Studies in Mycology 102 (June 2022)

ISSN 0166-0616

Diversity and taxonomy of food and indoor *Aspergillus*

Robert A. Samson, editor

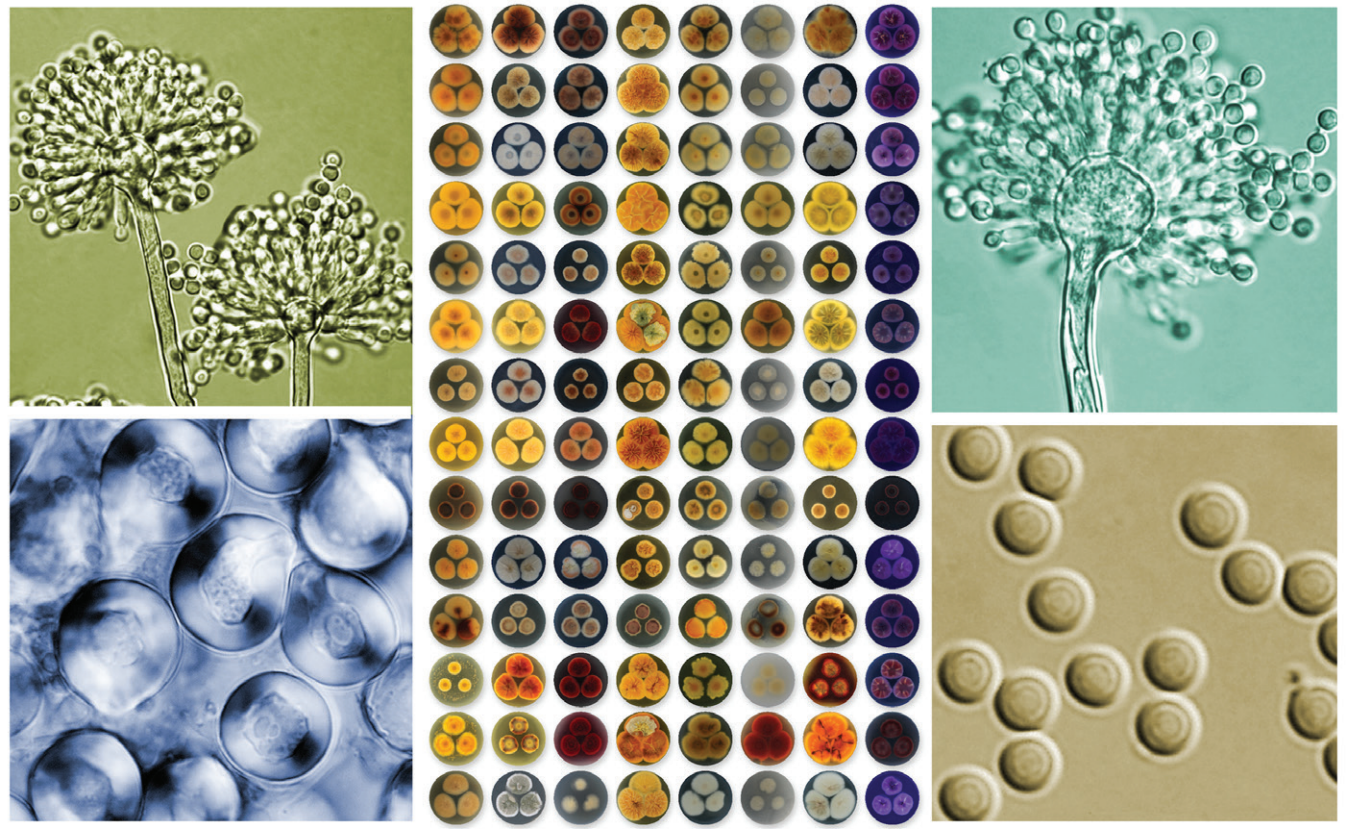

WESTERDIJK FUNGALBIO DIVERSITY INSTITUTE

An institute of the Royal Netherlands Academy of Arts and Sciences

ISBN/EAN: 978-94-91751-30-1

Cover: Top left: Conidiophores of *Aspergillus candidus*. Middle: Overview of macromorphological characters (reverse side of Petri dishes) within series *Versicolores* on eight cultivation media. Top right: Conidiophores of *A. subcandidus*. Bottom left: Hülle cells of *A. creber*. Bottom right: Conidia of *A. candidus*.

AIMS AND SCOPE

The Westerdijk Fungal Biodiversity Institute – an institute of the Royal Netherlands Academy of Arts and Sciences and situated in Utrecht, The Netherlands – maintains a world-renowned collection of living filamentous fungi, yeasts and bacteria. The institute's research programs principally focus on the taxonomy and evolution of fungi as well as on functional aspects of fungal biology and ecology, incorporating molecular and genomics approaches. The Westerdijk Fungal Biodiversity Institute employs circa 60 personnel, among whom circa 32 scientists.

Studies in Mycology is an international journal which publishes systematic monographs of filamentous fungi and yeasts, and special topical issues related to all fields of mycology, biotechnology, ecology, molecular biology, pathology and systematics. The journal is Open-Access and contains monographs or topical issues (5–6 papers per issue). There are no restrictions of length, although it is generally expected that manuscripts should be at least 50 A4 pages in print. The first issue was published in 1972.

Publication
Studies in Mycology is an open access journal that is freely available on the internet. All articles are open access under a Creative Commons BY-NC-ND (Attribution-NonCommercial-NoDerivatives) license. All manuscripts will undergo peer review before acceptance, and will be published as quickly as possible following acceptance. There are no page charges or length restrictions, or fees for colour plates. The official journal language is English. All content submitted to *Studies in Mycology* is checked for plagiarism.

Article submission
Authors who intend to submit monographs or topical issues should contact the Executive Editor in advance. Authors are obliged to meet the requirements as set out in our Instructions for Authors.

Hardcopies
From 2016 onwards hardcopies of new issues are no longer available. Single hardcopies of issues published prior to 2016 can be bought through the Westerdijk Fungal Biodiversity Institute Web shop. A 20% reduction on the list price applies only when 10 or more copies of a specific publication are bought at the same time.

Published by
Westerdijk Fungal Biodiversity Institute, Uppsalalaan 8, 3584 CT Utrecht, The Netherlands.

Hosted by
Ingenta Connect.

CONTENTS

WESTERDIJK FUNGALBIO DIVERSITY INSTITUTE

A monograph of *Aspergillus* section *Candidi*

K. Glässnerová[1], F. Sklenář[1,2], Ž. Jurjević[3], J. Houbraken[4], T. Yaguchi[5], C.M. Visagie[6], J. Gené[7], J.P.Z. Siqueira[7,8], A. Kubátová[1], M. Kolařík[1,2], V. Hubka[1,2,5]*

[1]*Department of Botany, Faculty of Science, Charles University, Prague, Czech Republic;* [2]*Laboratory of Fungal Genetics and Metabolism, Institute of Microbiology, Czech Academy of Sciences, Prague, Czech Republic;* [3]*EMSL Analytical, Cinnaminson, New Jersey, USA;* [4]*Westerdijk Fungal Biodiversity Institute, Utrecht, The Netherlands;* [5]*Medical Mycology Research Center, Chiba University, Chuo-ku, Chiba, Japan;* [6]*Department of Biochemistry, Genetics and Microbiology, Forestry and Agricultural Biotechnology Institute (FABI), University of Pretoria, Pretoria, South Africa;* [7]*Unitat de Micologia, Facultat de Medicina i Ciències de la Salut, IISPV, Universitat Rovira i Virgili, Reus, Spain;* [8]*Laboratório de Microbiologia, Faculdade de Medicina de São José do Rio Preto, São José do Rio Preto, Brazil*

**Corresponding author*: V. Hubka, vit.hubka@gmail.com

Abstract: *Aspergillus* section *Candidi* encompasses white- or yellow-sporulating species mostly isolated from indoor and cave environments, food, feed, clinical material, soil and dung. Their identification is non-trivial due to largely uniform morphology. This study aims to re-evaluate the species boundaries in the section *Candidi* and present an overview of all existing species along with information on their ecology. For the analyses, we assembled a set of 113 strains with diverse origin. For the molecular analyses, we used DNA sequences of three house-keeping genes (*benA*, *CaM* and *RPB2*) and employed species delimitation methods based on a multispecies coalescent model. Classical phylogenetic methods and genealogical concordance phylogenetic species recognition (GCPSR) approaches were used for comparison. Phenotypic studies involved comparisons of macromorphology on four cultivation media, seven micromorphological characters and growth at temperatures ranging from 10 to 45 °C. Based on the integrative approach comprising four criteria (phylogenetic and phenotypic), all currently accepted species gained support, while two new species are proposed (*A. magnus* and *A. tenebricus*). In addition, we proposed the new name *A. neotritici* to replace an invalidly described *A. tritici*. The revised section *Candidi* now encompasses nine species, some of which manifest a high level of intraspecific genetic and/or phenotypic variability (*e.g.*, *A. subalbidus* and *A. campestris*) while others are more uniform (*e.g.*, *A. candidus* or *A. pragensis*). The growth rates on different media and at different temperatures, colony colours, production of soluble pigments, stipe dimensions and vesicle diameters contributed the most to the phenotypic species differentiation.

Key words: *Aspergillus candidus*, *Aspergillus tritici*, genealogical concordance, integrative taxonomy, intraspecific variability, multispecies coalescent model.
Taxonomic novelties: New species: *Aspergillus magnus* Glässnerová & Hubka; *Aspergillus neotritici* Glässnerová & Hubka; *Aspergillus tenebricus* Houbraken, Glässnerová & Hubka.

Citation: Glässnerová K, Sklenář F, Jurjević Ž, Houbraken J, Yaguchi T, Visagie CM, Gené J, Siqueira JPZ, Kubátová A, Kolařík M, Hubka V (2022). A monograph of *Aspergillus* section *Candidi*. *Studies in Mycology* **102**: 1–51. doi: 10.3114/sim.2022.102.01
Received: 22 April 2022 ; **Accepted:** 3 August 2022; **Effectively published online:** 19 October 2022
Corresponding editor: Robert A. Samson

INTRODUCTION

Aspergillus is a large genus of filamentous fungi which is divided into 27 sections. *Aspergillus* section *Candidi* currently includes seven white- or yellow-sporulating species (Houbraken *et al.* 2020). Members of this section show a relatively uniform morphology and their identification to a species level is non-trivial when using only phenotypic characters. The first modern monograph of the section was published by Varga *et al.* (2007) who used a polyphasic approach for species delimitation (combination of morphology, physiology, exometabolite profiles and molecular data) and recognized *A. candidus* [MB 204868] and three other species: *A. tritici* [MB 309248] (Mehrotra & Basu 1976), *A. campestris* [MB 110495] (Christensen 1982) and *A. taichungensis* [MB 434473] (Yaguchi *et al.* 1995). Since then, another three species have been described, namely, *A. subalbidus* [MB 809190] (Visagie *et al.* 2014), *A. pragensis* [MB 800371] (Hubka *et al.* 2014) and *A. dobrogensis* [MB 821313] (Hubka *et al.* 2018b).

The studies of Varga *et al.* (2007), Visagie *et al.* (2014) and Hubka *et al.* (2014) used a combination of morphology, phylogeny and/or profiles of exometabolites for species description (polyphasic approach). Another widely used approach in fungal taxonomy, GCPSR (Genealogical Concordance Phylogenetic Species Recognition), has not been applied in section *Candidi*. This approach involves comparisons of topologies of single-locus phylogenetic trees and search for monophyletic genealogical groups that are concordantly well-supported (Taylor *et al.* 2000, Dettman *et al.* 2003a). More recently, new phylogenetic methods based on the multispecies coalescent model (MSC) have been implemented in taxonomy (Fujisawa *et al.* 2016). These methods take into account for example the incomplete lineage sorting, a most common reason for incongruences in tree topologies constructed on the basis of different loci (Edwards 2009, Mirarab *et al.* 2016). The application of these methods on section *Candidi* led to segregation of *A. candidus* into two species and description of *A. dobrogensis* (Hubka *et al.* 2018b).

The best known and the first described member of this section is *A. candidus*, a xerophilic species which is able to grow on substrates with low water activity like stored grains and seeds, where it can reduce the grains' germinability (Thom & Raper 1945, Papavizas & Christensen 1960, Raper & Fennell 1965). It is also

Studies in Mycology

frequently found in the indoor environment, on food products (flour, cereals, spices, nuts), in soil or in the marine environment (Weidenbörner & Kunz 1994, Pitt & Hocking 1997, Klich 2002, Wei *et al.* 2007, Visagie *et al.* 2017). The section also encompasses several clinically relevant representatives which occasionally cause superficial (onychomycosis or otitis externa) or invasive mycoses, or contaminate clinical samples. Among these, *A. tritici* and *A. candidus* are confirmed etiological agents of some infections, while *A. pragensis* and *A. dobrogensis* have only been isolated from clinical samples and their clinical significance remains questionable (Moling *et al.* 2002, Hubka *et al.* 2012, Hubka *et al.* 2014, Becker *et al.* 2015, Nouripour-Sisakht *et al.* 2015, Gupta *et al.* 2016, Masih *et al.* 2016, Carballo *et al.* 2020, Kaur *et al.* 2021).

Members of the section *Candidi* produce many industrially important enzymes and secondary metabolites with a biotechnological potential. For example, they produce extracellular lipases, xylanases and cellulases which have potential to be used in the waste degradation processes (Milala *et al.* 2009, Garai & Kumar 2013, Farias *et al.* 2015) or metabolites with antioxidant activity which can be used in the process of maturing foods (Grazia *et al.* 1986, Pitt & Hocking 1997, Sunesen & Stahnke 2003). The production of bioactive metabolites with pharmacological potential has been identified in some species, for example chlorflavonin with antibiotic and antifungal effects (Munden *et al.* 1970, Marchelli & Vining 1973, Hubka *et al.* 2014), compounds with significant anti-oxidative activity such as candidusin B, 3-hydroxyterphenyllin or dihydroxymethyl pyranone (Yen *et al.* 2001, Elaasser *et al.* 2011), cytotoxic candidusin A, preussin or *p*-terphenyl derivatives (Kobayashi *et al.* 1982, Malhão *et al.* 2019, Lin *et al.* 2021) and many other recently discovered compounds with antitumor, antimicrobial, cytotoxic or antiviral activities such as ascandinines (Zhou *et al.* 2021), taichunines (El-Desoky *et al.* 2021), unguisins (Li *et al.* 2020) or other *p*-terphenyl derivatives (Han *et al.* 2020, Shan *et al.* 2020, Wang *et al.* 2020). The production of most of these secondary metabolites is usually attributed to *A. candidus*, but it is likely that the producer was misidentified in some cases with other species from section *Candidi*. For instance, production of *p*-terphenyl derivative 4"-deoxy-2'-methoxyterphenyllin attributed to *A. candidus* is in fact produced by *A. subalbidus* (Shan *et al.* 2020). Such re-identifications are, however, only possible when the isolate is accessioned and preserved in culture collections or DNA sequence data are available which is gradually becoming a standard in studies on compounds produced by microorganisms.

Previous studies focused on section *Candidi* included only a small number of strains and consequently, little is known about intraspecific genetic and phenotypic variability. Section *Candidi* members are widespread worldwide and occur on a wide range of substrates, but at low frequencies. During our past projects, a large collection of over a hundred strains belonging to the section *Candidi* has been gathered from various substrates and countries, and a high genetic and morphological variability has been observed within species which were previously considered to be relatively homogeneous. To determine if this variability reflects undescribed species diversity or a high intraspecific variability, we compared the data from phenotypic analyses, classical phylogenetic methods, GCPSR approach and delimitation methods based on coalescence theory. According to the resulting taxonomic conclusions, we revised the descriptions of all supported species in the section.

MATERIALS AND METHODS

Strains

This study builds upon previous taxonomic studies dealing with section *Candidi* (Varga *et al.* 2007, Hubka *et al.* 2014, Visagie *et al.* 2014, Hubka *et al.* 2018b). The majority of new and yet unpublished strains were isolated from indoor environments, caves and dung. The isolation techniques mostly followed the procedures previously described by Jurjević *et al.* (2015), Nováková *et al.* (2018), Guevara-Suarez *et al.* (2020) and Visagie *et al.* (2021). Remaining strains were obtained from culture collections and collaborators, and originated from diverse substrates and countries. In total, we gathered 113 strains and detailed information about their provenance is listed in Table 1. Dried holotype and isotype specimens of the newly described species were deposited into the herbarium of the Mycological Department, National Museum, Prague, Czech Republic (PRM).

Phenotypic studies

Macromorphological characters were studied on malt extract agar (MEA; malt extract from Oxoid Ltd., Basingstoke, UK), Czapek Yeast Extract Agar (CYA; yeast extract from Oxoid Ltd.), Czapek-Dox Agar (CZA), and Czapek Yeast Extract Agar with 20 % sucrose (CY20S). For the agar media composition, see Samson *et al.* (2014). The strains were inoculated in three points on growth media in 90 mm Petri dishes and colony dimensions were measured after seven and 14 d of incubation at 25 °C. After 14 d, the photographs of colonies were taken, and after 28 d, the colonies were checked for presence of sclerotia and soluble pigment production as these characters are frequently expressed with delay. To determine the cardinal temperatures, the strains were grown for 14 d on MEA at 10, 15, 20, 25, 30, 35, 37, 40, and 45 °C. The description and names of colours followed Kornerup & Wanscher (1967). Colony details were documented with a Canon EOS 500D camera and a Leica M205C stereo microscope with a Leica DMC 5400 digital camera.

Micromorphological characters (length and width of stipe, vesicle diameter, length of metulae and phialides, length and width of conidia) were photographed and measured from 7–21-d-old colonies on MEA incubated at 25 °C. Lactic acid (60%) was used as mounting medium. Every morphological character was recorded at least 35 times for each strain. Statistical differences, in particular phenotypic characters, were tested with one-way ANOVA followed by Tukey's honest significant difference (HSD) test in R v. 4.1.2 (R Core Team 2021). Boxplots and violin graphs were created in R with package ggplot2 (Wickham 2016).

Microscopic photographs were taken using an Olympus BX51 microscope equipped with an Olympus DP72 camera. The photographic plates were made in CorelDRAW Graphic Suite 2021. Scanning electron microscopy (SEM) was performed using a JEOL-6380 LV microscope (JEOL Ltd. Tokyo, Japan) as described previously by Hubka *et al.* (2013b).

Molecular studies

Total genomic DNA was extracted from 7-d-old colonies growing on MEA using the ZR Fungal/ Bacterial DNA Kit™ (Zymo Research, Irvin, CA, USA). The quality of the isolated DNA was verified using a NanoDrop 1000 Spectrophotometer.

Table 1. List of strains from *Aspergillus* section *Candidi* examined in this study.

Species	Strain No.[a]	Provenance: country, locality, substrate, year, collector/isolator	GenBank/ENA/DDBJ accession Nos.			
			ITS	*benA*	*CaM*	*RPB2*
A. campestris	CBS 348.81^T = IMI 259099^T = NRRL 13001^T = IBT 13382^T = IBT 28561^T = ATCC 44563^T = IFM 50931^T = CCF 5596^T	USA, North Dakota, near Zap, storage pile of topsoil displaced from a native, mixed prairie (*Agropyron* spp., *Bouteloua gracilis*), 1979, R.M. Miller & S.M. Pippen	EF669577	EU014091	EF669535	EF669619
	IBT 17867 = CCF 5700	USA, Wyoming, Pillot Hill Road, Medicine Bow National Forest, near Laramie, soil, 1994, J.C. Frisvad	ON156368	ON164544	ON164594	ON164491
	CCF 5641 = IFM 66789 = EMSL 1816	USA, Wyoming, Gillette, air of living room, 2012, Ž. Jurjević	ON156369	ON164567	ON164616	ON164514
	FMR 15224 = CBS 142984 = CCF 6075 = IFM 66790	Spain, Castile and Leon, Palencia, Monte el Viejo, Deer Reserve Park, herbivore dung, 2016, J. Gené & J.Z. Siqueira	LT798902	LT798915	LT798916	LT798917
	FMR 15226 = CBS 142985 = CCF 6053	Spain, Castile and Leon, Palencia, Monte el Viejo, Deer Reserve Park, herbivore dung, 2016, J. Gené & J.Z. Siqueira	LT798903	LT798918	LT798919	LT798920
	IBT 23172 = IMI 073462 = CCF 5699 = IFM 66791	USA, California, rabbit (*Oryctolagus cuniculus*) dung, 1958, S. Stribling	ON156370	ON164568	ON164617	ON164515
	IMI 344489	South Africa, Pretoria, mouse dung, deposited into IMI collection in 1991, R.Y. Anelich	ON156371	ON164569	ON164618	ON164516
A. candidus	CBS 566.65^T = IMI 091889^T = NRRL 303^T = IBT 28566^T = ATCC 1002^T = CCF 5594^T	unknown, received by K.B. Raper and D.I. Fennell in 1909 from J. Westerdijk	EF669592	EU014089	EF669550	EF669634
	CCF 488 = IBT 32273	Czech Republic, tunnels of bark beetles, 1960, E. Kotýnková-Sychrová	FR733811	LT626977	LT626978	LT626979
	CCF 4029 = CMF ISB 1730 = IBT 32272	Romania, Meziad Cave, bat droppings, 2009, A. Nováková	FR733813	LT626980	FR751424	LT626981
	CCF 3996 = CBS 134394	Czech Republic, Prague, external auditory canal of 53-year-old man (otitis externa), 2010, P. Lysková	FR727137	FR775325	HE716843	LT626982
	CCF 5577	Romania, Ungurului Cave, old bat guano, 2010, A. Nováková	LT626946	LT626983	LT626984	LT626985
	NRRL 58579 = CCF 5843 = IBT 33371 = EMSL 914	USA, New York, indoor air of a home, 2008, Ž. Jurjević	LT626947	LT626986	LT626987	LT626988
	NRRL 58959 = CCF 5845 = EMSL 1252	USA, Pennsylvania, indoor air of a home, 2009, Ž. Jurjević	LT626948	LT626989	LT626990	LT626991
	CCF 4912 = EMSL 2295	USA, New Jersey, Cranbury, crawlspace metal duct (swab), 2014, Ž. Jurjević	LT626949	LT626992	LT626993	LT626994
	CCF 5172	Czech Republic, Prague, mouse excrements in grain store, 2000, J. Hubert	LT626953	LT627005	LT627006	LT627007
	CCF 4713	Romania, Ungurului Cave, bat guano, 2010, A. Nováková	LT626950	LT626995	LT626996	LT626997
	CCF 4659	Czech Republic, Hustopeče, toenail of 52-year-old woman, 2012, S. Dobiášová	HG915889	HG916672	HG916681	LT626998
	CCF 4915 = EMSL 1285	USA, Rhode Island, indoor air of living room, 2009, Ž. Jurjević	LT626951	LT626999	LT627000	LT627001
	NRRL 4646 = IMI 359076 = DTO 213-G2 = CBS 133061	USA, barn litter, D.I. Fennell	EF669605	EU014090	EF669563	EF669647
	CCF 5675 = EMSL 2403	USA, Pennsylvania, Feasterville, air in a basement of a house, 2014, Ž. Jurjević	LT626952	LT627002	LT627003	LT627004
	CCF 5576 = EMSL 2421	USA, New York, Binghamton, air in bedroom, 2014, Ž. Jurjević	LT626954	LT627008	LT627009	LT627010
	DTO 223-E5	The Netherlands, soil, 2012, M. Meijer	LT626955	LT627011	LT627012	LT627013
	CCF 6195 = EMSL 2721	USA, Minnesota, Minneapolis, classroom dust, 2015, Ž. Jurjević	ON156372	ON164545	ON164634	ON164492

Table 1. (Continued).

Species	Strain No.[a]	Provenance: country, locality, substrate, year, collector/isolator	GenBank/ENA/DDBJ accession Nos.			
			ITS	*benA*	*CaM*	*RPB2*
	CCF 6198 = EMSL 2863	USA, Ohio, Westerville, air in basement (settle plates), 2015, Ž. Jurjević	ON156373	ON164546	ON164595	ON164493
	CCF 6200 = EMSL 2895	USA, Massachusetts, Cohasset, air in bathroom, 2015, Ž. Jurjević	ON156374	ON164547	ON164596	ON164494
	CMW-IA 8 = CMW 58610 = CN138F7 = KAS 5864	Canada, Nova Scotia, Wolfville, house dust, 2015, C.M. Visagie & A. Walker	—	ON164548	ON164597	ON164495
	CMW-IA 9 = CMW 58611 = CN138F8 = KAS 6297	Canada, Nova Scotia, Little Lepreau, house dust, 2015, C.M. Visagie & A. Walker	—	ON164549	ON164598	ON164496
	CMW-IA 10 = CMW 58612 = CN138F9 = KAS 6134	Canada, Nova Scotia, Wolfville, house dust, 2015, C.M. Visagie & A. Walker	—	ON164550	ON164599	ON164497
	CMW-IA 11 = CMW 58613 = CN138G1 = KAS 6135	Canada, Nova Scotia, Wolfville, house dust, 2015, C.M. Visagie & A. Walker	—	ON164551	ON164600	ON164498
A. dobrogensis	CCF 4651^T = CCF 4655^T = NRRL 62821^T = IBT 32697^T = CBS 143370^T	Romania, Movile Cave, 2nd airbell, cave sediment, 2012, A. Nováková	LT626959	LT627027	LT558722	LT627028
	IBT 29476 = CCF 5823	Denmark, Høve Strand, mouse dung (in bed in summer house annex), 2007, J.C. Frisvad	LT907964	LT907967	LT907966	LT907969
	CCF 5567	Romania, Meziad Cave, bat droppings, 2009, A. Nováková	LT626960	LT627029	LT627030	LT627031
	CCF 5568	Romania, Liliecilor de la Guru Dobrogei Cave, Galeria Fossile, bat guano, 2010, A. Nováková	LT626961	LT627032	LT627033	LT627034
	CCF 4650 = CCF 4657 = NRRL 62820 = IBT 32699	Romania, Meziad Cave, cave sediment, 2010, A. Nováková	LT626962	LT627035	LT627036	LT627037
	CCF 4649 = IBT 32700	Romania, Liliecilor de la Guru Dobrogei Cave, Galeria Fossile, bat guano, 2010, A. Nováková	LT626963	LT627038	LT627039	LT627040
	CCF 5569	Romania, Liliecilor de la Guru Dobrogei Cave, Galeria Fossile, bat guano, 2010, A. Nováková	LT626964	LT627041	LT627042	LT627043
	CCF 5570	Romania, Liliecilor de la Guru Dobrogei Cave, Galeria Fossile, bat droppings, 2010, A. Nováková	LT626965	LT627044	LT627045	LT627046
	CCF 5573	Romania, Liliecilor de la Guru Dobrogei Cave, cave air, 2011, A. Nováková	LT626966	LT627047	LT627048	LT627049
	CCF 5571	Romania, Meziad Cave, hall in the upper floor, bat guano, 2010, A. Nováková	LT626967	LT627050	LT627051	LT627052
	CCF 5572	Romania, Liliecilor de la Guru Dobrogei Cave, cave air, 2013, A. Nováková	LT626968	LT627053	LT627054	LT627055
	CCF 5574	Romania, Liliecilor de la Guru Dobrogei cave, Galeria Fossile, bat droppings, 2014, A. Nováková	LT626969	LT627056	LT627057	LT627058
	CCF 5575	Czech Republic, nails of 31-year-old woman, 2014, P. Lysková	LT626970	LT627 059	LT627060	LT627061
	CBS 225.80 = DTO 031-E6	The Netherlands, human nail (contaminant), 1980, CBS	LT626971	LT627062	LT627063	LT627064
	DTO 025-I1	Germany, carpet, 2006	LT626972	LT627077	LT627078	LT627079
	DTO 013-C4 = IBT 28582	The Netherlands, Maastricht, indoor air, 2006, J. Houbraken	LT626973	LT627065	LT627066	LT627067
	DTO 001-F9 = IBT 28576	The Netherlands, surface of museum piece, 2004, J. Houbraken	LT626974	LT627068	LT627069	LT627070
	DTO 029-H2	Germany, carpet, 2006	LT626975	LT627071	LT627072	LT627073
	DTO 031-D9 = CBS 116945 = IBT 116945 = IBT 28573	The Netherlands, Tiel, dust in museum, 2004, J. Houbraken	LT626976	LT627074	LT627075	LT627076

Table 1. (Continued).

Species	Strain No.[a]	Provenance: country, locality, substrate, year, collector/isolator	GenBank/ENA/DDBJ accession Nos.			
			ITS	*benA*	*CaM*	*RPB2*
	CCF 5844 = EMSL No. 2810	USA, New York, Lockport, indoor air in basement (settle plate), 2015, Ž. Jurjević	LT907963	ON164552	LT907965	LT907968
	FMR 15444 = CBS 142752 = CCF 6119	Spain, Galicia, Lugo, Ribeira Sacra, herbivore dung, 2016, J. Guarro & M. Guevara-Suarez	LT798904	LT798921	LT798922	LT798923
	FMR 15601 = CCF 5846	Spain, Galicia, Orense, Cortegada, herbivore dung, 2016, J. Guarro & M. Guevara-Suarez	ON156375	LT962396	ON164601	ON164499
A. magnus	UAMH 1324^T = IBT 14560^T = CCF 6606^T	Canada, Alberta, Edmonton, mouse collected on horsefarm, 1962, J.W. Carmichael	ON156376	ON164570	ON164619	ON164517
A. neotritici	CCF 3853^T = IBT 32725^T	Czech Republic, Prague, toenail of 62-year-old man, 2008, M. Skořepová	FR727136	FR775327	HE661598	LT627021
	CBS 266.81 = IBT 21956 = CCF 5842	India, grains of *Triticum aestivum*, before 1976, B.S. Mehrotra	LT626958	EU076293	HG916678	LT627017
	CCF 4030 = CMF ISB 1300 = IBT 32729	Czech Republic, Frýdek-Místek, vermicompost, 2001, A. Nováková	FR733814	LT627018	FR751425	LT627019
	CCF 4653	Czech Republic, Prague, toenail of 58 -year-old woman, 2012, P. Lysková	HG915890	HG916674	HG916677	LT627020
	CCF 3314	Czech Republic, Prague, outdoor air, 1996, A. Kubátová	FR733812	LT627022	FR751426	LT627023
	CCF 1649	Czech Republic, Prague, flour, 1979, J. Svrčková	FR733810	LT627024	FR751427	LT627025
	NRRL 4847 = IMI 359077 = DTO 213-G3 = CBS 133055 = CCF 4809	Japan (?), unknown, received by K.B. Raper and D.I. Fennell from CBS as Nakazawa´s strain of *A. albus* var. *thermophilus*	ON156395	ON164587	ON164628	ON164537
	CCF 4658	Czech Republic, Prague, toenail of 69-year-old woman, 2008, M. Skořepová	HG915891	HG916675	HG916676	LT627026
	DTO 201-D3 = CBS 129260 = RMF 7641	USA, Nebraska, 1 mile north of Miller, loess soil, 6 feet deep, soil profile, 1984	ON156397	ON164591	ON164632	ON164541
	DTO 201-G7 = RMF TC 215 = CBS 129307	Unknown location, soil	ON156398	ON164592	ON164633	ON164542
	CCF 6202 = EMSL 3152	USA, Florida, Key West, air in bedroom (settle plates), 2015, Ž. Jurjević	ON156396	ON164588	ON164629	ON164538
	CCF 6397	Czech Republic, Havlíčkův Brod, abdominal cavity of 62-year-old male with disseminated mycosis (probably caused by *Rhizopus* sp. and *Trichosporon asahii*), 2020, D. Lžičařová	ON156394	ON164589	ON164630	ON164539
	CMW-IA 12 = CMW 58614 = CN117B9	South Africa, Free State, Viljoenskroon, sunflower seed, 2020, C.M. Visagie	—	ON164590	ON164631	ON164540
	IBT 12659	USA, New Mexico, Seviletta National Wildlife Refuge, Socorro County, soil in a kangaroo rat burrow, 1989, L. Hawkins	ON156393	ON164557	ON164606	ON164504
	CCF 4914 = IFM 66793 = EMSL 2182	USA, Arizona, Tucson, air in a hospital, 2013, Ž. Jurjević	ON156392	ON164556	ON164605	ON164503
A. pragensis	CCF 3962^T = CBS 135591^T = IBT 32274^T = NRRL 62491^T	Czech Republic, Prague, toenail of 58-year-old man, 2007, M. Skořepová	FR727138	HE661604	FR751452	LN849445
	CCF 4654 = IBT 32701	Czech Republic, Prague, toenail of 59-year-old man, 2013, P. Lysková	HG915888	HG916673	HG916680	LT627014
	CCF 5847 = EMSL 2216	USA, Pennsylvania, Feasterville, carpet in bedroom, 2013, Ž. Jurjević	LT908112	LT908040	LT908041	LT908042
	NRRL 58614 = CCF 4911 = EMSL 1057	USA, Pennsylvania, indoor air of a home, 2008, Ž. Jurjević	LT908111	LT908037	LT908038	LT908039

Table 1. (Continued).

Species	Strain No.[a]	Provenance: country, locality, substrate, year, collector/isolator	GenBank/ENA/DDBJ accession Nos.			
			ITS	*benA*	*CaM*	*RPB2*
	CCF 5693 EMSL 2397	USA, Maryland, Cohasset, outdoor air, 2014, Ž. Jurjević	LT908113	LT908043	LT908044	LT908045
	CMW-IA 13 = CMW 58615 = CN138F5 = KAS 6296	Canada, Nova Scotia, Little Lepreau, house dust, 2015, C.M. Visagie & A. Walker	—	ON164553	ON164602	ON164500
	CMW-IA 14 = CMW 58616 = CN138G6 = KAS 6138	Canada, Nova Scotia, Little Lepreau, house dust, 2015, C.M. Visagie & A. Walker	—	ON164554	ON164603	ON164501
	CMW-IA 15 = CMW 58617 = CN138G8 = KAS 6299	Canada, Nova Scotia, Little Lepreau, house dust, 2015, C.M. Visagie & A. Walker	—	ON164555	ON164604	ON164502
A. subalbidus	CBS 567.65^{T} = NRRL 312^{T} = ATCC 16871^{T} = IMI 230752^{T} = CCF 5822^{T}	Brazil, received by K.B. Raper and D.I. Fennell in 1939 from J. Reis (Instituto Biologica)	EF669593	KP987050	EF669551	EF669635
	CBS 112449 = DTO 031-E3 = DTO 039-E7	Germany, indoor environment	LT626956	EU076294	EU076307	LT627015
	NRRL 5214 = ATCC 26930 = IMI 16046 = CCF 4860	Ghana, vegetable lard, International Mycological Institute, Egham, England, 1933, H.A. Dade (strain GC601) sent to IMI	LT908114	LT908034	LT908035	LT908036
	CCF 5696 =EMSL 2674	USA, Georgia, Canton, settle plates in living room, 2015, Ž. Jurjević	ON156388	ON164571	ON164620	ON164518
	CCF 6199 = EMSL 2894	USA, Florida, Bradenton, air in bathroom (settle plates), 2015, Ž. Jurjević	ON156386	ON164572	ON164621	ON164519
	CMW-IA 16 = CMW 58618 = CN162C8 = DN12	Botswana, Okavango basin, Gcwihaba Caves, bat guano-contaminated soil, 2019, G. Modise, D. Nkwe & R. Mazebedi	—	ON164573	MW480718	ON164520
	CMW-IA 17 = CMW 58619 = CN162C9 = DN13	Botswana, Okavango basin, Gcwihaba Caves, bat guano-contaminated soil, 2019, G. Modise, D. Nkwe & R. Mazebedi	—	ON164574	MW480719	ON164521
	CMW-IA 18 = CMW 58620 = CN162D1 = DN62	Botswana, Okavango basin, Gcwihaba Caves, bat guano-contaminated soil, 2019, G. Modise, D. Nkwe & R. Mazebedi	—	ON164575	MW480764	ON164522
	CMW-IA 19 = CMW 58621 = CN162D2 = DN67	Botswana, Okavango basin, Gcwihaba Caves, bat guano-contaminated soil, 2019, G. Modise, D. Nkwe & R. Mazebedi	—	ON164576	MW480769	ON164523
	CMW-IA 20 = CMW 58622 = CN162D3 = DN68	Botswana, Okavango basin, Gcwihaba Caves, bat guano-contaminated soil, 2019, G. Modise, D. Nkwe & R. Mazebedi	—	ON164577	MW480770	ON164524
	CN162D4 = DN69	Botswana, Okavango basin, Gcwihaba Caves, bat guano-contaminated soil, 2019, G. Modise, D. Nkwe & R. Mazebedi	—	ON164578	MW480771	ON164525
	CN162D5 = DN75	Botswana, Okavango basin, Gcwihaba Caves, bat guano-contaminated soil, 2019, G. Modise, D. Nkwe & R. Mazebedi	—	ON164579	MW480777	ON164526
	CN162D6 = DN80	Botswana, Okavango basin, Gcwihaba Caves, bat guano-contaminated soil, 2019, G. Modise, D. Nkwe & R. Mazebedi	—	ON164580	MW480781	ON164527
	CN162D7 = DN82	Botswana, Okavango basin, Gcwihaba Caves, bat guano-contaminated soil, 2019, G. Modise, D. Nkwe & R. Mazebedi	—	ON164581	MW480783	ON164528
	CN162D8 = DN85	Botswana, Okavango basin, Gcwihaba Caves, bat guano-contaminated soil, 2019, G. Modise, D. Nkwe & R. Mazebedi	—	ON164582	MW480785	ON164529
	CCF 5642 = IFM 66794 = EMSL 410	USA, Connecticut, wall in a house, 2008, Ž. Jurjević	ON156377	ON164558	ON164607	ON164505
	CCF 6197 = IFM 66795 = EMSL 2731	USA, Illinois, Mokena, air in crawl space (settle plates), 2015, Ž. Jurjević	ON156378	ON164559	ON164608	ON164506
	CCF 5643 = EMSL 2181	USA, Maryland, Baltimore, carpet in living room, 2013, Ž. Jurjević	ON156380	ON164561	ON164610	ON164508

Table 1. (Continued).

Species	Strain No.[a]	Provenance: country, locality, substrate, year, collector/isolator	GenBank/ENA/DDBJ accession Nos.			
			ITS	*benA*	*CaM*	*RPB2*
	NRRL 4809 = ATCC 11380 = IFO 4310 = DTO 213-F7 = CBS 133057 = CCF 5595	Japan (?), chinese yeast cake, received by K.B. Raper and D.I. Fennell from the Institute for Fermentation, Osaka, Japan (No. 4319) as "*A. albus* var. 1", M. Yamazaki, 1946	EF669609	EU014092	EF669567	EF669651
	NRRL 58123 = CCF 6193 = IFM 66796 = EMSL 465	USA, California, wall in a house, 2008, Ž. Jurjević	ON156382	ON164565	ON164614	ON164512
	CCF 5697 = IFM 66797 = EMSL 2180	USA, New Jersey, Mont Clair, indoor air, 2013, Ž. Jurjević	ON156381	ON164562	ON164611	ON164509
	CCF 4913 = EMSL 2297	USA, Maryland, Baltimore, house dust (living room), 2014, Ž. Jurjević	ON156379	ON164560	ON164609	ON164507
	CCF 5698 = EMSL 2369	USA, Maryland, Baltimore, house dust (living room), 2014, Ž. Jurjević	ON156385	ON164563	ON164612	ON164510
	CCF 5848 = EMSL 2646	USA, California, Rancho Mirage, settle plates in living room, 2014, Ž. Jurjević	ON156387	ON164564	ON164613	ON164511
	CCF 6205 = EMSL 3325	USA, Texas, Harker Heights, air in basement (settle plates), 2015, Ž. Jurjević	ON156383	ON164566	ON164615	ON164513
	FMR 15733 = CBS 142983 = CCF 6052 = IFM 66798	Spain, Canary Islands, Gran Canaria, Santa Brígida, herbivore dung, 2016, J. Gené & J.Z. Siqueira	LT798905	LT798924	LT798925	LT798926
	FMR 15736 = CBS 142982 = CCF 6074	Spain, Canary Islands, Gran Canaria, Teror, herbivore dung, 2016, J. Gené & J.Z. Siqueira	LT798906	LT798927	LT798928	LT798929
	FMR 15877 = CBS 142667 = CCF 6058	Spain, Canary Islands, Gran Canaria, North Coast, herbivore dung, 2016, J. Gené & J.Z. Siqueira	LT798907	LT798930	LT798931	LT798932
	DTO 196-E4 = CBS 126836	Ecuador, Galapagos Islands, soil, 1965, D.P. Mahoney	ON156384	ON164583	ON164622	ON164530
A. taichungensis	IBT 19404^{T} = CCF 5597^{T}= DTO 031-C6^{T}	Taiwan, Taichung city, soil, 1994, T. Yaguchi	LT626957	EU076297	HG916679	LT627016
	CMW-IA 21 = CMW 58623 = CN162D9 = DN07	Botswana, Okavango basin, Gcwihaba Caves, bat guano-contaminated soil, 2019, G. Modise, D. Nkwe & R. Mazebedi	—	—	MW480714	ON164531
	DTO 266-G2 = CCF 5827 = IFM 66799	Mexico, house dust, 2013, C.M. Visagie	KJ775572	KJ866980	ON164627	ON164536
	DTO 270-C9 = CCF 5826	Mexico, house dust, 2013, C.M. Visagie	KJ775573	KJ866981	ON164626	ON164535
A. tenebricus	DTO 337-H7^{T} = CBS 147048^{T}	South Africa, Robben island, soil, 2015, P.W. Crous & M. Meijer	ON156389	ON164584	ON164623	ON164532
	DTO 440-E1 = CBS 147376	Australia, Queensland, soil, 2009, P.W. Crous, N. Yilmaz & T. Hoogenhuijzen	ON156390	ON164585	ON164624	ON164533
	DTO 440-E2	Australia, Queensland, soil, 2009, P.W. Crous & T. Hoogenhuijzen	ON156391	ON164586	ON164625	ON164534
***Aspergillus* sp.**	DTO 244-F1	New Zealand, indoor environment, E. Whitfield, K. Mwange & T. Atkinson	ON156399	ON164543	ON164593	ON164490

[a] Acronyms of culture collections in alphabetic order: ATCC, American Type Culture Collection, Manassas, Virginia; CBS, Westerdijk Fungal Biodiversity Institute (formerly Centraalbureau voor Schimmelcultures), Utrecht, the Netherlands; CCF, Culture Collection of Fungi, Department of Botany, Charles University, Prague, Czech Republic; CMF ISB, Collection of Microscopic Fungi of the Institute of Soil Biology, Academy of Sciences of the Czech Republic, České Budějovice, Czech Republic; CN, CMW & CMW-IA, working and formal culture collections housed at FABI (Forestry and Agricultural Biotechnology) Institute, University of Pretoria, South Africa; DN, working collection of David Nkwe, housed at the Department of Biological Sciences and Biotechnology, Botswana International University of Science and Technology, Botswana; DTO, Internal Culture Collection of The Department Applied and Industrial Mycology of the CBS-KNAW Fungal Biodiversity Centre, Utrecht, The Netherlands; EMSL, EMSL Analytical Inc., New Jersey, USA; FMR, Facultat de Medicina i Ciències de la Salut, Reus, Spain; FRR, Food Fungal Culture Collection, North Ryde, Australia; IBT, Culture Collection at Department of Biotechnology and Biomedicine, Lyngby, Denmark; IFM, Collection at the Medical Mycology Research Center, Chiba University, Japan; IFO, Institute for Fermentation, Osaka, Japan; IHEM (BCCM/IHEM), Belgian Coordinated Collections of Micro-organisms, Fungi Collection: Human and Animal Health, Sciensano, Brussels, Belgium; IMI, CABI's collection of fungi and bacteria, Egham, UK; KAS, fungal collection of Keith A. Seifert, internal working culture collection at DAOMC (Culture collection of the National Mycological Collections, Agriculture & Agri-Food Canada), Ottawa, Canada; NRRL, Agricultural Research Service Culture Collection, Peoria, Illinois, USA; RMF, Rocky Mountain Fungi, Dept. of Botany, University of Wyoming, Laramie; UAMH, University of Alberta Microfungus collection and Herbarium, Edmonton, Alberta, Canada.

The PCR reaction volume of 20 µL contained 1 µL (50 ng mL^{-1}) of DNA, 0.3 µL of both primers (25 pM mL^{-1}), 0.2 µL of MyTaq™ DNA Polymerase (Bioline, GmbH, Germany) and 4 µl of 5 × MyTaq PCR buffer. The standard thermal cycle profile was 93 °C—2 min; 38 cycles of 93 °C—30 s, 55 °C—30 s, 72 °C—60 s; and a final extension of 72 °C—10 min. The internal transcribed spacer rDNA region (ITS) was amplified using forward primer ITS1 (White *et al.* 1990) and reverse primers NL4 (O'Donnell 1993) or ITS4 (White *et al*. 1990); the partial β-tubulin gene region (*benA*) was amplified using forward primers Bt2a (Glass & Donaldson 1995), T10 (O'Donnell & Cigelnik 1997) or Ben2f (Hubka & Kolařík 2012) and reverse primer Bt2b (Glass & Donaldson 1995); the partial calmodulin gene region (*CaM*) was amplified using forward primers CF1L, CF1M (Peterson 2008) or cmd5 (Hong *et al.* 2006) and reverse primers CF4 (Peterson 2008) or cmd6 (Hong *et al.* 2006); and the partial RNA polymerase II second largest subunit gene region (*RPB2*) using forward primers fRPB2-5F (Liu *et al.* 1999) or RPB2-F50-CanAre (Jurjević *et al.* 2015) and reverse primer fRPB2-7cR (Liu *et al.* 1999). The PCR products were separated by electrophoresis on 1 % agarose gel and subsequently purified using ExoSAP-IT™ (Thermo Fisher Scientific, Vilnius, Lithuania).

Sequences were inspected and assembled using BioEdit v. 7.2.5 (Hall 1999) and deposited into the GenBank database under accession numbers listed in Table 1.

Phylogenetic studies

Alignments of the *benA*, *CaM* and *RPB2* loci were performed using the FFT-NS-i option implemented in the MAFFT online service (Katoh *et al.* 2019). ITS was excluded from analyses due to its low number of informative sites. The alignments were trimmed, concatenated and then analysed using maximum likelihood (ML), Bayesian inference (BI) and Maximum Parsimony (MP; this method was used only to construct single-gene phylogenies) methods. Suitable partitioning schemes and substitution models (Bayesian information criterion) for the analyses were selected using a greedy strategy implemented in PartitionFinder 2 (Lanfear *et al.* 2017) with settings allowing introns, exons and codon positions to be independent datasets. The optimal partitioning schemes for each analysed dataset along with basic alignment characteristics are listed in Table 2.

Maximum likelihood trees were constructed with IQ-TREE v. 1.4.4 (Nguyen *et al.* 2015) with nodal support determined by ultrafast bootstrapping (BS) with 100 000 replicates. Trees were rooted with the clade containing *A. neotritici* isolates. Bayesian posterior probabilities (PP) were calculated using MrBayes v. 3.2.6 (Ronquist *et al.* 2012). The analysis ran for 10^7 generations, two parallel runs with four chains each were used, every 1 000th tree was retained and the first 25 % of trees were discarded as burn-in. The convergence of the runs and effective sample sizes were checked in Tracer v. 1.6 (http://tree.bio.ed.ac.uk/software/tracer). Maximum parsimony (MP) trees were created using PAUP* v.4.0b10 (Swofford 2003). Analyses were performed using the heuristic search option with 100 random taxon additions; tree bisection-reconnection (TBR); maxtrees were set to 1 000. Branch support was assessed by bootstrapping with 500 replications.

The rules for the application of the GCPSR approach were adopted from Dettman *et al.* (2003a,b) and slightly modified to different design of this study (different number of loci and methods used). To recognize a clade as an evolutionary lineage, it had to satisfy either of two criteria: (a) genealogical concordance - the clade was present in the majority (2/3) of the single-locus genealogies; (b) genealogical nondiscordance - the clade was well supported in at least one single-locus genealogy, as judged

Table 2. Characteristics of alignments, partition-merging results and best substitution model for each partition according to the Bayesian information criterion.

Alignment	Length (bp)	Variable position	Parsimony informative sites	Phylogenetic method	Partitioning scheme (substitution model)
benA + *CaM* + *RPB2* (Fig. 1)	2069	455	353	Maximum likelihood (ML)	Five partitions: 1st codon positions of *benA, CaM* & *RPB2* & 2nd codon positions of *CaM* (TrN+I); 2nd codon positions of *benA* & *RPB2* (JC); 3rd codon positions of *benA* & *CaM* (HKY+G); 3rd codon positions of *RPB2* (K81uf+G); introns of *benA* & *CaM* (K80+G)
				Bayesian inference (BI)	Five partitions: 1st codon positions of *benA, CaM* & *RPB2* (HKY+I); 2nd codon positions of *benA, CaM* & *RPB2* (F81+I); 3rd codon positions of *benA* & *CaM* (HKY+G); 3rd codon positions of *RPB2* (HKY+G); introns of *benA* & *CaM* (K80+G)
benA (Fig. 2)	479	133	106	ML	Three partitions: 1st & 2nd codon positions (JC); 3rd codon positions (HKY+G); introns (K80+G)
				BI	Three partitions: 1st & 2nd codon positions (JC); 3rd codon positions (HKY+G); introns (K80+G)
CaM (Fig. 2)	576	120	88	ML	Three partitions: 1st & 2nd codon positions (TrN+I); 3rd codon positions (HKY+G); introns (K80+G)
				BI	Three partitions: 1st & 2nd codon positions (HKY+I); 3rd codon positions (HKY+G); introns (K80+G)
RPB2 (Fig. 2)	1014	202	159	ML	Three partitions: 1st codon positions (HKY+I); 2nd codon positions (JC); 3rd codon positions (K81uf+G)
				BI	Three partitions: 1st codon positions (HKY+I); 2nd codon positions (JC); 3rd codon positions (HKY+G)

by both ML and MP bootstrap proportions (≥70 %) and BI posterior probabilities (≥95 %), and was not contradicted in any other single-locus genealogy at the same level of support. When deciding which evolutionary lineages represent phylogenetic species, two additional criteria were applied and evaluated according to the combined phylogeny of three genes: (a) genetic differentiation - species had to be relatively distinct and well differentiated from other species to prevent minor tip clades from being recognized as a separate species; (b) all individuals had to be placed within a phylogenetic species, and no individuals were to be left unclassified.

In order to create hypotheses about species boundaries, we used one multi-locus multispecies coalescent (MSC) model-based method STACEY (Jones 2017) and four single-locus species MSC delimitation methods: (1) the general mixed Yule-coalescent method (GMYC) (Fujisawa & Barraclough 2013), (2) the Bayesian version of the general mixed yule-coalescent model (bGMYC) (Reid & Carstens 2012), (3) the Poisson tree processes model (PTP) and (4) the Bayesian Poisson tree processes model bPTP (Zhang *et al.* 2013).

For the single-locus species delimitation methods, we used the *haplotype* function from package PEGAS (Paradis 2010) in R to retain only unique sequences in alignments. The following nucleotide substitution models were selected by jModelTest v. 2.1.10 (Darriba *et al.* 2012) for *benA*, *CaM* and *RPB2* loci according to the Bayesian information criterion: K80+I, TrNef+G and TrN+I. The GMYC analysis was performed in R with the package SPLITS (Fujisawa & Barraclough 2013). The ultrametric input trees for the GMYC method were calculated in BEAST v. 2.6.6 (Bouckaert *et al.* 2014) with a chain length of 1×10^7 generations. As a model for creating input trees we set up Coalescent Constant Population prior and performed two tree reconstruction methods – one with Common Ancestor heights (CAh) setting and second with Median heights (Mh) setting. We only show delimitation results of both settings when they were different. The bGMYC analysis was performed with package BGMYC (Reid & Carstens 2012) in R v. 3.4.1. For this method, we firstly discarded the initial 25 % of the trees from the BEAST inference as burn-in and then we used R v. 4.1.2 the package APE (Paradis *et al.* 2004) in R to randomly select one hundred trees, which were then used as input. Two values (0.5 and 0.75) of bgmyc.point function were set up for all analyses. This function is crucial for the final division of strains into species. The authors of the software recommended value around 0.5, lower value delimits either the same number of species or less while a value >0.5 delimits the same number of species or more. For the PTP and bPTP method, 1 000 maximum likelihood standard bootstrap trees were calculated in IQ-TREE v. 1.6.12 (Nguyen *et al.* 2015) and used as input. The analysis was run in the Python v. 3 (van Rossum & Drake 2019) package PTP (Zhang *et al.* 2013).

The multi-locus species delimitation method STACEY was performed in BEAST v. 2.6.6 (Bouckaert *et al.* 2014) using the STACEY v. 1.2.5 add-on (Jones 2017). We set up the length of mcmc chain to 1×10^9 generations, the species tree prior was set to the Yule model, the molecular clock model was set to strict clock, growth rate prior was set to lognormal distribution (M = 5, S = 2), clock rate priors for all loci were set to lognormal distribution (M = 0, S = 1), PopPriorScale prior was set to lognormal distribution (M = -7, S = 2) and relativeDeathRate prior was set to beta distribution ($\alpha = 1$, $\beta = 1000$). The output was processed with SpeciesDelimitationAnalyzer (Jones 2015). For the presentation of the results of STACEY, we firstly created a plot showing how the number of delimited species and the probability of the most probable scenarios change in relation to the value of *collapseheight* parameter, and then we created similarity matrices using code from Jones *et al.* (2015) with two different values (0.007, 0.01) of *collapseheight* chosen from the plot (see Results section - *Species delimitation using STACEY*). Phylogenetic trees generated during STACEY analysis were then used for the presentation of species delimitation results analysis. The graphical outputs were created in iTOL (Interactive Tree Of Life) (Letunic & Bork 2021).

We also employed the recently developed software DELINEATE (Sukumaran *et al.* 2021) to independently test species boundaries hypotheses. Firstly, the dataset was split into hypothetical populations with "A10" analysis in BPP v. 4.3 (Yang 2015). Then, the species tree for these populations was estimated in starBEAST (Heled & Drummond 2009) implemented in BEAST v. 2.6.6 (Bouckaert *et al.* 2014). Finally, the populations delimited by BPP were lumped into species based on the results of species delimitation methods and phenotypic characters, with several populations always left unassigned to be delimited by DELINEATE. In total, nine models of species boundaries were set up. The analysis was run in Python v. 3 (van Rossum & Drake 2019) package DELINEATE (Sukumaran *et al.* 2021).

RESULTS

Integrative approach for determining species boundaries

For the species delimitation in section *Candidi*, three genetic loci (*benA*, *CaM* and *RPB2*) were examined across 113 strains, while phenotypic characters were measured and scored for 66 strains representing the genetic variability across the section. The results from the GCPSR approach were compared with MSC methods and phenotypic data to draw the final conclusions about species limits.

From the early beginning of this study, it was clear that creating initial hypotheses about species boundaries in section *Candidi* would be extremely difficult due to relatively uniform morphology and conflicting data from single-gene phylogenies. To overcome these difficulties and remain relatively consistent across the section, we decided to score support for delimitation of species and monitor four main criteria. In this integrative approach, we required that the delimited species meet at least three of the following four criteria: (1) no conflict in the assessment of species limits using the GCPSR approach, (2) support from the multi-locus MSC method STACEY (at least in one of the two most probable scenarios – see below), (3) support by the majority (10 from 18) of single-locus MSC methods and their settings (agreement on the delimitation of species in its exact form or delimitation of smaller entities within it but without any admixture with related species/populations) and (4) presence of phenotypic difference(s) from phylogenetically most closely related species. The resulting scoring is summarized in Table 3. Using this approach, delimitation of two novel species was supported, *A. magnus* and *A. tenebricus* (see below and section Taxonomy).

Phylogenetic analysis and GCPSR approach

The best scoring ML tree based on the concatenated and partitioned alignment of 113 strains is shown in Fig. 1. The topology of the tree inferred by BI was almost identical and the posterior probabilities are appended to nodes together with bootstrap support values from

Table 3. Support for delimitation of various species/populations using integrative approach consisting of four main components.

Examined species/populations	Support from four evaluated components				Overall support
	GCPSR	STACEY[1]	Single-locus MSC methods[2]	Morphology / physiology	(3–4/4)
A. campestris	NO	YES (2/2)	YES (12/18)	YES	YES
segregation of *A. campestris* into three species	NO[3]	NO (0/2)	NO (6/18)	NO	NO
A. candidus	YES	YES (1/2)	NO (7/18)	N/A (trend)	?
A. dobrogensis	YES	YES (1/2)	NO (7/18)	N/A (trend)	?
***Aspergillus* sp. DTO 244-F1**	N/A	YES (2/2)	YES (11/18)	N/A	?
A. magnus	N/A	YES (2/2)	YES (17/18)	YES	YES
A. neotritici	YES	YES (2/2)	YES (18/18)	YES	YES
segregation of CCF 4914 and IBT 12659 from *A. neotritici*	YES	NO (0/2)	NO (3/18)	YES	NO
A. pragensis	YES	YES (2/2)	YES (17/18)	YES	YES
A. subalbidus	YES	YES (1/2)	YES (17/18)	YES	YES
segregation of CCF 6199 and CCF 5642 (pop 6) from *A. subalbidus*	YES	YES (1/2)	NO (9/18)	NO	NO
A. taichungensis	YES	YES (2/2)	YES (13/18)	YES	YES
segregation of DTO 266-G2 from *A. taichungensis*	NO	NO (0/2)	YES (10/18)	NO	NO
A. tenebricus	YES	YES (2/2)	YES (13/18)	YES	YES

MCS – multispecies coalescent model-based methods; N/A – data not available or analysis could not be performed (non-viable strain DTO 244-F1 could not be analyzed phenotypically; species/populations represented by one strains could not be evaluated using GCPSR; a part of *A. dobrogensis* and *A. candidus* isolates cannot be distinguished morphologically – see sections Results, Discussion and Taxonomy).

[1]Support in at least one of the two most probable scenarios with *collapseheight* parameters 0.007 and 0.01 – see Fig. 4B.

[2]Support by the majority (at least 10 out of 18) of single-locus methods and their settings, *i.e.*, agreement on the delimitation of species in its exact form or delimitation of smaller entities within it but without any admixture with related species/populations – see Fig. 3.

[3]Support is ambiguous: although three evolutionary lineages are supported by two out of three single-gene genealogies (Fig. 2), they lack support in the combined tree (Fig. 1); „YES" scoring would not change the final decision about species limits using integrative approach.

ML analysis. Isolation source and geographical origin of strains are plotted on the tree (also listed in Table 1) together with the culture collection accession numbers. All alignments are available from the Dryad Digital Repository (https://doi.org/10.5061/dryad.3j9kd51mq) and basic alignment characteristics are listed in Table 2 together with partitioning scheme and substitution models used in the analyses.

Phylogenetic relationships between section *Candidi* members are well resolved in the combined phylogeny and the species clustered into three main monophyletic clades. The first clade included *A. candidus*, *A. dobrogensis*, *Aspergillus* sp. DTO 244-F1, *A. campestris* and *A. magnus*. Although it is highly probable that strain DTO 244-F1 represents an undescribed species according to this phylogeny and molecular analyses mentioned below, it is no longer viable and thus only molecular data could be analysed. The second clade comprised *A. subalbidus*, *A. taichungensis*, *A. tenebricus* and *A. pragensis*. *Aspergillus neotritici* formed a single-species lineage, relatively distant from the other species. This topology was almost identical to the trees generated in STACEY analysis and starBEAST with one notable exception. In the ML and BI trees, *A. campestris* was resolved as polyphyletic due to the position of the strain IBT 17867. This strain formed a single-strain lineage clustering with *Aspergillus* sp. DTO 244-F1, *A. candidus* and *A. dobrogensis*. This is caused by its atypical *RPB2* sequences influencing the topology not only of the *RPB2* tree (Fig. 2) but also of the whole multi-locus phylogeny (Fig. 1). The *RPB2* sequence of *A. campestris* IBT 17867 shares many variable positions with *A. candidus* and *A. dobrogensis* and probably represents a phenomenon of ancestral polymorphism/incomplete lineage sorting or could be caused by past recombination/hybridization. By contrast, in the tree from the multi-locus MSC method STACEY (Fig. 3) and starBEAST (see Delineate analysis), all seven strains of *A. campestris* formed a monophyletic clade. Other sequences and phenotypic characters of IBT 17867 were typical of *A. campestris*.

When comparing topologies of single-gene trees and applying rules of the GCPSR concept (Fig. 2), no conflicts were found between *A. candidus* and *A. dobrogensis* supporting definition of these species in their known limits (Hubka *et al.* 2018b). There was some exchange of isolates between clades within the *A. candidus* lineage and we thus consider this species a single phylogenetic species (PS). Three evolutionary lineages are supported among seven examined strains of *A. campestris*: IBT 17867 + CBS 348.81 (1), IMI 344489 + IBT 23172 (2) and FMR 15224 + FMR 15226 + CCF 5641 (3). Except for lineage 1, these lineages are present in all three single-gene trees without conflict. However, as mentioned above, the deviating *RPB2* sequence and phylogenetic position of IBT 17867 in the *RPB2* tree contradicts support of lineages 1 in the *RPB2* tree. It is difficult to decide if there is a support for three PS using GCPSR because lineage 1 does not occur in the combined phylogeny reconstructed using ML and BI (Fig. 1) but at the same time, it is present in the species trees from other multigene analyses as mentioned above.

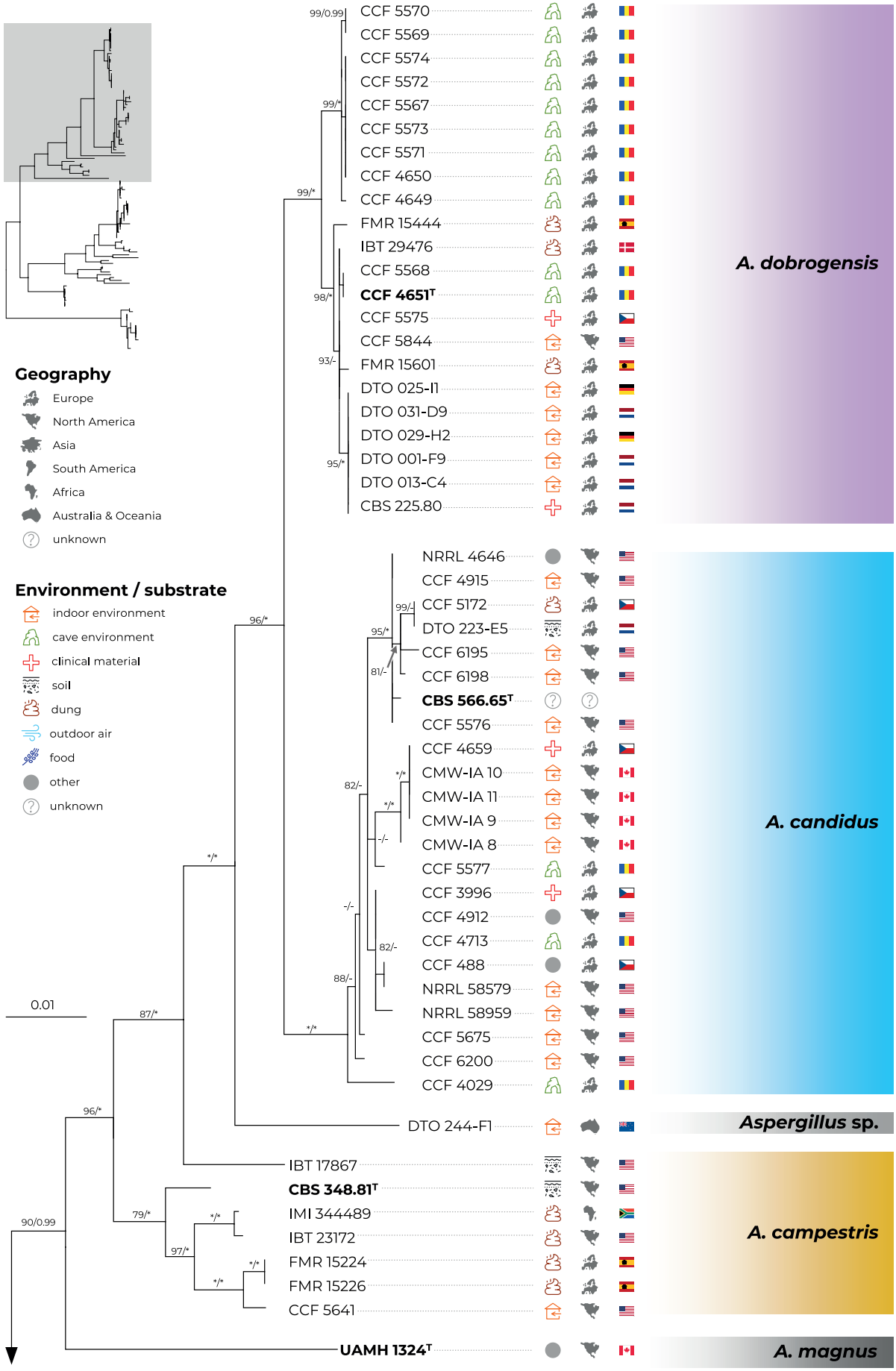

Fig. 1. Multi-locus phylogeny of *Aspergillus* section *Candidi* based on three loci (*benA*, *CaM*, *RPB2*) and comprising 113 isolates. Best scoring Maximum Likelihood tree inferred in the IQ-TREE is shown; Maximum likelihood bootstrap values and Bayesian posterior probabilities are appended to nodes; only support values higher than 70 % and 0.95, respectively, are shown. The ex-type strains are designated with a superscripted T and bold print. Alignment characteristics, partitioning scheme and substitution models are listed in Table 2. The information on geographic origin and isolation source was plotted on the tree – see legend.

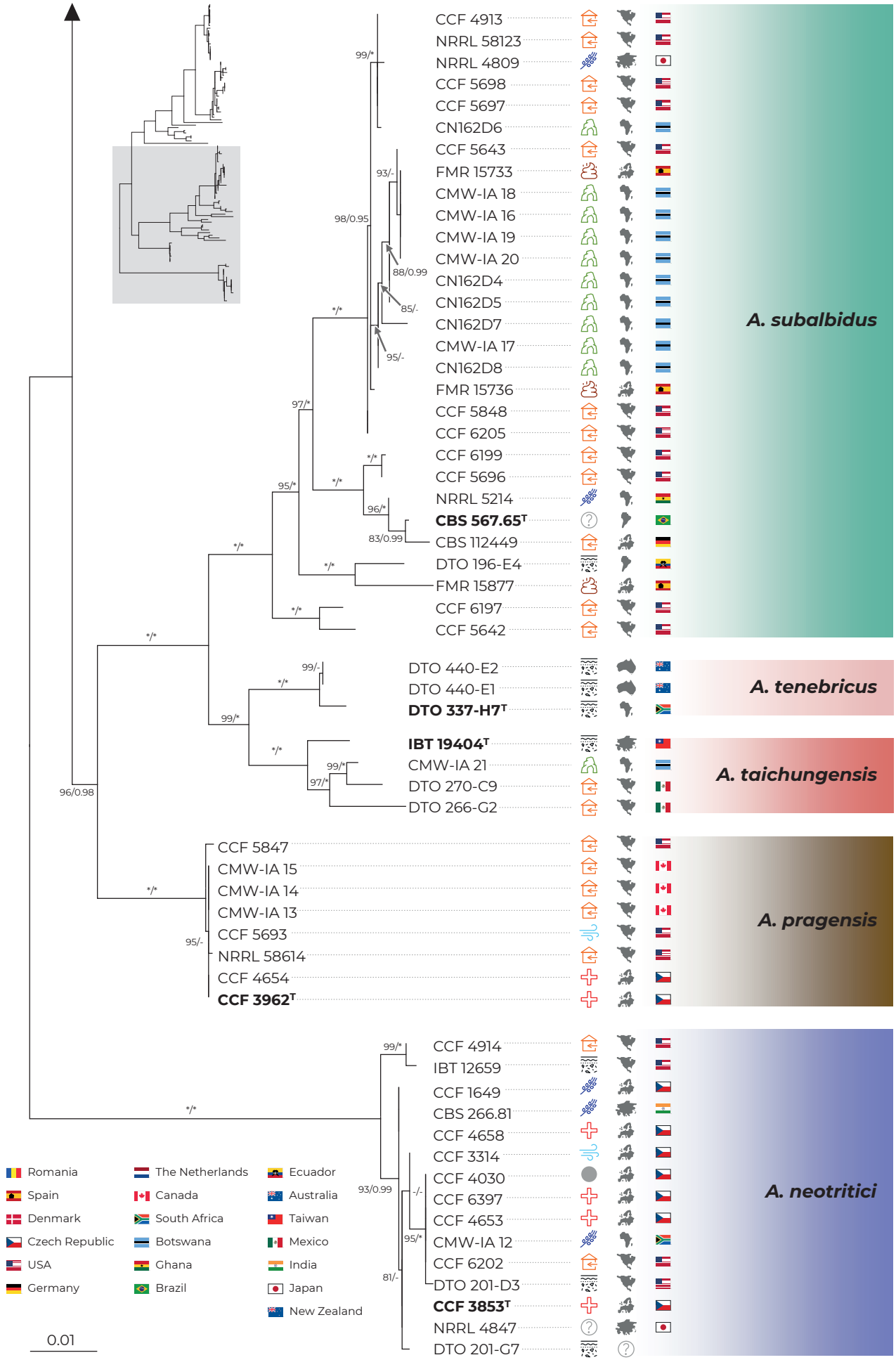

Fig. 1. (Continued).

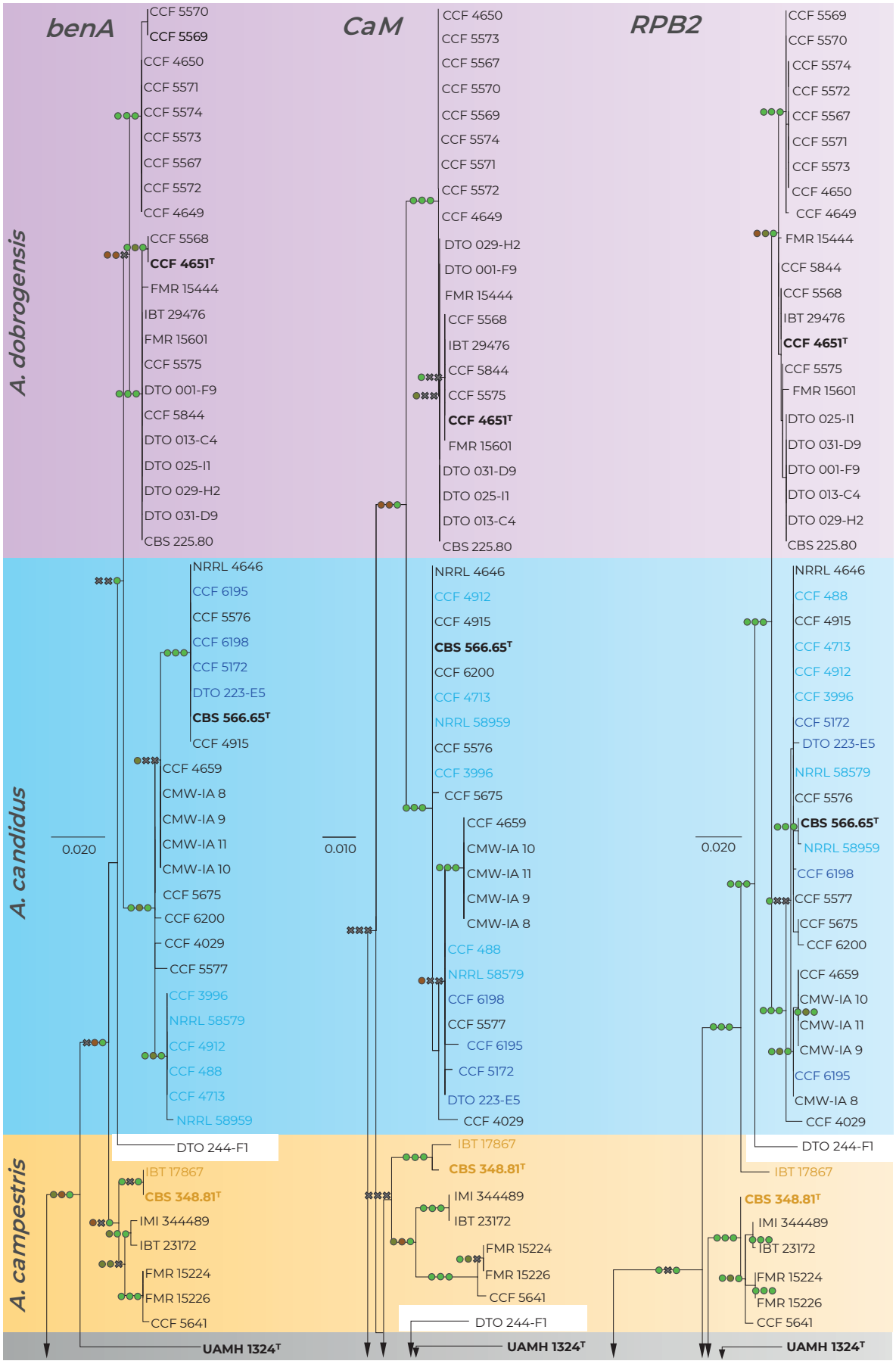

Fig. 2. Comparison of single-gene genealogies based on the alignments of *benA*, *CaM* and *RPB2* loci and created by three different phylogenetic methods. Single-locus maximum likelihood trees are shown; maximum likelihood bootstrap supports (MLBS), maximum parsimony bootstrap supports (MPBS) and Bayesian inference posterior probabilities (BIPP) are appended to nodes. Only MLBS and MPBS values ≥70 % and BIPP ≥0.95, respectively, are shown. A cross indicates lower statistical support for a specific node or the absence of a node in the MP and BI phylogenies. Selected strains or strain groups causing incongruences across single-gene phylogenies because of their unstable position are colour highlighted. The ex-type strains are designated with a superscripted T and bold print.

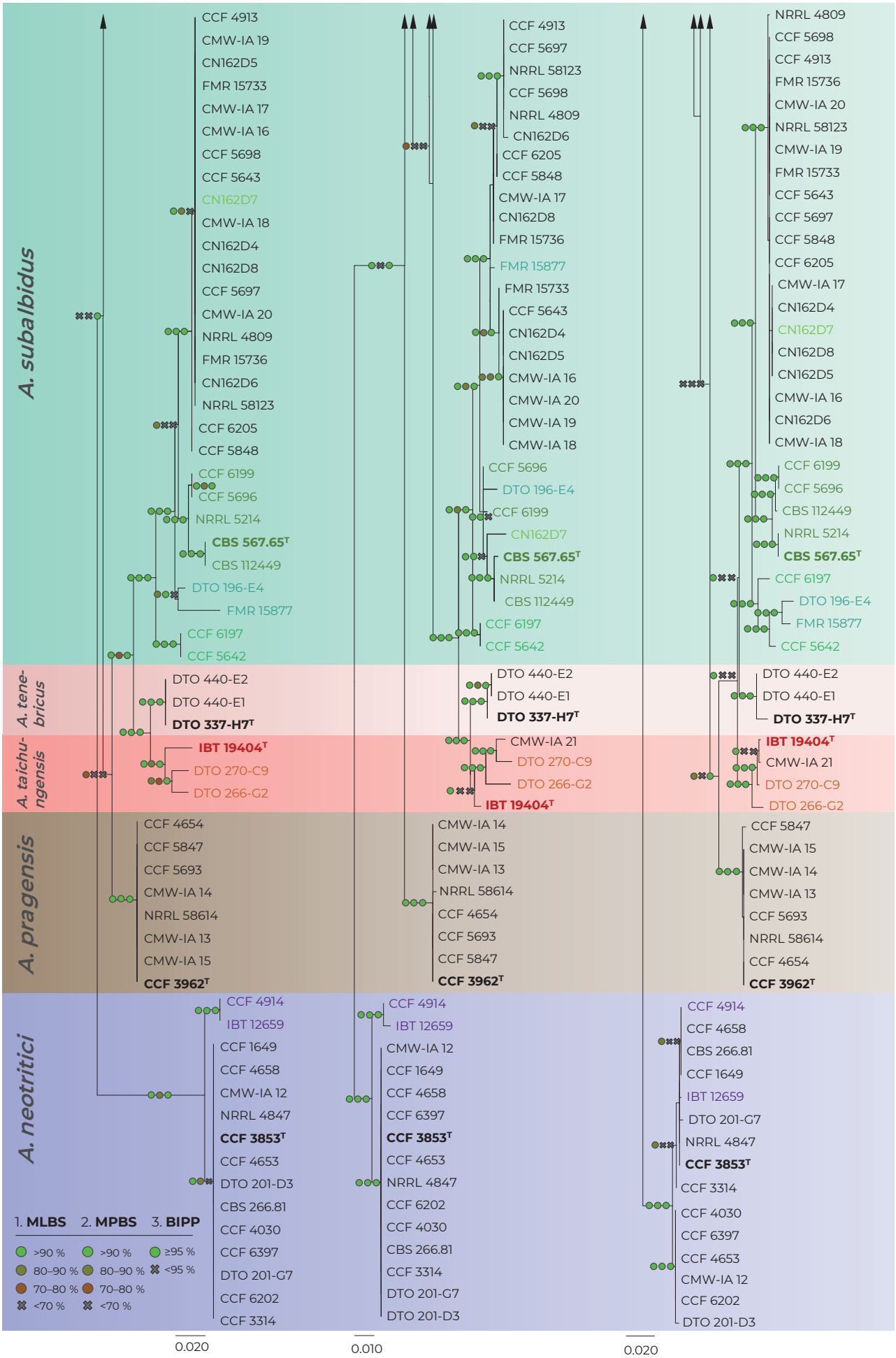

Fig. 2. (Continued).

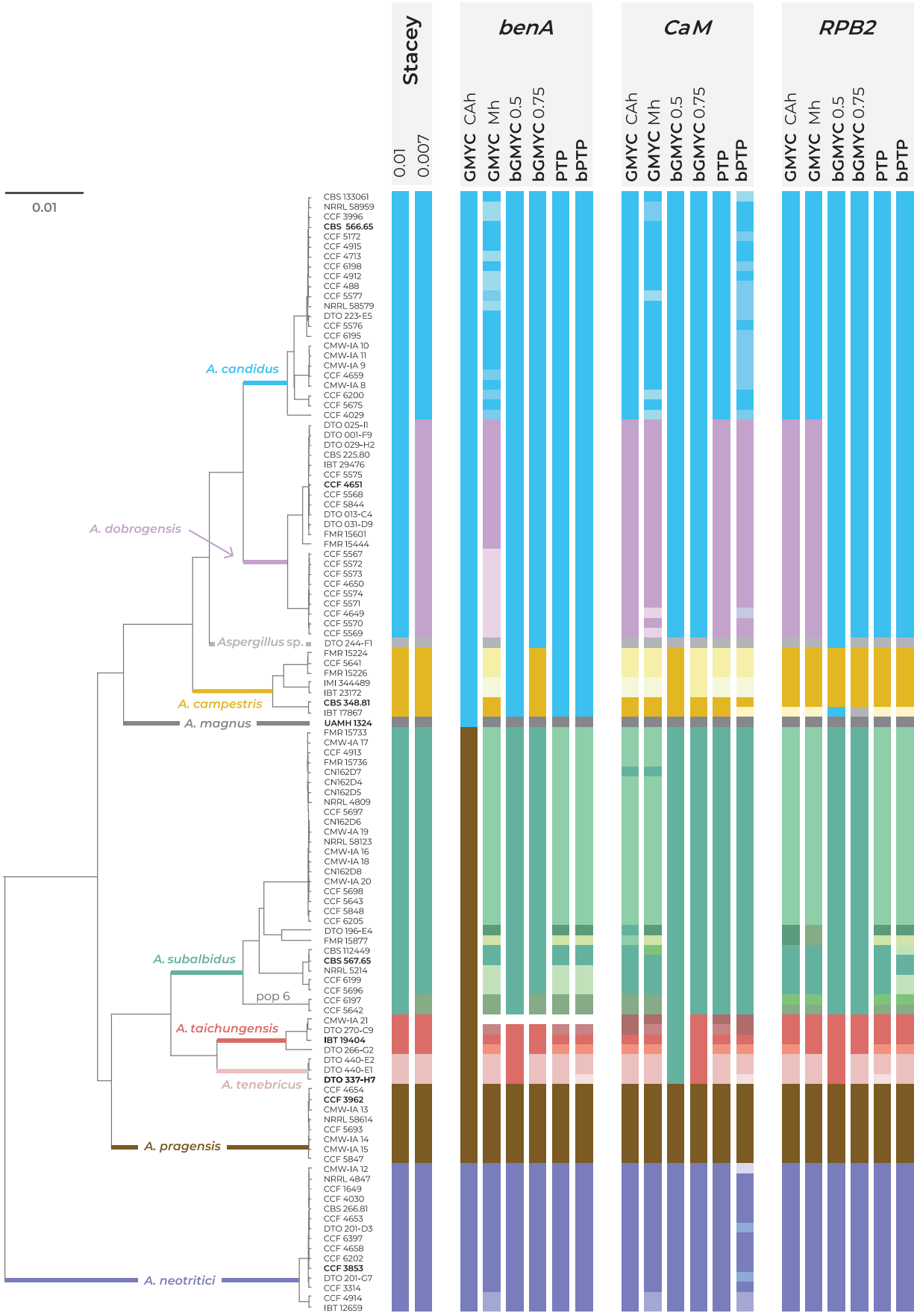

Fig. 3. Schematic representation of results of species delimitation methods in the section *Candidi*. One multi-locus method (STACEY) and five single-locus methods (GMYC, bGMYC, PTP, bPTP) were applied on dataset of three loci (*benA*, *CaM*, *RPB2*). The results are depicted by coloured bars with different colours or shades indicating tentative species delimited by specific method and setting. Ex-type isolates of accepted species are highlighted with bold print. STACEY results with two values of *collapseheight* parameter, 0.01 and 0.007, are shown. For the GMYC method, the Coalescent Constant Population tree model was used as an input with both common ancestor heights (CAh) and Median heights (Mh) settings. For the bGMYC method, values 0.5 and 0.75 were used for the *bgmyc.point* function. The phylogenetic tree was calculated in starBEAST analysis and it is used solely for the comprehensive presentation of the results from different methods.

Aspergillus pragensis received clear support because this lineage contained little intra-species variation and it is well separated from other species in all phylogenies. The GCPSR approach also clearly supported delimitation of *A. tenebricus* and its sister species *A. taichungensis*. There are some incongruences within the *A. taichungensis* lineage not allowing this species to be defined other than in the form of four strains (IBT 19404, DTO 266-G2, DTO 270-C9 and genetically invariable CMW-IA 21). Significant incongruences can be found in the robust and structured lineage of *A. subalbidus.* GCPSR approach supports segregation of basal clade with strains CCF 5642 and CCF 6197 (referred to as population "pop 6" according to the DELINEATE analysis – see below) from *A. subalbidus*. Speciafically, segregation of this PS is supported by *benA*, *CaM* and combined phylogenies but not by *RPB2* phylogeny (Figs 1–2).

All species belonging to the section *Candidi* are biseriate, however, within the lineage of *A. neotritici*, there is a subclade with two uniseriate strains CCF 4914 and IBT 12659 (no biseriate conidiophores observed) which is supported by *benA*, *CaM* and combined phylogenies but not by *RPB2* (Figs 1–2). Although GCPSR supported segregation of this subclade from *A. neotritici*, MSC methods preferred a broad concept of *A. neotritici* (see below).

Singleton lineages with unstable phylogenetic position, namely, *Aspergillus* sp. DTO 244-F1 and UAMH 1324 (*A. magnus*), were excluded from evaluation using GCPSR because it is not possible to evaluate potential discordant positions of similar isolates across genealogies. On the other hand, both strains formed their own singleton lineages in all single-gene and multigene trees.

Species delimitation using STACEY

Detailed results of the multi-locus method STACEY are shown in Fig. 4 where subfigure A illustrates the effect of the *collapseheight* parameter value on the number of delimited species. This *collapseheight* parameter is plotted on the x-axis while on the left y-axis, there is a number of delimited species with the given *collapseheight* value (black line). The support for the most probable scenario (red line), and the second most probable scenario (turquoise line) are shown; other less supported scenarios are omitted. The changing value o the *collapseheight* parameter has consequences especially for the delimitation of *A. dobrogensis*, *A. candidus*, and species in the clade containing *A. subalbidus*, *A. taichungensis* and *A. tenebricus*. There are two main scenarios which gained reasonable support, *i.e.*, with 9 and 11 delimited species (Fig. 4A). The vertical dashed lines in subfigure A represent these scenarios illustrated in detail in subfigures B (Fig. 4B) in the form of similarity matrices showing posterior probabilities of each pair of isolates being included in the same species.

The scenario with 11 species reached support of approximately 0.4 (y-axis on the right side; maximum is 1) when the *collapseheight* parameter value is around 0.007. In this scenario, *A. dobrogensis*, *A. candidus*, *A. taichungensis* and *A. tenebricus* are delimited as separate species. Strains of *A. subalbidus* are divided into two tentative species – status of the separate species is supported for the clade "pop 6" designated according to the DELINEATE analysis (see below).

In the scenario with 9 species and *collapseheight* parameter value of approximately 0.01, *A. subalbidus* is delimited as a single broad species, while *A. dobrogensis* is merged with *A. candidus*. Both *A. taichungensis* and *A. tenebricus* are still delimited but with lower support. The delimitation support of the other species was stable and with high support in both scenarios (*Aspergillus* sp. DTO 244-F1, *A. campestris*, *A. magnus*, *A. pragensis* and *A. neotritici*).

Delimitation using single-locus MSC methods

There was a high overall agreement across single-locus MSC methods and their different settings on the delimitation of *A. magnus*, *A. pragensis* and *A. neotritici* while for the other species, different methods generated a plethora of possible arrangements (Fig. 3). *Aspergillus pragensis* and *A. magnus* have been consistently defined from other species by all mentioned methods except the GMYC method with Common Ancestor node heights settings (GMYC CAh) based on *benA*. In this setting, *A. magnus* was lumped with *A. candidus*, *A. dobrogensis*, *A. campestris* and *Aspergillus* sp. DTO 244-F1, while *A. pragensis* was lumped with *A. subalbidus*, *A. taichungensis* and *A. tenebricus*. Only three analyses delimited one or more additional species within *A. neotritici* lineage, namely GMYC method with Median node heights setting (GMYC Mh) based on *benA* and *CaM* loci, and bPTP method based on *CaM* locus. All these three analyses agreed on the separation of clade containing uniseriate isolates CCF 4914 and IBT 12659 from *A. neotritici.* Most of the analyses (12/18) also supported delimitation of singleton species *Aspergillus* sp. DTO 244-F1 which is related to *A. candidus*, *A. dobrogensis* and *A. campestris*.

The agreement of the methods on the delimitation and arrangement of the remaining species was much lower. The majority of analyses did not support the delimitation of *A. dobrogensis* from *A. candidus* (Fig. 3). Only seven analyses distinguished *A. candidus* and *A. dobrogensis* or delimited a couple of additional species within these species. Delimitation of *A. campestris* in its broad concept (seven isolates) was only supported by bGMYC with value 0.5 for the *bgmyc.point* function (bGMYC 0.5) based on *CaM* locus and with value 0.75 (bGMYC 0.75) based on *benA* locus. This broad concept is in agreement with results of STACEY with both *collapseheight* parameters. Some analyses based on *benA* locus (PTP, bPTP, GMYC CAh and bGMYC 0.5 methods) lumped *A. campestris* with *A. candidus* and *A. dobrogensis.* All methods based on *CaM* locus except bGMYC 0.5 and also GMYC Mh based on *benA* locus delimited 2–4 species within *A. campestris.* Because the *RPB2* sequence of strain IBT 17867 is atypical and relatively dissimilar from other *A. campestris* isolates, all single-locus methods based on *RPB2* failed to connect this strain with *A. campestris*. This strain was either delimited as a singleton species or it was lumped with *Aspergillus* sp. DTO 244-F1 (bGMYC 0.75) or with the clade containing *A. candidus* and *A. dobrogensis* (bGMYC 0.5).

Aspergillus taichungensis was delimited as a species with four strains (IBT 19404, DTO 270-C9, DTO 266-G2 and CMW-IA 21) by STACEY with both values of the *collapseheight* parameter. This arrangement was only supported by three single-locus methods, namely, bGMYC 0.75 based on *benA* and *RPB2* and GMYC Mh based on *RPB2.* The majority of analyses (10/18) delimited 2–4 species within *A. taichungensis* (Fig. 3). Three analyses merged *A. taichungensis* with *A. tenebricus* and two analyses (bGMYC 0.5 based on *CaM and* GMYC Cah based on *benA*) even merged these species with *A. subalbidus* and/or *A. pragensis*. Similarly to STACEY, most of the analyses (10/18) delimited *A. tenebricus* as a species comprising three strains: DTO 337-H7, DTO 440-E1 and DTO 440-E2. Three analyses supported segregation into two species and the remaining five analyses merged *A. tenebricus* with related species as mentioned above. *Aspergillus subalbidus* was represented by a high number of strains (n = 29) which were structured into several clades and frequently delimited as separate species by single-locus MSC methods. STACEY proposed a broad concept of *A. subalbidus* with 29 or 27 strains, only supporting

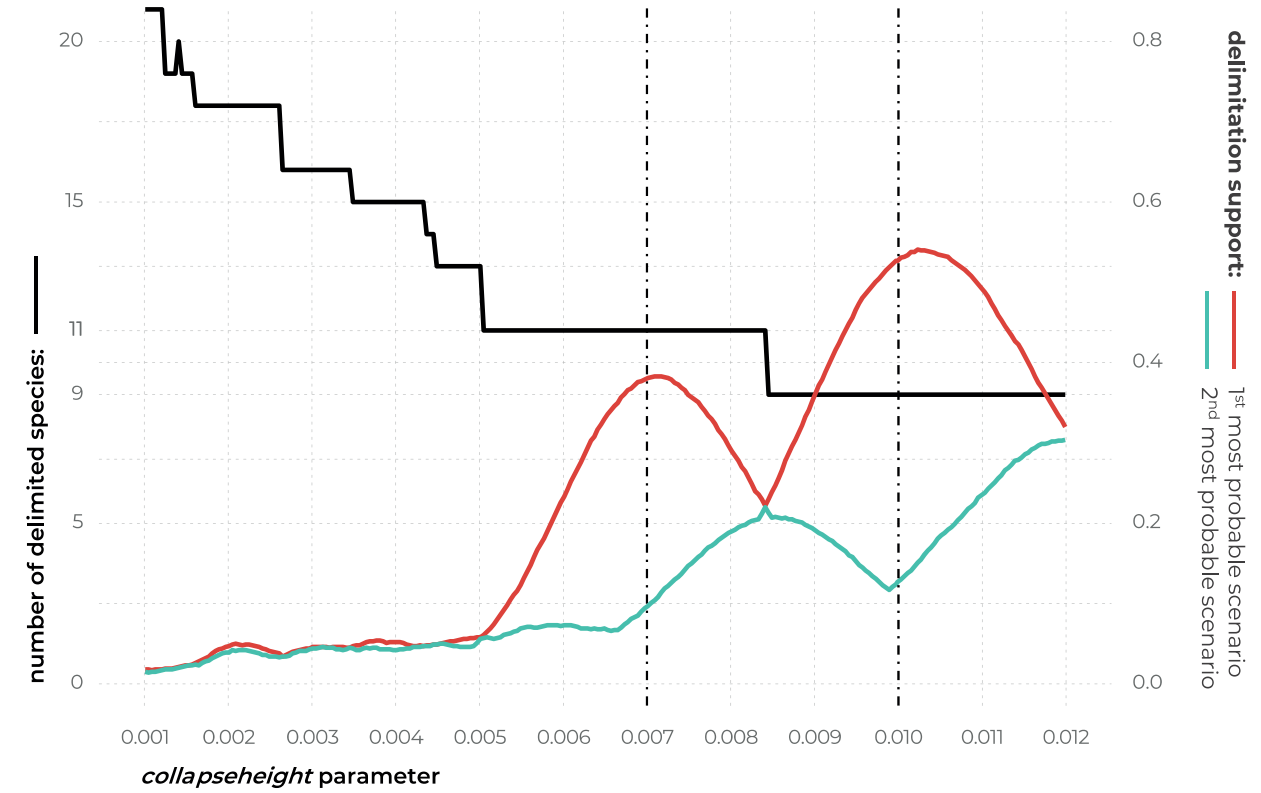

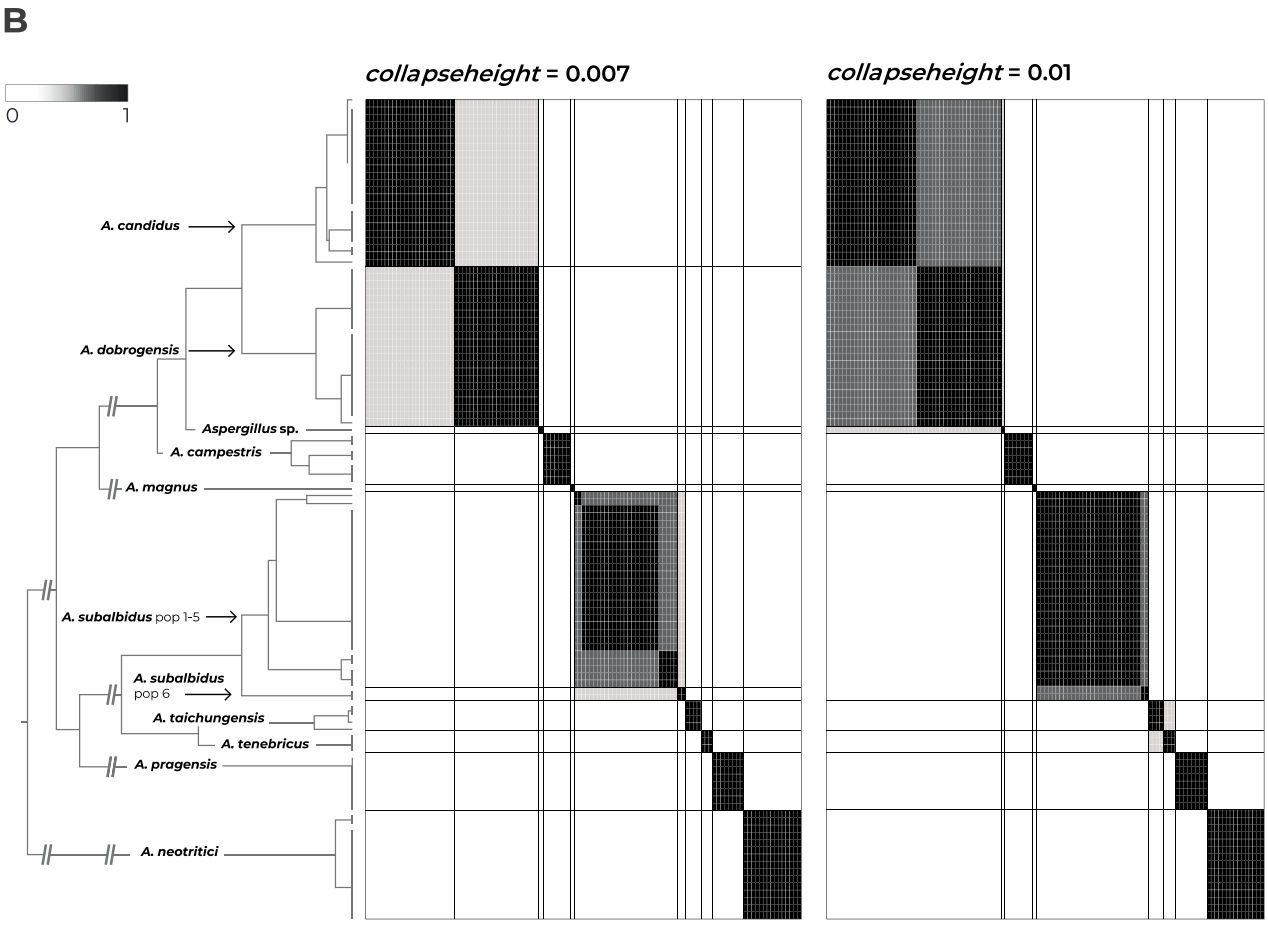

Fig. 4. The results of species delimitation by using STACEY method. **A.** Dependence of delimitation results on *collapseheight* parameter. The black solid line represents the number of delimited species (left y-axis) depending on the changing value of *collapseheight* parameter (x-axis). The red line represents the probability (range from 0 to 1, right y-axis) of the most probable scenario at specific *collapseheight* value. The turquoise line represents the probability of the second most probable scenario at specific *collapseheight* value. Dashed vertical lines mark two values (0.007, 0.01) of *collapseheight* parameter whose results are shown in detail by similarity matrices (subfigure B). **B.** The similarity matrices give the posterior probability of every two isolates belonging to the same multispecies coalescent cluster (tentative species). The darkest black shade corresponds to a posterior probability of 1, while the white colour is equal to 0. Thicker horizontal and vertical lines in the similarity matrices delimit species or their populations that gained delimitation support in some scenarios.

segregation of "pop 6" (see DELINEATE analysis below) in the setting with low *collapseheight* parameter (0.007). This broad concept of *A. subalbidus* was supported by six out of 18 single-locus MSC analyses and the remaining analyses usually segregated "pop 6" (nine out of 18) and/or delimited several additional species with variable arrangements. Two analyses lumped *A. subalbidus* with neighbouring species (Fig. 3).

Phenotypic analysis - macromorphology

All species were able to grow on the four cultivation media (MEA, CYA, CZA, CY20S) at 25 °C. Colony diameters on these media and selected macromorphological characters relevant for the species identification are summarized in Table 4. Almost all species have the largest colony diameter on CY20S compared to the other media with a lower sugar content. *Aspergillus magnus* and *A. pragensis* had the smallest colony diameters and their restricted growth was even more accentuated on CZA.

The overview of macromorphology of all species and their various morphotypes are shown in Fig. 5. Colony morphology of *A. candidus* is very similar to *A. dobrogensis*, but colonies of *A. dobrogensis* strains have a larger diameter on MEA, CYA and CY20S (Table 4). The colony colour of most species in the section *Candidi* is white or yellowish white, but shades of yellow dominate in *A. campestris* (usually yellow to sulphur yellow), *A. magnus* (greyish yellow on MEA, CYA and CY20S) and *A. taichungensis* (pastel yellow on CYA and MEA). Intraspecific variability in colony colour and dimensions is sometimes high. For instance, colonies of *A. campestris*, usually ascribed as yellow, sulphur yellow or bright yellow, were rather white or yellowish-white in FMR 15224. In addition, there were also significant differences in the shape and profile of colonies, production of soluble pigment and reverse colour among strains (Fig. 5), but without any phylogenetic pattern. Another phenotypically variable species was *A. subalbidus* with strains showing significant differences in their colony surfaces, dimensions and colours (Fig. 5). Two strains of *A. subalbidus* (DTO 196-E4 and FMR 15877) differed from other strains by their greyish beige colonies, but otherwise they did not display any other unique characteristics. Neither the other morphological variability observed in *A. subalbidus* displayed any phylogenetic pattern that could lead to considerations of segregation into multiple monophyletic species. Two strains of *A. neotritici* (CCF 4914 and IBT 12659), which formed their own subclade (Fig.1, Fig. 2, Fig. 3), differed from other strains by more velvety colony surface and significantly deviated in micromorphology (see below).

Production of sclerotia was observed in all species (except *A. magnus*), mostly on CZA, CYA and MEA (Table 4). Except A. *dobrogensis*, at least some strains of every species produced soluble pigments after 4 wk of cultivation, most often on CZA and CYA (Table 4). In general, the production of sclerotia and soluble pigments was mostly strain-specific rather than species-specific. But in several species represented by more strains, we observed some trends, and in few cases, production of pigments contributed to the species differentiation. For instance, a dark brown soluble pigment was produced by *A. tenebricus* compared to yellow soluble pigment produced by some strains of *A. taichungensis*. Dark soluble pigments were also produced by all strains of *A. campestris* and *A. pragensis* but with variable intensity and location. In contrast, soluble pigments were observed to be absent in *A. dobrogensis* strains while in the closely related *A. candidus*, five out of nine examined strains produced pigments.

Phenotypic analysis – micromorphology

Dimensions of micromorphological characters are summarized in Table 5 and statistical significances of differences in these characters between species are detailed in Supplementary Table S1. Interesting phenomenon can be seen in *A. neotritici* because some strains of this species produce atypically short and uniseriate conidiophores only (CCF 4914 and IBT 12659) in contrast to other *A. neotritici* isolates and other section *Candidi* species. These strains formed a separate clade in *benA* and *CaM* phylogenies and were delimited as separate species by three single-locus MSC methods. The strain CBS 266.81, a reference strain of invalidly described *A. tritici*, produces atypically short, distorted and septate conidiophores. Colonies of this strain also have a smaller diameter than other *A. neotritici* isolates on all media and the strain produces abundant sclerotia.

Results of the micromorphological analysis show that the most important characters for distinguishing species are the length and width of stipe, vesicle diameter and the length of metulae. In contrast, conidial dimensions are characters that do not contribute to species differentiation (Fig. 6). *Aspergillus magnus* is easily distinguishable from other species. It has the longest and widest stipes, the largest vesicle and the longest metulae. *Aspergillus dobrogensis* has larger dimensions of stipes, vesicles, metulae and phialides compared to the closely related *A. candidus* (Fig. 6). This statement is however valid only for the species as a whole as there are several individual strains not differing from *A. candidus* (Fig. 7). The possibilities of micromorphological differentiation between related species *A. subalbidus*, *A. taichungensis*, *A. tenebricus* and *A. pragensis* are limited. Among these species, *A. tenebricus* typically has longer phialides and metulae. It also has a larger vesicle than *A. taichungensis.* Some phylogenetic methods supported segregation of clade "pop 6" from *A. subalbidus* or segregation of DTO 266-G2 from *A. taichungensis*. We did not observe any specific feature connecting these strains and differentiating them from other *A. subalbidus* strains. The strain DTO 266-G2 also did not show unique characters compared to remaining *A. taichungensis* strains except much weaker production of yellow soluble pigment.

In some species, we observed remarkable differences in individual microscopic characters between strains. For example, in the *A. campestris* lineage, strain IMI 344489 produced larger conidia while strain CBS 348.81 had larger vesicles (Fig. 7). In the *A. subalbidus* lineage, strain DTO 196-E4 produced significantly larger stipes and vesicles, and among *A. neotritici* strains, CCF 4030 had longer metulae and CCF 3853 produced larger conidia (Fig. 7). These phenotypically exceptional strains did not form any well-defined phylogenetic units.

We did not observe any differences in surface ornamentation of conidia between species when using SEM (Fig. 8). Conidia of all species were smooth-walled or occasionally finely roughened.

Physiology

Cardinal temperatures were assessed on MEA at nine different temperatures ranging from 10 to 45 °C. The most common growth patterns are shown in Fig. 9. *Aspergillus neotritici* is the only species which is not able of growing or at least germinating at 10 °C and its optimal growth temperature is around 30 °C, while all other species have optima around 25 °C or do not grow faster at 30 °C compared to 25 °C. At least some strains of four species can grow at 37 °C, namely, *A. neotritici*, *A. subalbidus*, *A. taichungensis* and *A. tenebricus*. All strains of *A. taichungensis* and *A. neotritici*

Table 4. Overview of selected macromorphological characters and growth parameters at 25 °C.

Species (no. of examined strains)	**Colony diameter after 7 d** in mm (mean)				**Colony diameter after 14 d** in mm (mean)				**Colony colours**	**Soluble pigment** (present : absent)[1]	**Sclerotia** (present : absent)[1]
	MEA	**CYA**	**CZA**	**CY20S**	**MEA**	**CYA**	**CZA**	**CY20S**	(CYA and MEA)		
A. campestris (7)	11–17 (15)	14–20 (17)	6–14 (9)	10–21 (18)	16–28 (24)	22–36 (28)	10–20 (16)	25–34 (30)	yellow, sulphur yellow, yellowish white	7 : 0 (CZA > CYA > CY20S)	4 : 3 (CZA, CYA)
A. candidus (9)	12–17 (15)	15–21 (18)	9–15 (11)	16–25 (22)	20–27 (24)	20–32 (27)	16–25 (21)	25–45 (36)	white, white with a yellowish tinge	5 : 4 (CZA > CYA)	5 : 4 (CZA)
A. dobrogensis (10)	17–20 (19)	20–24 (21)	9–14 (10)	18–28 (24)	22–35 (29)	26–39 (32)	17–22 (19)	32–48 (41)	white, white with a yellowish tinge	0 : 10	2 : 8 (CZA > MEA, CYA, CY20S)
A. magnus (1)	12–14 (13)	12–14 (13)	4–6 (5)	13–15 (14)	20–22 (21)	16–17 (17)	11–13 (12)	19–20 (20)	pale yellow, yellowish gray	1 : 0 (CYA)	0 : 1
A. neotritici (11)	10–25 (18)	14–28 (22)	5–19 (12)	19–31 (27)	20–47 (31)	21–50 (38)	14–39 (25)	28–60 (51)	white, yellowish white	6 : 5 (CZA)	4 : 7 (CZA)
A. pragensis (5)	8–10 (9)	9–14 (12)	3–6 (5)	13–18 (15)	15–18 (16)	16–22 (20)	11–15 (12)	24–30 (27)	white	5 : 0 (CZA, CYA)	2 : 3 (CYA > MEA)
A. subalbidus (19)	11–17 (14)	14–24 (20)	8–18 (13)	18–27 (22)	18–30 (24)	24–42 (32)	16–26 (21)	24–45 (33)	white, yellowish white	12 : 7 (CYA > CZA)	7 : 12 (CZA > CYA > MEA > CY20S)
A. taichungensis (3)	16–18 (17)	22–28 (25)	10–12 (11)	28–31 (30)	25–29 (27)	33–43 (38)	19–21 (20)	40–51 (46)	pastel yellow	2 : 1 (CYA, MEA)	2 : 1 (CZA, CY20S)
A. tenebricus (3)	19–21 (20)	19–23 (21)	12–14 (13)	28–30 (29)	26–33 (30)	29–34 (31)	22–24 (23)	48–52 (50)	white, yellowish white	3 : 0 (CYA, CZA)	2 : 1 (CZA)

[1]Production was scored after 4 wk of cultivation on MEA, CYA, CZA and CY20S; the ratio shows the number of strains producing and not producing pigment/sclerotia; media on which pigment or slerotia were produced, are listed in the parentheses and sorted by frequency. See section Taxonomy for more details concerning colours of soluble pigments and sclerotia, and strain numbers..

grow or germinate at 40 °C (Fig. 10). An unusually wide variability was observed in the temperature maximum of *A. campestris*. Some strains of this species do not grow at 30 °C (IBT 17867, IBT 23172), while all others grow well at this temperature, and the ex-type strain (CBS 348.81) grows up to 35 °C. Similarly, only some strains (CBS 567.65, FMR 15736, NRRL 58123, FMR 15733, CCF 5643, NRRL 4809, CCF 5697, CCF 6197) of *A. subalbidus* were able to grow at 35 °C and only some strains of *A. subalbidus* (CCF 5643, CCF 5697, FMR 15733) and *A. tenebricus* (DTO 337-H7, DTO 440-E2) could grow at 37 °C (Table 6, Fig. 9, Fig. 10).

Species delimitation using DELINEATE software

The species hypotheses were independently tested in DELINEATE software where we set up nine different models. The results are summarized in Fig. 11. Individual populations were either assigned into species according to the previous results of species delimitation (Supplementary Table S2) - grey coloured bars, or they were left unassigned and free to be delimited - brown coloured bars. The red frames show the resulting solution proposed by DELINEATE for every model.

The first model left all populations of *A. candidus*, *A. dobrogensis*, *A. campestris*, *A. magnus* and *Aspergillus* sp. DTO 244-F1 unassigned and the other species were defined as follows: all populations of *A. subalbidus* formed one species (including "pop 6"), *A. taichungensis* was merged with *A. tenebricus*. In this setting, unassigned populations were divided into two species: *A. magnus* and a broad species comprising all other species (*A. candidus* + *A. dobrogensis* + *A. campestris* + *Aspergillus* sp. DTO 244-F1). The second model differed from the first by predefined species status of *A. magnus,* and also *A. tenebricus* was separated from *A. taichungensis*. In this setting, *A. campestris* and *Aspergillus* sp. DTO 244-F1 were recognized as a separate species, while *A. candidus* and *A. dobrogensis* remained lumped together. The third model differed from the second by predefined species status for subpopulation "pop 6" of *A. subalbidus*. When "pop 6" was separated, *A. candidus* and *A. dobrogensis* were supported as separate species in contrast to model 2. In the fourth model, populations of *A. dobrogensis*, *Aspergillus* sp. DTO 244-F1, *A. subalbidus*, *A. taichungensis* and *A. tenebricus* were left unassigned and other species were determined within their usual boundaries. This model resulted in recognizing *A. subalbidus* as a single species, *A. tenebricus* was divided from *A. taichungensis*, and *A. dobrogensis* was lumped together with *A. candidus*.

The remaining models focused on the clade containing *A. subalbidus*, *A. taichungensis* and *A. tenebricus*. In all models, there was a predefined species status for *A. dobrogensis* and all other species in their usual boundaries. In the fifth model, all populations of *A. subalbidus*, *A. taichungensis* and *A. tenebricus* were left free to be delimited. In this setting *A. subalbidus* "pop 6" was segregated from *A. subalbidus*, *A. tenebricus* was segregated from *A. taichungensis*, and *A. taichungensis* was divided into two species. The populations of *A. taichungensis* and *A.*

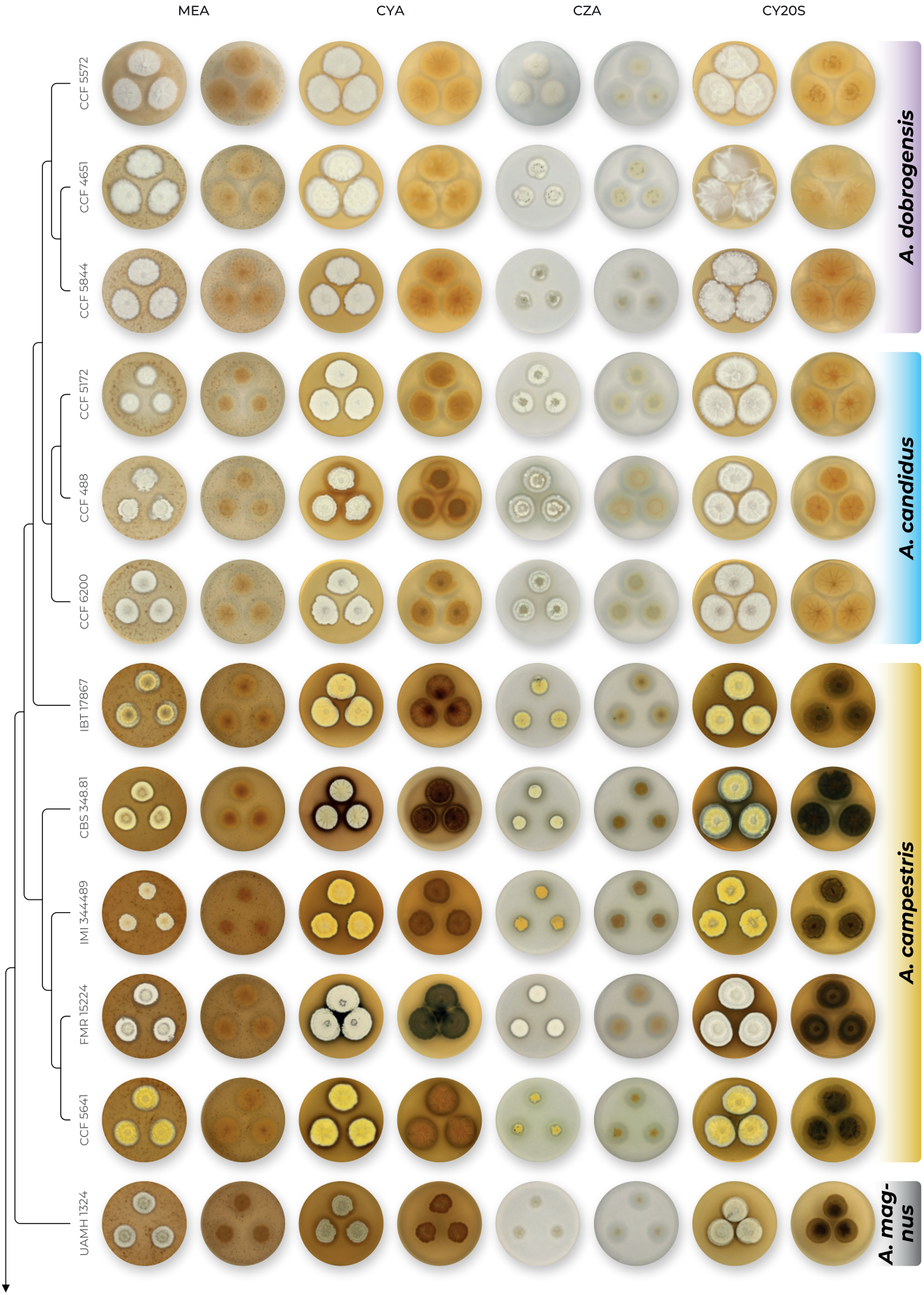

Fig. 5. Overview of macromorphological patterns (obverse and reverse) within section *Candidi* on four cultivation media (MEA, CYA, CZ, CY20S) grown for 14 d at 25 °C. Macromorphological characters were scored in detail for 68 isolates and only unique phenotypic patterns are shown for every species.

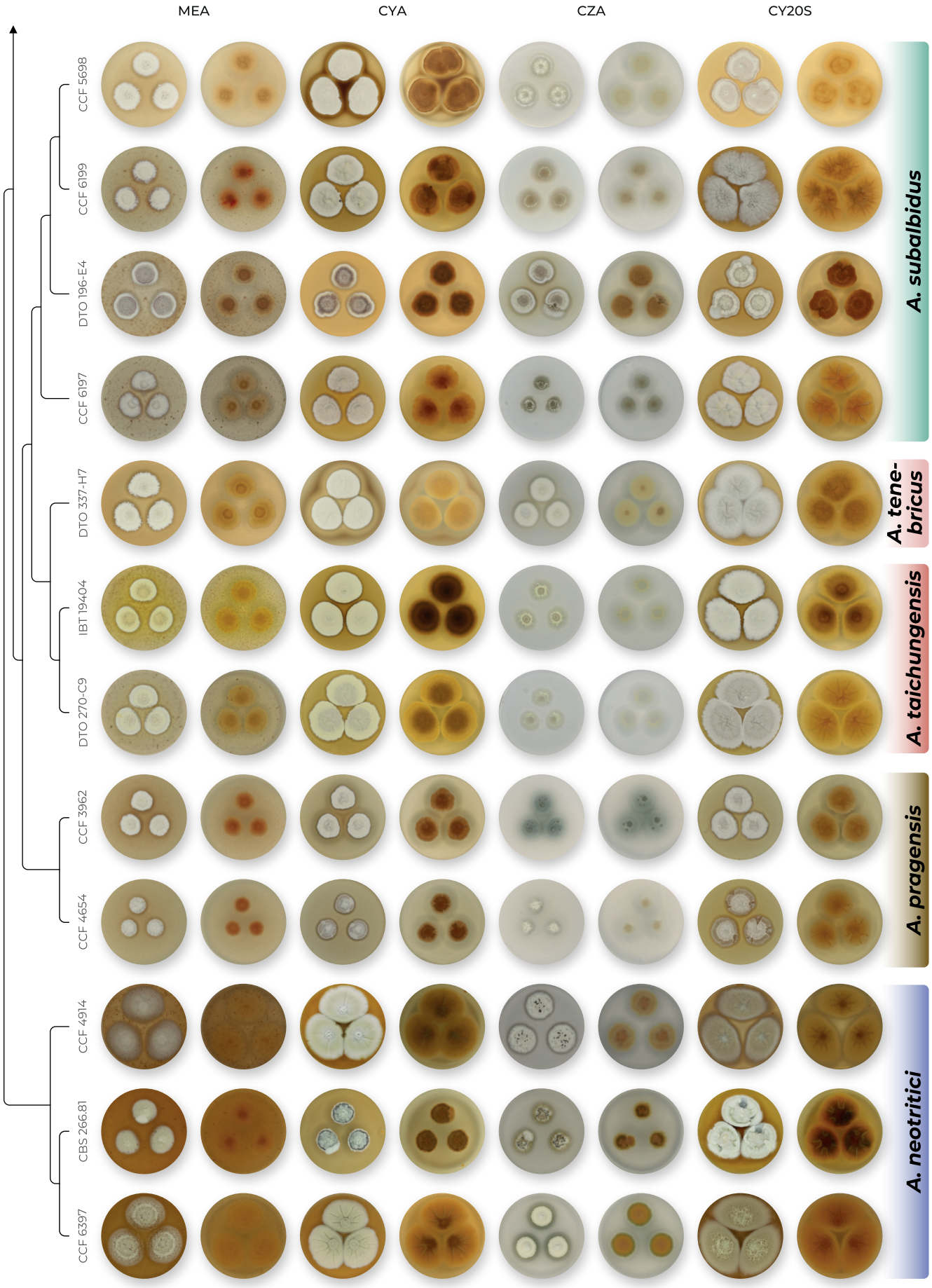

Fig. 5. (Continued).

tenebricus were the only unassigned populations in the sixth and seventh model. *Aspergillus subalbidus* was predefined as one (model 6) or two species (model 7) with "pop 6" treated as separate species. In both cases, *A. tenebricus* was recognized as a separate species, while *A. taichungensis* was divided into two species in the seventh model. In the last two models, only populations of *A. subalbidus* were left free to be delimited. In the eighth model, *A. subalbidus* was recognized as a single species in the situation when *A. taichungensis* and *A. tenebricus* were predefined as one species. By contrast, when *A. taichungensis* and *A. tenebricus* were predefined as separate species, population "*A. subalbidus* pop 6" was segregated from *A. subalbidus*.

Ecology

To analyse distribution and substrate preferences of section *Candidi* members, we downloaded all sequences of *benA*, *CaM* and *RPB2* and associated data from GenBank (accessed on 20 February 2022) (Supplementary Table S3) and analysed them together with sequences listed in Table 1. Then we constructed a combined tree (Supplementary Fig. S1), determined probable species limits and visualized ecological data (Fig. 12). Although there are many other records on the occurrence of section *Candidi* members in literature, we restricted our focus to data with identification verified by DNA sequencing of variable loci.

Eight from nine species (except *A. tenebricus*) have been found in North America from where we gathered 52 records (Supplementary Table S3), followed by Europe with 51 records representing seven species (except *A. magnus* and *A. tenebricus*). *Aspergillus neotritici* and *A. subalbidus* were the most geographically widespread species in our dataset occurring on five continents each.

The most common and diverse habitat for section *Candidi* is the indoor environment, where seven out of nine species were found (55 records), and only *A. magnus* and *A. tenebricus* were missing. Four species, *A. dobrogensis*, *A. candidus*, *A. subalbidus* and *A. taichungensis* have been isolated from caves (28 records). Food-borne species (19 records) comprised *A. neotritici*, *A. candidus*, *A. subalbidus*, *A. pragensis* and *A. taichungensis*. Four species are known as coprophilous (14 records), namely, *A. campestris*, *A. candidus, A. dobrogensis* and *A. subalbidus*. Clinical isolates (14 records) mostly belonged to *A. neotritici* (eight records) and

Table 5. Overview of micromorphological characters[1,2].

Species (no. of examined strains)	**Stipe**		**Metulae length;**	**Phialides length;**	**Vesicle diam;**	**Conidia (longer dimension);**
	Length; mean ± sd	**Width; mean ± sd**	**mean ± sd**	**mean ± sd**	**mean ± sd**	**mean ± sd**
A. campestris (7)	(90–)250–850(–1 300);	(4–)5–7.5(–9);	(7–)8–14(–17);	(4.5–)5–7(–9);	(10.5–)14–22(–31.5);	(2.8–)3–4.5(–4.9);
	507 ± 217.5	5.9 ± 1.1	10.1 ± 2.3	5.9 ± 0.8	17.1 ± 3.7	3.8 ± 0.5
A. candidus (9)	(70–)125–400(–520);	(2.5–)3.5–8.5(–9.5);	(4.5–)5.5–7.5(–8);	(4.5–)5–6.5(–7);	(8–)10–23(–33);	(3.1–)3.3–4(–4.3);
	242 ± 101.5	4.9 ± 1.6	6 ± 0.7	5.6 ± 0.5	14.7 ± 5.0	3.7 ± 0.2
A. dobrogensis (10)	(100–)150–1 150(–2 000);	(3–)5–7(–14);	(5–)5.5–12(–14);	(5–)5.5–7.5(–8.5);	(9–)10–30(–39.5);	(3–)3.4–4.1(–4.3);
	609 ± 330.2	6.2 ± 1.5	8.4 ± 1.9	6.4 ± 0.7	19.6 ± 5.6	3.7 ± 0.3
A. magnus (1)	(540–)810–1 150(–1 600);	(6–)9–13(–16);	(7.5–)9–14(–17);	(4.5–)5.5–7(–8);	(18–)33–49(–45);	(3.2–)3.4–3.6(–3.8);
	945 ± 225.8	11.2 ± 2.4	12.1 ± 2.8	6.1 ± 0.8	34.8 ± 8.0	3.5 ± 0.2
A. neotritici (9)	(140–)250–500(–700);	(3.5–)4–8(–9);	(4–)7–17(–21);	(2.5–)3.5–6(–8);	(11–)14–24(–28);	(2.6–)3–4.6(–5.1);
	363 ± 109.7[3]	6.1 ± 1.0[3]	9.9 ± 3.3[3]	4.5 ± 0.9	18.4 ± 3.7[3]	3.5 ± 0.5
A. pragensis (5)	(40–)110–260(–380);	(3–)3.5–5(–6);	(4–)5–6.5(–8);	(4–)5–6(–6.5);	(7–)10–17(–23);	(3.1–)3.5–4(–4.6);
	175 ± 82.1	4.3 ± 0.6	5.7 ± 0.8	5.3 ± 0.4	13.6 ± 3.1	3.7 ± 0.3
A. subalbidus (19)	(20–)50–330(–730);	(2.5–)3–8(–10);	(4–)6–11(–16.5);	(3.5–)4.5–6(–7.5);	(5–)7–23(–31);	(3–)3.2–4.2(–4.5);
	136 ± 91.0	4.2 ± 1.3	7.4 ± 1.5	5.4 ± 0.6	11.8 ± 4.7	3.7 ± 0.3
A. taichungensis (3)	(15–)40–90(–215);	(2–)3–4(–5);	(4–)5.5–7(–9.5);	(3.5–)4.5–6.5(–7.5);	(5–)7–11(–15);	(2.8–)3–3.8(–4.1);
	60 ± 31.4	3.3 ± 0.7	6.2 ± 0.8	5.0 ± 0.5	8.2 ± 2.0	3.4 ± 0.3
A. tenebricus (3)	(30–)80–140(–310);	(2.5–)3.5–5(–6.5);	(7–)8–12(–14);	(5.5–)6–7(–8.5);	(8.5–)11–18(–27);	(3.4–)3.6–3.9(–4.3);
	114 ± 57.9	4.2 ± 0.8	9.9 ± 1.3	6.7 ± 0.7	14.3 ± 3.4	3.8 ± 0.2

[1]Measured after 1–3 wk of cultivation on MEA at 25 °C.

[2]Statistical comparison of micromorphological characters between species is listed in Supplementary Table 1.

[3]Strains CCF 4914, IBT 12659 and CBS 266.81 were excluded because they produced short, uniseriate or atypical conidiophores.

the remaining strains were *A. pragensis*, *A. dobrogensis* and *A. candidus*. Five species (12 records) have been found in soil, *i.e.*, *A. candidus*, *A. campestris*, *A. subalbidus*, *A. neotritici*, *A. taichungensis* and *A. tenebricus*. Strains from outdoor air were poorly represented in our dataset and were restricted to *A. neotritici* and *A. pragensis*.

Our set of strains included many from less usual substrates (scored as "other") like vermicompost, tunnels of bark beetles, metal duct, egg-mass, barn litter and the newly described species, *A. magnus*, that was isolated from a mouse.

Based on the number of strains included in this study and number of sequences deposited in GenBank, *A. candidus* and *A. subalbidus* seem to be the most encountered species. None of the species which were represented by a high number of strains seem to be substrate-specific or geographically restricted.

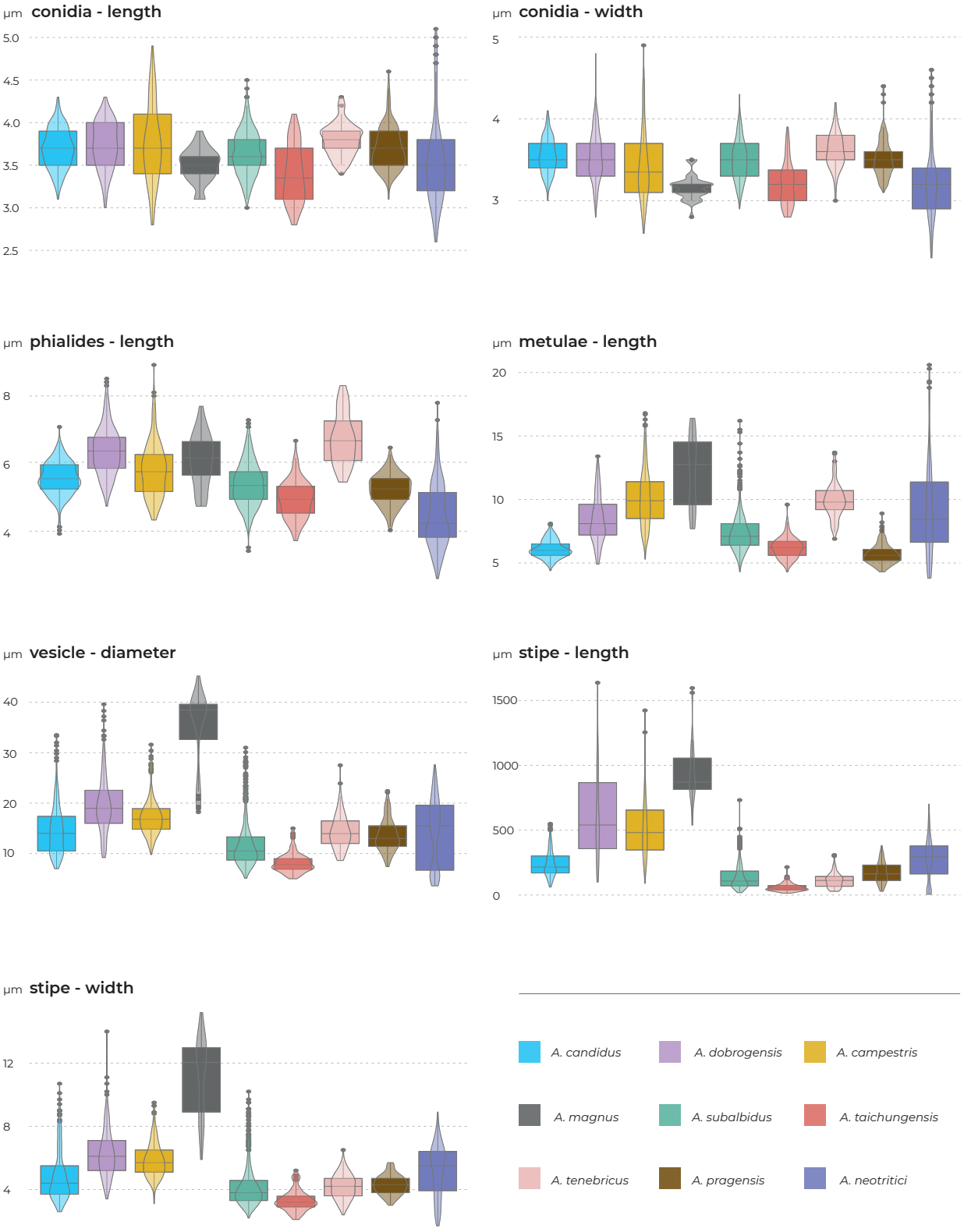

Fig. 6. Summary overview of seven micromorphological characters across species of section *Candidi*. Boxplots show median, interquartile range, values within ± 1.5 of interquartile range (whiskers) and outliers.

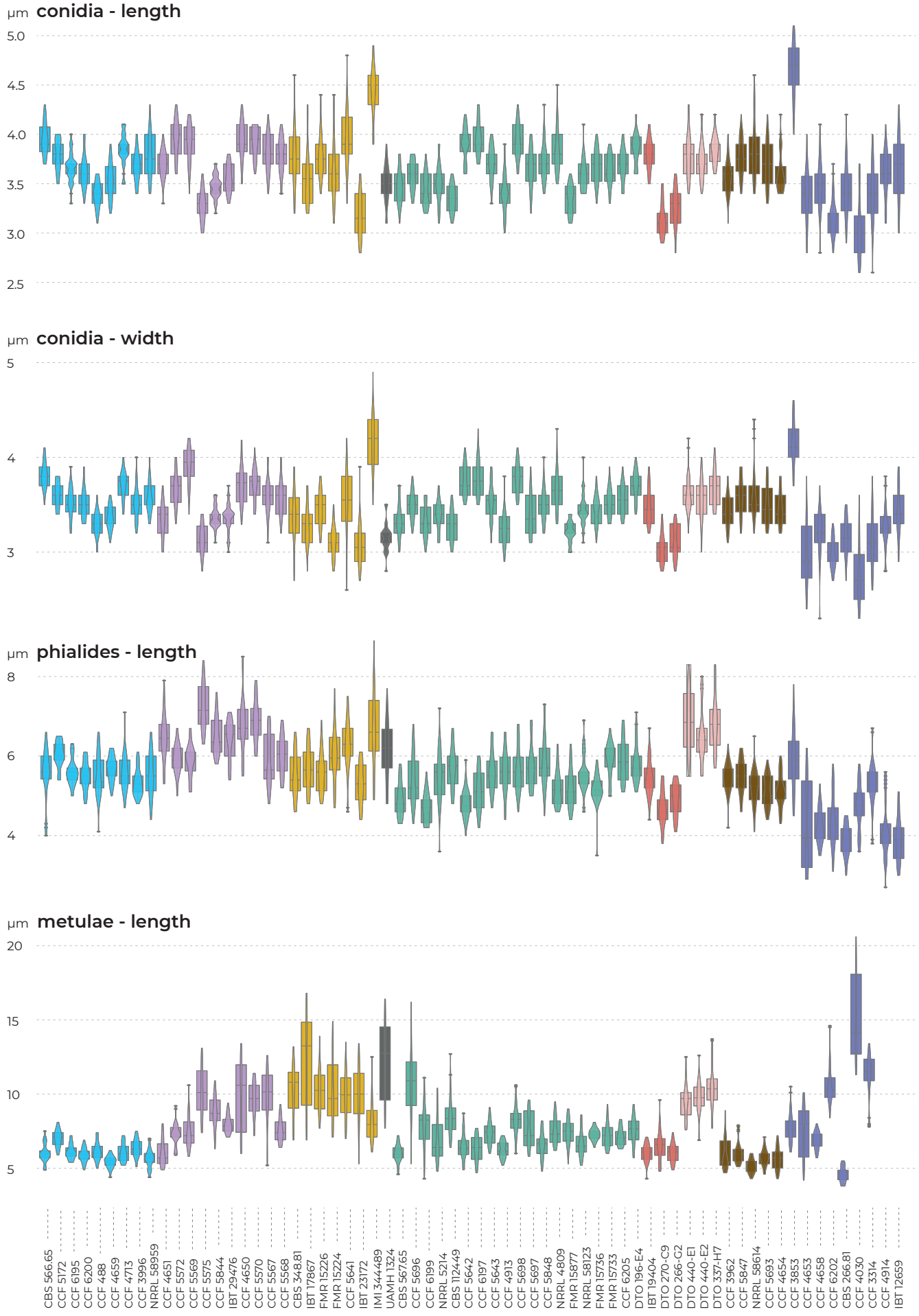

Fig. 7. A detailed overview of seven micromorphological characters at a strain level. Boxplots show median, interquartile range, values within ± 1.5 of interquartile range (whiskers) and outliers.

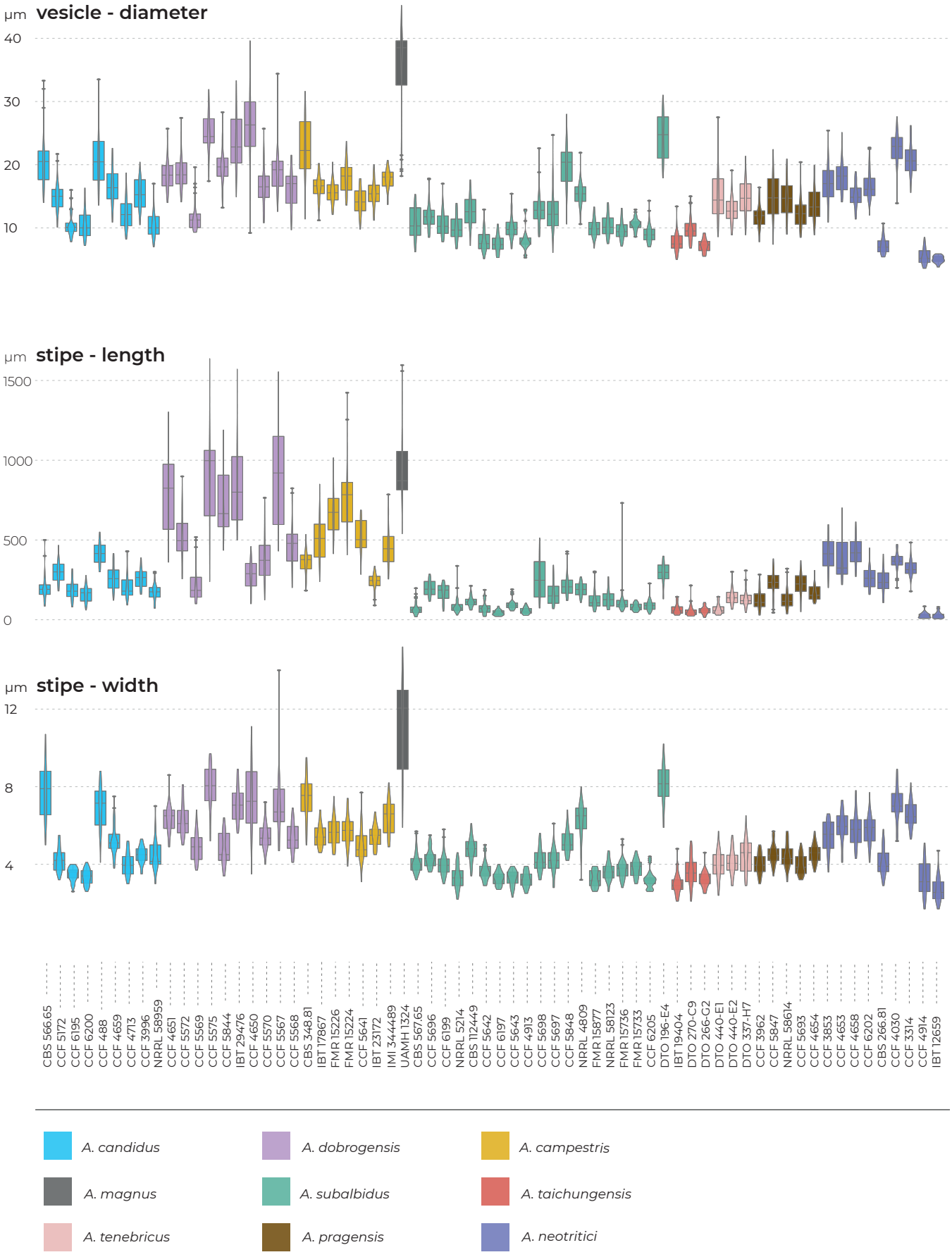

Fig. 7. (Continued).

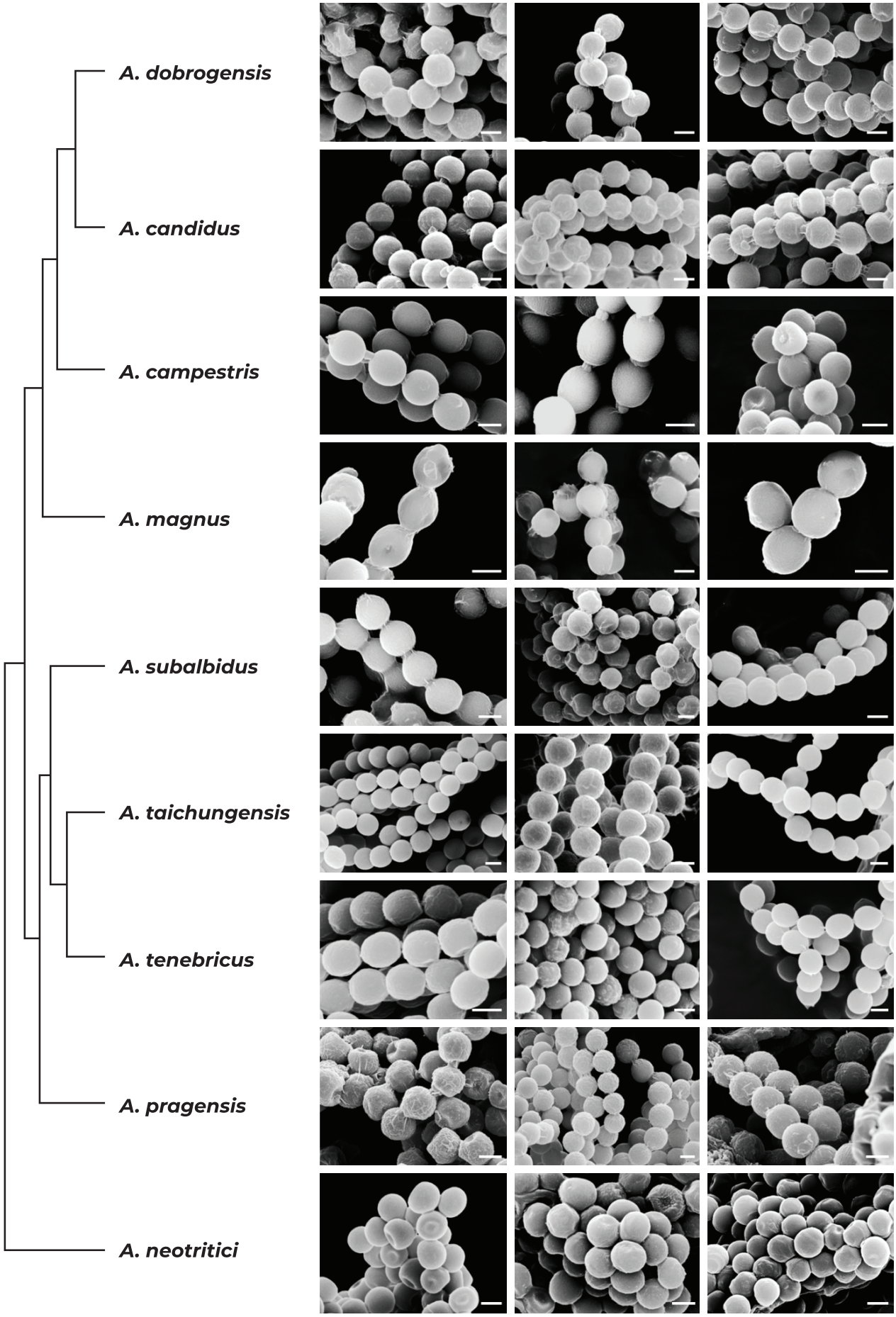

Fig. 8. Conidia under scanning electron microscopy (SEM). Examined strains from left to right: *A. dobrogensis* - CCF 4649, IBT 29476, IBT 29476; *A. candidus* - CCF 3996, CBS 566.65, CCF 3996; *A. campestris* - FMR 15224, FMR 15226, IBT 23172; *A. magnus* - UAMH 1324 only; *A. subalbidus* - FMR 15877, CBS 122449, CCF 5643; *A. taichungensis* - DTO 266-G2 only; *A. tenebricus* - DTO 440-E1, DTO 337-H7, DTO 337-H7; *A. pragensis* - CCF 4654, CCF 3962, CCF 4654; *A. neotritici* - CCF 4653, CBS 266.81, IBT 12659. Scale bars = 2 µm.

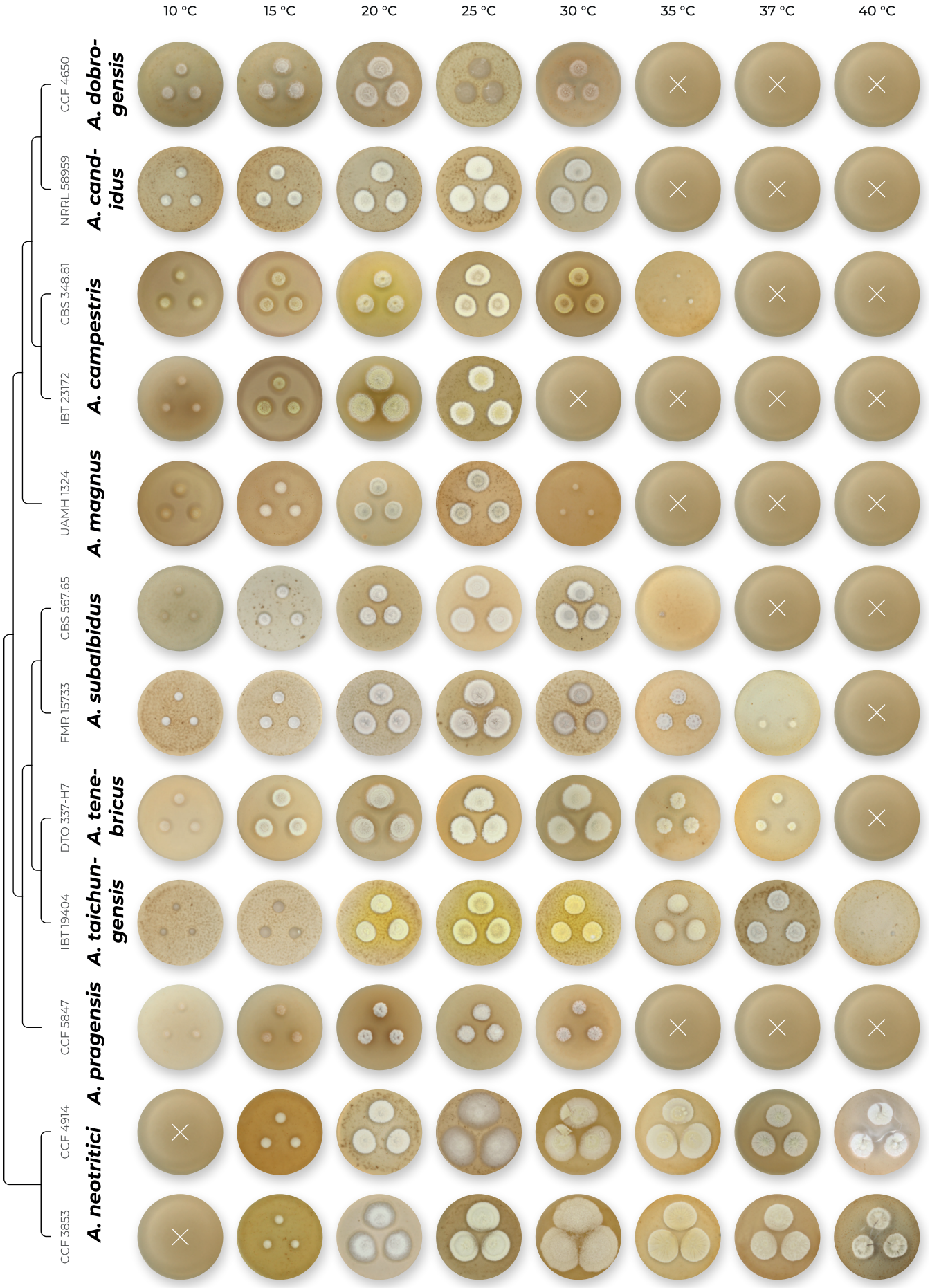

Fig. 9. Temperature growth profiles of *Aspergillus* section *Candidi* members after 14 d on MEA at temperatures ranging from 10 °C to 40 °C. Physiological characters were scored in detail for 52 isolates and only predominant patterns are shown for every species. For details, see Table 6 and section Taxonomy.

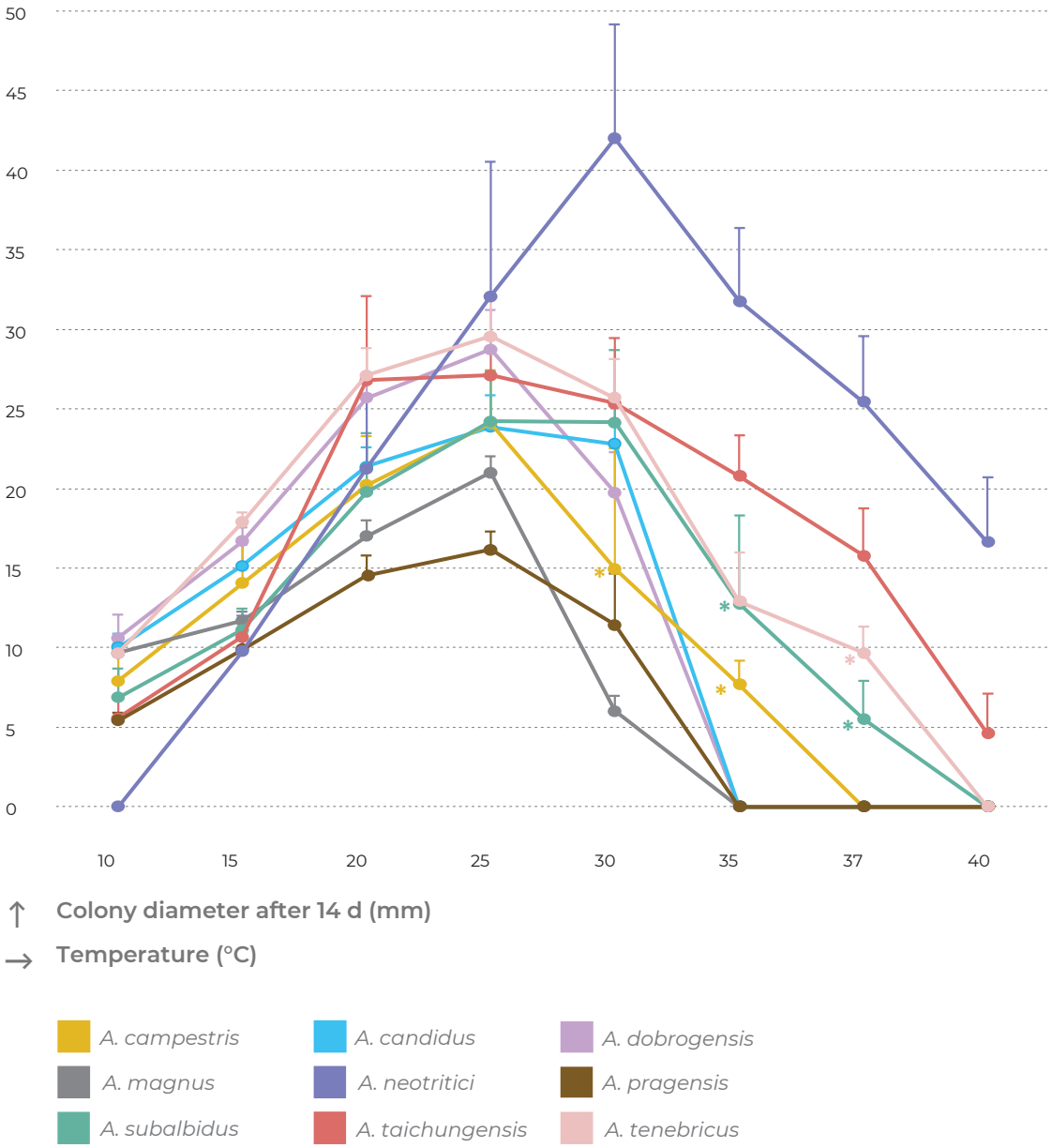

Fig. 10. Growth of section *Candidi* members after 14 d on MEA at temperatures ranging from 10 °C to 40 °C. The points on the curves show the mean values and standard deviations. When isolates of the same species differed in their maximum growth temperatures, zero values were omitted for calculation of mean values (these points are designated by asterisks).

Table 6. Overview of growth parameters at different temperatures.

Species (no. of examined strains)	**Colony diameter after 14 d of cultivation on MEA in mm (mean value)**							
	10 °C	**15 °C**	**20 °C**	**25 °C**	**30 °C**	**35 °C**	**37 °C**	**40 °C**
A. campestris (7)	4–10 (8)	10–17 (14)	15–26 (20)	16–28 (24)	0–22 (18)[1]	0–4 (3)[1]	—	—
A. candidus (5)	8–11 (10)	12–17 (15)	20–23 (21)	20–27 (24)	18–25 (23)	—	—	—
A. dobrogensis (6)	9–13 (11)	15–18 (17)	24–27 (26)	23–32 (29)	17–24 (20)	—	—	—
A. magnus (1)	9–10 (10)	11–12 (12)	16–18 (17)	20–22 (21)	5–7 (6)	—	—	—
A. neotritici (6)	—	4–13 (10)	11–26 (21)	23–47 (32)	32–51 (42)	30–42 (32)	18–33 (25)	4–22 (17)
A. pragensis (5)	5–6 (5)	9–11 (10)	13–17 (15)	15–18 (16)	3–14 (11)	—	—	—
A. subalbidus (16)	3–9 (7)	9–14 (11)	15–30 (20)	18–30 (24)	9–29 (24)	0–22 (13)[1]	0–9 (6)[1]	—
A. taichungensis (3)	4–7 (6)	9–12 (11)	20–32 (27)	25–29 (27)	20–29 (25)	18–25 (21)	12–20 (16)	1–7 (5)
A. tenebricus (3)	9–11 (10)	17–19 (18)	25–29 (27)	26–33 (30)	22–29 (26)	8–16 (13)	0–12 (10)[1]	—

[1]The mean was calculated from non-zero values only.

— no growth.

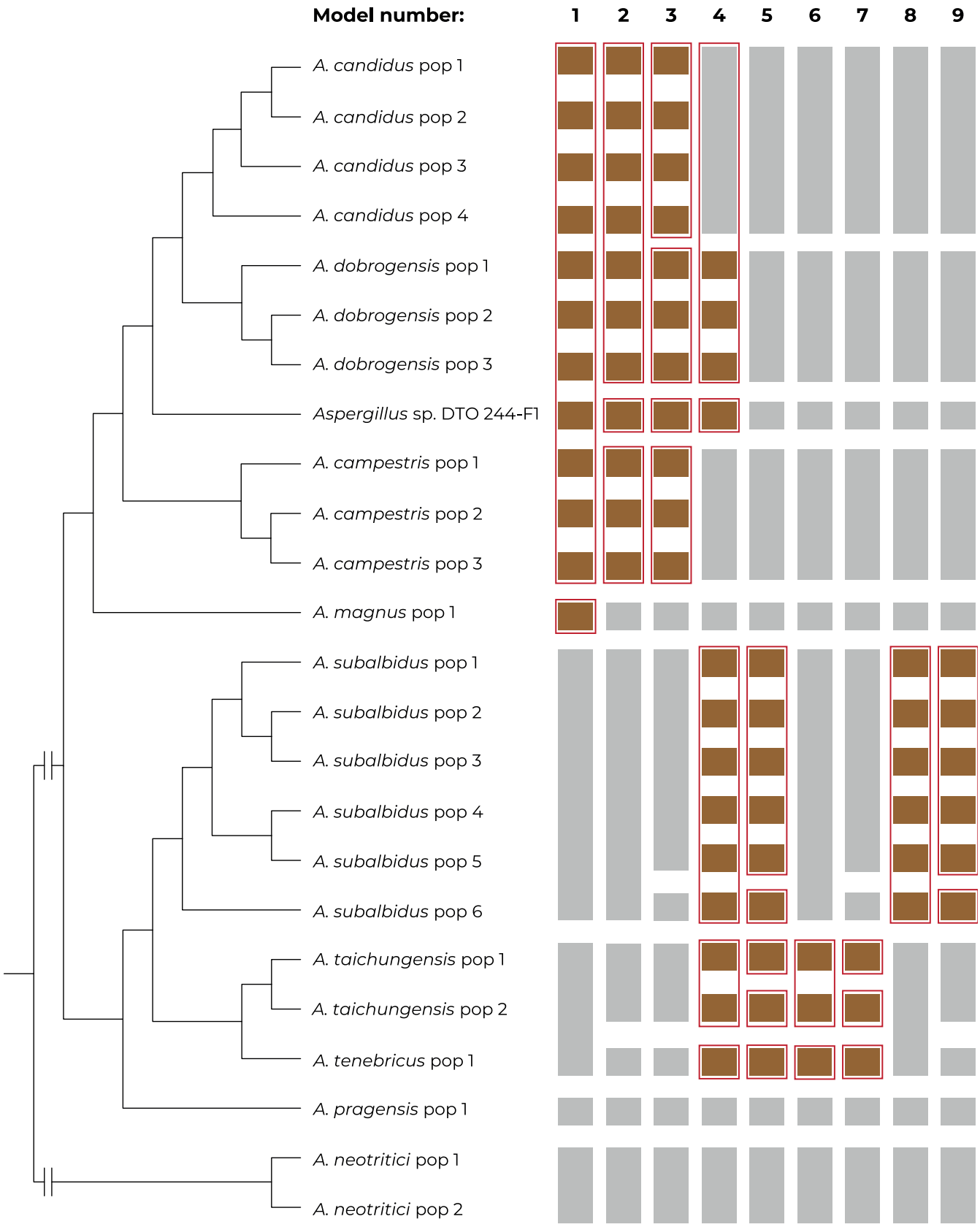

Fig. 11. The results of species validation using the software DELINEATE. Nine models of species boundaries were set up and tested. The brown bars represent unassigned populations left free to be delimited, while the grey bars represent the predefined species. The resulting solutions suggested by DELINEATE are depicted by red frames around bars. The populations of each species were delimited by BPP software (Supplementary Table S2) and the displayed tree was calculated in starBEAST.

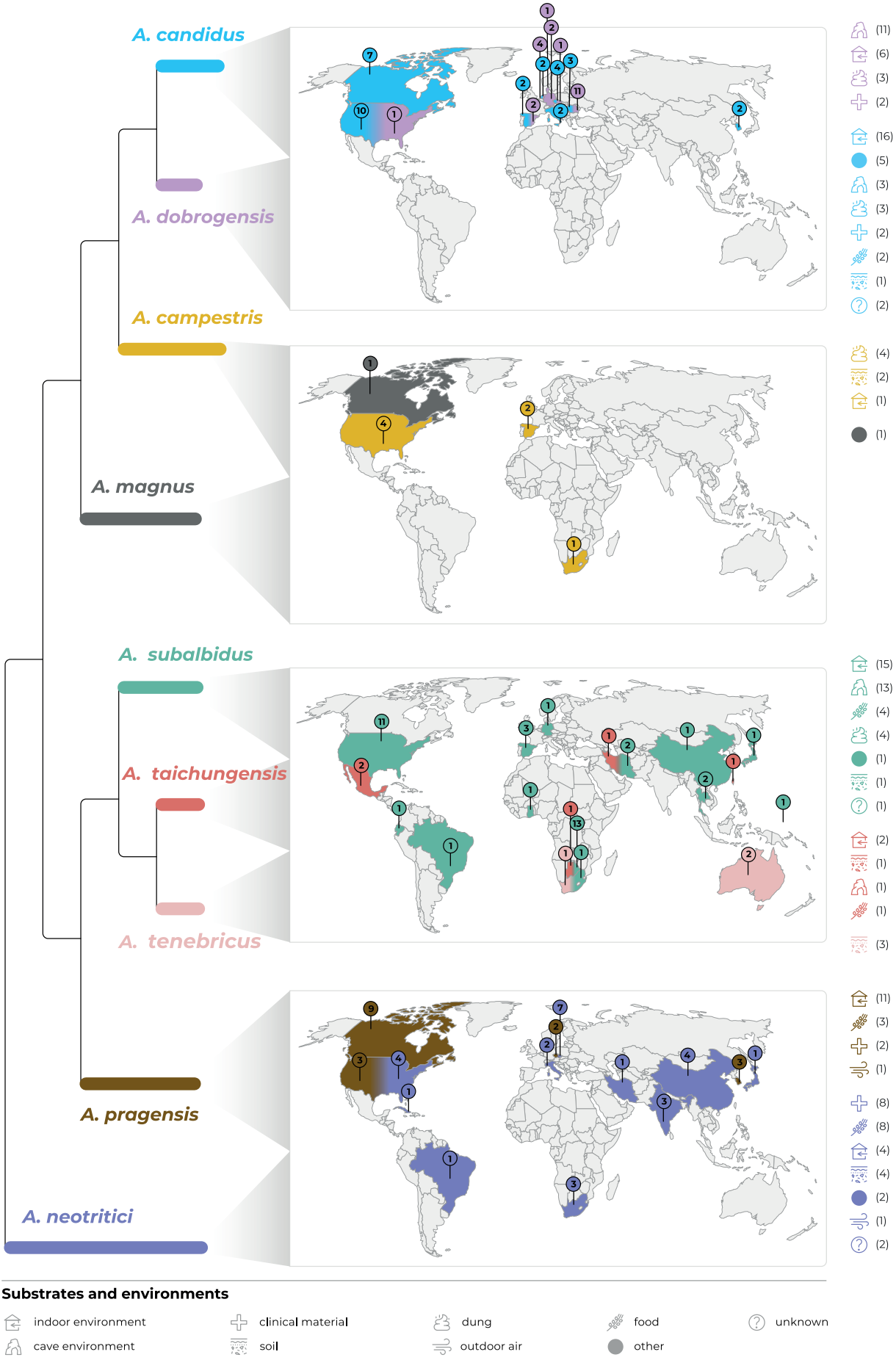

Fig. 12. Geographic distribution of *Aspergillus* section *Candidi* members based on available sequence data from *benA*, *CaM* and *RPB2* genes generated in this study (accession numbers are listed in Table 1) and available in the NCBI database (accession numbers in Supplementary Table S3), accessed on February 20, 2022. The numbers in the location pointers correspond to a total number of reliably identified strains reported from a specific country; the numbers following icons of substrates represent a total number of reliably identified strains reported from this substrate.

On the other hand, there were apparently preferred substrates/environments of occurrence in some species, for instance dung in *A. campestris*.

Species identification in practice using molecular and phenotypic characters

All nine species recognized in this study can be identified by using DNA sequencing of any of three phylogenetic markers employed, *i.e.*, *benA*, *CaM* and *RPB2*. The ITS region which was excluded from the phylogenetic analyses due to the low number of variable positions, can only be used for the identification of *A. campestris*, *A. taichungensis* and *A. neotritici*. The ITS rDNA sequences of these species include the following diagnostic positions which are mostly found in the ITS1 region (the numbering is according to the ITS alignment deposited in the DRYAD digital repository: https://doi.org/10.5061/dryad.3j9kd51mq): *A. campestris* position 95 T/C; *A. taichungensis* 109 T/C; and *A. neotritici* 89 A/G, 97 C/T and 498 C/T. Remaining species are indistinguishable from each other by ITS region.

As detailed above, the phenotypic species identification is non-trivial due to the relatively high intraspecific variability in morphological and physiological features detected in this work. Additionally, we do not have information about the degree of variability in species represented by one or few strains. For this reason, any identification key is burdened with a significant inaccuracy. For approximate phenotypic identification in practice, we have created the following synoptic key.

Synoptic key to accepted species in the *Aspergillus* section *Candidi*

A. campestris M. Chr. 1
A. candidus Link 2
A. dobrogensis A. Nováková *et al.* 3
A. magnus Glässnerová & Hubka 4
A. neotritici Glässnerová & Hubka 5
A. pragensis Hubka *et al.* 6
A. subalbidus Visagie, Hirooka & Samson 7
A. taichungensis Yaguchi, Someya & Udagawa 8
A. tenebricus Houbraken, Glässnerová & Hubka 9

I. Macromorphology

Isolates must be grown on the following media at 25 °C for 14 d and 28 d for the presence of soluble pigment.

Colony colour on MEA and CYA
white 2, 3, 5, 6, 7, 9
yellowish white/pale yellow/pastel yellow 1, 4, 5, 7, 8, 9
yellowish grey 1, 4, 7
sulphur yellow 1

Growth on MEA
≤ 25 mm 1, 2, 3, 4, 5, 6, 7, 8
26–34 mm 1, 2, 3, 5, 7, 8, 9
≥ 35 mm 3, 5

Growth on CYA
≤ 25 mm 1, 2, 4, 5, 6, 7
> 25 mm 1, 2, 3, 5, 7, 8, 9

Growth on CZA
≤ 15 mm 1, 4, 5, 6, 7, 8
> 15 mm 1, 2, 3, 5, 7, 8, 9

Growth on CY20S
≤ 30 mm 1, 2, 4, 5, 6, 7
31–45 mm 1, 2, 3, 5, 7, 8, 9
> 45 mm 3, 5, 8, 9

Soluble pigment on CZA
brown, dark brown, black 1, 2, 5, 7, 9
green, dark green, greyish green 1, 5, 6, 7
yellow, yellowish brown 2, 5
no soluble pigment 1, 2, 3, 4, 5, 7, 8

Soluble pigment on CYA
brown, dark brown 1, 2, 4, 6, 7, 9
yellow 8
no soluble pigment 1, 2, 3, 5, 6, 7, 8

II. Physiology

Isolates must be grown on MEA at specified temperatures for 14 d.

Growth at 10 °C
no growth 5
< 8 mm 1, 6, 7, 8
≥ 8 mm 1, 2, 3, 4, 9

Growth at 30 °C
≤ 25 mm 1, 2, 3, 4, 6, 7, 8, 9
26–30 mm 7, 8, 9
> 30 mm 5

Growth at 35 °C
no growth 1, 2, 3, 4, 6, 7
growth 1, 5, 7, 8, 9

Growth at 37 °C
no growth 1, 2, 3, 4, 6, 7, 9
growth 5, 7, 8, 9

Growth at 40 °C
no growth 1, 2, 3, 4, 6, 7
growth 5, 8

III. Micromorphology

Isolates must be grown on MEA at 25 °C for 7–21 d.

Length of stipes
< 500 µm 1, 2, 3, 5, 6, 7, 8, 9
500–800 µm 1, 3, 4, 5
> 800 µm 1, 3, 4

Width of stipe
≤ 6.5 µm 1, 2, 3, 4, 5, 6, 7, 8, 9
7–9.5 µm 1, 2, 3, 4, 5, 7
≥ 10 µm 7

Vesicle diameter
≤ 17 µm 1, 2, 3, 5, 6, 7, 8, 9
17–30 µm 1, 2, 3, 5, 6, 7, 9
> 30 µm 4

Length of metulae
≤ 8 µm 1, 2, 3, 5, 6, 7, 8
≥ 10 µm 1, 3, 4, 5, 7, 9

TAXONOMY

Aspergillus* section *Candidi W. Gams *et al*., Adv. Pen. Asp. Syst.: 61. 1986 [1985]. MB832512. Emended description.

Typus: Aspergillus candidus Link, Mag. Ges. Naturf. Freunde Berlin 3: 16. 1809.

Section *Candidi* encompasses nine species with white- or yellow-coloured colonies. *Conidiophores* biseriate (exceptionally uniseriate in some *A. neotritici* strains), *stipes* hyaline, smooth-walled, rarely finely roughened, non-septate or septate, *vesicles* usually globose or subglobose, typically reaching diameter of 10–30 µm (Table 5), *conidia* subglobose to globose, rarely elliptical, smooth-walled or finely roughened (smooth to microtuberculate in SEM).

The species are moderately xerophilic and grow more rapidly on media with higher content of osmotically active substances (*e.g.* CY20S) compared to conventional media such as MEA and CYA. The majority of species produce soluble pigments and/or sclerotia after 4 wk of cultivation (Table 4). *Sclerotia* are purple, brown to black. *Sexual state* has not been observed. All species (except for *A. neotritici*) are able to grow at 10 °C and some species (*A. neotritici*, *A. subalbidus*, *A. taichungensis* and *A. tenebricus*) are able to grow at 37 °C or even higher temperatures. The members of sect. *Candidi* are worldwide distributed across all climate zones and are mostly isolated from indoor and cave environments, stored food/feed, soil and clinical samples (Fig. 12).

The majority of species produce the secondary metabolites chloroflavonins, terphenyllins, candidusins and xanthoascins (Rahbæk *et al.* 2000, Varga *et al.* 2007, Hubka *et al.* 2014, Hubka *et al.* 2018b), in addition to taichunins (Kato *et al.* 2019) and taichunamides (Kagiyama *et al.* 2016) which are found in some species.

The members of the phylogenetically related section *Petersoniorum* (Jurjević *et al*. 2015) are not xerophilic and their occurrence is restricted to the tropical region. They produce conidia that are grey-green or blue-green on masse and have tuberculate surface. Their vesicles do not exceed 20 µm and sclerotia are yellow to brown. The secondary metabolites of section *Petersoniorum* are poorly explored but similarly to section *Candidi*, they produce terphenyl-type of secondary metabolites, arenarins (Oh *et al*. 1998).

Aspergillus campestris M. Chr., Mycologia 74: 212. 1982. MycoBank MB110495. Fig. 13.

Holotype: NY ST 2–3–1 (catalogue number 00936735). Culture ex-type: CBS 348.81 = NRRL 13001 = IBT 13382 = IBT 28561 = IMI 259009 = ATCC 44563 = IFM 50931 = CCF 5596.

Colony diam, 25 °C, 7 d / 14 d (mm): MEA: 11–17 / 16–28; CYA: 14–20 / 22–36; CZA: 6–14 / 10–20; CY20S: 10–21 / 25–34.

Cardinal temperatures (on MEA, after 2 wk): Aspergillus campestris is able to grow at 10 °C (4–10 mm) and its optimum growth temperature is 25 °C (16–28 mm). Some strains did not grow or only germinate at 30 °C (IBT 17867, IBT 23172), while all other strains grew well at this temperature (12–22 mm). The only strain capable of growing at 35 °C was CBS 348.81^{T} (3–4 mm). No growth at 37 °C.

Culture characteristics (at 25 °C after 2 wk): Colonies on MEA pale yellow (2A3), light yellow (3A5), yellowish white (2A2) or greyish yellow (4B4) with pale yellow margins (2A3), flat, texture granular or floccose, sporulation abundant, margins entire, exudate absent, soluble pigment absent, reverse yellow (3A6), light yellow (4A5) or greyish yellow (4B5). Colonies on CYA yellowish white (3A2), pale yellow (3A3), light yellow (3A5) or yellowish grey (4B2) with pale yellow margins (2A3), flat or centrally raised, usually radially wrinkled, texture granular or floccose, sporulation abundant, margins entire or delicately undulate, reverse yellowish brown (5D5), greyish yellow (4B5), brownish orange (5C5) or dark blond (5D4), exudate absent, soluble pigment dark brown after 4 wk in some strains with varying intensity or location: 4–5 mm large circle around colonies in CBS 348.81^{T} and CCF 5641; 1–3 mm large circle around colonies in FMR 15226 and IMI 344489; pigment in central area between colonies in FMR 15224. Colonies on CZA yellowish white (3A2), yellow (3A6) or light yellow (2A5), flat, texture granular or floccose, sporulation abundant, margins entire or irregular, reverse pale yellow (3A3), light yellow (3A5) or greyish yellow (3B5), exudate absent, soluble pigment present in some strains after 4 wk: dark brown to black in CBS 348.81^{T} and IMI 344489 (3–5 mm large circle around colonies), greenish grey in FMR 15226 (6–7 mm around colonies) and brown in IBT 17867, FMR 15224 and IBT 23172 (2 mm large circle around colonies). Colonies on CY20S yellowish white (3A2), pale yellow (3A3) or pastel yellow (3A4) with bluish grey margins (23D2), flat, centrally raised or umbonate, texture floccose, granular or downy, sporulation abundant, margins entire, less frequently undulate or irregular, reverse olive (2E5), olive yellow (3C8) or yellowish brown (5E4) with greyish yellow margins (3B5, 4B4), exudate absent, soluble pigment present in some strains after 4 wk: dark green to black in CBS 348.81^{T} (3 mm large circle around colonies), dark brown to black in FMR 15224 (5 mm around colonies), and brown in IBT 17867 and CCF 5641 (only central area between colonies). *Sclerotia* produced superficially after 4 wk of cultivation, in IBT 17867, CCF 5641, FMR 15226 and FMR 15224. Sclerotia absent in CBS 348.81^{T}, IBT 23172 and IMI 344489. Dark grey or black sclerotia were observed on CZA (IBT 17867, CCF 5641) and CYA (FMR 15224), dark brown sclerotia were present on CYA in strain FMR 15226. No sclerotia were observed in any strain on MEA and CY20S.

Micromorphology: Conidial heads radiate, biseriate. Diminutive conidiophores occasionally present. *Stipes* (excluding diminutive) hyaline, smooth-walled, occasionally finely roughened, undulate in CBS 348.81^{T}, usually non-septate, (90–)250–850(–1 300) × (4–)5–7.5(–9) µm, *vesicles* globose or subglobose, (10.5–)14–22(–31.5) µm diam, *metulae* cylindrical or wedge-shaped (V-shaped), (7–)8–14(–17) µm long, covering three quarters to entire surface of vesicle; *phialides* ampulliform, (4.5–)5–7(–9) µm long. *Conidia* subglobose to globose, ovate or limoniform, (2.5–)3–4.5(–5) (3.8 ± 0.5 µm) × (2.5–)3–4.5(–5) (3.4 ± 0.4 µm), smooth-walled, rarely finely roughened. In IMI 344489 conidia wider and broader, subglobose or ovate, (3.5–)4–4.5(–5) (4.4 ± 0.3 µm) × (3–)4–4.5(–5) (4.2 ± 0.3 µm).

Diagnosis: Aspergillus campestris is most closely related to *A. candidus, A. dobrogensis* and *A. magnus.* Strains of *A. campestris* are usually easily differentiated from other members of section *Candidi* by their bright yellow colonies. Conidiophores of *A. magnus* have longer and wider stipes and broader vesicles compared to *A. campestris*, while the stipes of *A. candidus* are shorter. In comparison with *A. dobrogensis, A. campestris* isolates produce dark soluble pigments and grow more restricted on all cultivation media. The remaining species in sect. *Candidi*, *i.e.*, *A. neotritici*, *A. pragensis*, *A. taichungensis, A. tenebricus* and *A. subalbidus* have shorter stipes than *A. campestris*. These species, except for *A. neotritici*, have also narrower stipes and smaller vesicles (Table 5). *Aspergillus campestris* colonies have a smaller diameter than *A. taichungensis*, *A. tenebricus* and *A. neotritici* on all media, but larger than *A. pragensis* (Table 4). In addition, the majority of strains of *A. subalbidus, A. taichungensis, A. tenebricus* and *A. neotritici* grow at 35 °C or higher temperatures (Table 6) in contrast to *A. campestris* where only one strain germinated at 35 °C (CBS 348.81^{T}).

Ecology (only records verified by DNA sequencing): The species is known on dung from herbivorous animals, indoor air and soil. It has been isolated in South Africa, Spain and the USA (Fig. 12, Table 1).

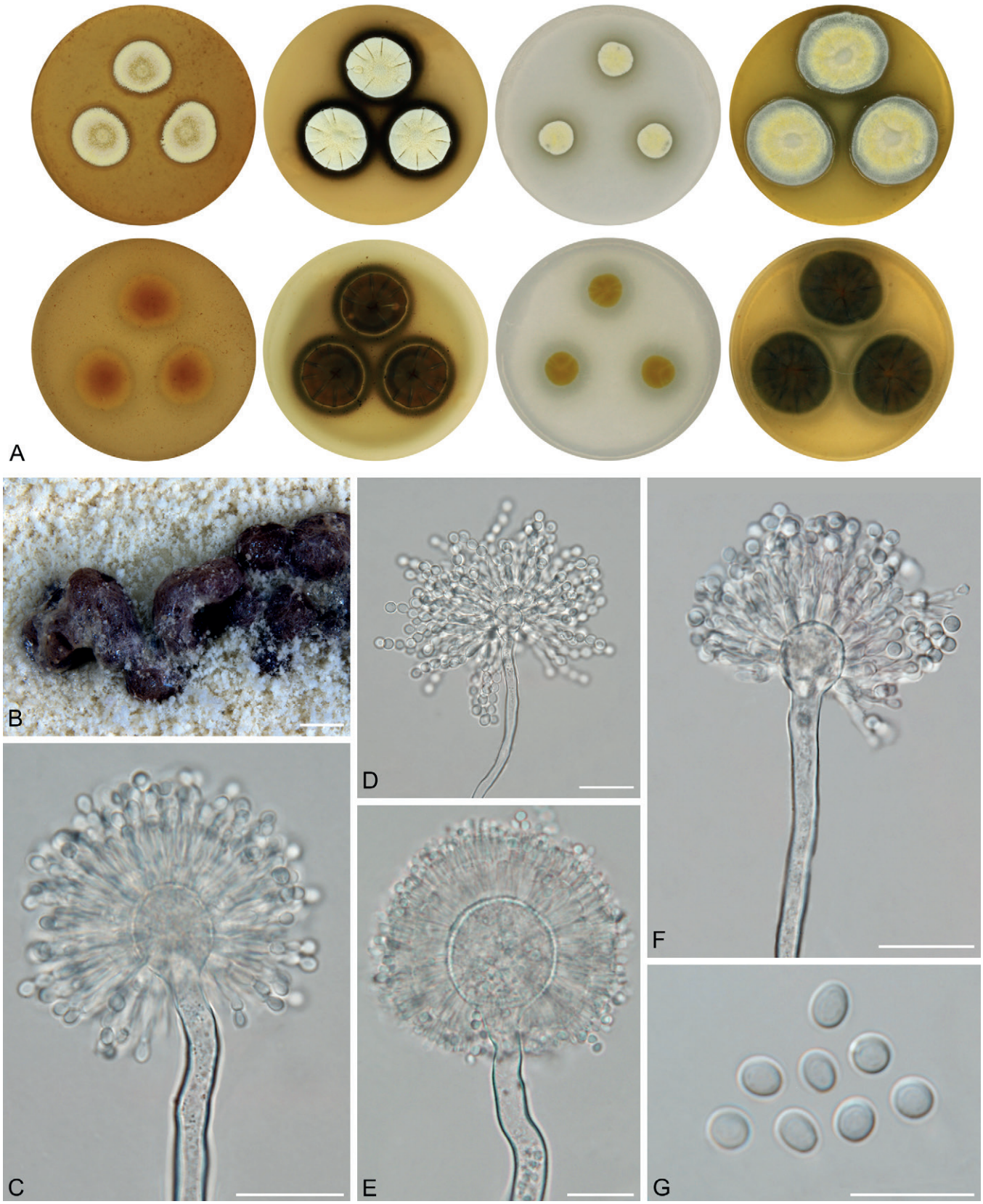

Fig. 13. Macromorphology and micromorphology of *Aspergillus campestris*. **A.** Colonies after 14 d at 25 °C, left to right: MEA, CYA, CZA, CY20S. **B.** Sclerotia produced on CYA (photograph taken after 28 d of cultivation). **C–F.** Conidiophores. **G.** Conidia. Scale bars: B = 500 µm; C–F = 20 µm, G = 10 µm.

Aspergillus candidus Link, Mag. Gesell. Naturf. Freunde, Berlin 3(1-2): 16. 1809. MycoBank MB 204868. Fig. 14.

Neotype (designated by Samson & Gams 1985): CBS 566.65. Culture ex-type: CBS 566.65 = NRRL 303 = IMI 091889 = ATCC 1002 = IBT 28566 = CCF 5594.

Colony diam, 25 °C, 7 d / 14 d (mm): MEA: 12–17 / 20–27; CYA: 15–21 / 20–32; CZA: 9–15 / 16–25; CY20S: 16–25 / 25–45.

Cardinal temperatures (on MEA, after 2 wk): Aspergillus candidus is able to grow at 10 °C (8−11 mm), the optimum growth temperature is 25 °C (20−27 mm). The maximum growth temperature is 30 °C

(18−25 mm). No growth at 35 °C.

Culture characteristics (at 25 °C after 2 wk): Colonies on MEA white (3A1) with a tint of yellowish white (4A2), flat, texture granular to floccose, sporulation abundant, margins entire, exudate absent, reverse light yellow (4A4) or pale yellow (4A3). Colonies on CYA white (3A1) with a tint of yellowish white (4A2) or orange white (5A2), flat or slightly centrally raised, texture granular to floccose, sporulation abundant, margins entire or slightly undulate, exudate absent, reverse light yellow (4A5) or brownish orange (5C3). Colonies on CZA white (3A1) to pale yellow (1A3, 3A3), flat, texture waxy to granular, sporulation weak, margins entire or irregular, exudate absent, reverse pale yellow (3A3) or light yellow (4A4). Colonies on CY20S white (3A1), flat or slightly centrally raised, texture floccose, granular or velvety, radially or irregularly folded, sporulation abundant, margins entire to diffuse or slightly erose, exudate absent, reverse light yellow (4A4, 4A5). *Soluble pigment* production after 4 wk was examined in nine strains: five of them (CCF 488, CCF 5172, CCF 6200, CCF 3996, NRRL 58959) were able to produce it and four (CBS 566.65^{T}, CCF 4659, CCF 4713, CCF 6195) not. Dark brown to black soluble pigment (3−4 mm around colonies) was observed on CZA in strains CCF 488 and CCF 6200. Brown soluble pigment was observed on CZA in strains CCF 5172 and CCF 3996 (2−4 mm around colonies) and on CYA in strain CCF 3996. Brownish yellow soluble pigment was observed on CZA in strain NRRL 58959. No soluble pigment was observed on MEA and CY20S in any strain. *Sclerotia* production after 4 wk was examined in nine strains. Five of them (CCF 488, CCF 5172, CCF 6200, CCF 3996, NRRL 58959) were able to produce sclerotia, while no sclerotia were observed in the remaining strains (CBS 566.65^{T}, CCF 4659, CCF 4713, CCF 6195). Brown to black sclerotia covered by mycelium were present on CZA in five mentioned strains. No sclerotia were observed on MEA, CYA and CY20S in any examined strain.

Micromorphology: Conidial heads radiate, biseriate. Diminutive conidiophores occasionally present. *Stipes* (excluding diminutive) hyaline, smooth-walled, usually non-septate, occasionally with septa, (70–)125–400(–520) × (2.5–)3.5–8.5(–9.5) µm, *vesicles* predominantly globose, (8–)10–23(–33) µm diam, *metulae* cylindrical or wedge-shaped (V-shaped), (4.5–)5.5–7.5(–8) µm long, usually covering entire surface of vesicle; *phialides* ampulliform, (4–)5–6.5(–7) µm long. *Conidia* globose to subglobose, (3–)3.5–4(–4.5) (3.7 ± 0.2) µm × (3–)3.5–4(–4.5) (3.5 ± 0.2 µm), smooth-walled, rarely finely roughened**.**

Diagnosis: Aspergillus candidus is sister to *A. dobrogensis* and closely related to *A. campestris* and *A. magnus.* In general, *A. candidus* has smaller vesicles, shorter and narrower stipes and also shorter phialides and metulae compared to *A. dobrogensis* (Table 5). *Aspergillus dobrogensis* colonies also have a larger diameter than *A. candidus* on MEA, CYA and CY20S (Table 4). However, most of these differences can be interpreted as a trend across the whole species, while some isolates show identical dimensions to *A. dobrogensis* strains (Fig. 7). Thus, distinguishing between them can be problematic in practice. *Aspergillus magnus* colonies have a smaller diameter and it has wider and longer stipes, vesicles and metulae than *A. candidus*. *Aspergillus campestris* has usually bright yellow colonies and produces stipes, vesicles and metulae which are longer/wider than in *A. candidus*. *Aspergillus pragensis* grows more restricted on all media while *A. neotritici, A. tenebricus* and *A. taichungensis* colonies have a larger diameter on MEA, CYA and CY20S. The latter three species grow at 35 °C or higher temperatures (Table 6). *Aspergillus taichungensis* and *A. tenebricus* produce shorter stipes and *A. tenebricus* has longer phialides and metulae compared to *A. candidus.*

Ecology (only records verified by DNA sequencing): The species is known from indoor environments (air, dust), caves, soil, dung, clinical samples, food, metal duct, tunnels of bark beetles, the red flour beetle (*Tribolium castaneum*) and egg-mass of *Arctoscopus japonicus. Aspergillus candidus* has been isolated in Canada, Czech Republic, Italy, the Netherlands, Romania, South Korea, Spain and the USA (Fig. 12, Table 1, Supplementary Table S3).

Aspergillus dobrogensis A. Nováková, Jurjević, F. Sklenar, Frisvad, Houbraken & Hubka, Int. J. Syst. Evol. Microbiol. 68: 1004. 2018. MycoBank MB 821313. Fig. 15.

Holotype: PRM 935751. Culture ex-type: CCF 4651 = CCF 4655 = CBS 143370 = NRRL 62821 = IBT 32697.

Colony diameters (at 25 °C, 7 d / 14 d, mm): MEA: 17–20 / 22–34; CYA: 20–24 / 26–39; CZA: 9–15 / 16–25; CY20S: 18–28 / 32–48.

Cardinal temperatures (on MEA, after 2 wk): Aspergillus dobrogensis is able to grow at 10 °C (9–13 mm) and the optimum growth temperature is 25 °C (23–32 mm). The maximum growth temperature is 30 °C (17–24 mm). No growth at 35 °C.

Culture characteristics (at 25 °C after 2 wk): Colonies on MEA white (4A1), sometimes with a tint of yellowish white (4A2), flat or slightly centrally raised, texture floccose, downy or granular, sporulation abundant, margins entire to slightly erose, exudate absent, soluble pigment absent, reverse pale yellow (4A3) or light yellow (4A4). Colonies on CYA white (4A1), sometimes with a tint of yellowish white (4A2), flat, centrally raised or umbonate, texture floccose, downy or granular, sporulation abundant, margins entire, exudate absent, soluble pigment absent, reverse light yellow (4A4, 4A5). Colonies on CZA white (3A1) to yellowish white (3A2, 4A2), flat, texture waxy to granular, sporulation weak and located in a small area in the colony, margins entire or irregular, exudate absent, soluble pigment absent, reverse yellowish white (4A2, 3A2) or pale yellow (3A3, 4A3). Colonies on CY20S white (3A1), flat, centrally raised or umbonate, texture floccose, granular or downy, velvety margins in some strains, sporulation abundant, margins entire, exudate absent, soluble pigment absent, reverse light yellow (4A4, 4A5). *Sclerotia* production after 4 wk was examined in 10 strains, two of them (CCF 4651^{T}, CCF 5570) were able to produce sclerotia and eight of them (CCF 5567, CCF 5568, CCF 4650, CCF 5844, IBT 29476, CCF 5575, CCF 5569 and CCF 5572) not. They were produced superficially, less commonly covered by felt of mycelium. Strain CCF 4651^{T} was able to produce sclerotia on all four media; dark brown sclerotia on MEA, CZA and CY20S and brown sclerotia on CYA. Dark brown sclerotia covered by felt of mycelium were present on CZA in CCF 5570. No sclerotia were observed on MEA, CYA and CY20S in remaining examined strains.

Micromorphology: Conidial heads radiate, biseriate. Diminutive conidiophores occasionally present. *Stipes* (excluding diminutive) hyaline, smooth-walled, occasionally finely roughened, usually non-septate, rarely septate, (100–)150–1 150(–2 000) × (3.5–)5–7(–14) µm, *vesicles* predominantly globose, sometimes subglobose or elongated, (9–)10–30(–39.5) µm diam, *metulae* cylindrical or

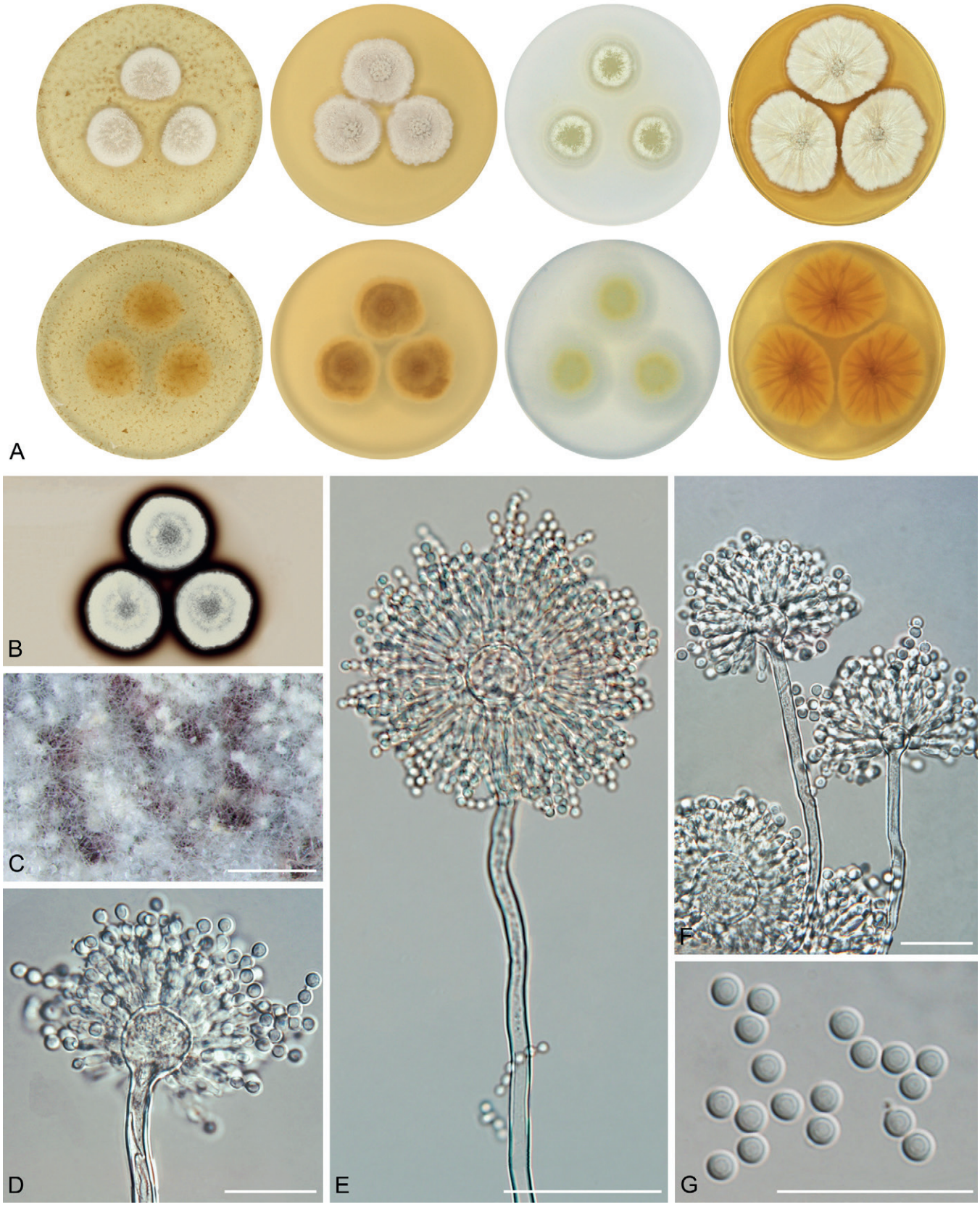

Fig. 14. Macromorphology and micromorphology of *Aspergillus candidus.* **A.** Colonies after 14 d at 25 °C, left to right: MEA, CYA, CZA, CY20S. **B.** Soluble pigment on CZA (photograph taken after 28 d of cultivation). **C.** Sclerotia produced on CZA (photograph taken after 28 d of cultivation). **D–F.** Conidiophores. **G.** Conidia. Scale bars: C = 1 mm; D, F, G = 20 µm; E = 50 µm.

wedge-shaped (V-shaped), (5–)5.5–12(–14) µm long, usually covering the entire surface of vesicle; *phialides* ampulliform, (5–)5.5–7.5(–8.5) µm long. *Conidia* globose to subglobose, (3–)3.5–4(–4.5) (3.7 ± 0.3) µm × (2.5–)3–4(–4.5) (3.5 ± 0.3 µm), smooth-walled, rarely finely roughened.

Diagnosis: See section "*Diagnosis*" of *A. candidus* for more details. *Aspergillus dobrogensis* differs from *A. candidus, A. pragensis, A. taichungensis*, *A. tenebricus* and *A. subalbidus* by its longer and broader stipes and larger vesicles (Table 5, Fig. 6). *Aspergillus campestris* can be differentiated by its yellow colonies. *Aspergillus dobrogensis*

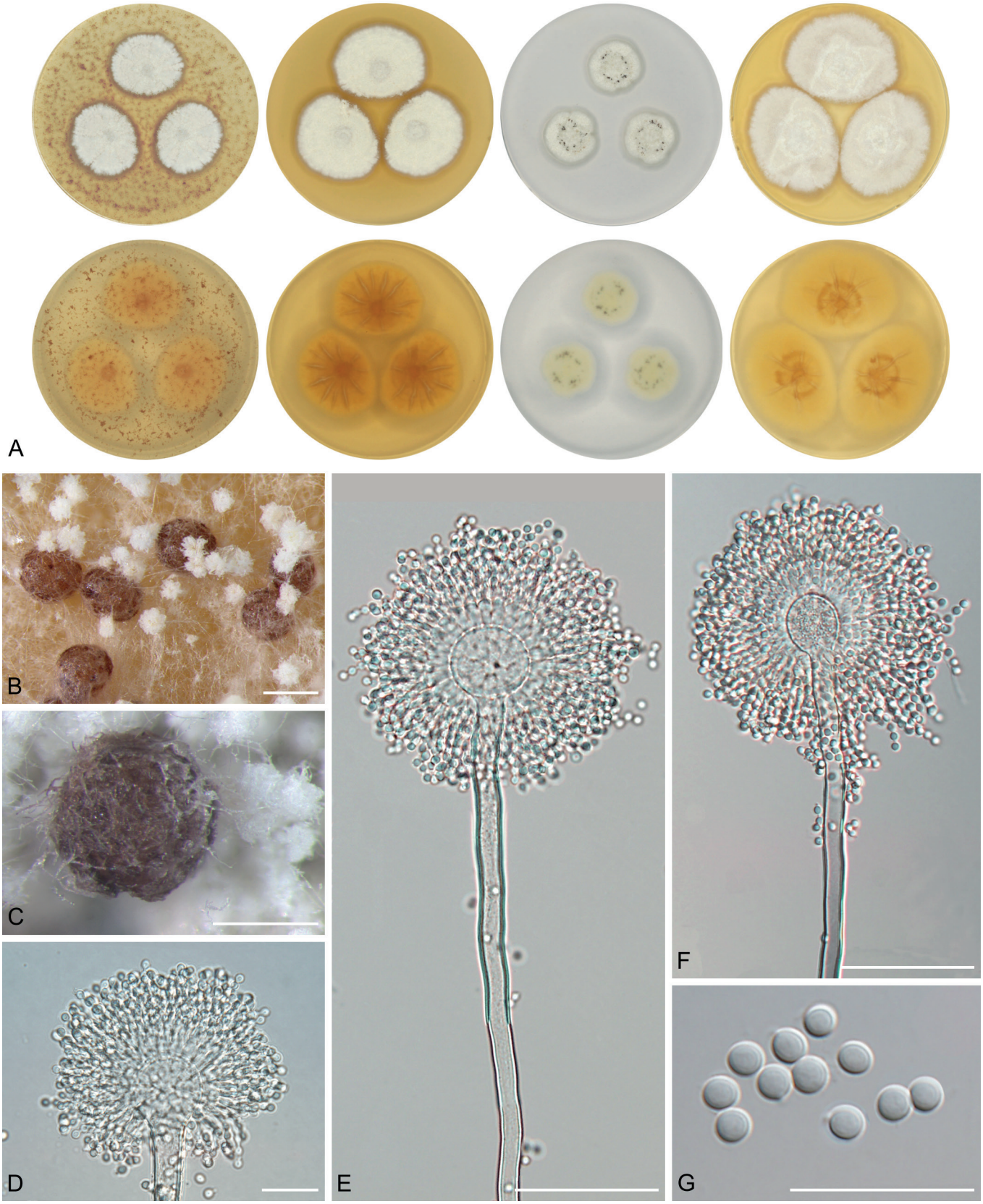

Fig. 15. Macromorphology and micromorphology of *Aspergillus dobrogensis*. **A.** Colonies after 14 d at 25 °C, left to right: MEA, CYA, CZA, CY20S. **B–C.** Sclerotia produced on CYA (B) and CZA (C), photographs taken after 28 d of cultivation. **D–F.** Conidiophores. **G.** Conidia. Scale bars: B = 750 µm; C = 500 µm; D, G = 20 µm; E, F = 50 µm.

colonies have a larger diameter than *A. campestris*, *A. candidus*, *A. pragensis*, *A. magnus* and *A. subalbidus* on MEA, CYA and CY20S, while *A. neotritici* and *A. taichungensis* colonies have a larger diameter than *A. dobrogensis* on these media (Table 4). *Aspergillus subalbidus, A. taichungensis*, *A. tenebricus* and *A. neotritici* can be differentiated by their ability to grow at 35 °C or even higher temperatures (Table 6).

Ecology (only records verified by DNA sequencing): The species is known from caves (bat droppings and guano, sediment, air), indoor environments (air, dust, carpet), mouse dung, herbivore dung and clinical material. It has been isolated in the Czech Republic, Denmark, Germany, the Netherlands, Romania, Spain and the USA (Fig. 12, Table 1).

Aspergillus magnus Glässnerová & Hubka, ***sp. nov.*** MycoBank MB 844202. Fig. 16.

Etymology: Latin adj. *magnus -a -um*, referring to its larger conidiophores (stipe length and width, metulae length and vesicle diameter) compared to related species.

Typus: **Canada**, Alberta, Edmonton, mouse collected on horse farm, 1962, J.W. Carmichael (**holotype** PRM 956934 (dried culture, metabolically inactive), **isotypes** PRM 956935–956937 (dried culture, metabolically inactive), culture ex-type UAMH 1324 = IBT 14560).

Colony diam, 25 °C, 7 d / 14 d (mm): MEA: 12–14 / 20–22; CYA: 12–14 / 16–17; CZA: 4–6 / 11–13; CY20S: 13–15 / 19–21.

Cardinal temperatures (on MEA, after 2 wk)*: Aspergillus magnus* is able to grow at 10 °C (9–10 mm) and the optimum growth temperature is 25 °C (20–22 mm). The maximum growth temperature is 30 °C (5–7 mm). No growth at 35 °C.

Culture characteristics (at 25 °C after 2 wk): Colonies on MEA yellowish grey to pale yellow (3C2–3A3) in the centre, yellowish white (3A2) on the margins, flat, texture floccose, sporulation abundant, margins entire, exudate absent, soluble pigment absent, reverse light yellow (4A4). Colonies on CYA pale yellow (3A3) in the centre, yellowish grey (4B2) on the margins, flat, texture floccose, sporulation abundant, margins entire, exudate absent, soluble pigment dark brown (3 mm around colonies after 4 wk), reverse greyish yellow to dark blond (4B4-5D4). Colonies on CZA pale yellow (3A3), flat, texture floccose, sporulation abundant, margins entire, exudate absent, soluble pigment absent, reverse pale yellow (3A3). Colonies on CY20S pale yellow (3A3), centrally raised, texture floccose, sporulation abundant, margins entire, exudate absent, soluble pigment absent, reverse greyish yellow to dark blond (4B4–5D4). *Sclerotia* production after 4 wk was not observed on any medium.

Micromorphology: Conidial heads radiate, biseriate. Diminutive conidiophores usually present. *Stipes* (excluding diminutive) hyaline, smooth-walled, occasionally finely roughened, non-septate or occasionally septate, (540–)810–1 150(–1 600) × (6–)9–13(–16) µm, *vesicles* globose to subglobose, (18–)33–39(–45) µm diam, *metulae* cylindrical or wedge-shaped (V-shaped), (7.5–)9–14(–17) µm long, covering the entire surface of vesicle; *phialides* ampulliform, (4.5–)5.5–7(–8) µm long. *Conidia* subglobose to globose, (3–)3.4–3.6(–4) (3.5 ± 0.2 µm) × (2.5–)3.1–3.3(–3.5) (3.2 ± 0.2 µm), occasionally broadly ellipsoidal, smooth-walled, rarely finely roughened**.**

Diagnosis: Aspergillus magnus differs from other section *Candidi* members by its larger vesicles, longer and wider stipes and longer metulae (Table 5, Fig. 6). Some strains of *A. dobrogensis* reach similar stipe lengths but they differ from *A. magnus* by other characters, especially its white colony colour. *Aspergillus magnus* grows more restricted than other species on all media except for *A. pragensis* (Table 4). *Aspergillus neotritici, A. tenebricus, A. taichungensis* and *A. subalbidus* can be differentiated by their ability to grow at 35 °C or even higher temperatures.

Ecology (only records verified by DNA sequencing): The species is known only from a single strain, isolated from a mouse collected on a horse farm in Canada.

Aspergillus neotritici Glässnerová & Hubka, ***sp. nov.*** MycoBank MB 844204. Fig. 17.
= *Aspergillus tritici* [as *triticus*] B.S. Mehrotra & M. Basu, Nova Hedwigia 27 (3-4): 599. 1976. MycoBank MB309248. Not validly published [Art. 8.1, Art. 8.4, Art 40.1, Art. 40.4 (Turland *et al.* 2018)].

Etymology: Latin preposition *neo-* referring to a new description of previously invalidly described species *A. tritici.*

Typus: **Czech Republic**, Prague, toenail of 62-year-old man, 2008, isolated by M. Skořepová (**holotype** PRM 956940 (dried culture, metabolically inactive), **isotypes** PRM 956938, PRM 956939 and PRM 956941 (metabolically inactive), culture ex-type CCF 3853 = IBT 32725).

Colony diam, 25 °C, 7 d / 14 d (mm): MEA: 10–25 / 20–47; CYA: 14–28 / 21–50; CZA: 5–19 / 14–39; CY20S: 19–31 / 28-60.

Cardinal temperatures (on MEA, after 2 wk): Aspergillus neotritici does not grow at 10 °C, and its minimum growth temperature is 15 °C (4–13 mm). The optimum growth temperature is 30 °C (32–51 mm) and the maximum growth temperature is 40 °C (4–22 mm). No growth at 45 °C.

Culture characteristics (at 25 °C after 2 wk): Colonies on MEA white (3A1) to yellowish white (2A2, 3A2), flat, texture floccose to granular, less commonly velvety (in CCF 4914 and IBT 12659), sporulation abundant, margins entire, exudate absent, soluble pigment absent, reverse light yellow (4A4), greyish yellow to golden yellow (4B5–5B7). Colonies on CYA white (3A1) to yellowish white (3A2), flat to centrally raised, usually radially wrinkled, texture floccose, velvety or floccose in CCF 4914 and IBT 12659, margins entire or diffuse, sporulation abundant, exudate usually absent, minute yellow droplets present in CCF 6202, soluble pigment absent, reverse greyish yellow (4B5), reddish yellow (4A6) or brownish orange (5B4) in the centre, light yellow (4A4) on margins. Colonies on CZA white (3A1) to yellowish white (3A2), flat to centrally raised, texture granular, floccose or downy, sporulation abundant, margins entire or irregular, exudate usually absent, minute yellow droplets present in CCF 6202, soluble pigment present in some strains after 4 wk, dark brown soluble pigment (1–2 mm around colonies) present in strains CCF 4030 and CCF 6397, dark green soluble pigment present in strain CCF 4653 (2 mm around colonies), yellow soluble pigment present in strains CCF 3314, CCF 3853^{T} and CCF 4914 (1–5 mm around or between colonies), reverse greyish yellow to pale orange (4B5–5A3). Colonies on CY20S white to yellowish white (1A1–2A2) or pale yellow in CCF 4914 and IBT 12659 (2A2–2A3), flat or centrally raised, radially wrinkled in some strains (CBS 266.81, CCF 4914 and IBT 12659), texture floccose, downy to velvety in CCF 4914 and IBT 12659, sporulation abundant, margins entire or diffuse, exudate absent, soluble pigment absent, reverse yellow to reddish yellow (3A6–4A6) or greyish yellow (4C5). Sporulation was abundant in all strains on all tested media except for strains NRRL 4847 (ex-type of *A. albus* var. *thermophilus*) and CCF 1649 which were sterile. *Sclerotia* were present on the colony surface after 4 wk of cultivation in strains CBS 266.81, CCF 3314, CCF 4914 and IBT 12659, absent in CCF 4030, CCF 4653, CCF 3853^{T}, CCF 4658, CCF 6202, CCF 1649 and CCF 6397. Purple sclerotia were present only on CZA in all mentioned strains, no sclerotia were observed on MEA, CYA and CY20S. Purple sclerotia were present in both strains on CZA only.

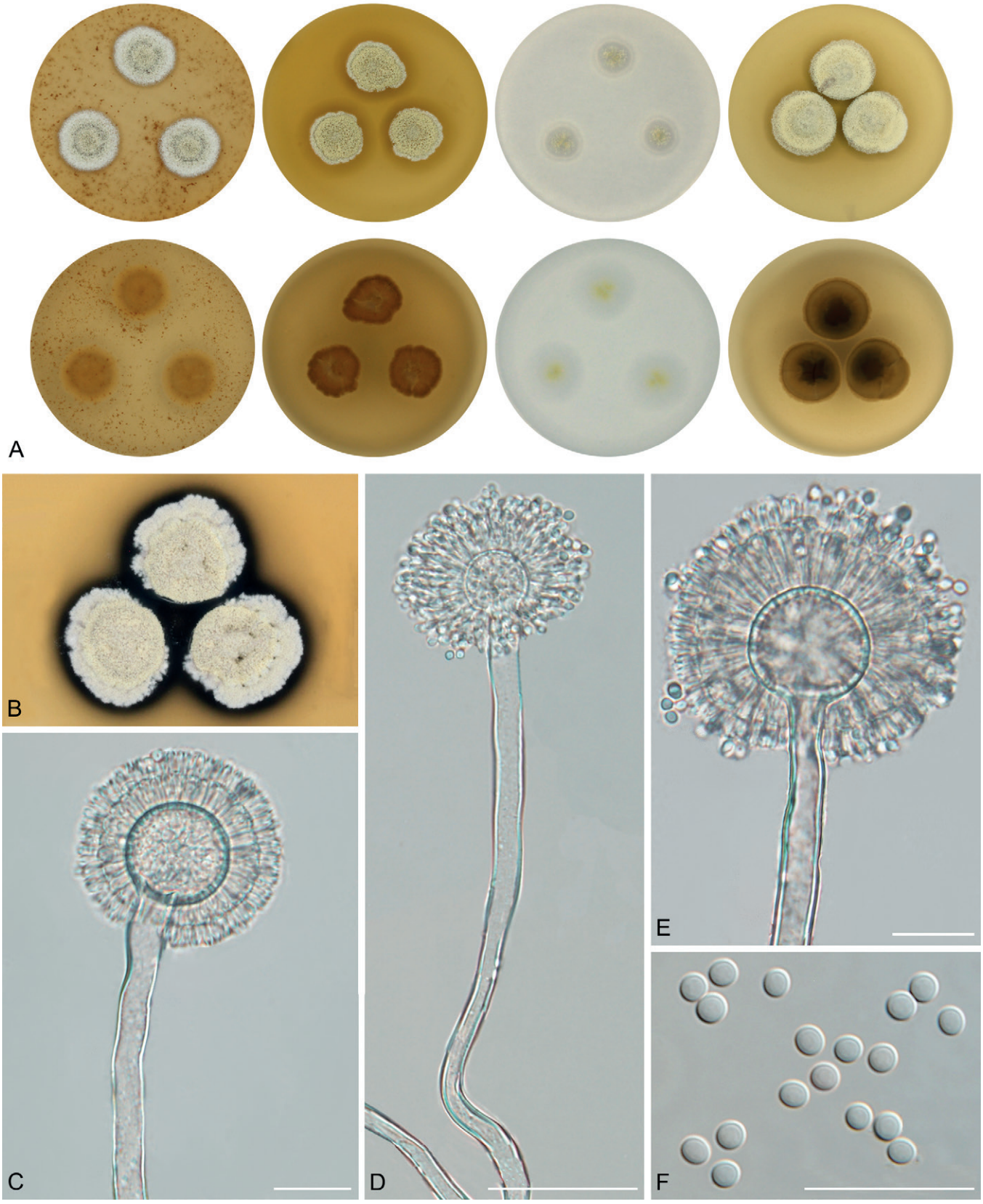

Fig. 16. Macromorphology and micromorphology of *Aspergillus magnus*. **A.** Colonies after 14 d at 25 °C, left to right: MEA, CYA, CZA, CY20S. **B.** Soluble pigment produced on CYA (photograph taken after 28 d of cultivation). **C–E.** Conidiophores. **F.** Conidia. Scale bars: C, E, F = 20 µm; D = 50 µm.

Micromorphology: Conidial heads radiate, predominantly biseriate, uniseriate in CCF 4914 and IBT 12659 (dimensions of micromorphological features are given separately in the next paragraph). Diminutive conidiophores occasionally present. *Stipes* (excluding diminutive) hyaline, smooth-walled or finely roughened, usually non-septate, occasionally with septa (extensively septate in CBS 266.81), (140–)200–500(–700) × (3.5–)4–8(–9) µm, *vesicles* globose, subglobose or elongated, (11–)14–24(–28) µm diam, (5–)6–8(–11) µm diam in CBS 266.81, *metulae* cylindrical or wedge-shaped (V-shaped), (4–)7–17(–21) µm long, (3.5–)4–5(–5.5) µm long in CBS 266.81, usually covering the entire surface of vesicle; *phialides* ampulliform, (2.5–)3.5–6(–8) µm long. *Conidia* (including

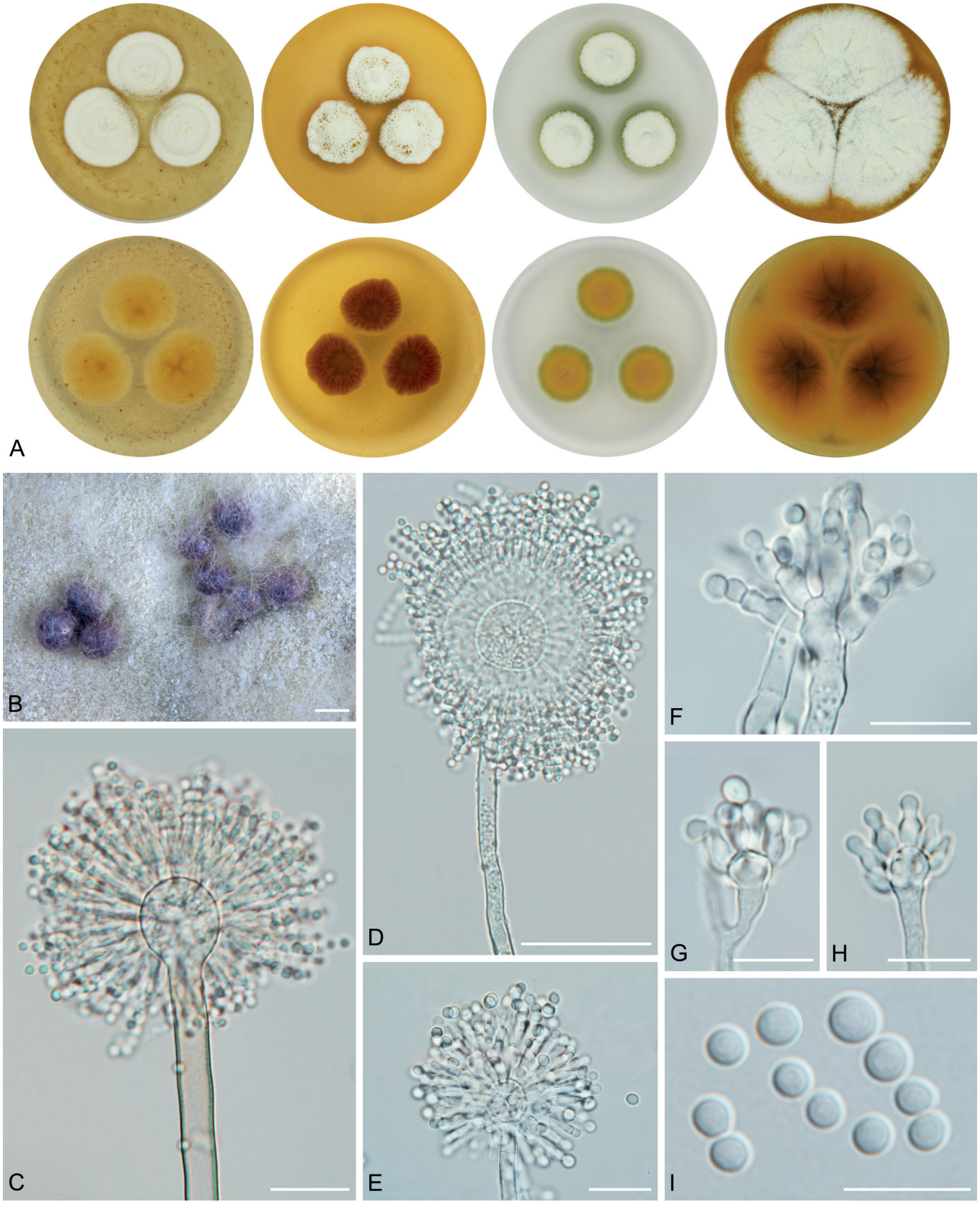

Fig. 17. Macromorphology and micromorphology of *Aspergillus neotritici.* **A.** Colonies after 14 d at 25 °C, left to right: MEA, CYA, CZA, CY20S. **B.** Sclerotia produced on CZA (photograph taken after 28 d of cultivation). **C–E.** Biseriate conidiophores (typical). **F.** Atypical biseriate conidiophores produced by strain CBS 266.81. **G–H.** Atypical uniseriate conidiophores produced by strains CCF 4914 and IBT 12659. **I.** Conidia. Scale bars: B = 500 µm; C, E, F = 20 µm; D = 50 µm; G–I = 10 µm.

CCF 4914 and IBT 12659) globose to subglobose or ellipsoidal, (2.5–)3–4.5(–5) (3.5 ± 0.5) µm × (2.5–)3–4(–4.5) (3.2 ± 0.5) µm, smooth-walled, rarely finely roughened**.**

Conidiophores in CCF 4914 and IBT 12659 short, uniseriate, *stipes* (6–)18–45(–85) × (2–)2.5–4(–5) µm, *vesicles* (3.5–)4–7(–8.5) µm, *phialides* (3–)3.5–4.5(–6) µm long, *conidia* had similar dimension to other strain, (3–)3.5–4(–4.5) (3.6 ± 0.3) µm × (3–)3–3.5(–4) (3.4 ± 0.3) µm.

Diagnosis: Aspergillus neotritici colonies have a larger diameter than *A. campestris*, *A. candidus*, *A. magnus* and *A. pragensis* on all media at 25 °C (Table 4). It grows better than any other species at 30–40 °C and its optimum growth temperature is 30 °C, while in other species, except for *A. subalbidus*, it is 25 °C (Table 6). It is also the only species which is not able to grow or at least germinate at 10 °C and can grow at 40 °C. *Aspergillus pragensis*, *A. dobrogensis*, *A. candidus*, *A. campestris* and *A. magnus* can be differentiated from *A. neotritici* by their inability to grow at 37 °C. The stipe length and vesicle diameter of *A. neotritici* is generally longer when compared to *A. subalbidus*, *A. pragensis, A. tenebricus* and *A. taichungensis* (Fig. 7), noting that this omits strains with atypical or uniseriate conidiophores.

Ecology (only records verified by DNA sequencing): The species is known from clinical samples, food (flour, corn, sunflower seed, cave cheese rind, grains of *Triticum sativum*), soil, indoor environments, outdoor air, vermicompost, and deep litter for pig raising. It has been reported in Brazil, China, Cuba, Czech Republic, India, Iran, Italy, South Africa, and the USA (Fig. 12, Table 1, Supplementary Table S3).

Aspergillus pragensis Hubka, Frisvad & M. Kolařík, Med. Mycol. 52: 570. 2014. MycoBank MB 800371. Fig. 18.

Holotype: PRM 922702. Culture ex-type: CCF 3962 = CBS 135591 = NRRL 62491 = IBT 32274.

Colony diam, 25 °C, 7 d / 14 d (mm): MEA: 8–10 / 15–18; CYA: 9–14 / 16–22; CZA: 3–6 / 11–15; CY20S: 13–18 / 24–30.

Cardinal temperatures (on MEA, after 2 wk): Aspergillus pragensis grows restrictedly at 10 °C (5–6 mm, colonies having character of minimally sporulating waxy drops) and the optimum growth temperature is 25 °C (15–18 mm). The maximum growth temperature is 30 °C (3–14 mm). No growth at 35 °C.

Culture characteristics (at 25 °C after 2 wk): Colonies on MEA white (3A1), slightly raised, crateriform in the centre, radially sulcate, texture velvety to downy, sporulation abundant, margins entire to slightly undulate, exudate absent, soluble pigment absent, reverse brownish yellow (5C6) in the centre, orange white (5A2) on the margins. Colonies on CYA white (3A1), centrally raised to umbonate, texture floccose to granular, sporulation abundant, margins entire or slightly undulate, exudate absent, soluble pigment dark brown in CCF 3962^{T}, CCF 4654, CCF 5693, CCF 5847 after 4 wk (4–6 mm wide circle around colonies or in the area between colonies), reverse light brown to brownish orange (5D5–5C4). Colonies on CZA white (3A1) or brownish grey (4D2), flat, texture waxy to floccose, sporulation weak and located only in the colony centre, margins irregular or submerged, exudate absent, soluble pigment intense dark green to greyish blue in all strains after 4 wk (3–6 mm around colonies), reverse yellowish grey (3D2). Colonies on CY20S white (3A1) with a tint of yellowish white (3A2), flat to slightly raised, texture downy, granular or floccose, sporulation abundant, margins entire, exudate absent, soluble pigment absent, reverse light yellow (4A5). *Sclerotia* were present after 4 wk of cultivation in NRRL 58614 and CCF 5847, absent in CCF 3962^{T}, CCF 4654 and CCF 5693. Dark brown to purple sclerotia covered by felt of mycelium were observed on CYA in NRRL 58614 and CCF 5847, and on MEA in CCF 5847. No sclerotia were observed on CZA and CY20S.

Micromorphology: Conidial heads radiate, biseriate. Diminutive conidiophores occasionally present. *Stipes* (excluding diminutive) hyaline, smooth-walled, occasionally finely roughened, usually non-septate, occasionally with septa, (40–)110–260(–380) × (3–)3.5–5(–6) µm, *vesicles* predominantly globose, sometimes subglobose, (7–)10–17(–23) µm diam, *metulae* cylindrical or wedge-shaped (V-shaped), (4–)5–6.5(–8) µm long, covering three quarters to entire surface of vesicle; *phialides* ampulliform, (4–)5–6(–6.5) µm long. *Conidia* globose to subglobose, (3–)3.5–4(–4.5) (3.7.± 0.3 µm) × (3–)3.5–4(–4.5) (3.5 ± 0.2 µm), smooth-walled, rarely finely roughened.

Diagnosis: Aspergillus pragensis is phylogenetically basal to *A. subalbidus*, *A. tenebricus* and *A. taichungensis*. Together with *A. magnus*, it is unique by its small colony diameters on all media, especially on CZA. *Aspergillus pragensis* and *A. magnus* can be easily distinguished by colony colour and strikingly different micromorphology (Fig. 5, Fig. 6). *Aspergillus subalbidus, A. taichungensis*, *A. tenebricus* and *A. neotritici* can be differentiated from *A. pragensis* by their ability to grow at 35 °C or higher temperatures (Table 6). *Aspergillus pragensis* differs from *A. dobrogensis, A. magnus* and *A. campestris* by its shorter and narrower stipes, shorter metulae and smaller vesicles (Table 5).

Ecology (only records verified by DNA sequencing): The species is known from indoor environments (indoor air, carpet, dust), food (rice bran), clinical samples and outdoor air. It has been isolated in Canada, Czech Republic, South Korea and the USA (Fig. 12, Table 1, Supplementary Table S3).

Aspergillus subalbidus Visagie, Hirooka & Samson, Stud. Mycol. 78: 101. 2014. MycoBank MB 809190. Fig. 19.

Holotype: CBS H-21807. Culture ex-type: CBS 567.65^{T} = NRRL 312 = IMI 230752 = ATCC 16871 = CCF 5822.

Colony diam, 25 °C, 7 d / 14 d (mm): MEA: 11–17 / 18–30; CYA: 14–24 / 24–42; CZA: 8–18 / 16–25; CY20S: 18–27 / 25–45.

Cardinal temperatures (on MEA, after 2 wk): Aspergillus subalbidus germinates or grows restrictedly at 10 °C (3–9 mm). The optimum growth temperature is between 25 °C (18–30 mm) and 30 °C (9–29 mm). Only eight out of 12 tested strains (CBS 567.65^{T}, FMR 15736, NRRL 58123, FMR 15733, CCF 5643, NRRL 4809, CCF 5697, CCF 6197) were able to grow at 35 °C (2–22 mm) and only three out of 12 tested strains (CCF 5643, CCF 5697 and FMR 15733) were able to grow at 37 °C (3–9 mm). No growth at 40 °C.

Culture characteristics (at 25 °C after 2 wk): Colonies on MEA white (4A1) to yellowish white (2A2, 3A2, 4A2), greyish yellow (4B3) in CBS 112449 and orange grey (5B2) in FMR 15877, flat, slightly raised to crateriform, texture floccose to granular, downy or fluffy, sporulation abundant, margins entire, less frequently slightly irregular or erose, exudate absent, soluble pigment absent, reverse greyish yellow (4B5), light yellow (4A5) or reddish orange (7B8) in the centre, pale yellow (4A3) or light orange (5A4) on margins. Colonies on CYA white (4A1), yellowish white (2A2, 3A2, 4A2), yellowish grey (4B2), brownish grey (8C2) or greyish brown (8E3) with white (8A1) margins, flat or centrally raised, texture granular, floccose, velvety or downy, sporulation abundant, margins entire, less frequently delicately undulate or erose, reverse brownish orange (5C4, 5C5), greyish yellow

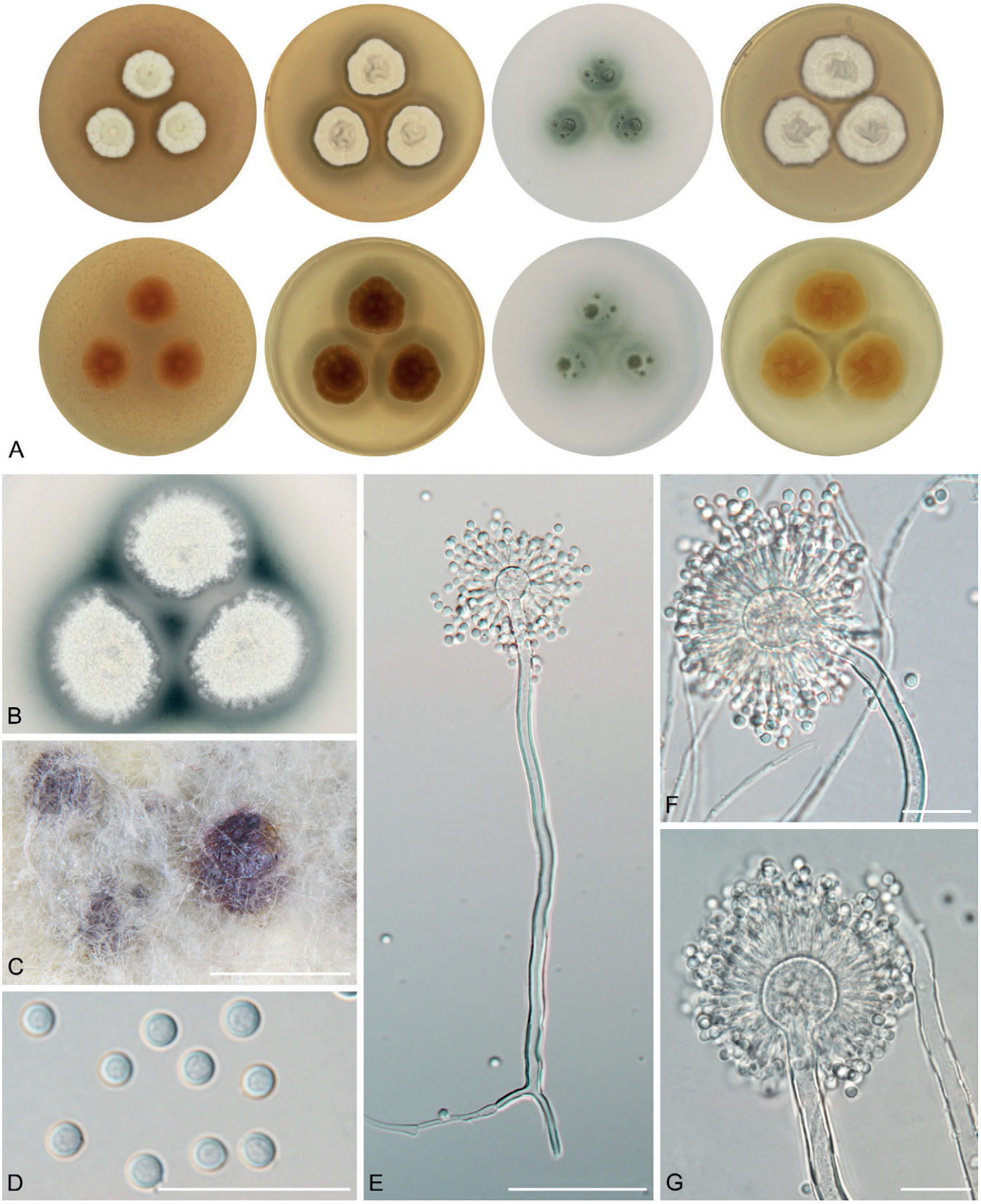

Fig. 18. Macromorphology and micromorphology of *Aspergillus pragensis*. **A.** Colonies after 14 d at 25 °C, left to right: MEA, CYA, CZA, CY20S. **B.** Soluble pigment produced on CZA (photograph taken after 28 d of cultivation). **C.** Sclerotia produced on CYA (photograph taken after 28 d of cultivation). **D.** Conidia. **E–G.** Conidiophores. Scale bars: C = 500 µm; D, F, G = 20 µm; E = 50 µm.

(4B4, 4B5, 4B6) or dark blond (5D4) in the centre, light yellow (4A4, 4A5) or golden brown (5D7) on margins, exudate absent, soluble pigment brown in some strains with varying intensity or location after 4 wk: central area between colonies in CCF 4913, CBS 112449, CCF 5697 and CBS 567.65^{T}; 3–4 mm large circle around colonies in NRRL 58123 and CCF 5698; 5–6 mm large circle around colonies in CCF 5643; slightly pigmented areas around sclerotia in strain CCF 6199; rusty brown soluble pigment was present in strain CCF 6197 (6–7 mm around colonies). Colonies on CZA white (4A1), yellowish white (1A2, 2A2, 3A2),

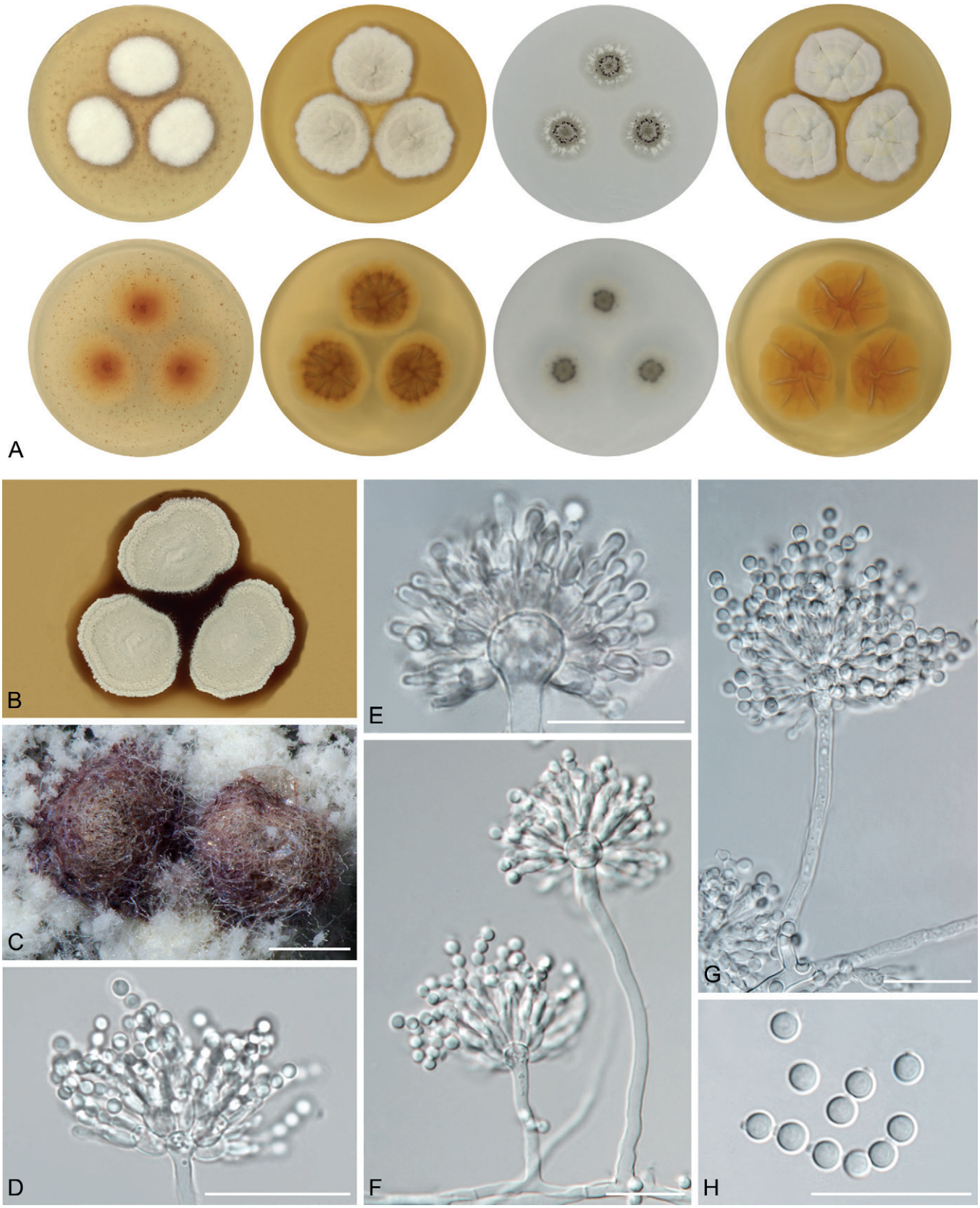

Fig. 19. Macromorphology and micromorphology of *Aspergillus subalbidus*. **A.** Colonies after 14 d at 25 °C, left to right: MEA, CYA, CZA, CY20S. **B.** Soluble pigment produced on CYA (photograph taken after 28 d of cultivation). **C.** Sclerotia produced on CZA (photograph taken after 28 d of cultivation). **D–G.** Conidiophores. **H.** Conidia. Scale bars: C = 250 µm; D–H = 20 µm.

greyish yellow (4B3) or reddish grey (7B2) in strain DTO 196-E4, flat or submerged, floccose, waxy or granular, sporulation usually abundant, weak in CCF 5696, CCF 6199, CCF 5642 and CCF 6197, margins entire, less frequently delicately undulate or erose, reverse pale yellow (3A3, 4A3), greyish brown (5E3, 5F3) or greyish yellow (4B3), exudate absent, soluble pigment present in some strains after 4 wk: dark green to black in FMR 15736, NRRL 58123, CCF 5643 (all over the Petri dish), in the central area between colonies in CBS 567.65^{T}, weak greyish green soluble pigment was present in the central area between colonies and

slightly around colonies in NRRL 5214, and dark brown soluble pigment was present in DTO 196-E4 (3 mm around colonies). Colonies on CY20S white (4A1), yellowish white (2A2, 3A2, 4A2) or yellowish grey (4B2), flat or centrally raised, irregularly folded, texture floccose, less frequently granular, downy or fluffy, sporulation abundant, margins entire, less frequently erose or undulate, exudate absent, soluble pigment absent, reverse brownish orange (5C5, 5C6), light yellow (4A5), greyish yellow (4B4, 4B5, 4B6) or reddish yellow (4A6) in the centre, light yellow (4A4, 4A5) on margins. *Sclerotia* were produced superficially, less commonly covered by felt of mycelium (NRRL 4809 and CCF 6199 on CZA). After 4 wk of cultivation, they were observed in CBS 567.65^{T}, NRRL 4809, FMR 15877, CCF 6197, CCF 6911, NRRL 5214 and CBS 112449, absent in CCF 5642, CCF 5696, DTO 196-E4, FMR 15733, CCF 4913, CCF 5848, CCF 5697, CCF 6205, CCF 5643, CCF 5698, NRRL 58123 and FMR 15736. Dark brown sclerotia were observed on MEA in FMR 15877, CCF 6197 and CCF 6199, on CYA in CBS 567.65^{T}, CCF 6197, CCF 6199, NRRL 5214 and CBS 112449, on CZA in CCF 6197 and on CY20S in CCF 6197. Brown sclerotia on CZA were observed in CBS 112449, on CY20S in FMR 15877, and sclerotia in various shades of brown were observed on CZA in FMR 15877.

Micromorphology: Conidial heads radiate, biseriate. Diminutive conidiophores occasionally present. *Stipes* (excluding diminutive) hyaline, smooth-walled, occasionally finely roughened, usually non-septate, (20–)50–330(–730) × (2.5–)3–8(–10) µm, *vesicles* globose or subglobose, (5–)7–23(–31) µm diam, *metulae* cylindrical or wedge-shaped (V-shaped), (4–)6–11(–16.5) µm long, usually covering the entire surface of vesicle; *phialides* ampulliform, (3.5–)4.5–6(–7.5) µm long. *Conidia* globose to subglobose, (3–)3.5–4(–4.5) (3.7 ± 0.3 µm) × (3–)3.5–4(–4.5) (3.5 ± 0.3 µm), smooth-walled, rarely finely roughened.

Diagnosis: Aspergillus subalbidus is closely related to *A. taichungensis* and *A. tenebricus*. *Aspergillus taichungensis* differs from *A. subalbidus* by its larger colony diameters on MEA, CYA, CY20S, and by its pastel yellow colonies and yellow soluble pigment produced by some strains on CYA and MEA (Table 4). *Aspergillus tenebricus* has longer phialides and metulae than *A. subalbidus*. *Aspergillus subalbidus* differs from *A. dobrogensis*, *A. magnus*, *A. neotritici*, *A. candidus* and *A. campestris* by its shorter and narrower stipes and smaller vesicles (Table 5, Fig. 6). *Aspergillus pragensis* and *A. magnus* colonies have a smaller diameter compared to *A. subalbidus*. *Aspergillus taichungensis* and *A. neotritici* can be differentiated by their larger colony diameters at 37 °C and by their ability to grow at 40 °C (Table 6).

Ecology (only records verified by DNA sequencing): The species is known from indoor environments (indoor air, walls, dust, carpet, settle plates), caves, food (Chinese yeast cake, vegetable lard, agriculture products), dung, soil, and from the Dubia roach (*Blaptica dubia*). It has been isolated in Botswana, Brazil, China, Federated States of Micronesia, Germany, Ghana, South Africa, Spain, Thailand and the USA (Fig. 12, Table 1, Supplementary Table S3).

Aspergillus taichungensis Yaguchi, Someya & Udagawa, Mycoscience 36: 421. 1995. MycoBank MB 434473. Fig. 20.

Holotype: PF1167. Culture ex-type: IBT 19404 = CCF 5597 = DTO 031-C6.

Colony diam, 25 °C, 7 d / 14 d (mm): MEA: 16–18 / 25–29; CYA: 22–28 / 33–43; CZA: 11–12 / 19–21; CY20S: 28–31 / 36–51.

Cardinal temperatures (on MEA, after 2 wk): Aspergillus taichungensis germinates or grows restrictedly at 10 °C (4–7 mm). The optimum growth temperature is between 20 °C (20–32 mm) and 25 °C (25–29 mm). *Aspergillus taichungensis* is able to grow at 37 °C (12–20 mm) and the maximum growth temperature is 40 °C (1–7 mm), but the strain IBT 19404^{T} only germinates at this temperature (1–2 mm).

Culture characteristics (at 25 °C after 2 wk): Colonies on MEA pastel yellow (1A4), flat, texture floccose to granular or velvety, sporulation abundant, margins entire, exudate absent, soluble pigment yellow (all over the Petri dish, predominantly around colonies) present in DTO 266-G2 and IBT 19404^{T}, reverse yellow (2A8, 3A6) or light yellow (2A5). Colonies on CYA pastel yellow (1A4) or pale yellow (1A3), flat, texture granular, sporulation abundant, margins entire to slightly undulate, exudate absent, soluble pigment yellow (all over the Petri dish) present in IBT 19404^{T} and DTO 266-G2, reverse yellow (3B8) or deep yellow (4B8) with vivid yellow margins (3A8) or yellowish brown (5D5) with reddish yellow (4A6) margins. Colonies on CZA pastel yellow (1A4), flat, texture granular or waxy, sporulation weak and located in irregular zones, margins irregular, exudate absent, soluble pigment absent, reverse pastel yellow (1A4, 2A4). Colonies on CY20S white (2A1) with a tint of yellowish white (2A2), flat to centrally raised, texture granular, downy or floccose, irregularly folded, sporulation abundant, margins entire to slightly erose, exudate absent, soluble pigment absent, reverse light yellow (4A5) or reddish yellow (4A6). *Sclerotia* produced superficially, less commonly covered by felt of mycelium (DTO 270-C9 on CY20S). After 4 wk of cultivation, they were observed in strains DTO 270-C9 and IBT 19404^{T}, absent in DTO 266-G2. Brown sclerotia were observed on CZA in strain IBT 19404^{T}, and dark brown to black sclerotia on CY20S in strain DTO 270-C9. No sclerotia were observed on MEA and CYA.

Micromorphology: Conidial heads radiate, biseriate. Diminutive conidiophores present. *Stipes* (excluding diminutive) hyaline, smooth-walled, occasionally finely roughened, usually non-septate, occasionally with septa, (15–)40–90(–215) × (2–)3–4(–5) µm, *vesicles* hemispherical, elongated, subglobose or globose, (5–)7–11(–15) µm diam, *metulae* cylindrical or wedge-shaped (V-shaped), (4–)5.5–7(–9.5) µm long, covering three quarters to entire surface of vesicle; *phialides* ampulliform, (3.5–)4.5–5.5(–6.5) µm long. *Conidia* globose to subglobose, (2.5–)3–3.5(–4) (3.4 ± 0.3 µm) × (2.5–)3–3.5(–4) (3.2 ± 0.3 µm), smooth-walled, rarely finely verrucose.

Diagnosis: Aspergillus taichungensis has the shortest and narrowest stipes and smallest vesicles in section *Candidi* (Table 5, Fig. 6). It is micromorphologically most similar to *A. tenebricus* and *A. subalbidus*, but differs from these by its pastel yellow colonies, production of yellow soluble pigment by some strains on CYA and MEA, and by its shorter stipes, metulae and phialides, and smaller vesicles. In addition, colonies of *A. taichungensis* have a larger diameter on CYA and CY20S compared to *A. tenebricus* and *A. subalbidus* (Table 4). *Aspergillus candidus*, *A. dobrogensis*, *A. magnus* and *A. pragensis* can be differentiated by their inability to grow at 37 °C. Colonies of *A. neotritici* have a larger diameter than *A. taichungensis* at 37 °C and 40 °C (Table 6).

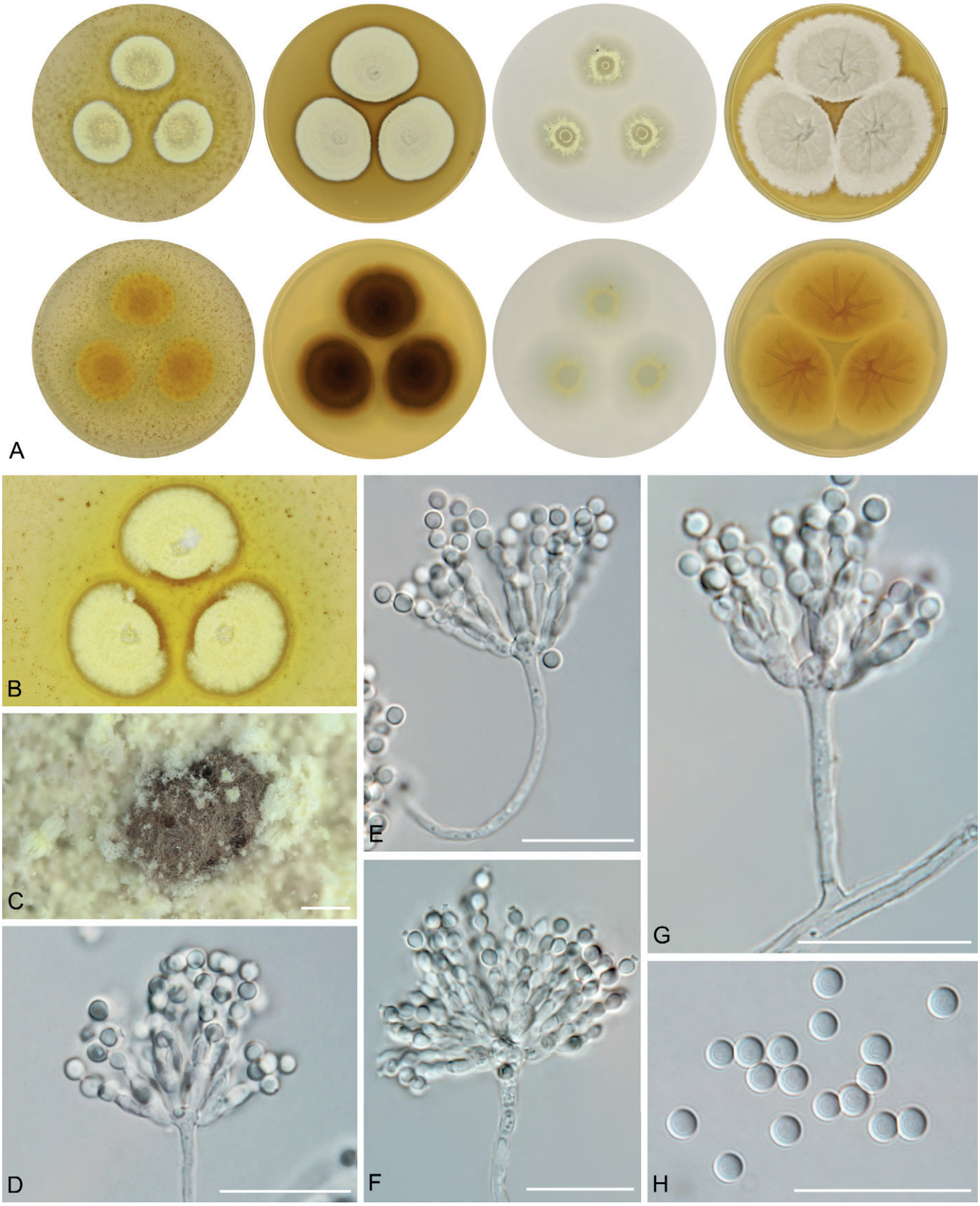

Fig. 20. Macromorphology and micromorphology of *Aspergillus taichungensis.* **A.** Colonies after 14 d at 25 °C, left to right: MEA, CYA, CZA, CY20S. **B.** Soluble pigment produced on CZA (photograph taken after 28 d of cultivation). **C.** Sclerotia produced on CY20S (photograph taken after 28 d of cultivation). **D–G.** Conidiophores. **H.** Conidia. Scale bars: C = 1.4 mm; D–H = 20 µm.

Ecology (only records verified by DNA sequencing): The species is known from soil, agriculture products, caves and house dust. It has been isolated in Iran, Mexico and Taiwan (Fig. 12, Table 1, Supplementary Table S3).

Aspergillus tenebricus Houbraken, Glässnerová & Hubka**, *sp. nov.*** MycoBank MB 844203. Fig. 21.

Etymology: Latin adj. *tenebricus -a -um*, referring to dark soluble pigment which is produced on CYA and CZA unlike its close relative *A. taichungensis*.

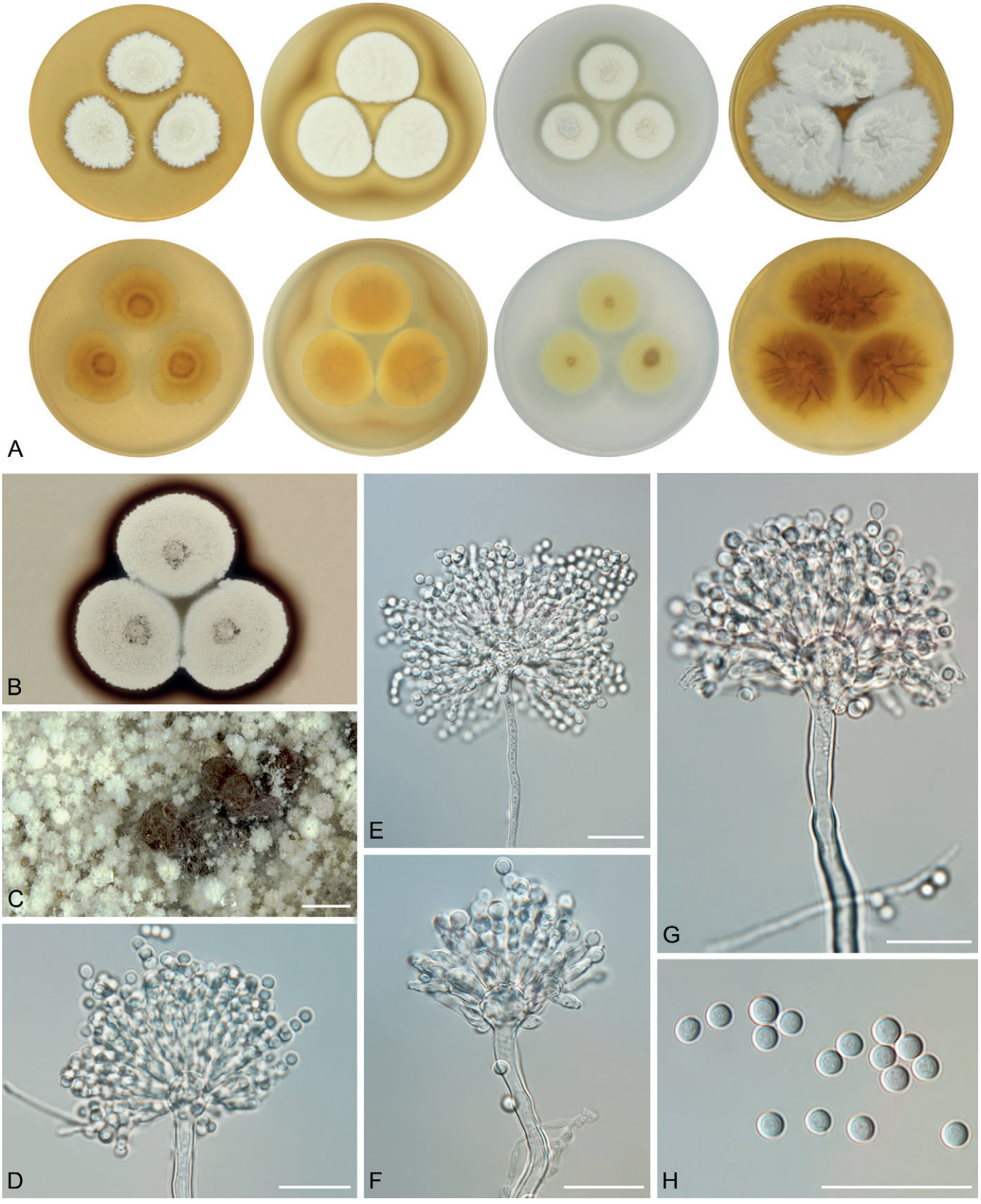

Fig. 21. Macromorphology and micromorphology of *Aspergillus tenebricus*. **A.** Colonies after 14 d at 25 °C, left to right: MEA, CYA, CZA, CY20S. **B.** Soluble pigment produced on CZA (photograph taken after 28 d of cultivation). **C.** Sclerotia produced on CZA (photograph taken after 28 d of cultivation). **D–G.** Conidiophores. **H.** Conidia. Scale bars: C = 1 mm; D–H = 20 µm.

Typus: **South Africa**, Robben Island, soil, 2015, collected by P.W. Crous and isolated by M. Meijer (**holotype** PRM 957108 (dried culture, metabolically inactive), **isotypes** PRM 957109–957110, culture ex-type DTO 337-H7 = CBS 147048).

Colony diam, 25 °C, 7 d / 14 d (mm): MEA: 19–21 / 26–33; CYA: 19–23 / 29–34; CZA: 12–14 / 22–24; CY20S: 28–30 / 48–52.

Cardinal temperatures (on MEA, after 2 wk): Aspergillus tenebricus is able to grow at 10 °C (9–11 mm). The optimum growth

temperature is 25 °C (26–33 mm). Strains DTO 337-H7^T and DTO 440-E2 are able to grow at 37 °C (7–12 mm) in contrast to strain DTO 440-E1. No growth at 40 °C.

Culture characteristics (at 25 °C after 2 wk): Colonies on MEA white (4A1) to yellowish white (4A2, 2A2), flat, texture floccose, sporulation abundant, margins slightly erose, exudate absent, soluble pigment absent, reverse greyish yellow (4B4). Colonies on CYA yellowish white (4A2), flat with slight radial folding, texture granular, sporulation abundant, margins entire, exudate absent, soluble pigment dark brown after 4 wk (3–6 mm large circle around colonies), reverse light yellow (4A5, 4A4) or dark blond (5D4). Colonies on CZA white (2A1) to yellowish white (2A2), flat, texture granular, sporulation abundant, margins entire, exudate absent, soluble pigment dark brown after 4 wk (3–5 mm large circle around colonies), reverse pale yellow (3A3). Colonies on CY20S white (2A1), flat, texture granular to floccose, irregularly folded, sporulation abundant, margins slightly erose or entire, exudate absent, soluble pigment absent, reverse greyish yellow (4C6) with pastel yellow (3A4) margins. *Sclerotia* were produced superficially and only on CZA after 4 wk of cultivation. Brown sclerotia were observed in strains DTO 440-E1 and DTO 337-H7^T, and absent in DTO 440-E2. No sclerotia were observed on MEA, CYA and CY20S in any of the examined isolates.

Micromorphology: Conidial heads radiate, biseriate. Diminutive conidiophores present. *Stipes* (excluding diminutive) hyaline, smooth-walled, occasionally finely roughened, usually non-septate, occasionally with septa, (30–)80–140(–310) × (2.5–)3.5–5(–6.5) µm, *vesicles* subglobose to globose, (8.5–)11–18(–27) µm diam, *metulae* cylindrical or wedge-shaped (V-shaped), (7–)8–12(–14) µm long, covering three quarters to entire surface of vesicle; *phialides* ampulliform, (5.5–)6–7(–8.5) µm long. *Conidia* subglobose to globose, (3–)3.5–4(–4.5) (3.8 ± 0.2 µm) × (3–)3.5–4(–4.5) (3.6 ± 0.2 µm), smooth-walled, rarely finely roughened.

Diagnosis: Aspergillus tenebricus is closely related to *A. taichungensis* and *A. subalbidus.* It has larger vesicles and longer phialides and metulae than *A. taichungensis*. *Aspergillus tenebricus* also produces a dark brown soluble pigment on CYA and CZA after 4 wk compared to *A. taichungensis,* which can produce a yellow soluble pigment on CYA and MEA. The length of phialides and metulae of *A. tenebricus* is comparable to *A. dobrogensis*, *A. campestris* and *A. magnus* but longer than other species (Table 5, Fig. 6). The colonies of *A. taichungensis* have a larger diameter than *A. tenebricus* on CYA and CY20S (Table 4). *Aspergillus candidus*, *A. dobrogensis*, *A. magnus* and *A. pragensis* can be differentiated by their inability to grow at 35–37 °C while colonies of *A. neotritici* and *A. taichungensis* have a larger diameter than *A. tenebricus* at 37 °C (Table 6).

Ecology (only records verified by DNA sequencing): The species is known only from soil. It has been isolated in Australia and South Africa (Fig. 12, Table 1).

DISCUSSION

A polyphasic approach (or consilient concept of species) incorporating phylogeny, morphology and/or extrolite data is currently a standard for species delimitations in *Aspergillus* (Samson *et al.* 2014). A key part of this approach is represented by phylogenetic methods, which are implemented in practice by different methodologies and approaches. To revise species limits and explore the intraspecific variability, we gathered a hitherto largest collection of section *Candidi* members (n = 113). To deal with conflicting or variable results from various methods and to maintain some consistency in the decision-making process about species limits, we defined an integrative approach consisting of four main components, three of which should be met to support the species (see Results section; Table 3). Two out of four criteria in this approach were devoted to MSC methods. We considered the results of STACEY to some extent superior to other MSC methods as it is based on several genes and thus it can better accommodate incomplete lineage sorting and similar phenomena. The criterion based on single-locus MSC methods required that the species is supported by the majority of single-locus MSC analyses in its exactly defined form or split into smaller entities, but without any admixture with neighbouring species/populations. Variability of results from single-gene MSC methods is relatively common between loci and settings, especially within genetically highly variable species. Oversplitting and conflicting delimitation results within specific lineages usually indicate ongoing gene flow and recombination within this lineage as previously observed for instance in *A. iizukae* (Sklenář *et al.* 2021), *A. restrictus*, *A. penicillioides* (Sklenář *et al.* 2017) and *A. udagawae* (Hubka *et al.* 2018a). Thus, splitting of species into multiple smaller lineages by one or several single-gene MSC methods is not a contradiction of a broader species definition. But the delimitation of "species" that involves some strains/populations from neighbouring species delimited by the majority of other methods is a clear conflict.

Among existing species, the least support was observed for *A. dobrogensis*. Its delimitation was clearly supported by GCPSR and by one scenario in STACEY, but support from other MSC methods was low (Fig. 3). Its delimitation was only supported by some models used in DELINEATE (Fig. 11) and morphological support was also ambiguous. The dimensions of the majority of micromorphological characters were larger in *A. dobrogensis* than in *A. candidus* (Fig. 6) and the species also has a slightly larger diameter of colonies at 25 °C than *A. candidus* (Table 4) in agreement with observations of Hubka *et al.* (2018b). However, we identified some isolates which were phenotypically indistinguishable from *A. candidus* (Fig. 7). We can conclude that we observe a clear trend towards the formation of larger colonies and conidiophores in *A. dobrogensis* compared to *A. candidus.* Because we did not observe any conflict between single-gene phylogenies, we decided not to synonymize these species. Recently, we made a similar decision regarding *A. polyporicola* and *A. spelaeus* in section *Flavipedes* (Sklenář *et al.* 2021). These two species were proposed by Hubka *et al.* (2015) based on phylogeny and the differences in their ecology and production of accessory conidia. After obtaining additional strains, it was shown that mentioned species are not distinguishable as previously thought, but they were retained as cryptic species (morphologically indistinguishable species which form a separate phylogenetic lineages and can be distinguished by molecular and phylogenetic methods) supported by GCPSR, STACEY and some other MSC methods.

Previous studies dealing with species boundaries in section *Candidi* contained only the ex-type strain of *A. campestris* (CBS 348.81) in the phylogenetic analyses (Varga *et al*. 2007, Hubka *et al*. 2014, Visagie *et al*. 2014, Hubka *et al*. 2018b). Among seven strains of this species included in the present study, we identified relatively high intraspecific variability. There were several subclades

in the trees without any specific morphological features that would trace the phylogenetic pattern. All strains of *A. campestris* were also lumped together by STACEY and DELINEATE analyses further supporting the broad concept of this species. It is apparent from the example of deviating the *RPB2* sequence of IBT 17867 that the multi-locus MSC method STACEY can better deal with incongruent phylogenies and incomplete lineage sorting. This method correctly lumped this strain with *A. campestris* and resolved the whole species as monophyletic (Fig. 3) in contrast to polyphyletic resolution in ML and BI trees (Fig. 1).

In the remaining species, the species delimitation results were either very clear and consistent (*A. magnus*, *A. neotritici* and *A. pragensis*) or species limits were identified by a combination of approaches. Incongruences between single-gene phylogenies basically did not give much space for a different solution in *A. tenebricus* and *A. taichungensis* than that proposed here (Figs 1–3). The most controversial was the inclusion of the basal clade "pop 6" in *A. subalbidus*. This clade was delimited as separate species using GCPSR, and one half of MSC methods including one STACEY scenario. Interestingly, in models simulated in DELINEATE, *A. dobrogensis* has never been delimited from *A. candidus* when this subpopulation was treated as an integral part of *A. subalbidus*. If this population was segregated from *A. subalbidus*, DELINEATE also supported segregation of DTO 266-G2 (*A. taichungensis* population "pop 2", Fig. 11) from *A. taichungensis*. In the case of "pop 6" where delimitation results were very ambiguous, we followed the results of phenotypic studies which did not support delimitation of "pop 6" from *A. subalbidus* in contrast to a pair *A. dobrogensis* and *A. candidus*. We also believe that ambiguous support of "pop 6" may be further compromised in future with the addition of further isolates from other localities. These are the main reasons why we decided to be taxonomically conservative and not describe this potential species.

In general, the studies of intraspecific variability in *Aspergillus* are relatively rare and limited to a few extensively studied species or species complexes (Peronne *et al.* 2006, Drott *et al.* 2021, Lofgren *et al.* 2021, Bian *et al*. 2022, Sklenář *et al*. 2022). In this aspect, the present study is unique in showing both genetic and phenotypic variability in multiple markers and characters across strains of several related species. We showed that dimensions of morphological features, morphology of colonies and cardinal temperatures display significant variability within some species. Gathering of a considerable number of strains is needed to capture the full spectrum of variability and to identify taxonomically informative features. We also observed that atypical strains, significantly deviating from values typical for the whole species, are relatively common. This fact also contributed to the proposal of *A. tritici* which was described based on a single strain showing numerous atypical characters. Before the molecular era, such strains were frequently a cause of erroneous taxonomic conclusions and descriptions of superfluous species. For instance, we can find many examples where a single atypical isolate was proposed as a new species based on its inability to develop normal ascomata, or production of atypical ascospores, conidia and other characters. Such cases were very common especially in sections *Aspergillus* (Hubka *et al.* 2013a, Chen *et al.* 2017) and *Nidulantes* (Chen *et al.* 2016, Hubka *et al.* 2016) and most of these species were synonymized in the molecular era. Exceptionally, these species names, proposed on the basis of incorrect assumptions about their uniqueness, provide a name for the whole species thanks to the priority rules. In these cases, the type is morphologically dissimilar from other representatives of the same species (*e.g. A. proliferans*). This would be also the case of *A. tritici*, but this species name was not validly published. We redescribed this species in the present study as *A. neotritici* for which we selected a holotype better representing typical species morphology (see section Taxonomy).

We believe that collecting more strains or sequencing more genes in future will help to better understand speciation processes in section *Candidi* and to resolve persistent ambiguities in the definition of species limits in some species. It is possible that the markers used in this study are suboptimal for section *Candidi*, and that they do not reflect the predominant phylogenetic signal that would be detected when analysing more markers or the entire genomes. It is believed that the phylogenetic methods spanning the whole genome will allow for a systematic and comparable metric of species differentiation in fungi. Reciprocal monophyly and high level of concordance between thousands of markers on the genome scale should allow differentiation between processes such as recombination, incomplete lineage sorting and speciation in most cases (Kobmoo *et al.* 2019, Matute & Sepúlveda 2019, Mavengere *et al.* 2020). The differentiation of these processes is non-trivial in practice, especially if a low number of markers and strains per species are available, as this study has shown.

DECLARATION ON CONFLICT OF INTEREST

The authors declare that there is no conflict of interest.

ACKNOWLEDGEMENTS

The project was supported by Czech Ministry of Health (grant NU21-05-00681), the Charles University Research Centre program no. 204069 and Czech Academy of Sciences Long-term Research Development Project (RVO: 61388971). Kateřina Glässnerová was supported by the project of Charles University Grant Agency (GAUK140520). We are grateful to Radek Zmítko and Jan Karhan for the help with graphical adjustments of some analysis outputs. We thank Milada Chudíčková and Lenka Zídková for their invaluable assistance in the laboratory. We thank Miroslav Hyliš and Jana Nebesářová for technical assistance with scanning electron microscopy. Vit Hubka is grateful for the support from the Japan Society for the Promotion of Science Postdoctoral Fellowships for Research in Japan (Standard). This study was partially supported by the Grant-in-aid for JSPS research fellow (No. 20F20772). Cobus M Visagie was financially supported by the Future Leaders - African Independent Research fellowship programme (FLAIR, FLR\R1\201831). The FLAIR Fellowship Programme is a partnership between the African Academy of Sciences and the Royal Society funded by the UK Government's Global Challenges Research Fund. We would like to acknowledge Keith A Seifert, David Nkwe and Stephen W. Peterson who provided some strains used in this study.

REFERENCES

Becker A, Sifaoui F, Gagneux M*, et al.* (2015). Drug interactions between voriconazole, darunavir/ritonavir and tenofovir/emtricitabine in an HIV-infected patient treated for *Aspergillus candidus* lung abscess. *International Journal of STD & AIDS* **26**: 672–675.

Bian C, Kusuya Y, Sklenář F, *et al.* (2022). Reducing the number of accepted species in *Aspergillus* series *Nigri*. *Studies in Mycology* 102: under review.

Bouckaert R, Heled J, Kühnert D*, et al.* (2014). BEAST 2: a software platform for Bayesian evolutionary analysis. *PLoS Computational Biology* **10**: 1–6.

Carballo GM, Miranda JA, Arechavala A*, et al.* (2020). Onicomicosis en paciente inmunocompetente por *Aspergillus* sección *Candidi*. *Ars*

Medica **45**: 42–46.
Chen A, Frisvad JC, Sun B, *et al.* (2016). *Aspergillus* section *Nidulantes* (formerly *Emericella*): Polyphasic taxonomy, chemistry and biology. *Studies in Mycology* **84**: 1–118.
Chen A, Hubka V, Frisvad JC, *et al.* (2017). Polyphasic taxonomy of *Aspergillus* section *Aspergillus* (formerly *Eurotium*), and its occurrence in indoor environments and food. *Studies in Mycology* **88**: 37–135.
Christensen M (1982). The *Aspergillus ochraceus* group: two new species from western soils and a synoptic key. *Mycologia* **74**: 210–225.
Darriba D, Taboada GL, Doallo R, *et al.* (2012). jModelTest 2: more models, new heuristics and parallel computing. *Nature Methods* **9**: 772–772.
Dettman JR, Jacobson DJ, Taylor JW (2003a). A multilocus genealogical approach to phylogenetic species recognition in the model eukaryote *Neurospora*. *Evolution* **57**: 2703–2720.
Dettman JR, Jacobson DJ, Turner E, Pringle A, Taylor JW (2003b) Reproductive isolation and phylogenetic divergence in *Neurospora*: comparing methods of species recognition in a model eukaryote. *Evolution* **57**: 2721–2741.
Drott MT, Rush TA, Satterlee TR, *et al.* (2021). Microevolution in the pansecondary metabolome of *Aspergillus flavus* and its potential macroevolutionary implications for filamentous fungi. *Proceedings of the National Academy of Sciences* **118**: e2021683118.
Edwards SV (2009). Is a new and general theory of molecular systematics emerging? *Evolution: International Journal of Organic Evolution* **63**: 1–19.
El-Desoky AH, Inada N, Maeyama Y, *et al.* (2021). Taichunins E–T, Isopimarane Diterpenes and a 20-nor-Isopimarane, from *Aspergillus taichungensis* (IBT 19404): Structures and inhibitory effects on RANKL-induced formation of multinuclear osteoclasts. *Journal of Natural Products* **84**: 2475–2485.
Elaasser MM, Abdel-Aziz MM, El-Kassas RA (2011). Antioxidant, antimicrobial, antiviral and antitumor activities of pyranone derivative obtained from *Aspergillus candidus*. *Journal of Microbiology and Biotechnology* **1**: 5–17.
Farias CM, De Souza OC, Sousa MA, *et al.* (2015). High-level lipase production by *Aspergillus candidus* URM 5611 under solid state fermentation (SSF) using waste from *Siagrus coronata* (Martius) Becari. *African Journal of Biotechnology* **14**: 820–828.
Fujisawa T, Barraclough TG (2013). Delimiting species using single-locus data and the Generalized Mixed Yule Coalescent approach: a revised method and evaluation on simulated data sets. *Systematic Biology* **62**: 707–724.
Fujisawa T, Aswad A, Barraclough TG (2016). A rapid and scalable method for multilocus species delimitation using Bayesian model comparison and rooted triplets. *Systematic Biology* **65**: 759–771.
Garai D, Kumar V (2013). Response surface optimization for xylanase with high volumetric productivity by indigenous alkali tolerant *Aspergillus candidus* under submerged cultivation. *3 Biotech* **3**: 127–136.
Glass NL, Donaldson GC (1995). Development of primer sets designed for use with the PCR to amplify conserved genes from filamentous ascomycetes. *Applied and Environmental Microbiology* **61**: 1323–1330.
Grazia L, Romano P, Bagni A, *et al.* (1986). The role of moulds in the ripening process of salami. *Food Microbiology* **3**: 19–25.
Guevara-Suarez M, García D, Cano-Lira J, *et al.* (2020). Species diversity in *Penicillium* and *Talaromyces* from herbivore dung, and the proposal of two new genera of penicillium-like fungi in *Aspergillaceae*. *Fungal Systematics and Evolution* **5**: 39–76.
Gupta A, Gupta G, Jain H, *et al.* (2016). The prevalence of unsuspected onychomycosis and its causative organisms in a multicentre Canadian sample of 30 000 patients visiting physicians' offices. *Journal of the European Academy of Dermatology and Venereology* **30**: 1567–1572.
Hall T (1999). *BioEdit: a user-friendly biological sequence alignment editor and analysis program for Windows 95/98/NT*. *Nucleic Acids Symposium Series*: 95–98.
Han J, Lu F, Bao L, *et al.* (2020). Terphenyl derivatives and terpenoids from a wheat-born mold *Aspergillus candidus*. *The Journal of Antibiotics* **73**: 189–193.
Heled J, Drummond AJ (2009). Bayesian inference of species trees from multilocus data. *Molecular Biology and Evolution* **27**: 570–580.
Hong S-B, Cho H-S, Shin H-D, *et al.* (2006). Novel *Neosartorya* species isolated from soil in Korea. *International Journal of Systematic and Evolutionary Microbiology* **56**: 477–486.
Houbraken J, Kocsubé S, Visagie C, *et al.* (2020). Classification of *Aspergillus*, *Penicillium*, *Talaromyces* and related genera (*Eurotiales*): An overview of families, genera, subgenera, sections, series and species. *Studies in Mycology* **95**: 5–169.
Hubka V, Kolařík M (2012). β-tubulin paralogue *tubC* is frequently misidentified as the *benA* gene in *Aspergillus* section *Nigri* taxonomy: primer specificity testing and taxonomic consequences. *Persoonia* **29**: 1–10.
Hubka V, Kubatova A, Mallatova N, *et al.* (2012). Rare and new etiological agents revealed among 178 clinical *Aspergillus* strains obtained from Czech patients and characterized by molecular sequencing. *Medical Mycology* **50**: 601–610.
Hubka V, Kolařík M, Kubátová A, *et al.* (2013a). Taxonomic revision of *Eurotium* and transfer of species to *Aspergillus*. *Mycologia* **105**: 912–937.
Hubka V, Peterson SW, Frisvad JC, *et al.* (2013b). *Aspergillus waksmanii sp. nov.* and *Aspergillus marvanovae sp. nov.*, two closely related species in section *Fumigati*. *International Journal of Systematic and Evolutionary Microbiology* **63**: 783–789.
Hubka V, Lyskova P, Frisvad JC, *et al.* (2014). *Aspergillus pragensis sp. nov.* discovered during molecular reidentification of clinical isolates belonging to *Aspergillus* section *Candidi*. *Sabouraudia* **52**: 565–576.
Hubka V, Nováková A, Kolařík M, *et al.* (2015). Revision of *Aspergillus* section *Flavipedes*: seven new species and proposal of section *Jani sect. nov. Mycologia* **107**: 169–208.
Hubka V, Nováková A, Peterson SW, *et al.* (2016). A reappraisal of *Aspergillus* section *Nidulantes* with descriptions of two new sterigmatocystin-producing species. *Plant Systematics and Evolution* **302**: 1267–1299.
Hubka V, Barrs V, Dudová Z, *et al.* (2018a). Unravelling species boundaries in the *Aspergillus viridinutans* complex (section *Fumigati*): opportunistic human and animal pathogens capable of interspecific hybridization. *Persoonia* **41**: 142–174.
Hubka V, Nováková A, Jurjević Ž, *et al.* (2018b). Polyphasic data support the splitting of *Aspergillus candidus* into two species; proposal of *Aspergillus dobrogensis sp. nov. International Journal of Systematic and Evolutionary Microbiology* **68**: 995–1011.
Jones G, Aydin Z, Oxelman B (2015). DISSECT: an assignment-free Bayesian discovery method for species delimitation under the multispecies coalescent. *Bioinformatics* **31**: 991–998.
Jones G (2017). Algorithmic improvements to species delimitation and phylogeny estimation under the multispecies coalescent. *Journal of Mathematical Biology* **74**: 447–467.
Jurjević Ž, Kubátová A, Kolařík M, *et al.* (2015). Taxonomy of *Aspergillus* section *Petersonii sect. nov.* encompassing indoor and soil-borne species with predominant tropical distribution. *Plant Systematics and Evolution* **301**: 2441–2462.
Kagiyama I, Kato H, Nehira T, *et al.* (2016). Taichunamides: prenylated indole alkaloids from *Aspergillus taichungensis* (IBT 19404). *Angewandte Chemie International Edition* **55**: 1128–1132.
Katoh K, Rozewicki J, Yamada KD (2019). MAFFT online service: multiple sequence alignment, interactive sequence choice and visualization. *Briefings in Bioinformatics* **20**: 1160–1166.
Kaur M, Singla N, Bhalla M, *et al.* (2021). *Aspergillus candidus* eumycetoma with review of literature. *Journal of Medical Mycology* **31**: 1–4.
Klich MA (2002). Biogeography of *Aspergillus* species in soil and litter. *Mycologia* **94**: 21–27.
Kato H, Sebe M, Nagaki M, *et al.* (2019). Taichunins A–D, norditerpenes from *Aspergillus taichungensis* (IBT 19404). *Journal of Natural Products* **82**: 1377-1381.
Kobayashi A, Takemura A, Koshimizu K, *et al.* (1982). Candidusin A and B: new p-terphenyls with cytotoxic effects on sea urchin embryos. *Agricultural and Biological Chemistry* **46**: 585–589.
Kobmoo N, Mongkolsamrit S, Arnamnart N, *et al.* (2019). Population genomics revealed cryptic species within host-specific zombie-ant

fungi (*Ophiocordyceps unilateralis*). *Molecular Phylogenetics and Evolution* **140**: 106580.
Kornerup A, Wanscher JH (1978). Methuen handbook of colour (ten nazev kurzivou). 3rd ed. Eyre Methuen, London.
Lanfear R, Frandsen PB, Wright AM*, et al.* (2017). PartitionFinder 2: new methods for selecting partitioned models of evolution for molecular and morphological phylogenetic analyses. *Molecular Biology and Evolution* **34**: 772–773.
Letunic I, Bork P (2021). Interactive Tree Of Life (iTOL) v5: an online tool for phylogenetic tree display and annotation. *Nucleic Acids Research* **49**: W293–W296.
Li W, Jiao F-W, Wang J-Q*, et al.* (2020). Unguisin G, a new kynurenine-containing cyclic heptapeptide from the sponge-associated fungus *Aspergillus candidus* NF2412. *Tetrahedron Letters* **61**: 1–5.
Lin Y-K, Xie C-L, Xing C-P*, et al.* (2021). Cytotoxic p-terphenyls from the deep-sea-derived *Aspergillus candidus*. *Natural Product Research* **35**: 1627–1631.
Liu YJ, Whelen S, Hall BD (1999). Phylogenetic relationships among ascomycetes: evidence from an RNA polymerse II subunit. *Molecular Biology and Evolution* **16**: 1799–1808.
Lofgren LA, Ross BS, Cramer RA, Stajich JE (2021) Combined pan-, population-, and phylo-genomic analysis of *Aspergillus fumigatus* reveals population structure and lineage-specific diversity. *bioRxiv* 2021.12.12.472145; doi: 10.1101/2021.12.12.472145.
Malhão F, Ramos AA, Buttachon S*, et al.* (2019). Cytotoxic and antiproliferative effects of Preussin, a hydroxypyrrolidine derivative from the marine sponge-associated fungus *Aspergillus candidus* KUFA 0062, in a panel of breast cancer cell lines and using 2D and 3D cultures. *Marine Drugs* **17**: 1–27.
Marchelli R, Vining L (1973). The biosyethetic origin of chlorflavonin, a flavonoid antibiotic from *Aspergillus candidus*. *Canadian Journal of Biochemistry* **51**: 1624–1629.
Masih A, Singh PK, Kathuria S*, et al.* (2016). Identification by molecular methods and matrix-assisted laser desorption ionization–time of flight mass spectrometry and antifungal susceptibility profiles of clinically significant rare *Aspergillus* species in a referral chest hospital in Delhi, India. *Journal of Clinical Microbiology* **54**: 2354–2364.
Matute DR, Sepúlveda VE (2019). Fungal species boundaries in the genomics era. *Fungal Genetics and Biology* **131**: 1–9.
Mavengere H, Mattox K, Teixeira MM*, et al.* (2020). *Paracoccidioides* genomes reflect high levels of species divergence and little interspecific gene flow. *MBio* **11**: 1–18.
Mehrotra B, Basu M (1976). Some interesting new isolates of *Aspergillus* from stored wheat and flour. *Nova Hedwigia* **27**: 597–607.
Milala M, Shehu B, Zanna H*, et al.* (2009). Degradation of agro-waste by cellulase from *Aspergillus candidus*. *Asian Journal of Biotechnology* **1**: 51–56.
Mirarab S, Bayzid MS, Warnow T (2016). Evaluating summary methods for multilocus species tree estimation in the presence of incomplete lineage sorting. *Systematic Biology* **65**: 366–380.
Moling O, Lass-Floerl C, Verweij P*, et al.* (2002). Chronic and acute *Aspergillus* meningitis. *Mycoses* **45**: 504–511.
Munden J, Butterworth D, Hanscomb G*, et al.* (1970). Production of chlorflavonin, an antifungal metabolite of *Aspergillus candidus*. *Applied Microbiology* **19**: 718–720.
Nguyen L-T, Schmidt HA, Von Haeseler A*, et al.* (2015). IQ-TREE: a fast and effective stochastic algorithm for estimating maximum-likelihood phylogenies. *Molecular Biology and Evolution* **32**: 268–274.
Nouripour-Sisakht S, Mirhendi H, Shidfar M*, et al.* (2015). *Aspergillus* species as emerging causative agents of onychomycosis. *Journal de Mycologie Medicale* **25**: 101–107.
Nováková A, Hubka V, Valinová Š*, et al.* (2018). Cultivable microscopic fungi from an underground chemosynthesis-based ecosystem: a preliminary study. *Folia Microbiologica* **63**: 43–55.
O'Donnell K (1993). *Fusarium* and its near relatives. In: *The Fungal Holomorph: Mitotic, Meiotic and Pleomorphic Speciation in Fungal Systematics* (Reynolds DR, Taylor JW, eds). CAB International, Wallingford: 225–233.
O'Donnell K, Cigelnik E (1997). Two divergent intragenomic rDNA ITS2 types within a monophyletic lineage of the fungus *Fusarium* are nonorthologous. *Molecular Phylogenetics and Evolution* **7**: 103–116.
Oh H, Gloer JB, Wicklow DT, Dowd PF (1998). Arenarins A−C: new cytotoxic fungal metabolites from the sclerotia of *Aspergillus arenarius*. *Journal of Natural Products* **61**: 702–705.
Papavizas G, Christensen C (1960). Grain storage studies. XXIX. Effect of invasion by individual species and mixtures of species of *Aspergillus* upon germination and development of discolored germs in wheat. *Cereal Chemistry* **37**: 197–203.
Paradis E, Claude J, Strimmer K (2004). APE: analyses of phylogenetics and evolution in R language. *Bioinformatics* **20**: 289–290.
Paradis E (2010). pegas: an R package for population genetics with an integrated–modular approach. *Bioinformatics* **26**: 419–420.
Perrone G, Susca A, Epifani F*, et al*. (2006). AFLP characterization of Southern Europe population of *Aspergillus* section *Nigri* from grapes. *International Journal of Food Microbiology* **111**: S22–S27.
Peterson SW (2008). Phylogenetic analysis of *Aspergillus* species using DNA sequences from four loci. *Mycologia* **100**: 205–226.
Pitt JI, Hocking AD (1997). *Aspergillus* and related teleomorphs. In: *Fungi and Food Spoilage* (Pitt JI,Hocking AD, eds). Springer, London: 339–416.
R Core Team (2021). R: A language and environment for statistical computing, Vienna, Austria.
Rahbæk L, Frisvad JC, Christophersen C (2000) An amendment of *Aspergillus* section *Candidi* based on chemotaxonomical evidence. *Phytochemistry* **53**: 581–586.
Raper KB, Fennell DI (1965). *The genus Aspergillus.* Baltimore, Williams & Wilkins.
Reid NM, Carstens BC (2012). Phylogenetic estimation error can decrease the accuracy of species delimitation: a Bayesian implementation of the general mixed Yule-coalescent model. *BMC Evolutionary Biology* **12**: 1–11.
Ronquist F, Teslenko M, Van Der Mark P*, et al.* (2012). MrBayes 3.2: efficient Bayesian phylogenetic inference and model choice across a large model space. *Systematic Biology* **61**: 539–542.
Samson RA, Gams W (1985). Typification of the species of *Aspergillus* and associated teleomorphs. In: *Advances in Penicillium and Aspergillus systematics* (Samson RA, Pitt JI, eds). Plenum Press, New York: 31–54.
Samson RA, Visagie CM, Houbraken J*, et al.* (2014). Phylogeny, identification and nomenclature of the genus *Aspergillus*. *Studies in Mycology* **78**: 141–173.
Shan T, Wang Y, Wang S*, et al.* (2020). A new p-terphenyl derivative from the insect-derived fungus *Aspergillus candidus* Bdf-2 and the synergistic effects of terphenyllin. *PeerJ* **8**: e8221.
Sklenář F, Jurjević Ž, Zalar P*, et al.* (2017). Phylogeny of xerophilic aspergilli (subgenus *Aspergillus*) and taxonomic revision of section *Restricti*. *Studies in Mycology* **88**: 161–236.
Sklenář F, Jurjević Ž, Houbraken J*, et al.* (2021). Re-examination of species limits in *Aspergillus* section *Flavipedes* using advanced species delimitation methods and description of four new species. *Studies in Mycology* **99**: 1–30.
Sklenář F, Glässnerová K, Jurjević Ž, *et al*. (2022). Taxonomy of *Aspergillus* series *Versicolores*: species reduction and lesson learned about intraspecific variability. *Studies in Mycology* **102**: under revision.
Sukumaran J, Holder MT, Knowles LL (2021). Incorporating the speciation process into species delimitation. *PLoS Computational Biology* **17**: 1–19.
Sunesen L, Stahnke L (2003). Mould starter cultures for dry sausages-selection, application and effects. *Meat Science* **65**: 935–948.
Swofford DL (2003) PAUP* Phylogenetic analysis using parsimony, (*and other methods); version 4.0 b10; Sunderland, Sinauer Associates.
Taylor JW, Jacobson DJ, Kroken S*, et al.* (2000). Phylogenetic species recognition and species concepts in fungi. *Fungal Genetics and Biology* **31**: 21–32.
Thom C, Raper K (1945). *A Manual of the Aspergilli.* Baltimore, Williams & Wilkins.
Turland NJ, Wiersema JH, Barrie FR*, et al.* (2018). *International Code of Nomenclature for algae, fungi, and plants (Shenzhen Code) adopted*

by the Nineteenth International Botanical Congress Shenzhen, China, July 2017. Koeltz Botanical Books.
Van Rossum G, Drake F (2019). Python language reference, version 3. *Python Software Foundation*.
Varga J, Frisvad JC, Samson RA (2007). Polyphasic taxonomy of *Aspergillus* section *Candidi* based on molecular, morphological and physiological data. *Studies in Mycology* **59**: 75–88.
Visagie CM, Goodwell M, Nkwe D (2021). *Aspergillus* diversity from the Gcwihaba Cave in Botswana and description of one new species. *Fungal Systematics and Evolution* **8**: 81–89.
Visagie CM, Hirooka Y, Tanney JB*, et al.* (2014). *Aspergillus*, *Penicillium* and *Talaromyces* isolated from house dust samples collected around the world. *Studies in Mycology* **78**: 63–139.
Visagie CM, Yilmaz N, Renaud JB*, et al.* (2017). A survey of xerophilic *Aspergillus* from indoor environment, including descriptions of two new section *Aspergillus* species producing eurotium-like sexual states. *MycoKeys* **19**: 1–30.
Wang D, Qu P, Zhou J*, et al.* (2020). p-Terphenyl alcohols from a marine sponge-derived fungus, *Aspergillus candidus* OUCMDZ-1051. *Marine Life Science & Technology* **2**: 262–267.
Wei H, Inada H, Hayashi A*, et al.* (2007). Prenylterphenyllin and its dehydroxyl analogs, new cytotoxic substances from a marine-derived fungus *Aspergillus candidus* IF10. *The Journal of Antibiotics* **60**: 586–590.
Weidenbörner M, Kunz B (1994). Contamination of different muesli components by fungi. *Mycological Research* **98**: 583–586.
White TJ, Bruns T, Lee S*, et al.* (1990). Amplification and direct sequencing of fungal ribosomal RNA genes for phylogenetics. *PCR Protocols: a Guide to Methods and Applications* **18**: 315–322.
Wickham H (2016). *ggplot2: elegant graphics for data analysis.* Verlag, New York, Springer.
Yaguchi T, Someya A, Udagawa S-I (1995). *Aspergillus taichungensis*, a new species from Taiwan. *Mycoscience* **36**: 421–424.
Yang Z (2015). The BPP program for species tree estimation and species delimitation. *Current Zoology* **61**: 854–865.
Yen G-C, Chang Y-C, Sheu F*, et al.* (2001). Isolation and characterization of antioxidant compounds from *Aspergillus candidus* broth filtrate. *Journal of Agricultural and Food Chemistry* **49**: 1426–1431.
Zhang J, Kapli P, Pavlidis P*, et al.* (2013). A general species delimitation method with applications to phylogenetic placements. *Bioinformatics* **29**: 2869–2876.
Zhou G, Sun C, Hou X*, et al.* (2021). Ascandinines A–D, indole diterpenoids, from the sponge-derived fungus *Aspergillus candidus* HDN15-152. *The Journal of Organic Chemistry* **86**: 2431–2436.

Supplementary Material: https://studiesinmycology.org/

Fig. S1. Multi-locus phylogenetic tree (*benA*, *CaM* and *RPB2* loci) of *Aspergillus* section *Candidi* comprising isolates from GenBank (Supplementary Table S3) and those included in Table 1. Best scoring Maximum Likelihood tree inferred in the IQ-Tree is shown, bootstrap values are appended to nodes, only support values higher than 70 % are shown. The ex-type strains are designated with a superscripted T and bold print.
Table S1. Comparison of micromorphological characters between species of *Aspergillus* section *Candidi* and statistical significances.
Table S2. Delimitation of isolates into populations by BPP v. 4.3.
Table S3. *Aspergillus* isolates from the section *Candidi* used in the analysis of ecology together with strains listed in Table 1.

Taxonomy of *Aspergillus* series *Versicolores*: species reduction and lessons learned about intraspecific variability

F. Sklenář[1,2*], K. Glässnerová[1], Ž. Jurjević[3], J. Houbraken[4], R.A. Samson[4], C.M. Visagie[5], N. Yilmaz[5], J. Gené[6], J. Cano[6], A.J. Chen[7], A. Nováková[2], T. Yaguchi[8], M. Kolařík[2], V. Hubka[1,2,8*]

[1]*Department of Botany, Faculty of Science, Charles University, Prague, Czech Republic;* [2]*Laboratory of Fungal Genetics and Metabolism, Institute of Microbiology, Czech Academy of Sciences, Prague, Czech Republic;* [3]*EMSL Analytical, Cinnaminson, New Jersey, USA;* [4]*Westerdijk Fungal Biodiversity Institute, Utrecht, The Netherlands;* [5]*Department of Biochemistry, Genetics, and Microbiology, Forestry and Agricultural Biotechnology Institute, University of Pretoria, Pretoria, South Africa;* [6]*Unitat de Micologia, Facultat de Medicina i Ciències de la Salut, IISPV, Universitat Rovira i Virgili, Reus, Spain;* [7]*Microbiome Research Center, Moon (Guangzhou) Biotech Ltd., Guangzhou, China;* [8]*Medical Mycology Research Center, Chiba University, Chuo-ku, Chiba, Japan*

**Corresponding author*: V. Hubka, vit.hubka@gmail.com; F. Sklenář, frantisek.sklenar@natur.cuni.cz

Abstract: *Aspergillus* series *Versicolores* members occur in a wide range of environments and substrates such as indoor environments, food, clinical materials, soil, caves, marine or hypersaline ecosystems. The taxonomy of the series has undergone numerous re-arrangements including a drastic reduction in the number of species and subsequent recovery to 17 species in the last decade. The identification to species level is however problematic or impossible in some isolates even using DNA sequencing or MALDI-TOF mass spectrometry indicating a problem in the definition of species boundaries. To revise the species limits, we assembled a large dataset of 518 strains. From these, a total of 213 strains were selected for the final analysis according to their calmodulin (*CaM*) genotype, substrate and geography. This set was used for phylogenetic analysis based on five loci (*benA*, *CaM*, *RPB2*, *Mcm7*, *Tsr1*). Apart from the classical phylogenetic methods, we used multispecies coalescence (MSC) model-based methods, including one multilocus method (STACEY) and five single-locus methods (GMYC, bGMYC, PTP, bPTP, ABGD). Almost all species delimitation methods suggested a broad species concept with only four species consistently supported. We also demonstrated that the currently applied concept of species is not sustainable as there are incongruences between single-gene phylogenies resulting in different species identifications when using different gene regions. Morphological and physiological data showed overall lack of good, taxonomically informative characters, which could be used for identification of such a large number of existing species. The characters expressed either low variability across species or significant intraspecific variability exceeding interspecific variability. Based on the above-mentioned results, we reduce series *Versicolores* to four species, namely *A. versicolor, A. creber*, *A. sydowii* and *A. subversicolor*, and the remaining species are synonymized with either *A. versicolor* or *A. creber*. The revised descriptions of the four accepted species are provided. They can all be identified by any of the five genes used in this study. Despite the large reduction in species number, identification based on phenotypic characters remains challenging, because the variation in phenotypic characters is high and overlapping among species, especially between *A. versicolor* and *A. creber*. Similar to the 17 narrowly defined species, the four broadly defined species do not have a specific ecology and are distributed worldwide. We expect that the application of comparable methodology with extensive sampling could lead to a similar reduction in the number of cryptic species in other extensively studied *Aspergillus* species complexes and other fungal genera.

Key words: *Aspergillus creber*, *Aspergillus sydowii*, *Aspergillus versicolor*, indoor fungi, multispecies coalescent model, osmotolerance, species delimitation, sterigmatocystin

Citation: Sklenář F, Glässnerová K, Jurjević Ž, Houbraken J, Samson RA, Visagie CM, Yilmaz N, Gené J, Cano J, Chen AJ, Nováková A, Yaguchi T, Kolařík M, Hubka V (2022). Taxonomy of *Aspergillus* series *Versicolores*: species reduction and lessons learned about intraspecific variability. *Studies in Mycology* **102**: 53–93. doi: 10.3114/sim.2022.102.02

Received: 29 June 2022 ; **Accepted:** 26 October 2022; **Effectively published online:** 16 November 2022

Corresponding editor: J.Z. Groenewald

INTRODUCTION

Aspergillus is an important genus of filamentous fungi with almost 450 accepted species and a large number of newly described species every year since the advent of molecular phylogenetics (Houbraken *et al.* 2020). The taxonomy of the clade comprising *A. versicolor* and related species has been turbulent and the clade is now recognized as series *Versicolores* within the section *Nidulantes*. Originally, the '*Aspergillus versicolor* group' was introduced by Thom & Church (1926) and later revised by Thom & Raper (1945) who accepted four species. Raper & Fennell (1965) then expanded the group to 18 species, but only two of those species remained in the series in its current form. Because group is not a recognized taxonomic rank, Gams *et al.* (1985) replaced groups with sections and created section *Versicolores*. Kozakiewicz (1989) reallocated seven species from section *Versicolores* to other sections based on the evaluation of conidial surface ornamentation using scanning electron microscope. Klich (1993) revised the section using cluster analysis by average linkage based on macro- and micromorphological measurements. As a result, the species removed by Kozakiewicz (1989) were transferred back to the section and the section was expanded again to contain 23 species. Peterson (2008) performed the first comprehensive revision of *Aspergillus* using DNA sequence data, including data from *benA*, *CaM*, *RPB2* and ITS-LSU region of rDNA. The preceding conceptions of the section were shattered as only *A. versicolor* and *A. sydowii* remained in the phylogenetically defined section. Other species were transferred into different sections, mainly sections *Usti* and *Nidulantes*. In addition, the whole section was considered superfluous because of its internal phylogenetic position within section *Nidulantes*. Jurjević *et al.* (2012) analyzed strains closely related to *A. versicolor* and *A. sydowii* which were collected mainly

Studies in Mycology

from the indoor environments in the USA, and obtained from the NRRL culture collection. They performed a phylogenetic analysis based on DNA sequences from six loci, accepted *A. amoenus*, *A. protuberus*, *A. sydowii*, *A. tabacinus* and *A. versicolor* as section members and proposed nine new species. As a result, the number of accepted species increased to 14. The authors also suggested that the section rank should be retained because it forms a monophyletic cluster, and the designation is broadly used in practice. Hubka *et al.* (2016) considered the concept of section *Versicolores* untenable as it formed only a clade within section *Nidulantes*, confirming the result of Peterson (2008). Houbraken *et al.* (2020) expanded the classification of *Aspergillus* with the series rank and reduced section *Versicolores* to series level. Since the expansion of series *Versicolores* by Jurjević *et al.* (2012), three additional species have been described, increasing the total number of accepted species to 17. Visagie *et al.* (2014) described *A. griseoaurantiacus* from house dust in Micronesia, Thailand and Mexico, Tsang *et al.* (2016) described *A. hongkongensis* from a human clinical sample collected in Hong Kong, and Jakšić Despot *et al.* (2017) described *A. pepii* from indoor air in a grain mill in Croatia.

The representatives of series *Versicolores* are often described as ubiquitous because they are frequently isolated from a wide range of substrates, mainly soil, indoor environments, food, feed, plants, caves, and clinical material (Domsch *et al.* 2007, Pitt & Hocking 2009, Jurjević *et al.* 2012, Zahradnik *et al.* 2013, Siqueira *et al.* 2016, Nováková *et al.* 2018). Series *Versicolores* members are xerophilic, which means that they can grow on substrates with a low water activity (a_w < 0.9) (Janda-Ulfig *et al.* 2009, González-Abradelo *et al.* 2019). The abundant presence of these species in indoor environments and bioaerosols increases their potential to pose health risks to humans (Micheluz *et al.* 2015, Géry *et al.* 2021). The spores of these species can cause allergies, aggravate asthma and they are associated with sick building syndrome (Schwab & Straus 2004, Géry *et al.* 2022). Almost all species can also produce mycotoxins, most notably sterigmatocystin, which is recognized as a potential carcinogen (class 2B - possible human carcinogen) (Veršilovskis & De Saeger 2010, Rank *et al.* 2011, Jurjević *et al.* 2013, Jakšić Despot *et al.* 2017). There are also numerous reports on the isolation of series *Versicolores* species from human and animal clinical specimens and rare cases of proven or suspected infections (Siqueira *et al.* 2016, Bongomin *et al.* 2018, Borgohain *et al.* 2019, Jia *et al.* 2019, Swain *et al.* 2020).

There are many studies reporting the isolation of bioactive compounds from series *Versicolores*, showing the great potential of these fungi for biotechnology, *e.g.* diphenyl ethers with antimicrobial and cytotoxic activity from *A. tennesseensis*, beta-glucosidase applicable in cellulose degradation from *A. versicolor*, or chitinase with antifungal activity from *A. griseoaurantiacus* (Kato *et al.* 2015, Li *et al.* 2018, Shehata *et al.* 2018, Sakhri *et al.* 2019, Danagoudar *et al.* 2021, Dobolyi *et al.* 2021, Huang *et al.* 2021). Genome sequences for seven species from the series have been deposited to the NCBI GenBank database [accessed 23rd of March 2022]. Among the most notable findings, the sterigmatocystin biosynthetic gene cluster was found to be absent for *A. sydowii*, explaining the inability of this species to produce this mycotoxin (Rank *et al.* 2011). Additionally, mating-type loci (both *MAT-1-1-1* and *MAT-1-2-1*), which are crucial for sexual development, are present in the genomes of series *Versicolores* species, suggesting their heterothallic mode of reproduction, even though the sexual state is yet to be observed (De Vries *et al.* 2017).

The correct identification of series *Versicolores* species is of great importance as evidenced by their diverse above-mentioned significances. However, a large part of these species cannot be identified morphologically due to their similarity or high intraspecific variability (Jurjević *et al.* 2012, Siqueira *et al.* 2016, Géry *et al.* 2021). Additionally, the broadly used identification method MALDI-TOF MS (matrix-assisted laser desorption ionization time-of-flight mass spectrometry) is not able to discriminate species within the series. This significantly limits the possibilities of correct identification, especially in clinical practices (Vidal-Acuña *et al.* 2018, Imbert *et al.* 2019, Shao *et al.* 2022). There is also increasing evidence that some isolates cannot be reliably identified with sequence data because BLAST similarity searches with different genes result in different identifications (our observations and personal communication). These problems may indicate that the concept of species is too narrow and motivated the present taxonomic revision.

One requirement of the species delimitation methods, which often fails to be met in studies involving fungi, is the presence of within-species variability which is ensured by the quality of sampling in terms of geography and/or substrates (Ahrens *et al.* 2016, Sklenář *et al.* 2020). Without large enough depth of sampling, boundaries between intraspecific and interspecific variability can easily be misinterpreted. Thanks to the omnipresence of series *Versicolores* and the ease of their isolation, these species represent the perfect model group for studying species limits on a large scale. For this study, we assembled a collection of more than 500 isolates from various substrates and continents. A subset of genetically unique isolates was subjected to the detailed analysis by various phylogenetic methods building upon the previous studies using this approach for *Aspergillus* (Sklenář *et al.* 2017, Hubka *et al.* 2018, Sklenář *et al.* 2021). Aside from the phylogenetic part, we also studied traditional phenotypic characters including micromorphology, macromorphology on eight cultivation media, and the growth rate at different temperatures and in an osmotic gradient. The synthesis of the resulting data and the consideration of practical taxonomic implications have led to the proposal of a drastic reduction in the number of species as detailed below.

MATERIALS AND METHODS

Strains

Some strains and/or DNA sequences were obtained from previously published studies of Jurjević *et al.* (2012) and Siqueira *et al.* (2016), which focused on the indoor environment and clinical material in the USA, respectively. Furthermore, we included strains from various countries and substrates deposited in culture collections such as CBS culture collection housed at the Westerdijk Fungal Biodiversity Institute (WI), working collection DTO of the Food and Indoor Mycology department housed at the WI, Culture Collection of Fungi, Department of Botany, Charles University (CCF, Czech Republic), working collections of the Applied Mycology group (CN) and the Forestry and Agricultural Biotechnology Institute (CMW) at the University of Pretoria (South Africa), and China General Microbiological Culture Collection Center (CGMCC, China). Additionally, we supplemented the dataset with newly isolated strains mainly originating from the indoor environment and caves. The isolation techniques mostly followed the procedures described by Jurjević *et al.* (2015), Nováková *et al.* (2012) and Nováková *et al.* (2018). Detailed information about the provenance of strains is listed in Table 1.

Table 1. *Aspergillus* series *Versicolores* strains examined in this study.

Species	Strain No.[1]	Provenance (locality, substrate, year of isolation, isolator/collector)	GenBank/ENA/DDBJ accession Nos.					
			ITS	*benA*	*CaM*	*RPB2*	*Mcm7*	*Tsr1*
A. creber	**NRRL 58592^T = IBT 32277^T = DTO 225-G7^T = CBS 145749^T**	USA, CA, indoor air, 2008, Ž. Jurjević	NR_135442	JN853980	JN854043	JN853832	JQ301890	JN853887
	EMSL 4757	USA, MO, Festus, basement, swab, 2018, Ž. Jurjević	–	ON807803	ON807940	ON808233	ON808106	ON808375
	NRRL 58672	USA, GA, indoor air, 2009, Ž. Jurjević	–	JN853992	JN854055	JN853844	JN854122	JN853878
	UTHSCSA 09-3357 = FMR 14151	USA, PA, bronchoalveolar lavage, 2009, D.A. Sutton	LN898684	LN898838	LN898761	LN898915	ON808105	ON808374
	NRRL 58675	USA, OH, indoor air, 2009, Ž. Jurjević	–	JN853994	JN854058	JN853847	JN854124	JN853891
	NRRL 58612	USA, NJ, indoor air, 2009, Ž. Jurjević	–	JN853990	JN854051	JN853840	JN854121	JN853880
	UTHSCSA 03-2409 = FMR 14132	USA, TX, hospital air, 2003, D.A. Sutton	LN898681	LN898835	LN898758	LN898912	ON808104	–
	NRRL 58607	USA, PA, indoor air, 2009, Ž. Jurjević	–	JN853989	JN854050	JN853839	JN854120	JN853890
	UTHSCSA 10-1327 = FMR 14201	USA, MN, human nail, 2010, D.A. Sutton	LN898687	LN898841	LN898764	LN898918	ON808103	–
	DTO 180-A5 = KAS 3914	South Africa, house dust, 2010, C.M. Visagie	–	ON807802	ON807939	ON808232	ON808102	ON808373
	NRRL 58601	USA, NJ, indoor air, 2009, Ž. Jurjević	–	JN853987	JN854047	JN853836	JN854119	JN853882
	S 478	Spain, Cueva del Tesoro, cave sediment, 2012, A. Nováková	–	ON807801	ON807938	ON808231	ON808101	ON808372
	DTO 357-E7	Netherlands, cystic fibrosis patient, between 2011–2013, collector unknown	–	ON807800	ON807937	ON808230	ON808100	ON808371
	NRRL 58673	USA, GA, indoor air, 2009, Ž. Jurjević	–	JN853993	JN854056	JN853845	JN854123	JN853889
	DTO 319-E4 = IBT 26409	Greenland, Pakitsoq, ice sample (approximately 11500 years old), 2014, J.C. Frisvad	–	ON807799	ON807936	ON808229	ON808099	ON808370
	S 216	Romania, Magura Cave, bat guano, 2009, A. Nováková	–	ON807798	ON807935	ON808228	ON808098	ON808369
	DTO 319-D6 = IBT 22306	USA, MD, indoor air, 2014, B. Jarvis	–	ON807797	ON807934	ON808227	ON808097	ON808368
	EMSL 4775	USA, WA, Shoreline, bathroom - swab, 2018, Ž. Jurjević	–	ON807796	ON807933	ON808226	ON808096	ON808367
	NRRL 58587	USA, CA, indoor air, 2008, Ž. Jurjević	–	JN853985	JN854042	JN853831	JN854118	JN853886
	CGMCC 3.05281	China, fruit peel, 1999, collector unknown	–	ON807795	ON807932	ON808225	ON808095	ON808366
	S 448	Spain, Cueva del Tesoro, cave sediment, 2012, A. Nováková	–	ON807794	ON807931	ON808224	ON808094	ON808365
	S 321	Slovakia, Demanovská Peace Cave, dead marten, 2011, A. Nováková	–	ON807793	ON807930	ON808223	ON808093	ON808364
	CMW-IA 29 = CMW 58631 = CN 090-F5	South Africa, Goeiehoek Silo, Gauteng, soybean, 2020, S. Bezuidenhout	–	ON807792	ON807929	ON808222	ON808092	ON808363
	UTHSCSA 14-188 = FMR 14168	USA, DE, bronchoalveolar lavage, 2014, D.A. Sutton	LN898685	LN898839	LN898762	LN898916	ON808091	–
	EMSL 4759	USA, NY, Buffalo, bathroom wall - swab, 2018, Ž. Jurjević	–	ON807791	ON807928	ON808221	ON808090	ON808362
	NRRL 58670	USA, NJ, indoor air, 2009, Ž. Jurjević	–	JN853991	JN854053	JN853842	–	JN853888
	NRRL 58584	USA, PA, indoor air, 2008, Ž. Jurjević	–	JN853984	JN854041	JN853830	–	JN853894
	NRRL 13147 = CBS 145753 = DTO 225-F4 (ex-type of *A. venenatus*)	USA, TN, toxic dairy cattle feed, 1984, B.W. Horn	JQ301896	JN854003	JN854014	JN853803	JN854129	JN853876
	EMSL 4847	USA, NJ, Trenton, office building – indoor air, 2018, Ž. Jurjević	–	ON807809	ON807947	ON808240	ON808113	ON808382

Table 1. (Continued).

Species	Strain No.[1]	Provenance (locality, substrate, year of isolation, isolator/ollector)	GenBank/ENA/DDBJ accession Nos.					
			ITS	*benA*	*CaM*	*RPB2*	*Mcm7*	*Tsr1*
	NRRL 35641 = CBS 145750 = DTO 225-G5 = IBT 32284 (ex-type of *A. puulaauensis*)	USA, HI, dead hardwood branch, 2003, D.T. Wicklow	JQ301893	JN853979	JN854034	JN853823	JN854127	JN853895
	CCF 5173	Czech Republic, Prague, mouse excrements in seed store, 2000, J. Hubert	–	OP762559	ON807946	OP762579	OP762565	OP762573
	UTHSCSA 11-1436 = FMR 14159	USA, WA, bronchoalveolar lavage, 2014, D.A. Sutton	LN898715	LN898869	LN898792	LN898946	OP688453	–
	S 376	Spain, Cueva del Tesoro, cave sediment, 2012, A. Nováková	–	ON807808	ON807945	ON808238	ON808111	ON808380
	DTO 321-G4	Netherlands, polyethylene foil, 2014, J. Houbraken	–	ON808380	ON807944	ON808237	ON808110	ON808379
	S 344	Slovakia, Šingliarova Abyss, organic matter in cave, 2008, A. Nováková	–	ON807806	ON807943	ON808236	ON808109	ON808378
	NRRL 58602	USA, WV, indoor air, 2009, Ž. Jurjević	–	JN853999	JN854048	JN853837	JN854128	JN853896
	S 191	Romania, Meziad Cave, bat droppings, 2009, A. Nováková	–	ON807805	ON807942	ON808235	ON808108	ON808377
	DTO 324-F6	Netherlands, cystic fibrosis patient, 2014, collector unknown	–	ON807804	ON807941	ON808234	ON808107	ON808376
	CGMCC 3.07849	China, 2005, substrate unknown, 2005, collector unknown	–	ON807790	ON807927	ON808220	ON808089	ON808361
	NRRL 58593	USA, CA, indoor air, 2008, Ž. Jurjević	–	JN853998	JN854044	JN853833	JN854111	JN853869
	DTO 019-A3	USA, NJ, soil, isolation date and collector unknown	–	ON807789	ON807926	ON808219	ON808088	ON808360
	UTHSCSA 10-479 = FMR 14153	USA, OH, hospital air, 2010, D.A. Sutton	LN898695	LN898849	LN898772	LN898926	ON808087	ON808359
	NRRL 230	China, soy sauce, 1917, Round	–	JN853973	JN854023	JN853812	JN854109	JN853867
	NRRL 4642	Unknown, 1969	EF652467	JN853975	EF652379	EF652203	JN854110	JN853868
	NRRL 227 = CBS 599.65 = ATCC 16853 = IMI 211379 (ex-type of *A. cvjetkovicii*)	USA, New Jersey, soil, 1915, G.W. Wilson	EF652440	EF652264	EF652352	EF652176	JN854108	JN853866
	CMW-IA 30 = CMW 58632 = CN 093-G3	South Africa, Free State, Kroonstad, maize (white), 2020, C.M. Visagie	–	ON807788	ON807925	ON808218	ON808086	ON808358
	CMW-IA 31 = CMW 58633 = CN 096-A1	South Africa, Mpumalanga, Bethal, soybean, 2020, S. Bezuidenhout	–	ON807787	ON807924	ON808217	ON808085	ON808357
	CMW-IA 27 = CMW 58629 = CN 089-A2	South Africa, Gauteng, Afrikaskop, soybean, 2020, S. Bezuidenhout	–	ON807786	ON807923	ON808216	ON808084	ON808356
	CMW-IA 33 = CMW 58635 = CN 116-D2	South Africa, Free State, Heuningspruit, sunflower, 2020, C.M. Visagie	–	ON807785	ON807922	ON808215	ON808083	ON808355
	DTO 319-F2 = IBT 28293	Denmark, Fano, seawater, 2014, E.K. Lynne	–	ON807784	ON807921	ON808214	ON808082	ON808354
	DTO 319-D2 = IBT 14828	United Kingdom, wheat, 2014, M. Hetmanski	–	ON807783	ON807920	ON808213	ON808081	ON808353
	DTO 268-C6	Uruguay, Montevideo, house dust, 2008, Z. Torrano	–	ON807782	ON807919	ON808212	ON808080	ON808352
	S 384	Spain, Nerja Cave, cave sediment, 2012, A. Nováková	–	ON807781	ON807918	ON808211	ON808079	ON808351
	CMW-IA 25 = CMW 58627 = CN 088-I9	South Africa, Gauteng, Afrikaskop, soybean, 2020, S. Bezuidenhout	–	ON807780	ON807917	ON808210	ON808078	ON808350
	CMW-IA 28 = CMW 58630 = CN 089-A3	South Africa, Gauteng, Afrikaskop, soybean, 2020, S. Bezuidenhout	–	ON807779	ON807916	–	ON808077	ON808349
	CMW-IA 26 = CMW 58628 = CN 089-A1	South Africa, Gauteng, Afrikaskop, soybean, 2020, S. Bezuidenhout	–	ON807778	ON807915	ON808209	ON808076	ON808348
	NRRL 13150 = CBS 145752 = DTO 225-F5 = IBT 32283 (ex-type of *A. tennesseensis*)	USA, TN, toxic dairy cattle feed, 1984, B.W. Horn	JQ301895	JN853976	JN854017	JN853806	JN854113	JN853872

Table 1. (Continued).

Species	Strain No.[1]	Provenance (locality, substrate, year of isolation, isolator/ollector)	GenBank/ENA/DDBJ accession Nos.					
			ITS	*benA*	*CaM*	*RPB2*	*Mcm7*	*Tsr1*
	CCF 5066	Spain, Nerja Cave, cave air, 2011, A. Nováková	–	OP762558	ON807914	OP762578	OP762564	OP762572
	CMW-IA 24 = CMW 58636 = CN 116-D4	South Africa, Free State, Heuningspruit, sunflower, 2020, C.M. Visagie	–	ON807776	ON807913	ON808207	ON808074	ON808346
	CMW-IA 23 = CMW 58625 = CN 066-E9	South Africa, Gauteng, Afrikaskop, soybean, 2020, S. Bezuidenhout	–	ON807775	ON807912	ON808206	ON808073	ON808345
	NRRL 229	Unknown, 1917, R. Thaxter	–	JN853972	JN854022	JN853811	–	JN853870
	DTO 178-C5 = KAS 3787	South Africa, house dust, 2010, C.M. Visagie	–	ON807774	ON807911	ON808205	ON808072	ON808344
	DTO 019-A6 = CBS 556.90	Japan, dried *Lentinus edodes*, 1990, J.C. Frisvad	–	ON807773	ON807910	ON808204	ON808071	ON808343
	CGMCC 3.05345	China, moon cake, 1999	–	ON807772	ON807909	ON808203	ON808070	ON808342
	CGMCC 3.05331	China, moldy oil, 1999	–	ON807771	ON807908	ON808202	ON808069	ON808341
	DTO 321-F4	Netherlands, cystic fibrosis patient material, between 2011–2013	–	ON807770	ON807907	ON808201	ON808068	ON808340
	S 475	Spain, Nerja Cave, cave air, 2012, A. Nováková	–	ON807769	ON807906	ON808200	ON808067	ON808339
	S 139	Romania, Limanu Cave, cave air, 2012, A. Nováková	–	ON807768	ON807905	ON808199	ON808066	ON808338
	S 309	Slovakia, Ardovská Cave, cave air, 2009, A. Nováková	–	ON807767	ON807904	ON808198	ON808065	ON808337
	UTHSCSA 10-71 = FMR 14200	USA, CT, bronchoalveolar lavage, 2010, D.A. Sutton	LN898703	LN898857	LN898780	LN898934	ON808064	ON808336
	UTHSCSA 09-425 = FMR 14234	USA, UT, human nail, 2009, D.A. Sutton	LN898704	LN898858	LN898781	LN898935	ON808063	ON808335
	S 371	Spain, Cueva del Tesoro, cave sediment, 2012, A. Nováková	–	ON807766	ON807903	ON808197	ON808062	ON808334
	DTO 319-F6 = IBT 31894	Japan, Noto, Peninsula, Mediterranean mussel (*Mytilus galloprovinciales*) 2014, M. Tzukamoto	–	ON807765	ON807902	ON808196	ON808061	ON808333
	NRRL 58671	USA, PA, indoor air, 2009, Ž. Jurjević	–	JN854008	JN854054	JN853843	JN854104	JN853864
	NRRL 58600 (ex-type of *A. jensenii*)	USA, MT, indoor air, 2008, Ž. Jurjević	JQ301892	JN854007	JN854046	JN853835	JN854103	JN853863
	EMSL 4720	USA, MA, Cohasset, air, apartment, 2018, Ž. Jurjević	–	ON807764	ON807901	–	ON808060	ON808332
	DTO 303-H3	Netherlands, Leerdam, surface of archive material, 2014, M. Meijer	–	ON807763	ON807900	–	ON808059	ON808331
	CMW-IA 39 = CMW 58641 = CN 138-G5	Canada, Nova Scotia, Little Lepreau, house dust, 2015, C.M. Visagie	–	ON807762	ON807899	–	ON808058	ON808330
	S 315	Slovakia, Ochtinská Aragonitová Cave, cave air, 2010, A. Nováková	–	ON807761	ON807898	–	ON808057	ON808329
	UTHSCSA 10-327 = FMR 14152	USA, PA, sputum, 2010, D.A. Sutton	LN898700	LN898854	LN898777	LN898931	–	ON808328
	CGMCC 3.05297	China, moldy shoe, 1999, collector unknown	–	ON807760	ON807897	ON808195	ON808056	ON808327
	S 317	Slovakia, Krásnohorská Cave, cave air, 2006, A. Nováková	–	ON807759	ON807896	ON808194	ON808055	ON808326
	DTO 138-B3	Germany, indoor air, 2010, collector unknown	–	–	ON807895	ON808193	ON808054	ON808325
	EMSL 4825	USA, OH, Pepper Pike, bedroom, settle plates, 2018, Ž. Jurjević	–	ON807758	ON807894	ON808192	ON808053	ON808324
	S 447	Spain, Cueva del Tesoro, cave sediment, 2012, A. Nováková	–	ON807757	ON807893	ON808191	ON808052	ON808323
	EMSL 4785	USA, NJ, Cherry Hill, office - indoor air, 2018, Ž. Jurjević	–	ON807756	ON807892	ON808190	ON808051	ON808322
	NRRL 240	USA, NY, rhizosphere of pepper plants, 1911, C.N. Jensen	–	JN854002	JN854030	JN853819	JN854102	JN853862
	NRRL 235	United Kingdom, London, paraffin, 1930, H. Raistrick	–	JN854001	JN854027	JN853816	JN854101	JN853860

Table 1. (Continued).

Species	Strain No.[1]	Provenance (locality, substrate, year of isolation, isolator/ollector)	GenBank/ENA/DDBJ accession Nos.					
			ITS	*benA*	*CaM*	*RPB2*	*Mcm7*	*Tsr1*
	NRRL 225	United Kingdom, substrate unknown, 1913, collector unknown	–	JN854000	JN854020	JN853809	JN854100	JN853858
	DTO 319-D8 = IBT 23103	Slovenia, soil salterns, 2014, N. Gunde-Cimerman	–	ON807755	ON807891	ON808189	ON808050	ON808321
	UTHSCSA 05-3600 = FMR 14136	USA, MN, sputum, 2005, D.A. Sutton	LN898698	LN898852	LN898775	LN898929	ON808049	–
	S 207	Romania, Meziad Cave, Capela, bat guano, 2010, A. Nováková	–	ON807754	ON807890	ON808188	ON808048	ON808320
A. subversicolor	**NRRL 58999^{T} = CBS 145751^{T} = DTO 225-G9^{T}**	India, Karnataka, coffee berry, 1970, B. Muthappa	JQ301894	JN853970	JN854010	JN853799	JN854069	JN853857
	DTO 353-D8 = URM 7878	Brazil, Recife, Honey of *Melipona scutellaris*, 2014, R. Barbosa	–	ON807753	ON807889	–	ON808047	ON808319
	DTO 353-A7 = URM 7877	Brazil, Recife, Honey of *Melipona scutellaris*, 2014, R. Barbosa	–	ON807752	ON807888	–	ON808046	ON808318
A. sydowii	**NRRL 254^{T} = CBS 593.65^{T} = IMI 211384^{T} = NRRL 250^{T} = ATCC 16844^{T}**	USA, GA, clinical material, isolation date unknown, M.M. Harris	EF652451	LC589353	LC589325	EF652187	–	JN853897
	CMW-IA 46 = CMW 58648 = CN 164B6 = DN 86	Botswana, Gcwihaba Cave, guano-contaminated cave sediment, 2019, G. Modise & D. Nkwe	–	ON807751	ON807887	ON808187	ON808045	ON808317
	CMW-IA 44 = CMW 58646 = CN 164B4 = DN 47	Botswana, Gcwihaba Cave, guano-contaminated cave sediment, 2019, G. Modise & D. Nkwe	–	ON807750	ON807886	ON808186	ON808044	ON808316
	CMW-IA 42 = CMW 58644 = CN 164B2 = DN 30	Botswana, Gcwihaba Cave, guano-contaminated cave sediment, 2019, G. Modise & D. Nkwe	–	ON807749	ON807885	ON808185	ON808043	ON808315
	CMW-IA 41 = CMW 58643 = CN 164B1 = DN 6	Botswana, Gcwihaba Cave, guano-contaminated cave sediment, 2019, G. Modise & D. Nkwe	–	ON807748	ON807884	ON808184	ON808042	ON808314
	S 41	Spain, near Castañar de Ibor Cave, outdoor air, 2009, A. Nováková	–	ON807747	ON807883	ON808183	ON808041	ON808313
	S 15	Spain, Cueva del Tesoro, Sala de Marco Craso, cave air, 2010, A. Nováková	–	ON807746	ON807882	ON808182	ON808040	ON808312
	UTHSCSA 06-2780 = FMR 14185	USA, MN, bronchus, 2006, D.A. Sutton	LN898721	LN898875	LN898798	LN898952	ON808039	–
	S 23	Czech Republic, Moravian Karst, New Amateur Cave, „Dóm Ráztoka“ Dome, cave sediment, 2009, A. Nováková	–	ON807745	ON807881	ON808181	ON808038	ON808311
	DTO 145-G7	Egypt, tomb of dogs, 2010, M. Meijer	–	ON807744	ON807880	ON808180	ON808037	ON808310
	DTO 268-C2	Uruguay, Montevideo, house dust, 2008, Z. Torrano	–	ON807743	ON807879	ON808179	ON808036	ON808309
	CGMCC 3.06723	China, fermented crop, 2004, collector unknown	–	ON807742	ON807878	ON808178	ON808035	ON808308
	UTHSCSA 09-1708 = FMR 14338	USA, UT, lung tissue, 2009, D.A. Sutton	LN898732	LN898886	LN898809	LN898963	ON808034	ON808307
	CMW-IA 35 = CMW 58637 = CN 117-C2	South Africa, Viljoenskroon, sunflower, 2020, C.M. Visagie & N. Yilmaz	–	ON807741	ON807877	ON808177	ON808033	ON808306
	UTHSCSA 12-934 = FMR 14210	USA, MN, bronchoalveolar lavage, 2012, D.A. Sutton	LN898725	LN898879	LN898802	LN898956	ON808032	ON808305
	UTHSCSA 11-204 = FMR 14155	USA, PA, clinical sample - eye, 2011, D.A. Sutton	LN898717	LN898871	LN898794	LN898948	ON808031	ON808304
	CGMCC 3.13937	China, shoe, 2009, collector unknown	–	ON807740	ON807876	ON808176	ON808030	ON808303
	UTHSCSA 13-2518 = FMR 14164	USA, UT, clinical sample - eye, 2013, D.A. Sutton	LN898718	LN898872	LN898795	LN898949	ON808029	ON808302

Table 1. (Continued).

Species	Strain No.[1]	Provenance (locality, substrate, year of isolation, isolator/ollector)	GenBank/ENA/DDBJ accession Nos.					
			ITS	*benA*	*CaM*	*RPB2*	*Mcm7*	*Tsr1*
	CCF 3621	Czech Republic, Olomouc, endotracheal secret of man, 2003, P. Hamal	–	FR775355	ON807875	OP762580	OP762566	OP762574
	DTO 002-H3 = CBS 117771	South Korea, Yeongi, hot pepper from pepper field, 2003, S.B. Hong	–	ON807738	ON807874	ON808174	ON808027	ON808300
	DTO 266-H9	Federated States of Micronesia, Malem, house dust, 2009, W. Law	–	ON807737	ON807873	ON808173	ON808026	–
	CCF 5063	Spain, Cueva del Tesoro, cave sediment, 2011, A. Nováková	–	FR775337	ON807872	OP762581	OP762567	OP762575
	DTO 004-G1 = CBS 118475	Netherlands, tattoo paint, isolate date and collector unknown	–	ON807735	ON807871	–	ON808024	ON808298
A. versicolor	**NRRL 238^{T} = CBS 583.65^{T} = ATCC 9577^{T} = IFO 33027^{T} = IMI 229970^{T} = JCM 10258^{T} = UAMH 4956^{T} = UAMH 9314^{T}**	USA, unknown substrate and year of isolation, V.K. Charles	EF652442	LC589363	EF652354	EF652178	JN854079	JN853911
	CMW-IA 22 = CMW 58624 = CN 054-B5	South Africa, North West Province, Ottosdal, maize (white), 2020, C.M. Visagie & N. Yilmaz	–	ON807734	ON807870	–	ON808023	ON808297
	UTHSCSA 03-3679 = FMR 14181	USA, FL, bronchoalveolar lavage, 2003, D.A. Sutton	LN898740	LN898894	LN898817	LN898971	ON808022	ON808295
	DTO 241-I4	Indonesia, surface in medical rehabilitation room, 2012, A. Sidar	–	ON807733	ON807869	ON808171	ON808021	–
	DTO 270-D1	Mexico, Sayulita, house dust, 2009, A. Amend	–	ON807732	ON807868	ON808170	ON808020	ON808296
	DTO 174-H9	Imported from Madagascar, vanilla sticks, 2012, J. Houbraken	–	ON807731	ON807867	ON808169	ON808019	ON808294
	DTO 319-E9 = IBT 28029 = ATCC 32662	USA, TX, soil, 2014, H.W. Schroeder	–	ON807730	ON807866	ON808168	ON808018	ON808293
	NRRL 13144 = NRRL A-27273	USA, TN, toxic dairy cattle feed, 1984, B.W. Horn	–	JN853949	JN854011	JN853800	JN854081	JN853915
	NRRL 3505 = CBS 602.74 = ATCC 18990 (ex-type of *A. protuberus*)	former Yugoslavia, rubber coated electrical cables, before 1968, M. Muntañola-Cvetkovic	EF652460	EF652284	EF652372	EF652196	JN854088	LC004923
	CCF 5055	Spain, Nerja Cave, cave sediment, 2011, A. Nováková	–	OP762562	OP650540	OP762584	OP762570	–
	DTO 019-D4 = CBS 601.74 = IMI 278378	former Yugoslavia, rubber coated electrical cables, before 1968, M. Muntañola-Cvetkovic	–	ON807728	ON807864	ON808166	ON808016	–
	EMSL 4703	USA, CA, Lawndale, framing below balcony, swab, 2018, Ž. Jurjević	–	ON807727	ON807863	ON808165	ON808015	–
	UTHSCSA 11-269 = FMR 14156	USA, IL, bronchoalveolar lavage, 2011, D.A. Sutton	LN898707	LN898861	LN898784	LN898938	ON808014	ON808292
	S 49	Spain, Nerja Cave, cave sediment, 2011, A. Nováková	–	ON807726	ON807862	ON808164	ON808013	ON808291
	UTHSCSA 06-2837 = FMR 14328	USA, bronchoalveolar lavage, 2006, D.A. Sutton	LN898713	LN898867	LN898790	LN898944	ON808012	–
	S 450	Spain, Cueva del Tesoro, cave sediment, 2012, A. Nováková	–	ON807725	ON807861	ON808163	ON808011	ON808290
	CCF 5370	Romania, Movile Cave, cave air, 2013, A. Nováková	–	OP762563	OP650500	OP762585	OP762571	–
	EMSL 4753	USA, FL, Jacksonville, bedroom, settle plates, 2018, Ž. Jurjević	–	ON807723	ON807859	–	ON808009	–
	UTHSCSA 09-246 = FMR 14148	USA, CT, animal clinical specimen, 2009, D.A. Sutton	LN898706	LN898860	LN898783	LN898937	ON808008	ON808289
	S 445	Spain, Cueva del Tesoro, cave sediment, 2012, A. Nováková	–	ON807722	ON807858	ON808161	ON808007	ON808288
	EMSL 4846	USA, NJ, Trenton, office building - indoor air, 2018, Ž. Jurjević	–	ON807721	ON807857	ON808160	ON808006	–
	UTHSCSA 11-2175 = FMR 14205	USA, AL, Ohio, sputum, 2011, D.A. Sutton	LN898710	LN898864	LN898787	LN898941	ON808005	ON808287

Table 1. (Continued).

Species	Strain No.[1]	Provenance (locality, substrate, year of isolation, isolator/ollector)	GenBank/ENA/DDBJ accession Nos.					
			ITS	*benA*	*CaM*	*RPB2*	*Mcm7*	*Tsr1*
	S 39	Spain, Cueva del Tesoro, cave air, 2010, A. Nováková	–	ON807720	ON807856	ON808159	ON808004	ON808286
	DTO 247-E7	Mexico, Sayulita, house dust, 2009, A. Amend	–	ON807719	ON807855	ON808158	ON808003	–
	DTO 019-D6	Montenegro, Ulcinj, seawater, isolation year unknown, M. Muntañola-Cvetkovic	–	ON807718	ON807854	ON808157	ON808002	–
	UTHSCSA 08-1574 = FMR 14336	USA, CO, bronchoalveolar lavage, 2008, D.A. Sutton	LN898714	LN898868	LN898791	LN898945	ON808001	–
	UTHSCSA 06-4104 = FMR 14140	USA, MD, bronchoalveolar lavage, 2006, D.A. Sutton	LN898705	LN898859	LN898782	LN898936	ON808000	ON808285
	NRRL 233 = CBS 145748 = DTO 225-D8 (ex-type of *A. austroafricanus*)	South Africa, Cape Town, 1922, V.A. Putterill	JQ301891	JN853963	JN854025	JN853814	JN854086	JN853916
	DTO 268-A1	Thailand, Songkla, house dust, 2009, P. Noonim	–	ON807717	ON807853	ON808156	ON807999	ON808284
	DTO 237-D1	Indonesia, Yogyakarta, food and nutrient library, 2012, R. Rahmawati	–	ON807716	ON807852	ON808155	ON807998	OP688454
	CBS 145671 = HKU49 = NBRC 110693 = NCPF 7870 = BCRC FU30360 = DTO 351-C3 (ex-type of *A. hongkongensis*)	Hong Kong, human toenail, 2013	NR_138262	LC000552	LC000565	LC000578	LC000583	LC000584
	S 627	Spain, Cueva del Tesoro, cave air, 2012, A. Nováková	–	ON807715	ON807851	ON808154	ON807997	ON808283
	DTO 267-G2	South Africa, Stellenbosch, house dust, 2009, K. Jacobs	–	ON807714	ON807850	ON808153	ON807996	ON808282
	CMW-IA 45 = CMW 58647 = CN 164B5 = DN 52	Botswana, Gcwihaba Cave, guano-contaminated cave sediment, 2019, G. Modise & D. Nkwe	–	ON807713	ON807849	ON808152	ON807995	ON808281
	NRRL 4838 = NRRL 236 = CBS 111.32 = CBS 600.65 = DTO 019-A4 = IMI 211400 = ATCC 16845 (ex-type of *A. amoenus*)	Germany, Münster, botanical garden, fruit of *Berberis* sp., 1930, M. Roberg	EF652480	EF652304	EF652392	EF652216	JN854074	JN853907
	DTO 246-D6	South Africa, *Gonatophragmium* sp., 2013, J. Houbraken	–	ON807712	ON807848	ON808151	ON807994	ON808280
	DTO 268-I7	Federated States of Micronesia, Lelu, house dust, 2008, W. Law	–	ON807711	ON807847	ON808150	ON807993	ON808279
	EMSL 4790	USA, MD, Aberdeen, bathroom wall, swab, 2018, Ž. Jurjević	–	ON807710	ON807846	ON808149	ON807992	ON808278
	DTO 319-D5 = IBT 21121 = CCRC 32142	Taiwan, Hwalien City, stored sesame seeds, 2014, S.S. Tzean	–	ON807709	ON807845	ON808148	ON807991	–
	UTHSCSA 09-2582 = FMR 14368	USA, MA, lung tissue, 2009, D.A. Sutton	LN898677	LN898831	LN898754	LN898908	ON807990	ON808277
	DTO 319-E2 = NRRL 35600 = IBT 29647	USA, HI, Kapuka Pauula, basidiomata of *Ganoderma australe*, 2014, D.T. Wicklow	–	JN853952	JN854033	JN853822	JN854073	JN853908
	DTO 267-F7	Federated States of Micronesia, Lelu, house dust, 2008, W. Law	–	–	ON807844	ON808147	ON807989	–
	DTO 269-A7	Federated States of Micronesia, Lelu, house dust, 2008, W. Law	–	ON807708	ON807843	ON808146	ON807988	ON808276
	DTO 319-D3 = IBT 16439 = IMI 096225	United Kingdom, hay, 2014, M.E. Lacey	–	ON807707	ON807842	ON808145	ON807987	ON808275
	S 333	Romania, Fânaţe Cave, bat guano, 2010, A. Nováková	–	ON807706	ON807841	ON808144	ON807986	–
	EMSL 4779	USA, TX, Tyler, bedroom, vent - swab, 2018, Ž. Jurjević	–	ON807705	ON807840	ON808143	ON807985	ON808274
	DTO 248-D1	Mexico, Sayulita, house dust, 2009, A. Amend	–	ON807704	ON807839	ON808142	ON807984	ON808273
	UTHSCSA 06-4284 = FMR 14188	USA, South Carolina, bronchoalveolar lavage, 2006, D.A. Sutton	LN898672	LN898826	LN898749	LN898903	ON807983	–

Table 1. (Continued).

Species	Strain No.[1]	Provenance (locality, substrate, year of isolation, isolator/ollector)	GenBank/ENA/DDBJ accession Nos.					
			ITS	*benA*	*CaM*	*RPB2*	*Mcm7*	*Tsr1*
	S 310	Spain, Cueva del Tesoro, cave sediment, 2010, A. Nováková	–	ON807703	ON807838	ON807982	ON808141	ON808272
	S 459	Spain, Cueva del Tesoro, cave sediment, 2012, A. Nováková	–	ON807702	ON807837	ON808140	ON807981	ON808271
	CCF 5038	Spain, Nerja Cave, cave air, 2011, A. Nováková	–	OP762561	OP650489	OP762583	OP762569	OP762577
	UTHSCSA 09-125 = FMR 14198	USA, MD, bronchoalveolar lavage, 2009, D.A. Sutton	LN898673	LN898827	LN898750	LN898904	ON807979	ON808270
	CMW-IA 38 = CMW 58640 = CN 137-I5	South Africa, animal feed, 2021, C.M. Visagie & N. Yilmaz	–	ON807700	ON807835	–	ON807978	–
	NRRL 239 = CBS 584.65 ATCC 16856 = IMI 211385 (ex-type of *A. fructus*)	USA, CA, date fruit (*Phoenix dactylifera*), 1939, D.E. Bliss	EF652449	EF652273	EF652361	EF652185	JN854076	JN853917
	FMR 15740	Argentina, soil, 2016, A.M. Stchigel	LT903690	LT903681	LT903684	LT903687	–	ON808269
	CMW-IA 32 = CMW 58634 = CN 116-D1	South Africa, Heuningspruit, sunflower, 2020, C.M. Visagie & N. Yilmaz	–	ON807699	ON807834	ON808138	ON807977	ON808268
	DTO 319-D4	USA, WY, Farson, dungy soil under *Artemisia tridentata*, 2014, J.C. Frisvad	–	ON807698	ON807833	ON808137	ON807976	ON808267
	CMW-IA 40 = CMW 58642 = CN 164A9 = DN 2	Botswana, Gcwihaba Cave, guano-contaminated cave sediment, 2019, G. Modise & D. Nkwe	–	ON807697	ON807832	ON808136	ON807975	ON808266
	NRRL 241	Unknown, pomegranate fruit, 1916, L. McCulloch	–	JN853943	JN854031	JN853820	JN854087	JN853918
	DTO 267-G8	South Africa, Stellenbosch, house dust, 2009, K. Jacobs	–	ON807696	ON807831	ON808135	ON807974	ON808265
	S 434	Spain, near Nerja Cave, soil, 2012, A. Nováková	–	ON807695	ON807830	ON808134	ON807973	ON808264
	UTHSCSA 12-3194 = FMR 14162	USA, CA, pericardium, 2012, D.A. Sutton	LN898696	LN898850	LN898773	LN898927	ON807972	ON808263
	DTO 019-A2	USA, CA, fruit of *Phoenix dactylifera,* isolation date and collector unknown	–	ON807694	ON807829	ON808133	ON807971	ON808262
	CBS 142028 = MFBF AV11051B IX = SZMC 22333 (ex-type of *A. pepii*)	Croatia, Zagreb, grain mill - indoor air, 2012, D. Jakšić Despot	KU613368	KU613371	KU613365	–	–	–
	DTO 243-G4	Indonesia, polyclinic for children, 2012, A. Sidar	–	ON807693	OP650454	ON808132	ON807970	ON808261
	CBS 138191 = DTO 267-D8 (ex-type of *A. griseoaurantiacus*)	Federated States of Micronesia, Yela of Kosrae Island, house dust, 2010, E. Whitfield & K. Mwange	KJ775553	KJ775086	KJ775357	KU866988	–	–
	CMW-IA 43 = CMW 58645 = CN 164B3 = DN 40	Botswana, Gcwihaba Cave, guano-contaminated cave sediment, 2019, G. Modise & D. Nkwe	–	ON807692	ON807828	ON808131	ON807969	ON808260
	S 465	Spain, near Nerja Cave, cave air, 2012, A. Nováková	–	ON807691	ON807827	ON808130	ON807968	–
	DTO 276-F9	Iran, bronchoalveolar lavage, 2013, J. Najafzadeh	–	ON807690	ON807826	ON808129	ON807967	ON808259
	DTO 138-A3	Germany, airconditioning system, 2010, collector unknown	–	ON807689	ON807825	ON808128	ON807966	ON808258
	S 334	Romania, Zidita Cave, bat guano, 2009, A. Nováková	–	ON807688	ON807824	ON808127	ON807965	ON808257
	S 215	Romania, Zidita Cave, bat guano, 2009, A. Nováková	–	ON807687	ON807823	ON808126	ON807964	ON808256
	CMW-IA 36 = CMW 58638 = CN 131-G9	South Africa, animal feed, 2021, C.M. Visagie & N. Yilmaz	–	ON807686	ON807822	–	ON807963	ON808255
	DTO 245-F5 = CBS 138189	Mexico, Sayulita, house dust, 2009, A. Amend	–	ON807685	ON807821	ON808125	ON807962	ON808254
	CMW-IA 37 = CMW 58639 = CN 132-C9	South Africa, animal feed, 2021, C.M. Visagie & N. Yilmaz	–	ON807684	ON807820	ON808124	ON807961	ON808253

Table 1. (Continued).

Species	Strain No.[1]	Provenance (locality, substrate, year of isolation, isolator/ollector)	GenBank/ENA/DDBJ accession Nos.					
			ITS	*benA*	*CaM*	*RPB2*	*Mcm7*	*Tsr1*
	EMSL 4723	USA, NJ, Morris Plains, bathroom wall, swab, 2018, Ž. Jurjević	–	ON807683	ON807819	ON808123	ON807960	ON808252
	DTO 337-C3	Germany, school material, 2015, U. Hack	–	ON807682	ON807818	ON808122	ON807959	ON808251
	DTO 267-D2 = CBS 138190	Federated States of Micronesia, Lelu, house dust, 2009, W. Law	–	ON807681	ON807817	ON808121	ON807958	ON808250
	NRRL 4791 = CBS 122718 = IFO 4098 (ex-type of *A. tabacinus*)	Unknown, tobacco, before 1934, Y. Nakazawa	EF652478	EF652302	EF652390	EF652214	JN854084	JN853922
	DTO 337-B9	Germany, wallpaper, 2015, U. Hack	–	ON807680	ON807816	ON808120	ON807957	ON808249
	EMSL 4820	USA, NY, New York, bedroom, swab, 2018, Ž. Jurjević	–	ON807679	ON807815	ON808119	ON807956	ON808248
	UTHSCSA 07-2427 = FMR 14190	USA, bronchoalveolar lavage, 2007, D.A. Sutton	LN898737	LN898891	LN898814	LN898968	ON807955	ON808247
	DTO 319-E6 = IBT 26806	India, Kerala, green coffee beans, 2014, M. Franck	–	ON807678	ON807814	ON808118	ON807954	ON808246
	ANV 16-4K	Czech Republic, Prague, book in library, 2018, Nováková	–	ON807677	ON807813	ON808117	ON807953	ON808245
	CCF 3690	Czech Republic, Liberec, toenail of woman, 2006, J. Doležalová	–	OP762560	FR751430	OP762582	OP762568	OP762576
	NRRL 5031 (ex-type of *A. versicolor* var. *magnus*)	Unknown country and source, before 1962, Y. Sasaki	–	JN853947	JN854036	JN853825	–	JN853920
	DTO 019-D2	South Korea, Daejeon, soil from pepper field, 2003, S.B. Hong	–	ON807675	ON807811	ON808115	ON807951	ON808243
	UTHSCSA 03-1197 = FMR 14179	USA, FL, sputum, 2003, D.A. Sutton	LN898736	LN898890	LN898813	LN898967	ON807950	ON808242
	UTHSCSA 08-2898 = FMR 14232	USA, bronchoalveolar lavage, 2008, D.A. Sutton	LN898739	LN898893	LN898816	LN898970	ON807949	–
	CGMCC 3.05288	China, moldy broom, 1999, collector unknown	–	ON807674	ON807810	ON808114	ON807948	ON808241
	DTO 319-E3	Thailand, Hua Hin, soil under bush, 2014, J.C. Frisvad	–	OP82096	OP650458	OP820970	OP820969	–

[1] Acronyms of culture collections in alphabetic order: ATCC, American Type Culture Collection, Manassas, Virginia; BCRC, Bioresource Collection and Research Center, Hsinchu, Taiwan; CBS, Westerdijk Fungal Biodiversity Institute (formerly Centraalbureau voor Schimmelcultures), Utrecht, the Netherlands; CCF, Culture Collection of Fungi, Department of Botany of Charles University, Prague, Czech Republic; CGMCC, China General Microbiological Culture Collection Center, China; CMW, CMW-IA & CN, working and formal culture collections housed at FABI (Forestry and Agricultural Biotechnology Institute) and Innovation Africa, University of Pretoria, South Africa; DN, working collection of David Nkwe, housed at the Department of Biological Sciences and Biotechnology, Botswana International University of Science and Technology, Palapye, Botswana; DTO, Internal Culture Collection of the Department of Applied and Industrial Mycology of the CBS-KNAW Fungal Biodiversity Centre, Utrecht, The Netherlands; EMSL, EMSL Analytical Inc., New Jersey, USA; FMR, Facultat de Medicina i Ciències de la Salut, Reus, Spain; HKU,The University of Hong Kong Mycological Herbarium, Hong Kong; IBT, Culture Collection at the Department of Biotechnology and Biomedicine, Lyngby, Denmark; IFO, Institute for Fermentation, Osaka, Japan (IFO strains were transferred to the NBRC NITE collection); IMI, CABI's collection of fungi and bacteria, Wallingford, UK; JCM, Japan Collection of Microorganisms, Tsukuba, Japan; KAS, fungal collection of Keith A. Seifert, internal working culture collection at DAOMC (Culture collection of the National Mycological Collections, Agriculture & Agri-Food Canada), Ottawa, Canada; MFBF, collection of the Department of Microbiology, Faculty of Pharmacy and Biochemistry, University of Zagreb, Croatia; NBRC (NITE), National Institute of Technology and Evaluation, Biological Resource Center, Department of Biotechnology, Kisarazu, Chiba, Japan; NCPF, The National Collection of Pathogenic Fungi, Bristol, UK; NRRL, Agricultural Research Service Culture Collection, Peoria, Illinois, USA; SZMC, Szeged Microbiological Collection at the Department of Microbiology, Faculty of Science and Informatics, University of Szeged, Hungary; UAMH, UAMH Centre for Global Microfungal Biodiversity (formerly University of Alberta Microfungus collection and Herbarium), Gage Research Institute, University of Toronto, Toronto, Canada; URM, culture collection at the Federal University of Pernambuco, Recife, Brazil; UTHSCSA, Collection of Fungus Testing Laboratory, University of Texas, Health Science Center, San Antonio, USA. Other: ANV, S, personal designation of strains isolated by A. Nováková (no permanent preservation of cultures).

Molecular studies

Total genomic DNA was isolated from 7-d-old cultures with the NucleoSpin® Soil (Macherey–Nagel, Düren, Germany) DNA isolation kit and its quality was verified using a NanoDrop 1 000 Spectrophotometer.

Sequences of the ITS region of rDNA were not obtained for the majority of strains because the variability of this locus within series *Versicolores* is low (Jurjević *et al.* 2012). A part of the β-tubulin gene (*benA*) was amplified using forward primers Bt2a (Glass & Donaldson 1995) or T10 (O'Donnell & Cigelnik 1997) and reverse primer Bt2b (Glass & Donaldson 1995). A part of the calmodulin gene (*CaM*) was amplified using forward primers CF1L, CF1M (Peterson 2008) or cmd5 (Hong *et al.* 2006) and reverse primers CF4 (Peterson 2008) or cmd6 (Hong *et al.* 2006). A part of the *Mcm7* gene encoding the minichromosome maintenance factor 7 was amplified using either universal primers Mcm7-709for and Mcm7-1348rev (Schmitt *et al.* 2009) or newly developed primers specific for the series *Versicolores*, namely Mcm7-Aver710for (5'-CACGAGTATCAGATGTTAAACCG-3') and Mcm7-Aver1354rev (5'- GATTTGGCAACACCAGGGTC -3'). A part of the RNA polymerase II second largest subunit gene (*RPB2*) was amplified using forward primer fRPB2-5F and reverse primer fRPB2-7CR (Liu *et al.* 1999). Finally, a part of the *Tsr1* gene encoding the ribosome biogenesis protein was amplified with primers Tsr1-1453for and Tsr1-2308rev (Schmitt *et al.* 2009).

The PCR was performed with standard or touchdown protocol and the PCR products were purified with ethanol and sodium acetate. All procedures and amplification conditions are described in detail by Sklenář *et al.* (2021).

The resulting DNA sequences were assembled in BioEdit v. 7.0.5 (Hall 1999) and deposited in GenBank. Obtained accession numbers are listed in Table 1. The sequences were aligned in MAFFT v. 7 (Katoh & Standley 2013) using the G-INS-I strategy. The best fitting model of evolution for every alignment was determined in jModelTest v. 2.1.7 (Posada 2008) using Bayesian information criterion with the following results. For the alignment of *benA s*equences, K80+G was selected as the best fitting model; TrNef+G for the alignment of *CaM* sequences; K80+G for the alignment of *Mcm7* sequences; TrNef+G for the alignment of *RPB2* sequences; and TrN+I for the alignment of *Tsr1* sequences. The TrNef+I+G model was chosen as the best fitting model for the alignment of 518 *CaM* sequences, and the TrNef model for the alignment of 48 ITS rDNA sequences. All alignments (together with input data for phylogenetic methods) were deposited into the Dryad Digital Repository (https://doi.org/10.5061/dryad.63xsj3v5q).

Phylogenetic analysis and species delimitation

We first assembled *CaM* sequences of 518 strains belonging to series *Versicolores* and calculated a Maximum Likelihood (ML) tree in IQ-TREE v. 2.1.2 (Minh *et al.* 2020). The branch support was determined by 1 000 standard bootstrap replicates. The graphical output was prepared in iTOL v. 6.5.6 (Letunic & Bork 2016) with colour strips next to the phylogenetic tree representing the geographic origin and substrate/environment. The provenance of strains used in the analysis is listed in Supplementary Table S1.

Based on the results of this *CaM p*hylogenetic tree, we selected 213 strains to be used for further analyses and thus obtained additional sequences from four loci for them. The ML analysis based on a concatenated dataset was then calculated in IQ-TREE v. 2.1.2. Each locus was set up as a separate partition and the branch support was determined by 1 000 standard bootstrap replicates.

To further demonstrate the relationships between currently accepted species in series *Versicolores*, we calculated the species tree in starBEAST v. 2.0 (Drummond *et al.* 2012). The strains were assigned to 17 species according to the best scoring ML tree calculated from the concatenated dataset. The length of the mcmc chain was 1×10^9 generations, the molecular clock model was set to strict clock, and the *species tree* prior was set to the Coalescent constant population model. To present the results of this analysis we employed the program Densitree v. 2.2.7 (Bouckaert & Heled 2014).

To investigate the stability and robustness of identification across the currently accepted 17 species and different DNA loci, we performed BLAST (basic local alignment search tool) searches with all available sequences from all species against the local BLAST database consisting of only ex-type strains sequences. To demonstrate the results, we prepared colour strips in iTOL and plotted them on the ML tree.

Five single-locus species delimitation methods (GMYC, bGMYC, PTP, bPTP, ABGD) were performed with alignments reduced to unique sequences. The reduction was carried out in R v. 4.1.2 (R Core Team 2015) using the *haplotype* function from the package PEGAS (Paradis 2010). The GMYC method was performed in R v. 4.1.2 with the package SPLITS (Fujisawa & Barraclough 2013) based on the phylogenetic tree calculated in BEAST v. 2.6.7 (Bouckaert *et al.* 2019) with the chain length of 1×10^7 generations, strict molecular clock, and tree prior set to Yule model. The same source material was used for the bGMYC method, but instead of using one consensus tree, we used 100 randomly selected trees after discarding the initial 25 % of trees as burn-in. The analysis was performed in R v. 3.4.1 using the package BGMYC (Reid & Carstens 2012). PTP and bPTP utilized one thousand ML standard bootstrap trees calculated in IQ-TREE v. 2.1.2. Both PTP and bPTP analyses were performed in Python v. 3 (van Rossum & Drake 2019) with the package PTP (Zhang *et al.* 2013). The ABGD (Automatic Barcode Gap Discovery) (Puillandre *et al.* 2012) was performed on the ABGD web server (available online: http://wwwabi.snv.jussieu.fr/public/abgd/abgdweb.html). Alignments of unique sequences were used as input and the distance matrix was calculated on the server with the K2P model of evolution. The default value of parameter X (1.5) resulted in all strains delimited as one species, so a lower value (1.2) was used. Since ABGD analysis results in a number of different delimitation schemes, the decision on which result to consider was based on the recommendation of Puillandre *et al.* (2012) and Kekkonen & Hebert (2014) and therefore we chose the results of the initial partition which was closest to P = 0.01.

To prepare input for the multilocus method STACEY, we first merged all single-locus alignments into one, then we reduced this alignment to unique sequences using the *haplotype* function (the number of strains was reduced from 214 to 195), and finally we split the concatenated dataset back into separate single-locus alignments. The analysis was performed in BEAST v. 2.6.7 with the STACEY v. 1.2.5 add-on (Jones 2017). The following settings were selected: the length of mcmc chain was 1×10^9 generations, the molecular clock model was set to strict clock, the *species tree* prior was set to the Yule model, *growth rate* prior was set to lognormal distribution (M = 5, S = 2), *clock rate* priors for all loci were set to lognormal distribution (M = 0, S = 1), *PopPriorScale* prior was set to lognormal distribution (M = -7, S = 2) and *relativeDeathRate* prior was set to beta distribution (α = 1, β = 1 000). The output was processed with SpeciesDelimitationAnalyzer (Jones 2017). The results of STACEY are presented in two ways. Firstly, we

created a plot to show how the number of delimited species and the probability of the most probable and the second most probable scenario change in relation to the value of *collapseheight* parameter (the input data and the R script written for the production of this plot can be found in the Dryad Digital Repository: https://doi.org/10.5061/dryad.63xsj3v5q). Secondly, we created similarity matrices using code from Jones *et al.* (2015) with three different values of *collapseheight* parameter (0.005, 0.007 and 0.009) chosen from the plot.

Finally, we formulated six hypotheses about species boundaries based on the current taxonomy of the series and the results of the species delimitation methods, and we tested them with DELINEATE software (Sukumaran *et al.* 2021). The dataset was split into hypothetical populations with "A10" analysis in BPP v. 4.3 (Yang 2015) and the species tree of these populations was created in starBEAST v. 2.0 (Drummond *et al.* 2012) implemented in BEAST v. 2.6.7. Then we set up six scenarios, lumping some populations into defined species and leaving others to be delimited as either part of those defined species or separate species. The analysis was run in Python v. 3 with the package DELINEATE (Sukumaran *et al.* 2021).

Morphology

The macromorphological characters of colonies were observed on eight cultivation media, namely malt extract agar (MEA; Oxoid, Melbourne, Australia), Czapek yeast autolysate agar (CYA; Fluka, Buchs, Switzerland), Czapek-Dox agar (CZA), yeast extract Sucrose agar (YES), dichloran 18 % glycerol agar (DG18), oatmeal agar (OA; Difco, La Ponte de Claix, France), CYA supplemented with 20 % sucrose (CY20S), and creatine sucrose agar (CREA) (Samson *et al.* 2014). The strains were inoculated at three equidistant points on 90 mm Petri dishes and incubated at 25 °C in darkness. For the description of colony colours, we used the hexadecimal colour codes and the names were assigned according to website https://coolors.co/. After 14 d incubation, the plates were photographed, and strains incubated for a further one wk to check Hülle cells production. The strains were also grown on MEA for 14 d at 10, 15, 20, 25, 30, 35, 37, and 40 °C, in darkness, to determine cardinal temperatures.

Micromorphological characters were observed from 14-d-old colonies grown on MEA. Every character (conidia length and width, stipe length and width, vesicle diameter, length of phialides and metulae) was measured at least 35 times for each strain. Lactic acid (60 %) was used as the mounting medium. Photographs were taken on an Olympus BX51 microscope equipped with an Olympus DP72 camera. Based on the measurements, we created boxplots using R v. 4.1.2 and the package GGPLOT2 (Wickham 2016). The statistical differences in phenotypic characters between species were calculated using one-way ANOVA followed by Tukey's honest significant difference (HSD) test in R v. 4.1.2 and displayed using the package GGSIGNIF (Ahlmann-Eltze & Patil 2021). The linear discriminant analysis based on the measurements of the above-mentioned micromorphological features was performed in R v. 4.1.2 with the packages MASS (Venables & Ripley 2002) and GGORD (Beck 2017).

Physiology

To test the osmotic tolerance of strains/species, we cultivated strains at 25 °C on MEA supplemented with 0 %, 5 %, 10 %, and 15 % NaCl. The growth increment was measured each day for ten days. Based on these measurements, we created primary growth curves for every strain and NaCl concentration. Then we extracted the slope values from these curves and used them to create secondary growth curves which represent the growth rate of the strains in relation to the NaCl concentration. The secondary growth curves were calculated using the *loess* function in R v. 4.1.2 with the package GGPLOT2.

RESULTS

Phylogeny and ecology

A Maximum Likelihood (ML) phylogenetic tree based on *CaM* from 518 strains is presented in Fig. 1, with geographic origin and substrate (if known) plotted on the tree using the colour strips. The phylogenetic reconstruction shows full support for four large clades, but then the support is lost towards the terminal branches. There was no clear pattern in the distribution of localities or substrates of isolation. The two most common combinations overrepresented throughout the tree included, *i.e.*, North America / indoor environment and Europe / cave, but this condition is caused by sampling bias and is not limited to particular species or group of species.

Figure 2 shows the ML reconstruction based on a concatenated alignment of five loci from the representative dataset of 213 strains covering genetic and ecological variability (mostly selected based on *CaM* genotype, locality and substrate). There are still four main fully supported lineages in the tree corresponding to those in the *CaM* tree. For practical reasons, we named these lineages based on the priority rules as follows: *A. subversicolor* lineage and *A. sydowii* lineage contain only single species, while the *A. versicolor* lineage contains nine species (*A. amoenus*, *A. austroafricanus*, *A. fructus*, *A. griseoaurantiacus*, *A. hongkongensis*, *A. pepii*, *A. protuberus*, *A. tabacinus*, and *A. versicolor*), and the *A. creber* lineage contains six species (*A. creber*, *A. cvjetkovicii*, *A. jensenii*, *A. puulaauensis*, *A. tennesseensis*, and *A. venenatus*). The bootstrap support values in the combined tree are high on many branches even for the small terminal clades. It is however well-known that bootstrap values in the concatenated trees are often falsely high (Kubatko & Degnan 2007, Seo 2008). If only the monophyly and statistical support of branches in this tree would be considered, all currently recognized species could be accepted. To retain monophyly, however, several new species would have to be described in the *A. versicolor* lineage, especially in the proximity of *A. austroafricanus*/*A. hongkongensis*/*A. amoenus* and also in the clade containing *A. griseoaurantiacus* and *A. tabacinus*. The geography and substrate of isolation showed no clear patterns that could be associated with particular species similarly to *CaM* tree.

A species tree calculated in starBEAST (Drummond *et al.* 2012) is shown in Fig. 3 with strains assigned to species based on the current taxonomy. The visualization by Densitree (Bouckaert & Heled 2014) demonstrates the incongruences in the dataset, which are apparent in both the *A. versicolor* lineage (within the clade containing *A. pepii*, *A. fructus*, and *A. versicolor*, and within the clade containing the remaining species) and the *A. creber* lineage (between all species except *A. venenatus*).

Incongruences between single gene datasets: evidence from species tree and BLAST searches

To show practical consequences of incongruences between single-gene datasets, we created a local BLAST database containing

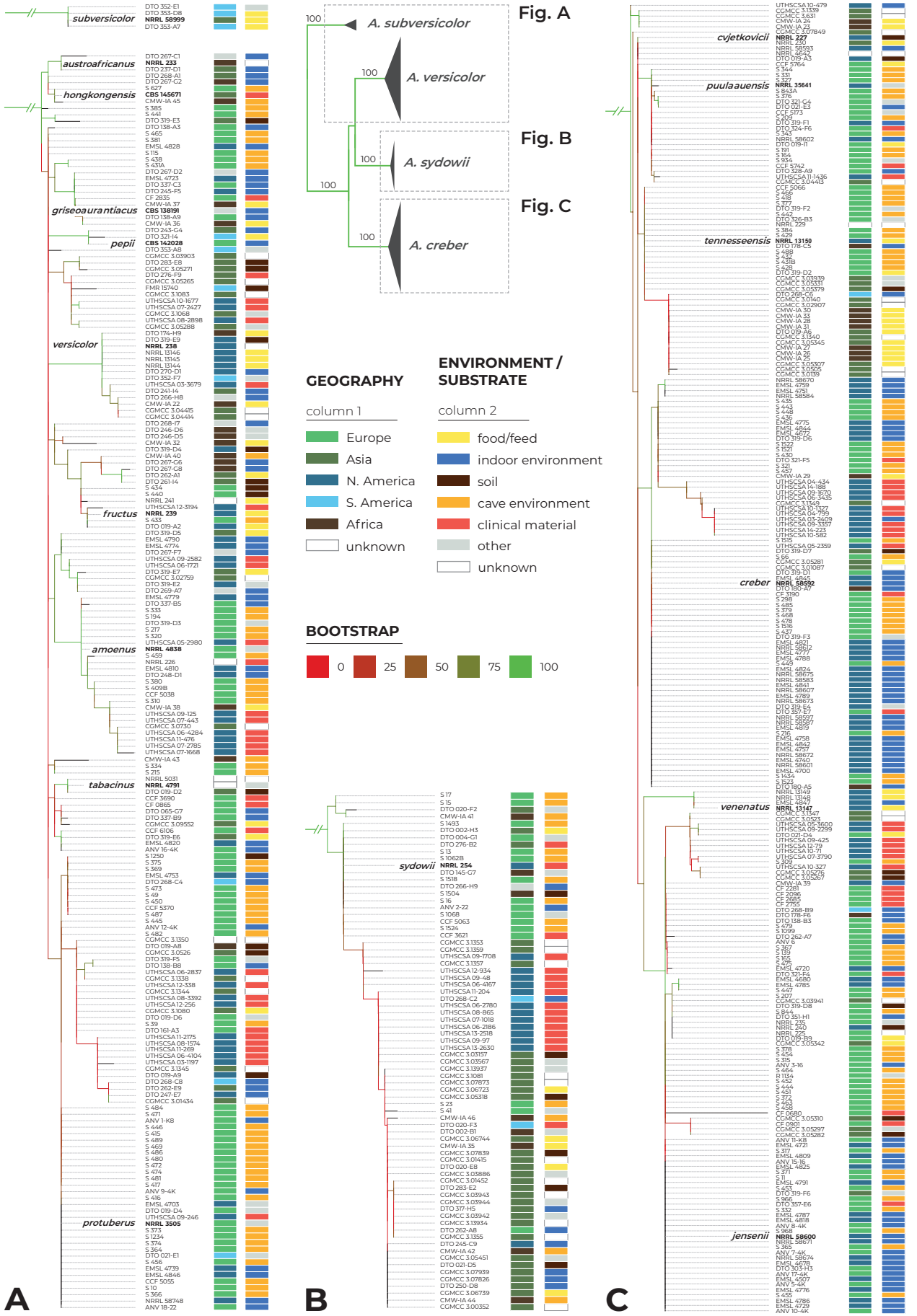

Fig. 1. Phylogenetic tree of 518 series *Versicolores* strains based on *CaM*. The tree was calculated in IQ-TREE with 1 000 standard bootstrap replicates. The tree is split into three parts for better readability: **A.** *Aspergillus versicolor* lineage and *A. subversicolor*. **B.** *A. sydowii*, and **C.** *A. creber* lineage. Coloured stripes placed to the right of the strain codes represent the geographic origin of strains (continent) and source of isolation (substrate or environment). Tree branches are coloured according to their bootstrap supports, red colour representing bootstrap value of 0 and green colour bootstrap value of 100. Ex-type isolates are highlighted with bold font.

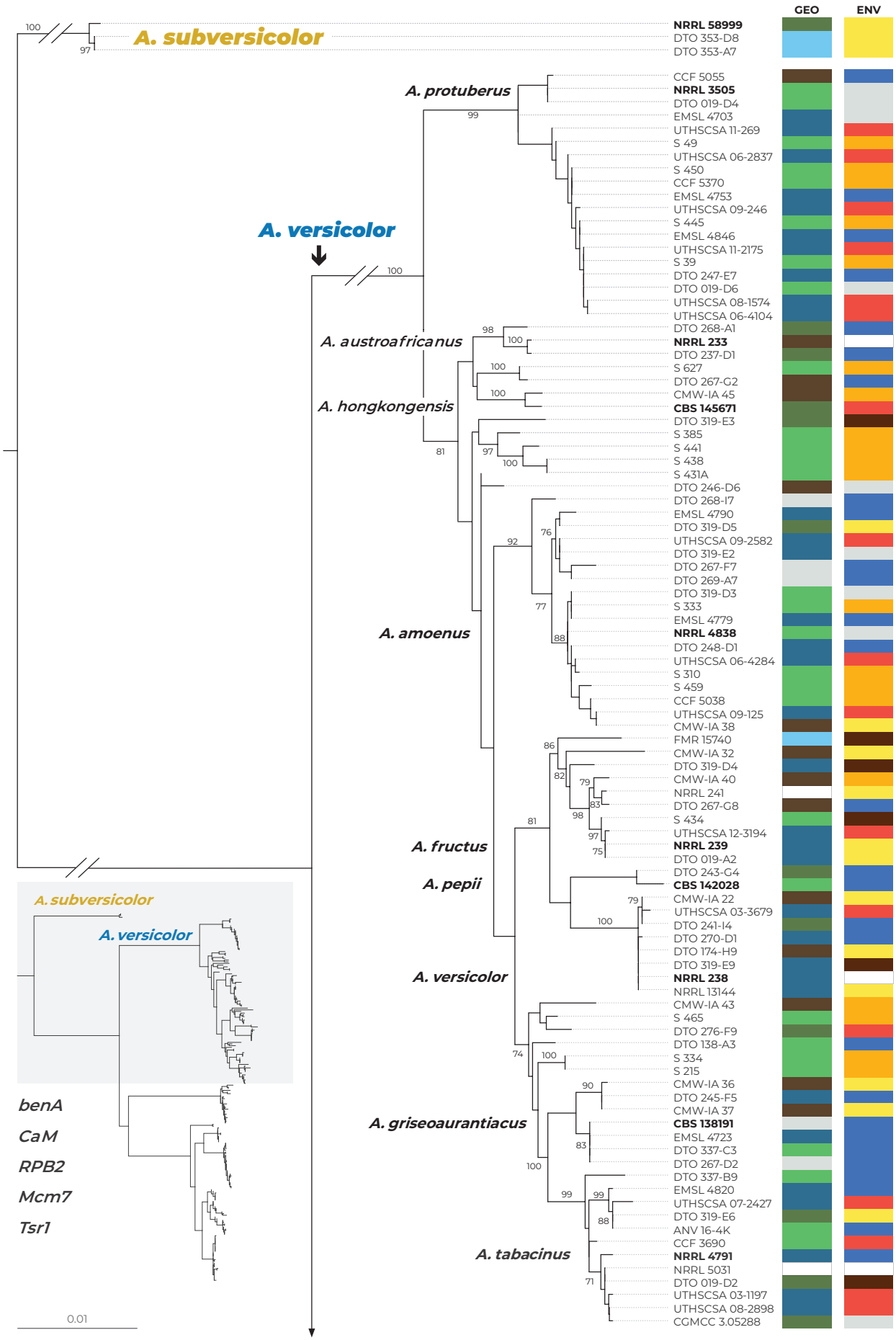

Fig. 2. Multilocus phylogeny of *Aspergillus* series *Versicolores* based on five loci (*benA*, *CaM*, *RPB2*, *Mcm7*, *Tsr1*) and comprising 213 strains. The displayed tree was calculated employing a Maximum likelihood method in IQ-TREE using partitioned analysis. The support was assessed by 1 000 standard bootstrap replicates, only values higher than 70 % are displayed. Coloured stripes next to strain codes represent the geographic origin of strains (continent) and the source of isolation (substrate or environment). Ex-type isolates are highlighted with bold font.

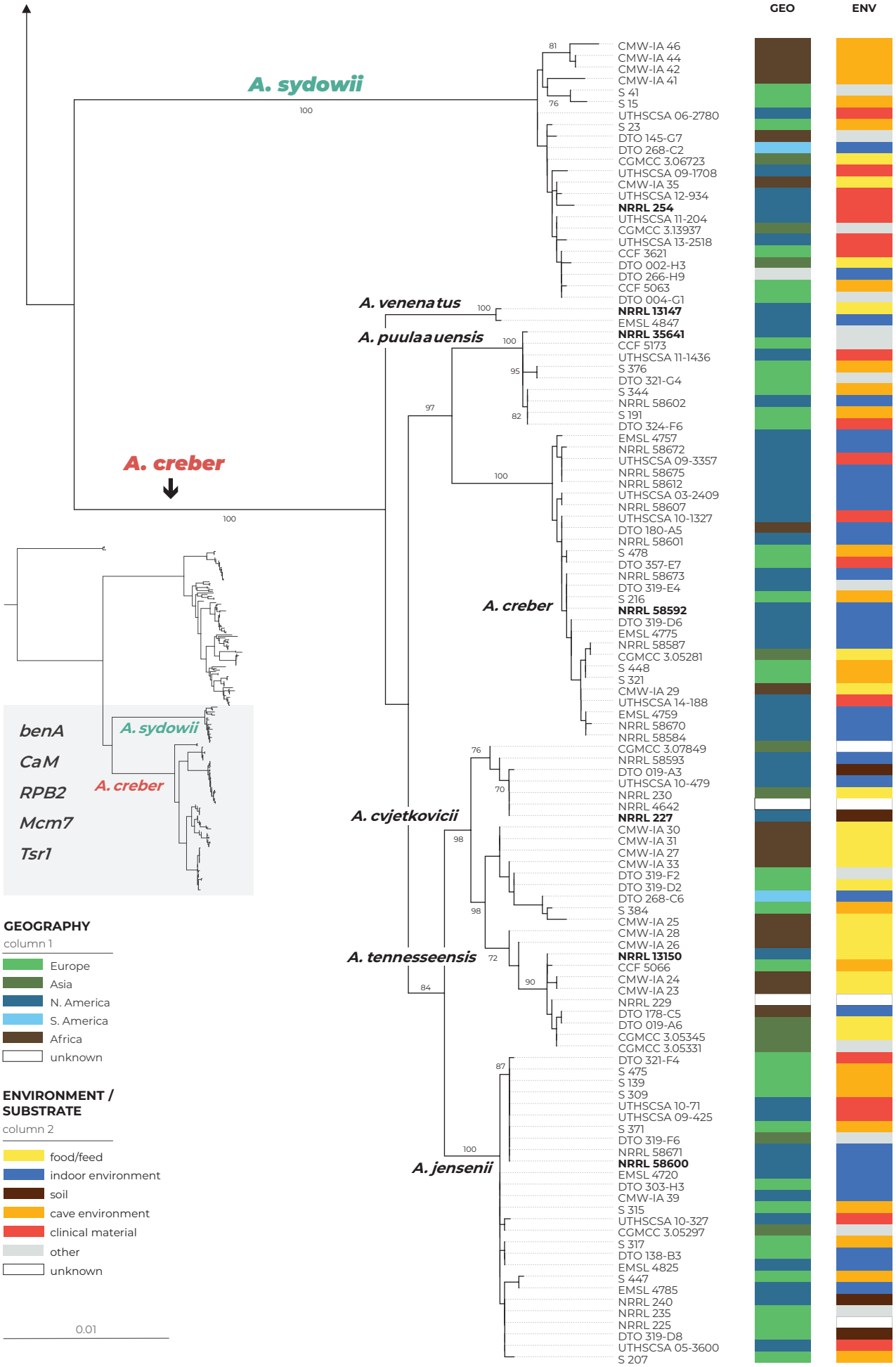

Fig. 2. (Continued).

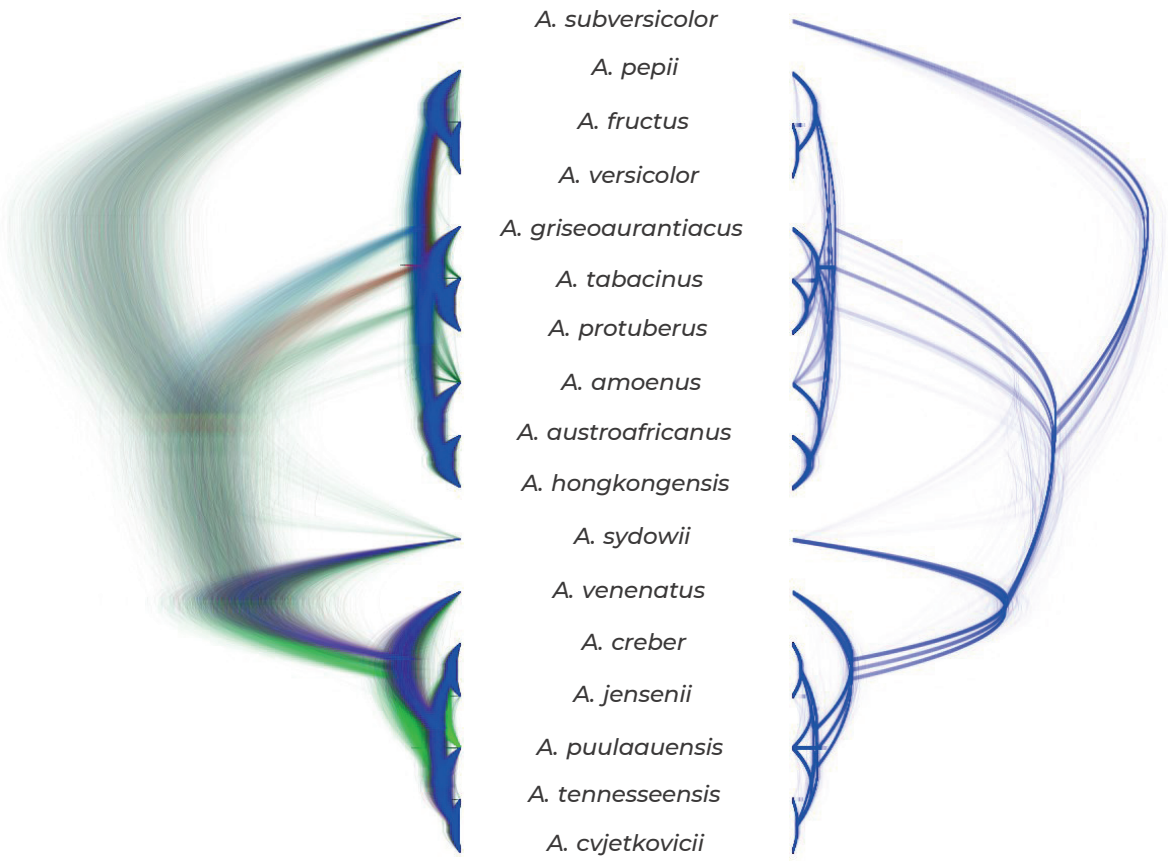

Fig. 3. Species tree inferred with starBEAST and visualized in DensiTree. All trees created in the analysis with the exception of the first 25 % (burn-in) are displayed on the left side. Trees with the most common topology are depicted by blue lines, trees with the second most common topology by red, trees with the third most common topology by light green, and all other trees by dark green. The consensus trees of the three most common topologies are displayed on the right side.

sequences from five genes of all 17 ex-type strains. Then we performed BLAST searches for all sequences from five loci we gathered for 213 isolates against this database. The results of BLAST searches and the closest similarities to the ex-type strains are presented in Fig. 4. We can see that sequences of different genes from the same strain frequently resulted in closest sequence similarities with ex-type strains of different species and this results in different species identifications. This phenomenon does not involve *A. subversicolor* and *A. sydowii.* In the *A. creber* lineage, the switching between different accepted species is present in *A. cvjetkovicii* and *A. tennesseensis*, while in the *A. versicolor* lineage, the unstable identification is very prevalent and present among all species except *A. pepii* and *A. versicolor*. At first glance, *A. protuberus* seems to be isolated from other species and well-defined phylogenetically in the combined ML tree, but there are conflicts in identification of some strains as well, suggesting the ongoing recombination with other representatives of the *A. versicolor* lineage. This is apparent for strains S 627 and DTO 267-G2, identified as *A. austroafricanus* and *A. hongkongensis* using *benA*, *CaM*, *and RPB2*, which had closest hits to *A. protuberus* using *Tsr1*. Similarly, strains S 465, S 334, and S 214, which belong to the clade containing ex-type strains of *A. griseoaurantiacus* and *A. tabacinus*, were identified as *A. protuberus* using *CaM*. The most extreme situation is present in the intermediate clade located between *A. austroafricanus*/*A. hongkongensis* and *A. amoenus* comprising strains DTO 319-E3, S 385, S 441, S 438, and S 431A. BLAST searches of almost every locus in this clade resulted in the closest hit to different species. This clearly demonstrates that there are no barcode gaps between many species and that there are phylogenetic conflicts between individual loci.

There are also 13 cases of *benA* sequences with equal similarity to three or more ex-type strains. This number is high in comparison with other loci (2 cases in *CaM*, no cases in any other locus), but it is most likely caused by shorter length of *benA* sequences and thus also their lower discriminatory power compared to the other loci.

Species delimitation

The results of various species delimitation methods, mostly based on the MSC model, are displayed in Fig. 5. The majority of methods and their various settings (19 out of 28) support the delimitation of four species in series *Versicolores*, *i.e.*, *A. subversicolor*, *A. sydowii*, *A. versicolor* (lineage containing nine species names), and *A. creber* (lineage with six species names). Two out of 28 analyses delimited less than four species, and seven delimited more than four species. The highest number of delimited species by any method was seven. The GMYC and ABGD methods based on *RPB2* sequences delimited only *A. subversicolor* and lumped all the remaining strains into one hypothetical species. Few methods delimited more than one species within the *A. versicolor* and *A. creber* lineages. Namely, STACEY delimited three species in the *A. creber* lineage with *collapseheight* value 0.005 and two species in the *A. creber* lineage with *collapseheight* value 0.007; GMYC and bGMYC based on *benA* sequences delimited two species in the *A. creber* lineage and three species in the *A. versicolor* lineage; bPTP based on *RPB2* sequences delimited two species in the *A. versicolor* lineage; bGMYC based on *Mcm7* sequences delimited two species in the *A. creber* lineage and two species in *A. versicolor*

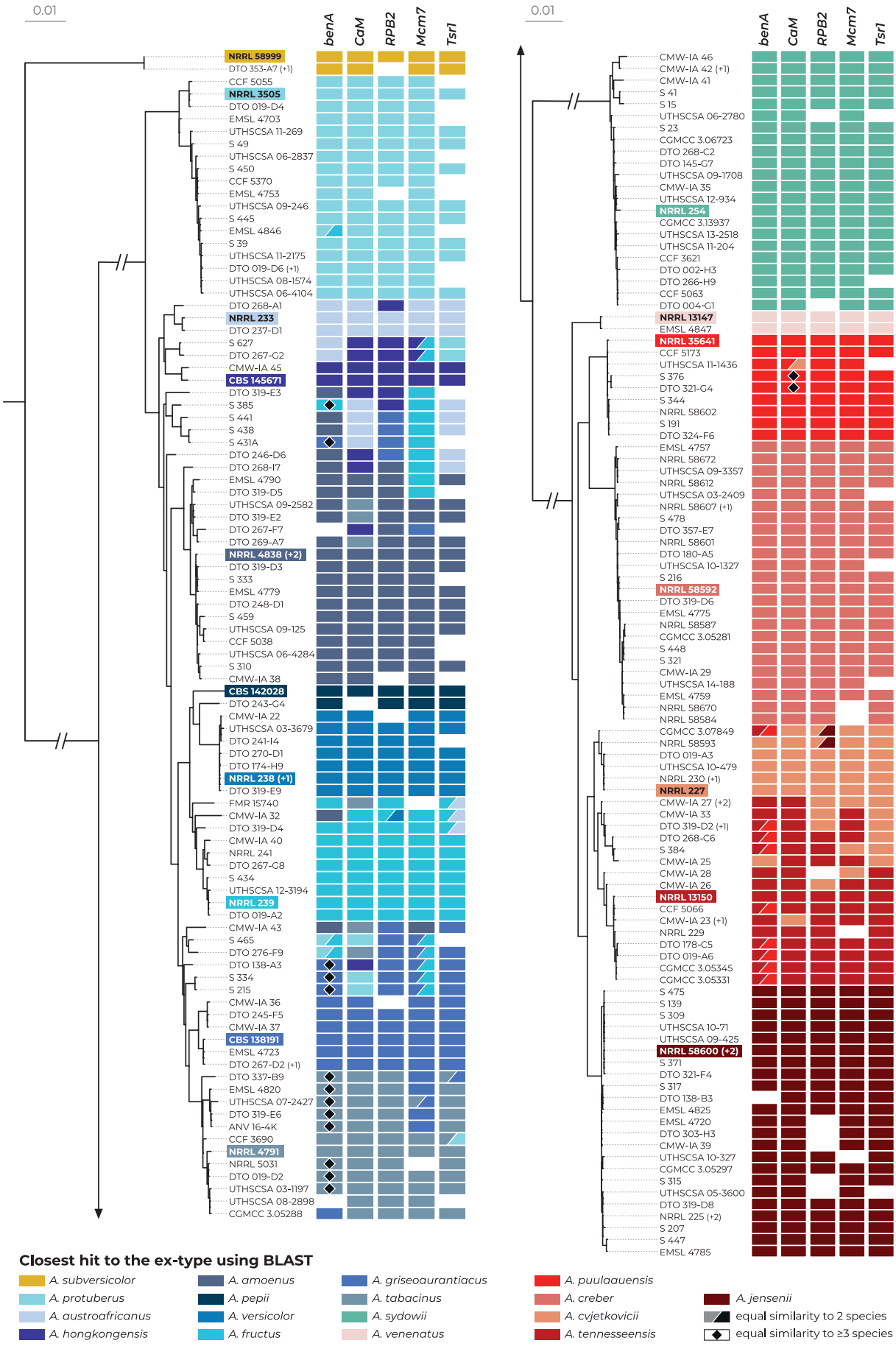

Fig. 4. The results of BLAST similarity searches of five unlinked loci (*benA*, *CaM*, *RPB2*, *Mcm7* and *Tsr1*) derived from 195 strains (only unique multilocus haplotypes were used) across the genetic diversity of series *Versicolores*. Coloured rectangles represent the closest hits to one of the 17 ex-type strains (every species has unique colour). If there was an identical similarity to two or more ex-type strains, the rectangles were diagonally divided or marked with a rhombus, respectively. Blank spaces represent missing sequences. Ex-type isolates are marked with bold font and coloured background. The phylogenetic tree was calculated in IQ-TREE using partitioned analysis and 1 000 ultrafast bootstrap replicates.

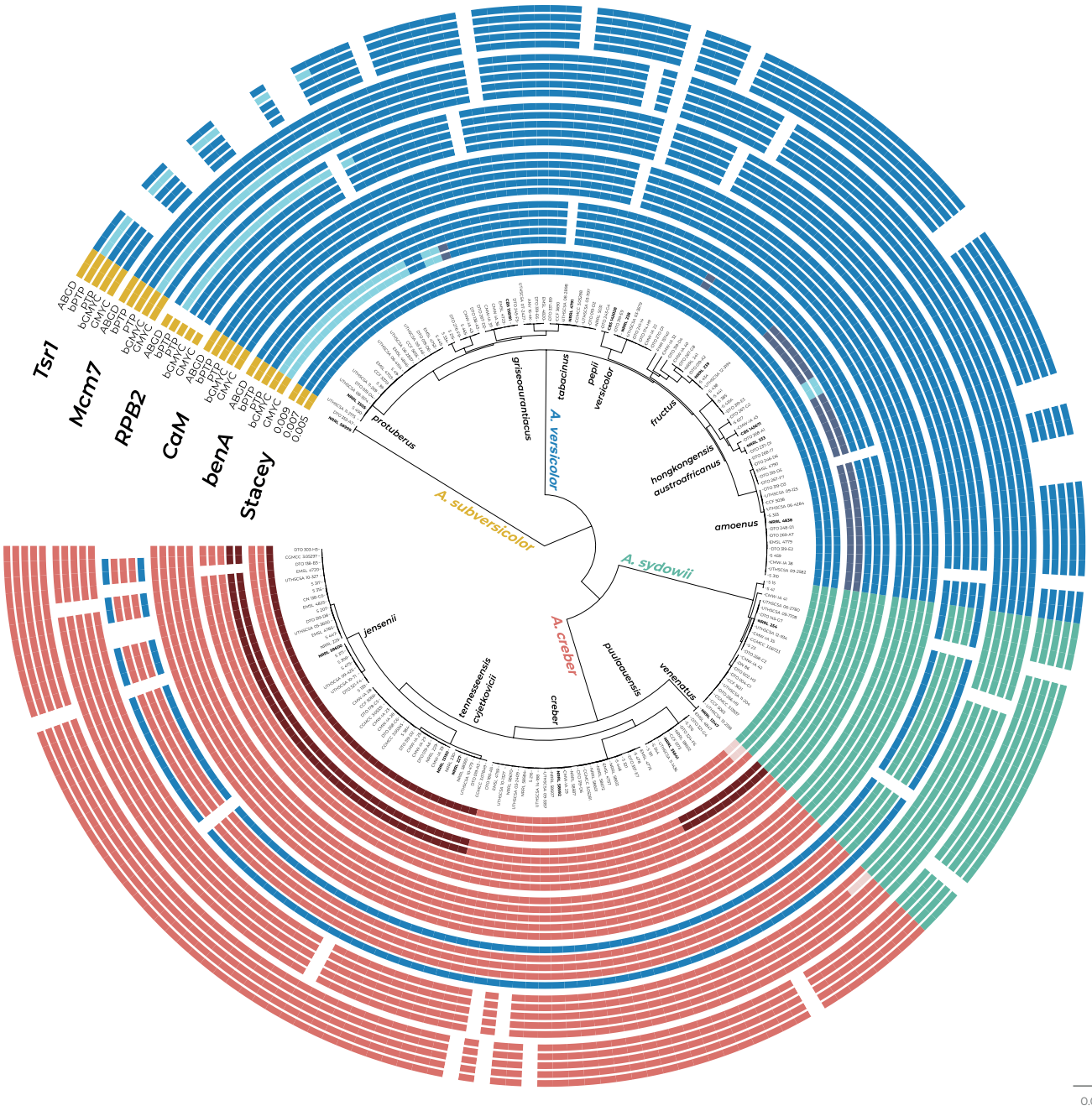

Fig. 5. Schematic representation of results of species delimitation methods in the series *Versicolores*. One multilocus method (STACEY) and five single-locus methods (ABGD, bPTP, PTP, bGMYC and GMYC) were applied on a dataset consisting of five loci (*benA*, *CaM*, *RPB2*, *Mcm7* and *Tsr1*). The dataset was reduced to strains with unique multilocus haplotypes. The results are depicted by coloured circles (blank spaces are missing sequence data for specific isolates) with different colours indicating tentative species delimited by each method. All ex-type isolates are highlighted with a bold font and the species are epithets written with black colour. The results of STACEY are presented with three different values of *collapseheight* parameter (0.005, 0.007 and 0.009). The phylogenetic tree was calculated during the STACEY analysis and is used solely for the comprehensive presentation of the results from different methods.

lineage; bPTP based on *Tsr1* sequences delimited two species in the *A. versicolor* lineage. Among the seven methods/settings which supported more than four species in series *Versicolores*, there was only very low agreement on the arrangement of these species. Most commonly, *A. protuberus* and *A. venenatus* gained support as additional species (3/28 methods).

The results of the multilocus method STACEY are presented in Fig. 6. Subfigure A illustrates the effect of *collapseheight* parameter value on the number of delimited species. This parameter is plotted on the x-axis, while on the y-axis on the left side, there is the number of delimited species with the given *collapseheight* value (black line). The support for the most probable scenario (red line), and the support for the second most probable scenario (turquoise line) are shown; other less supported scenarios were omitted. When the *collapseheight* value is low (0.001–0.005), the number of delimited species is high, but the probability for each delimitation is very low (the probabilities are plotted on the y-axis on the right side; the sum of probabilities of all scenarios at each *collapseheight* value is equal to one). The scenario with six species (three species in *A. creber* lineage) only received support slightly higher than 0.25, with several other scenarios receiving similar support at the respective *collapseheight* value. The scenario with five species (*A. venenatus* separated from *A. creber* lineage) is the first scenario with a relatively high support separating itself from the other scenarios at

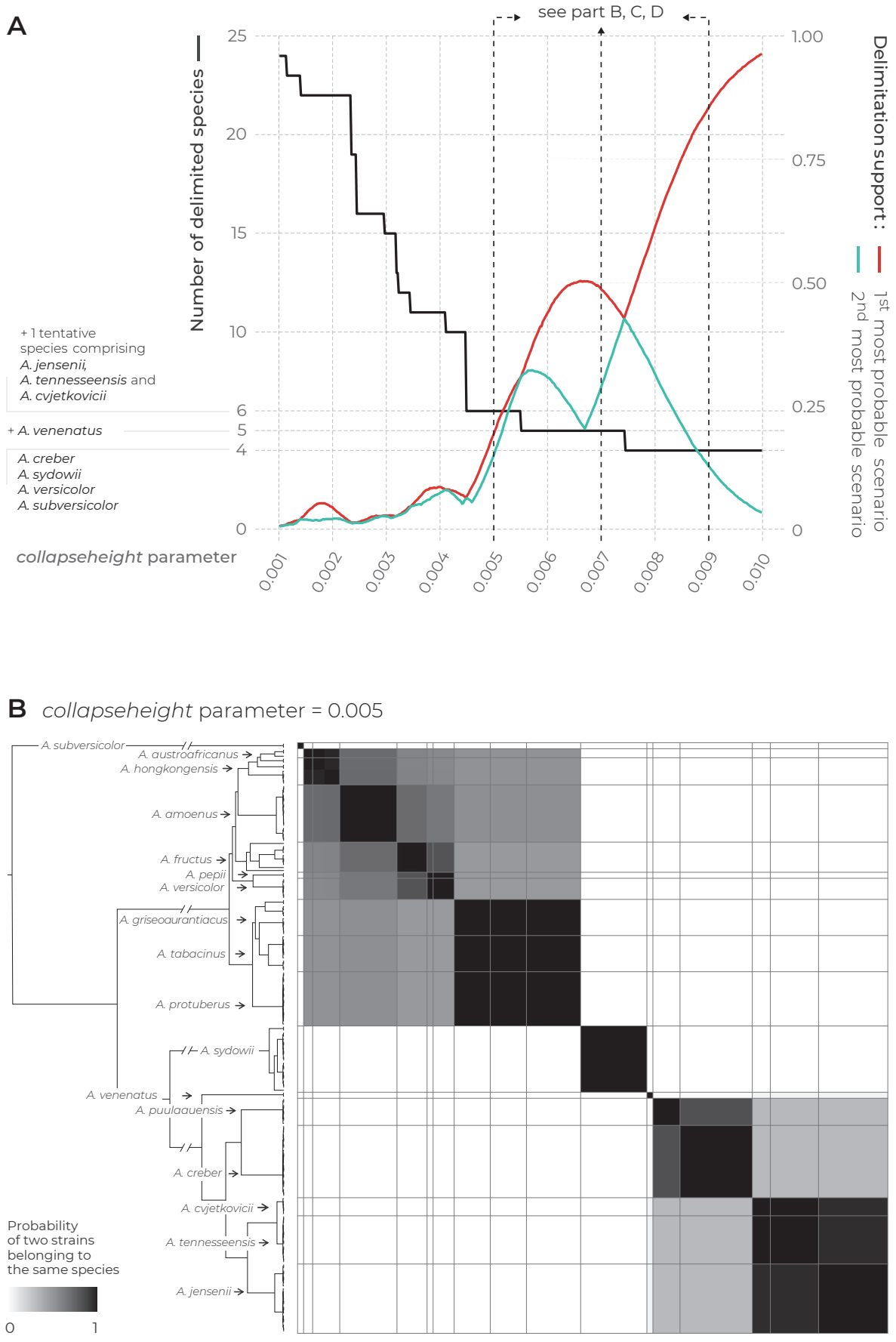

Fig. 6. The results of species delimitation by STACEY. **A.** Dependence of delimitation results on *collapseheight* parameter. The black solid line represents the number of delimited species (left y-axis) depending on the changing value of *collapseheight* parameter (x-axis). The red line represents the probability (right y-axis; range from 0 to 1) of the most probable scenario at specific *collapseheight* value. The turquoise line represents the probability of the second most probable scenario at specific *collapseheight* value. Dashed vertical lines mark three values (0.005, 0.007 and 0.009) of *collapseheight* parameter whose results are shown in detail by similarity matrices (**B**, **C**, **D**). The similarity matrices give the posterior probability of every two isolates belonging to the same multi-species coalescent cluster (tentative species). Black colour corresponds to a posterior probability of 1, while the white colour is equal to 0. Thicker horizontal and vertical lines in the similarity matrices depict the approximate boundaries of species in their narrow concept.

C *collapseheight* parameter = 0.007

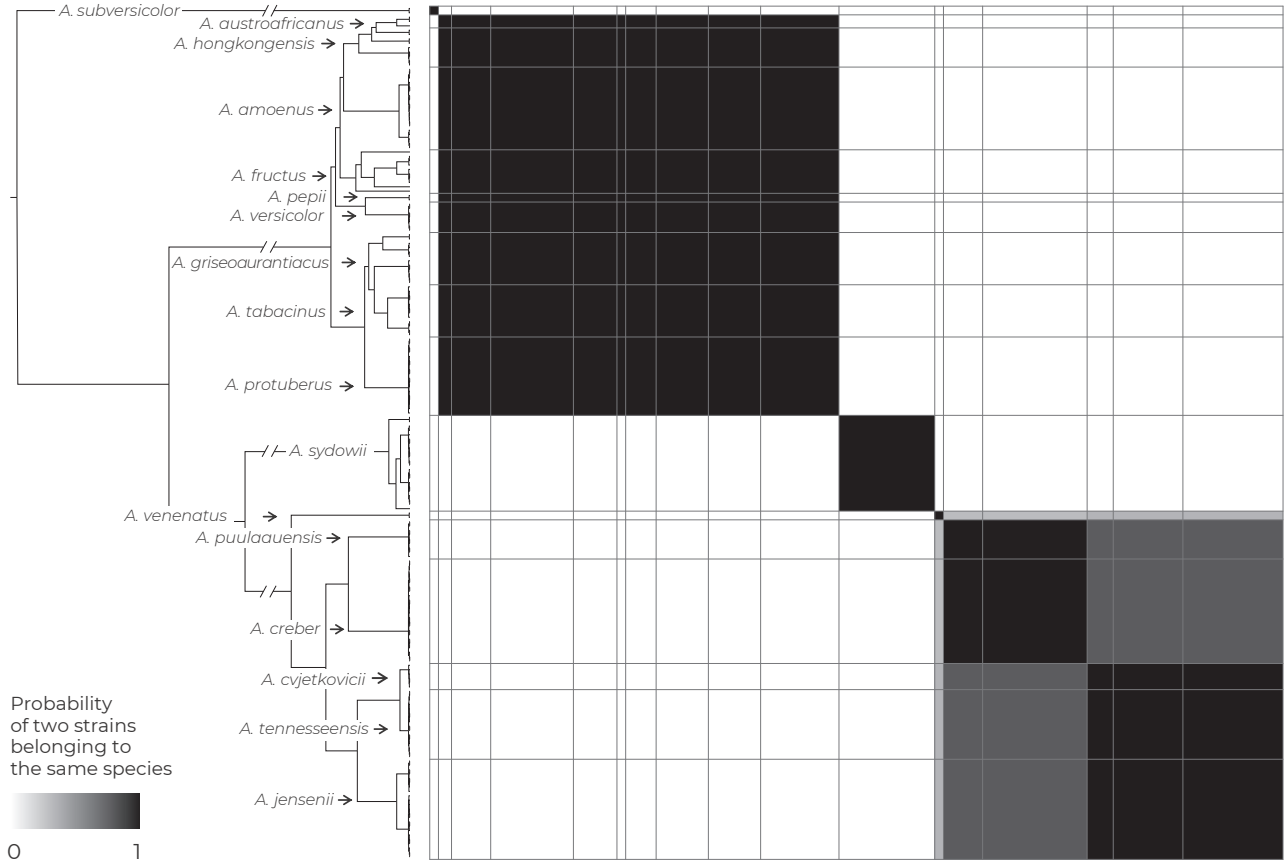

D *collapseheight* parameter = 0.009

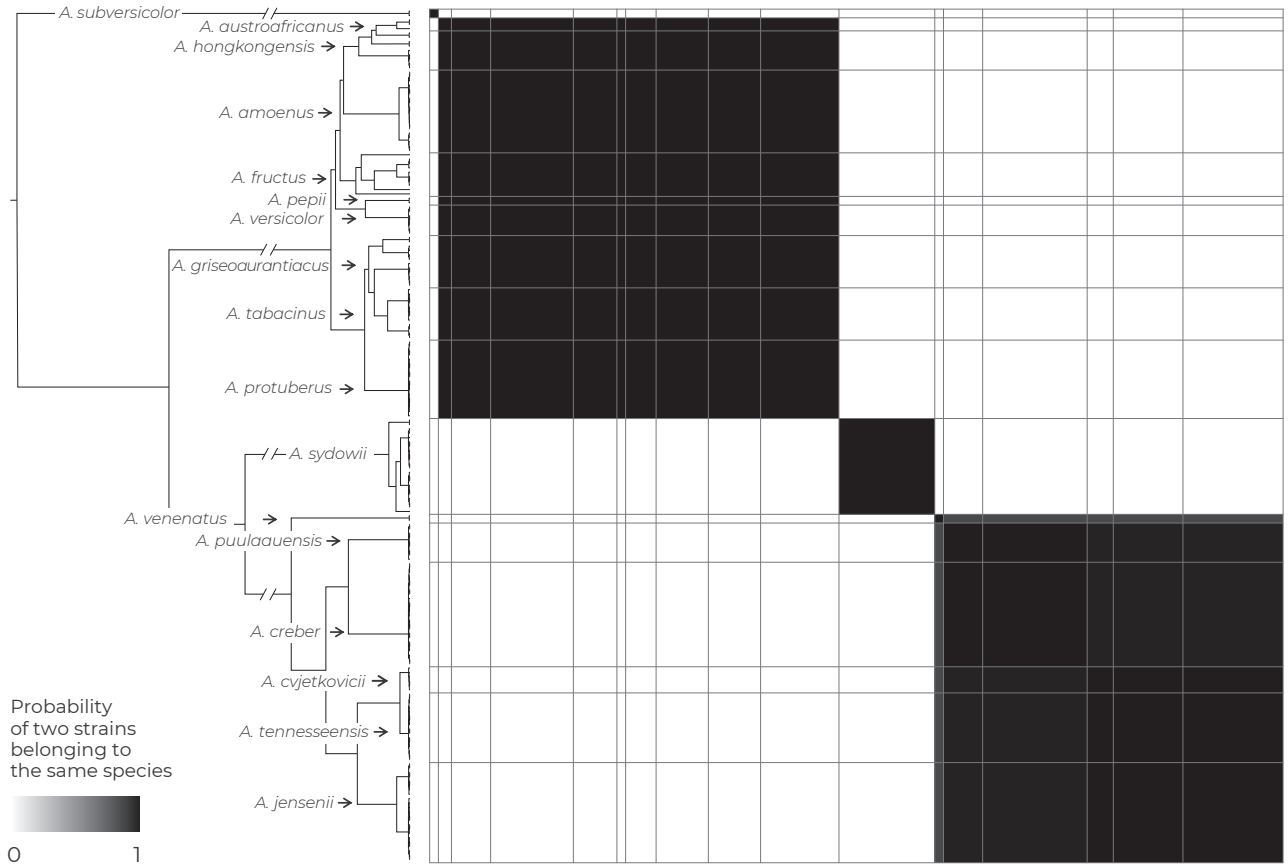

Fig. 6. (Continued).

collapseheight parameter around 0.006. At the *collapseheight* value of 0.0075, the delimitation of four species (*A. creber*, *A. sydowii*, *A. versicolor*, *A. subversicolor*) becomes the most supported scenario and its probability rises to almost 1.0 with increasing *collapseheight* value. The vertical dashed lines in Fig. 6A represent the scenarios illustrated in detail in subfigures B, C, and D in the form of similarity matrices. At the *collapseheight* of 0.005 (Fig. 6B), there are three species in the *A. creber* lineage (*A. venenatus*; *A. puulaauensis* + *A. creber*; *A. cvjetkovicii* + *A. tennesseensis* + *A. jensenii*) and there is also some visible structure in the *A. versicolor* lineage (*A. austroafricanus* + *A. hongkongensis* + *A. amoenus* + *A. fructus* + *A. pepii* + *A. versicolor*; *A. griseoaurantiacus* + *A. tabacinus* + *A. protuberus*). At *collapseheight* of 0.007 (Fig. 6C), the structure within *A. versicolor* and *A. creber* lineages disappears except for the strains of *A. venenatus* which remain separate from the *A. creber* lineage. At *collapseheight* of 0.009 (Fig. 6D), *A. venenatus* becomes part of the broad *A. creber* species.

The species hypotheses were independently tested with DELINEATE (Sukumaran *et al.* 2021) and the results are summarized in Fig. 7. We set up six models with *A. subversicolor* and *A. sydowii* always fixed as separate species and various parts of the *A. versicolor* and *A. creber* lineages left to be delimited. All populations from the *A. creber* lineage were left unassigned in models 1 and 2. In the first model, we assigned all populations from the *A. versicolor* lineage to one species, and in the second model, we split the *A. versicolor* lineage into three hypothetical species based

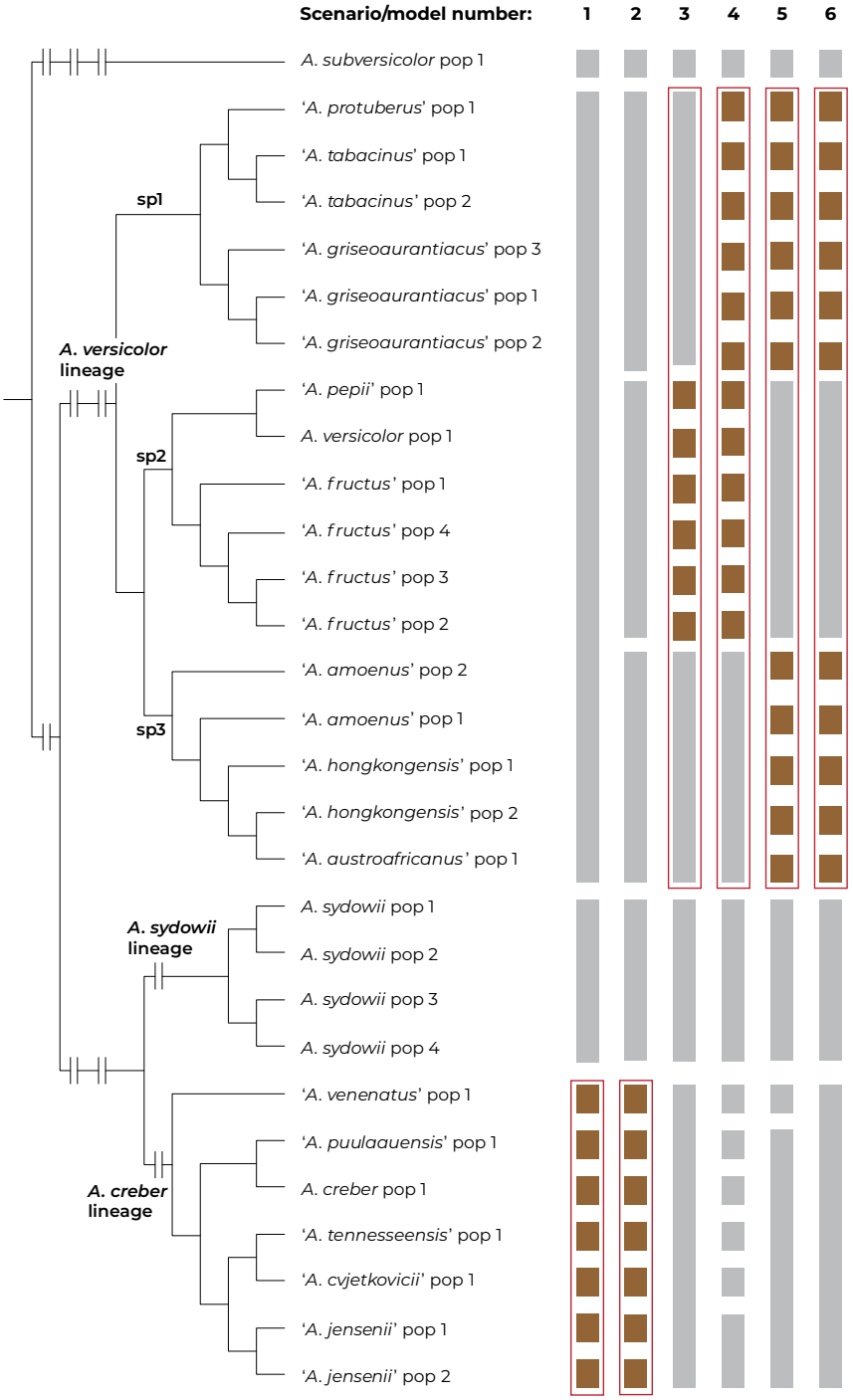

Fig. 7. Overview of species delimitation by DELINEATE. The populations were delimited with BPP and the species tree was calculated in starBEAST. The bars depict the setting and result of every scenario/model (numbered 1 to 6). The grey bars represent the predefined species (locked in the specific model), the brown bars represent unassigned populations, which were left free to be delimited. The red rectangles represent the species boundaries proposed by DELINEATE.

on the tree from starBEAST (Fig. 3) and the results of STACEY with a low *collapseheight* parameter of 0.005 (Fig. 6B): "versicolor sp1" (*A. protuberus*, *A. tabacinus*, and *A. griseoaurantiacus*) "versicolor sp2" (*A. pepii*, *A. versicolor*, and *A. fructus*) and "versicolor sp3" (*A. amoenus*, *A. hongkongensis*, and *A. austroafricanus*) (Fig. 7). Both models 1 and 2 resulted in delimitation of a single wide species in *A. creber* lineage.

Models 3-6 focused on *A. versicolor* lineage. In model 3, there were three fixed species: the whole *A. creber* lineage, clade "versicolor sp1", and clade "versicolor sp3", while the populations of "versicolor sp2" were left unassigned. In model 4, *A. creber* lineage was split into six currently accepted species, clade "versicolor sp3" was fixed as one species and all other populations in *A. versicolor* lineage were left to be delimited. In models 5 and 6, clade "versicolor sp2" was fixed as one species and all populations of clades "versicolor sp1" and "versicolor sp3" were left unassigned. The difference between models 5 and 6 was in the setting of *A. creber* lineage, where *A. venenatus* was set as separate species in model 5 and lumped together with the rest of the lineage in model 6. Models 3–6 resulted in lumping all the populations in *A. versicolor* lineage into a single wide species.

Morphology

Figures 8 and 9 and Supplementary Table S2 demonstrate the macromorphological variability within the series *Versicolores*. The conclusion we can draw from this comparison is that the strains in this series are extremely variable in terms of colony obverse and reverse colour and colony dimensions, and it is extremely hard to differentiate the phylogenetically defined clades/species from this series based on macromorphology. Even *A. sydowii*, a species usually considered as morphologically and physiologically well-defined can produce colonies with very different colours and texture on some media, *e.g.*, CYA, CZA, OA, CREA (Figs 8, 9). On the other hand, its typical blue-green colonies seem to be almost always present on MEA with exception of several strains examined by us, isolated from clinical material and caves which constantly produced light pink colonies on MEA (not shown). *Aspergillus subversicolor* generally produced smaller colonies than other species, but not exclusively and it could be in some cases misidentified as a member of the *A. creber* lineage based solely on macromorphological characters. Even phylogenetically very closely related strains of the same species frequently produce dissimilar colonies under the same conditions and vice versa, phylogenetically distant strains sometimes produce similar pattern of colonies (Figs 8, 9). Some differences, *e.g.*, the lack of sporulation, can be attributed to the long-term preservation of some strains (NRRL 238 or NRRL 227). On the other hand, in some other recently isolated strains, the lack of sporulation on some media seems to be rather random than specific to media. The production of Hülle cells is also rather random and not limited to some clades or media (Supplementary Table S3). The strain NRRL 239 was the only examined strain which produced Hülle cells regularly on all media except CREA. In conclusion, it is difficult to find macromorphological patterns specific for the narrow species or even for the main lineages. The variability within the two main lineages of *A. versicolor* and *A. creber* is extreme and largely overlapping between themselves.

Figures 10 and 11 display an overview of the dimensions of micromorphological characters separately for each strain and for the four main lineages. The plot showing the results of Linear Discriminant Analysis in Fig. 10 suggests that it is possible to differentiate the *A. versicolor* lineage, *A. sydowii* and *A. subversicolor* based on micromorphological measurements, but that the *A. creber* lineage interferes with all other lineages. The characters most useful for the discrimination were the length and width of conidia. Although the differences in measurements between the main lineages were mostly small, they were often evaluated as significant even using Tukey's HSD test, probably due to a large number of measurements. The variability of micromorphological characters between individual strains showed sometimes large differences even between phylogenetically closely related strains. The length and width of conidia were the most stable characters throughout the main lineages (smaller conidia in *A. versicolor* lineage compared to other lineages). The degree of stability within species/lineage is much lower in measurements of phialides and metulae, and completely lost in vesicle diameters and stipe lengths. The stipe width is rather similar throughout the whole series.

Physiology

The growth rates at variable temperatures and in osmotic gradient were measured for the same set of strains that were characterized macromophologically (Supplementary Tables S2, S3). The ability to grow at different temperatures differentiates *A. sydowii* and *A. subversicolor* from the remaining species/lineages (Fig. 12). Only some isolates of *A. sydowii* are capable of growing at 37 °C and this species grows moderately at 35 °C. *Aspergillus subversicolor* differs from all species by its inability of growing at 10 °C. It grows at 35 °C in contrast to strains from *A. creber* and *A. versicolor* lineages. All tested isolates of the *A. versicolor* and *A. creber* lineages grew restrictedly at 10 °C and none of them grew at 35 °C. There are very small differences between the *A. versicolor* and *A. creber* lineages in colony dimensions at 10, 15 and 30 °C. The strains of the *A. versicolor* lineage attained on average slightly larger colony diameters (in mm) after 14 d at 30 °C than *A. creber* lineage strains (minimum–average–maximum; *A. versicolor*: 18–30–43; *A. creber*: 10–20–32), and slightly smaller colony diameter at 10 °C (*A. versicolor*: 2–4.5–7; *A. creber*: 7–8.5–10) and 15 °C (*A. versicolor*: 10–13–17; *A. creber*: 15–17–19). The temperature optimum of the *A. versicolor* lineage is therefore higher than the optimum of the *A. creber* lineage.

The growth pattern in an osmotic gradient (Fig. 13) was similar to the growth rates at different temperatures, *i.e.*, *A. sydowii* and *A. subversicolor* being clearly different from other species, while *A. versicolor* and *A. creber* lineages expressed a similar growth profile (Fig. 13B). The biggest differences between the strains can be observed at 5 % NaCl concentration. *Aspergillus sydowii* grows much faster at this concentration than other species, while *A. subversicolor* is on the other side of the spectrum. Similar results but with less pronounced differences can be seen on MEA without NaCl and on MEA with 10 % NaCl. All tested strains grew very restrictedly at 15 % NaCl concentration. Figure 13A displays the variable growth rate within the *A. versicolor* and *A. creber* lineages. The differences between representatives of different clades/species are more distinct within the *A. versicolor* lineage with *A. hongkongensis* growing the fastest at 5 % and 10 % NaCl and *A. tabacinus* and *A. fructus* growing at the slowest rate. The fastest growing species in the *A. creber* lineage at 5 % and 10 % NaCl were *A. cvjetkovicii* and *A. tennesseensis* but the differences from other species were very small.

Fig. 8. Overview of macromorphological characters (obverse side of Petri dishes) within series *Versicolores* on eight cultivation media (MEA, CYA, CZA, YES, DG18, OA, CY20S, CREA) grown for 14 d at 25 °C.

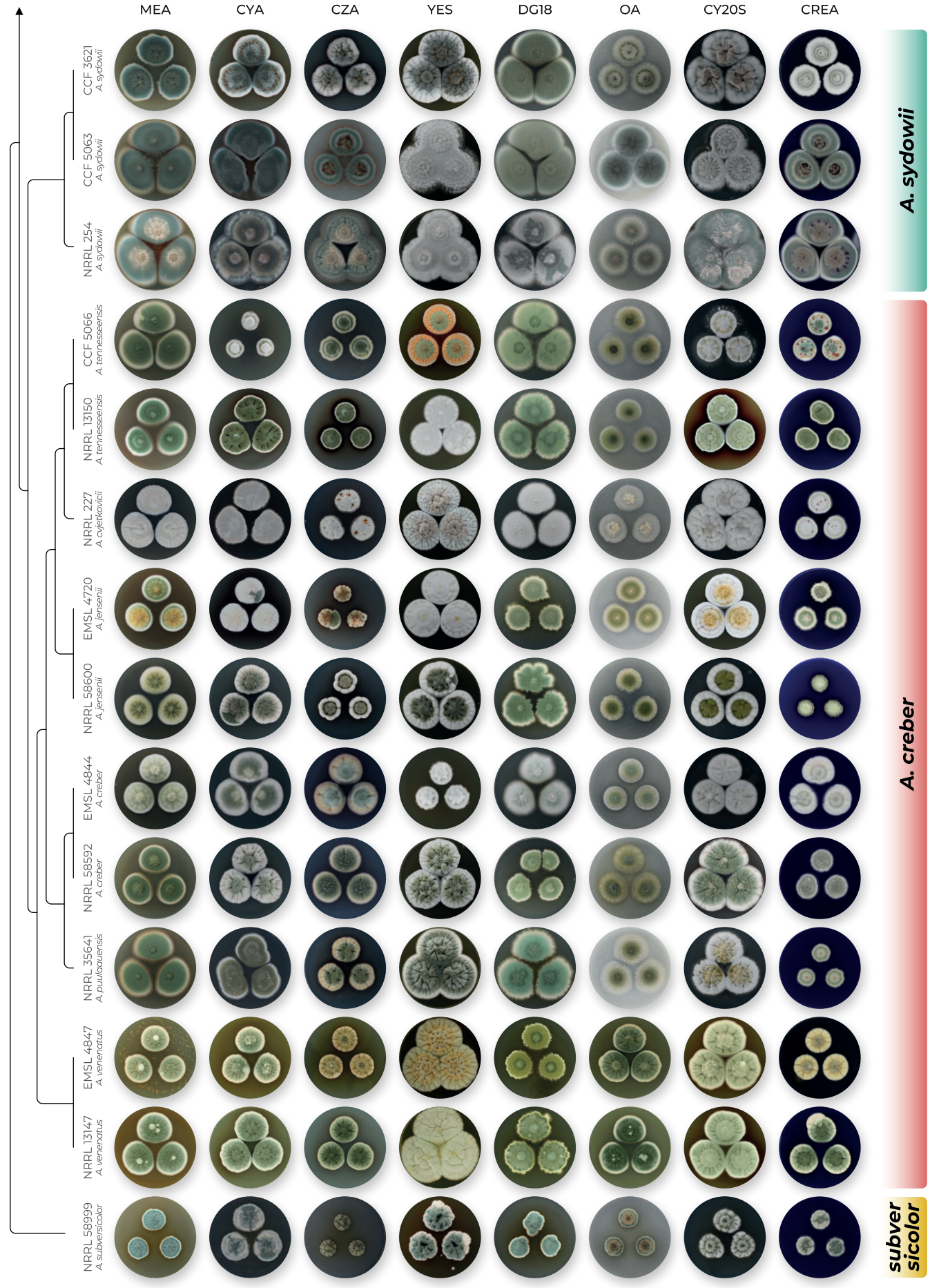

Fig. 8. (Continued).

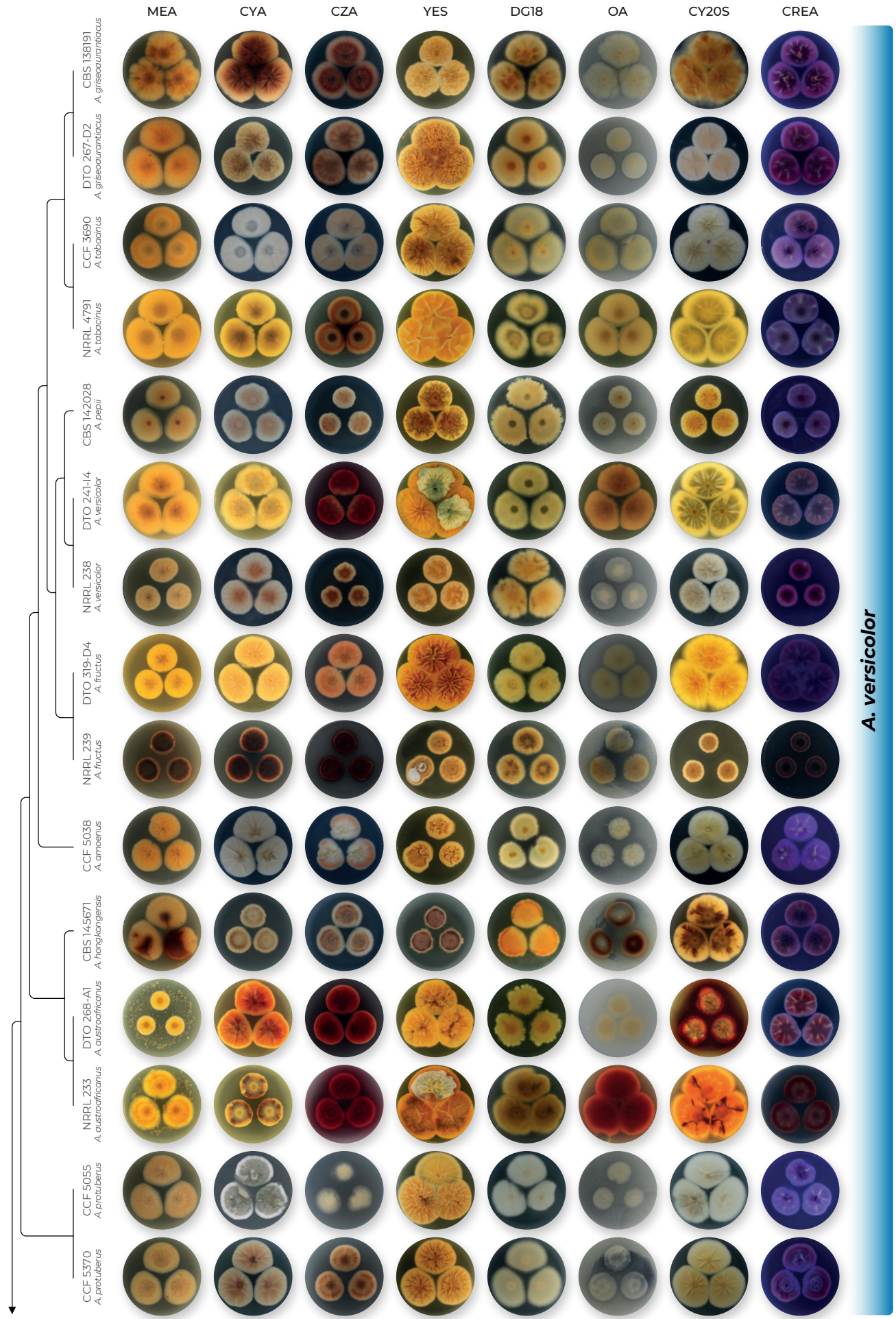

Fig. 9. Overview of macromorphological characters (reverse side of Petri dishes) within series *Versicolores* on eight cultivation media (MEA, CYA, CZA, YES, DG18, OA, CY20S, CREA) grown for 14 d at 25 °C.

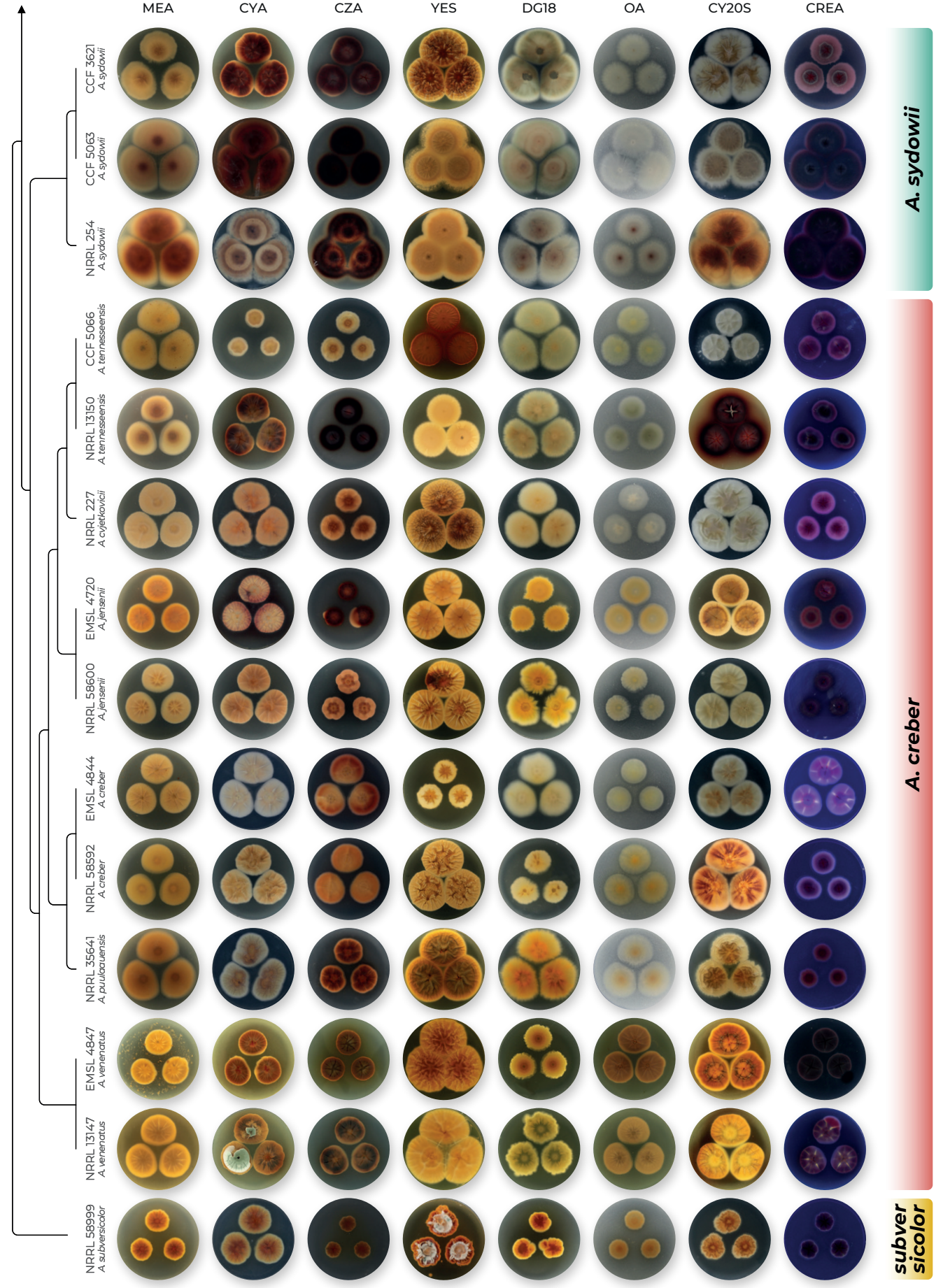

Fig. 9. (Continued).

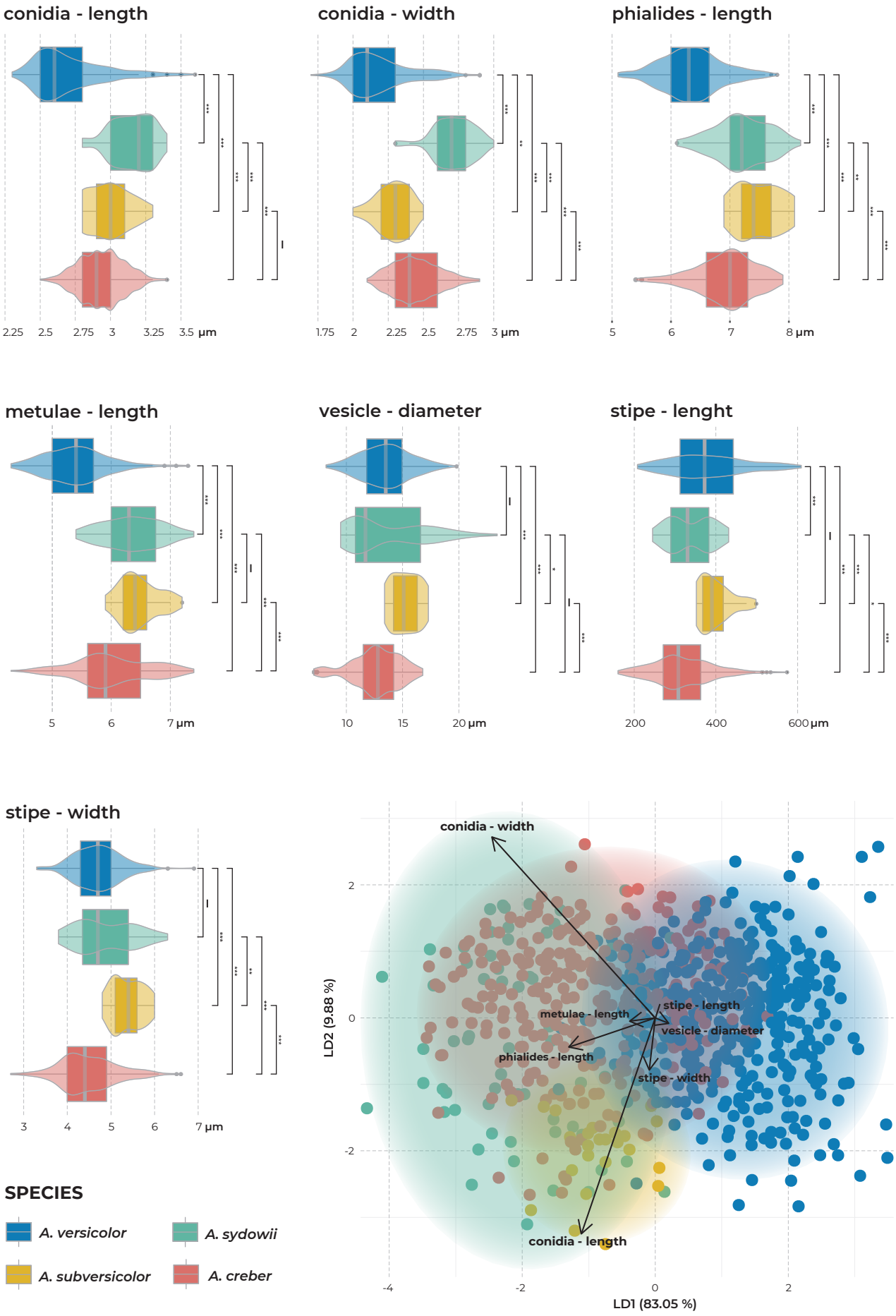

Fig. 10. Overview of dimensions of seven micromorphological characters. Box plots and violin plots of measurements distributed into four broadly defined species. Box plots show interquartile range, values within ± 1.5 of interquartile range (whiskers) and outliers. Asterisks on the right side of each plot express the statistical significance of pairwise comparisons using the Tukey's HSD test (* < 0.05; ** < 0.01; *** < 0.001). The lower right subfigure shows the results of linear discriminant analysis based on micromorphological measurements distributed into four broadly defined species.

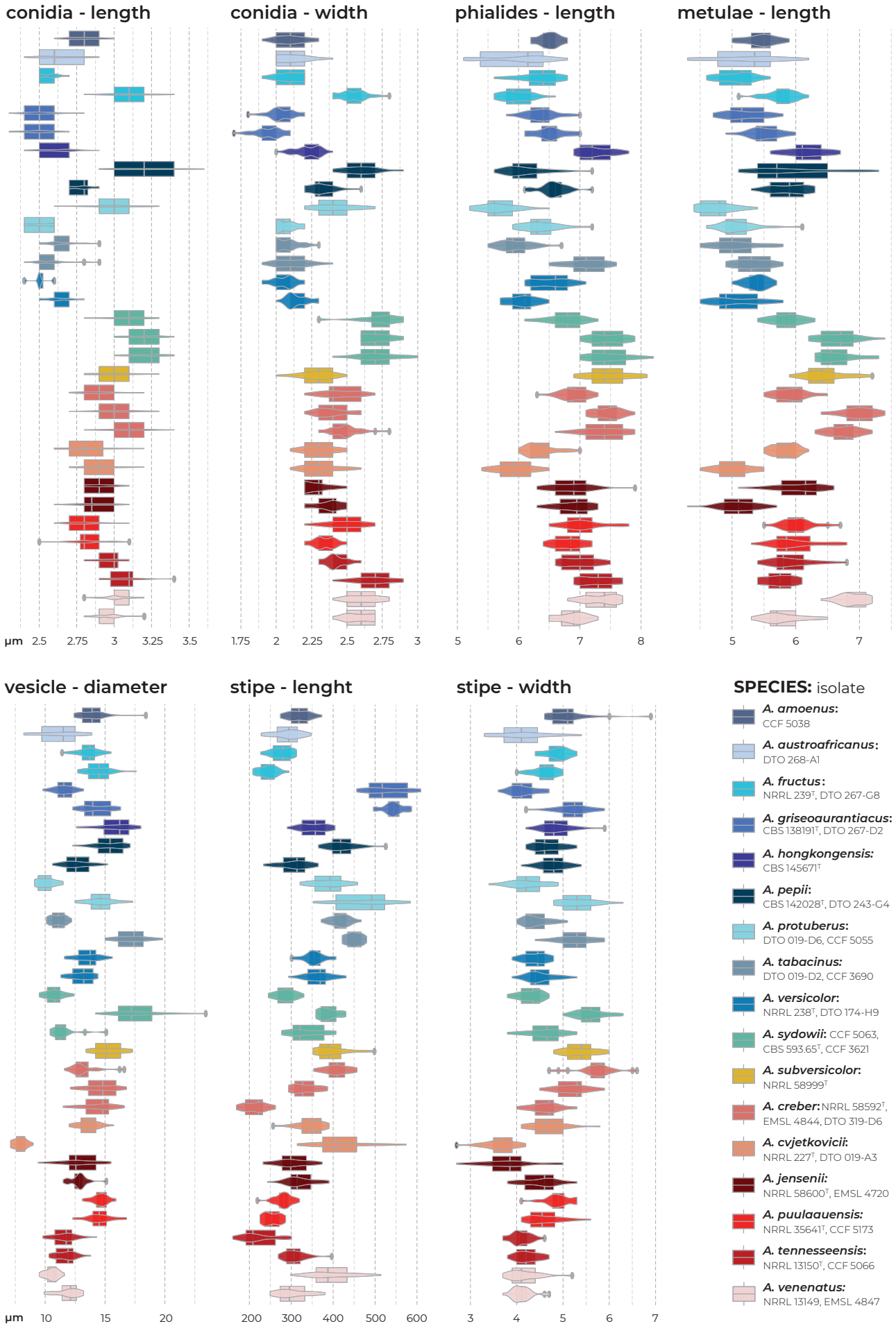

Fig. 11. Dimensions of seven micromorphological characters across isolates of narrowly defined species in the series *Versicolores* shown in the form of box plots and violin plots. Box plots show interquartile range, values within ± 1.5 of interquartile range (whiskers) and outliers.

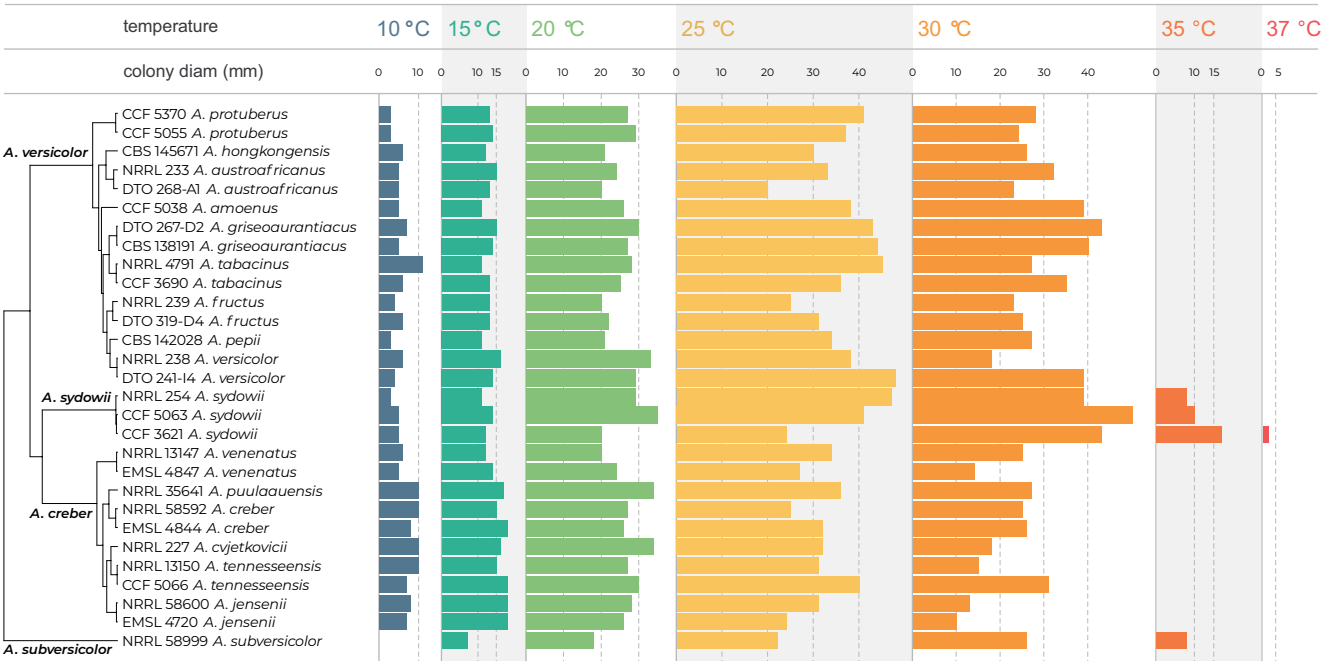

Fig. 12. Comparison of growth rates on MEA at temperatures ranging from 10 °C to 37 °C after 14 d of cultivation. Phylogenetic tree is based on the *CaM* sequences of selected strains and calculated in IQ-TREE; bar plots representing the colony size at specific temperature are displayed on the right.

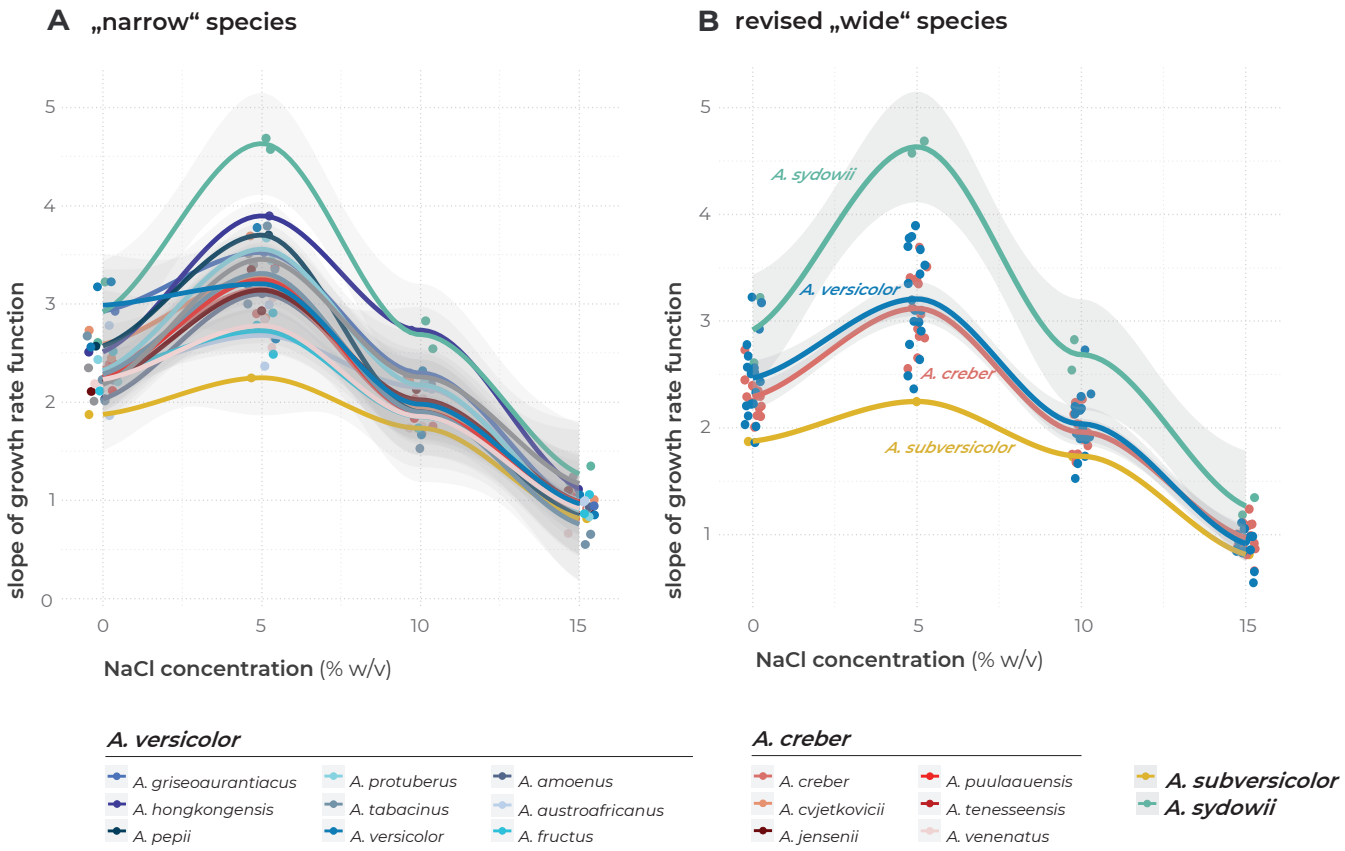

Fig. 13. Growth rates of species in osmotic (NaCl) gradient. Each point represents the slope value of the linear trendline from the growth curve of strains and NaCl concentration (0, 5, 10, 15 % w/v). The curve was created using the LOESS function in R package ggplot2, grey zones represent 95 % confidence intervals. **A.** Strains distributed into 17 narrow species. **B.** Strains distributed into four main lineages.

TAXONOMY

Aspergillus creber Jurjević, S.W. Peterson & B.W. Horn, IMA Fungus 3: 69. 2012. MycoBank MB 800598. Fig. 14.
= *Aspergillus cvjetkovicii* Jurjević, S.W. Peterson & B.W. Horn, IMA Fungus 3: 69. 2012. MycoBank MB 800599.
= *Aspergillus jensenii* Jurjević, S.W. Peterson & B.W. Horn, IMA Fungus 3: 70. 2012. MycoBank MB 800601.
= *Aspergillus puulaauensis* Jurjević, S.W. Peterson & B.W. Horn, IMA Fungus 3: 71. 2012. MycoBank MB 800602.
= *Aspergillus tennesseensis* Jurjević, S.W. Peterson & B.W. Horn, IMA Fungus 3: 73. 2012. MycoBank MB 800604.
= *Aspergillus venenatus* Jurjević, S.W. Peterson & B.W. Horn, IMA Fungus 3: 73. 2012. MycoBank MB 800605.

Typus: BPI 800912. Culture ex-type: CBS 145749 = NRRL 58592 = DTO 225-G7 = IBT 32277.

Colony diam, *25 °C (if not otherwise stated)*, *14 d (mm)*: MEA: 25–40; CYA: 18–38; CZA: 21–30; YES: 23–52; DG18: 25–51; OA: 22–36; CY20S: 26–47; CREA: 22–31. MEA 10 °C: 7–10; MEA 15 °C: 15–19; MEA 20 °C: 26–34; MEA 30 °C: 10–32; MEA 35 °C: 0.

Culture characteristics, *25 °C*, *14 d*: MEA: Colonies centrally raised, in some strains radially wrinkled; texture velutinous, floccose in the centre; margins entire to delicately filiform; mycelial areas white (#ffffff); sporulation bottle green (#006a4e) or viridian green (#40826d), at first white; orange yellow crayola patches with Hülle cells occasionally present; reverse centrally windsor tan (#a75502) to maximum yellow red (#f2ba49) in margins. CYA: Colonies centrally raised, radially wrinkled in some strains; texture velutinous; margins undulate; mycelial areas white to wheat (#f5deb3); sporulation at first white to wheat (#f5deb3), xanadu (#738678) or fern green (#4d744d); reverse centrally ochre (#cc7722) to gold crayola (#e6be8a) in margins, saddle brown (#964b00) when sporulation is dense. CZA: Colonies centrally raised, radially wrinkled in some strains; texture velutinous to floccose; margins undulate; exudate in the form of clear droplets present in some strains; bistre (#3d2b1f) soluble pigment present in some strains; mycelial areas jasmine (#f8de7e) or white; sporulation middle green (#4d8c57) or viridian (#40826d); reverse centrally seal brown (#59260b) or maximum yellow red (#f2ba49), in margins alloy orange (#c46210) or bistre (#3d2b1f) when soluble pigment is present. YES: Colonies centrally raised, significantly, irregularly wrinkled; texture floccose; margins entire, delicately undulate in some strains; mycelial areas white, in some strains bright yellow crayola (#ffaa1d); sporulation russian green (#679267), asparagus (#87a96b) or ash gray (#b2beb5); reverse centrally saddle brown (#964b00) or sepia (#704214) to naples yellow (#fada5e) in margins. DG18: Colonies flat or umbonate; texture velutinous; margins undulate to filiform; mycelial areas white; sporulation at first white, dark sea green (#8fbc8f) or green sheen (#6eaea1); reverse alloy orange (#c46210) to orange yellow crayola (#f8d568), in margins flax (#eedc82). OA: Colonies centrally raised; texture floccose to granular; margins entire, irregular in some strains; sporulation brunswick green (#1b4d3e) to yellow green crayola (#c5e384), in margins white; reverse orange peel (#ff9f00) to flax (#eedc82) in margins. CY20S: Colonies centrally raised, radially wrinkled; texture velutinous to floccose; margins entire to filiform; bistre (#3d2b1f) soluble pigment present in some strains; mycelial areas white in margins, maize crayola (#f2c649) in central areas; sporulation russian green (#679267), asparagus (#87a96b), ash gray (#b2beb5) or white; reverse centrally alloy orange (#c46210) or golden brown (#996515), in margins maize crayola (#f2c649) or medium champagne (#f3e5ab). CREA: Colonies centrally raised; texture velutinous to floccose; margins entire to delicately filiform; exudate in the form of clear droplets present in some strains; bistre (#3d2b1f) soluble pigment present in some strains; mycelial areas white; sporulation dark sea green (#8fbc8f) or cambridge blue (#a3c1ad); reverse dark purple (#301934), fuchsia crayola (#c154c1) or bistre (#3d2b1f); no acid production.

Micromorphology: *Ascomata* absent. *Hülle cells* present in some strains, most commonly on MEA or CZA (Supplementary Table S3), hyaline, subglobose, usually 18–21 × 16–19 µm. *Conidial heads* radiate, remaining compact, *conidiophores* biseriate. *Stipes* smooth, hyaline or light brown, (200–)250–350(–400) × 4–6 µm; *vesicles* hyaline, pyriform to subglobose, (10–)12–16 µm diam; *metulae* hyaline, cylindrical to barrel-shaped, 5–7 µm long, covering three quarters of the vesicle; *phialides* hyaline, flask-shaped, 6.5–7.5 µm long. *Conidia* globose to subglobose, verrucose, hyaline 2.5–3 (2.9 ± 0.2) × 2–2.5 (2.4 ± 0.2) µm.

Cardinal temperatures: *Aspergillus creber* grows at 10 °C, and the optimum growth temperature is between 20 and 25 °C. This species is able to grow well at 30 °C but does not grow at 35 °C.

Distinguishing characters: *Aspergillus creber* and *A. versicolor* are two species that possess huge genetic and phenotypic variability. It is impossible to distinguish these two species, because all morphological and physiological characters measured in this study largely overlap. The conidia of *A. versicolor* tend to be the smallest among the series members (*A. versicolor* 2.6 ± 0.2 × 2.1 ± 0.1 µm *vs A. creber* 2.9 ± 0.2 × 2.4 ± 0.2 µm). The strains of *A. versicolor* are usually growing slightly faster than those of *A. creber* on MEA supplied with 5 % NaCl (Fig. 13). The temperature optimum of these two species is also slightly different: *A. versicolor* strains grows faster at 30 °C and strains of *A. creber* grows faster at 10 and 15 °C. (Fig. 12) For distinguishing characters from *A. subversicolor* and *A. sydowii*, see the respective paragraphs below.

Aspergillus subversicolor Jurjević, S.W.Peterson & B.W. Horn, IMA Fungus 3: 69. 2012. MycoBank MB 800603. Fig. 15.

Typus: BPI 880918. Culture ex-type: CBS 145751 = NRRL 58999 = DTO 225-G9.

Colony diam, *25 °C (if not otherwise stated)*, *14 d (mm)*: MEA: 22; CYA: 31; CZA: 12; YES: 29; DG18: 22; OA: 19; CY20S: 25; CREA: 17. MEA 10 °C: 0; MEA 15 °C: 7; MEA 20 °C*:* 18; MEA 30 °C: 26; MEA 35 °C: 8.

Culture characteristics, *25 °C*, *14 d*: MEA: Colonies centrally raised, moderately wrinkled; texture velutinous; margins undulate; mycelial areas white (#ffffff); sporulation verdigris (#43b3ae); reverse centrally alloy orange (#c46210) to jasmine (#f8de7e) in margins. CYA: Colonies centrally raised, moderately wrinkled; texture floccose; margins undulate; mycelial areas white; sporulation polished pine (#5da493); reverse centrally burnt orange (#cc5500) to flax (#eedc82) in margins. CZA: Colonies crateriform (raised with central depression), significantly wrinkled; texture floccose; margins undulate; exudate present in the form of clear droplets; mycelial areas white; sporulation pine green (#01796f) to olivine (#9ab973); reverse saddle brown (#964b00) with medium champagne

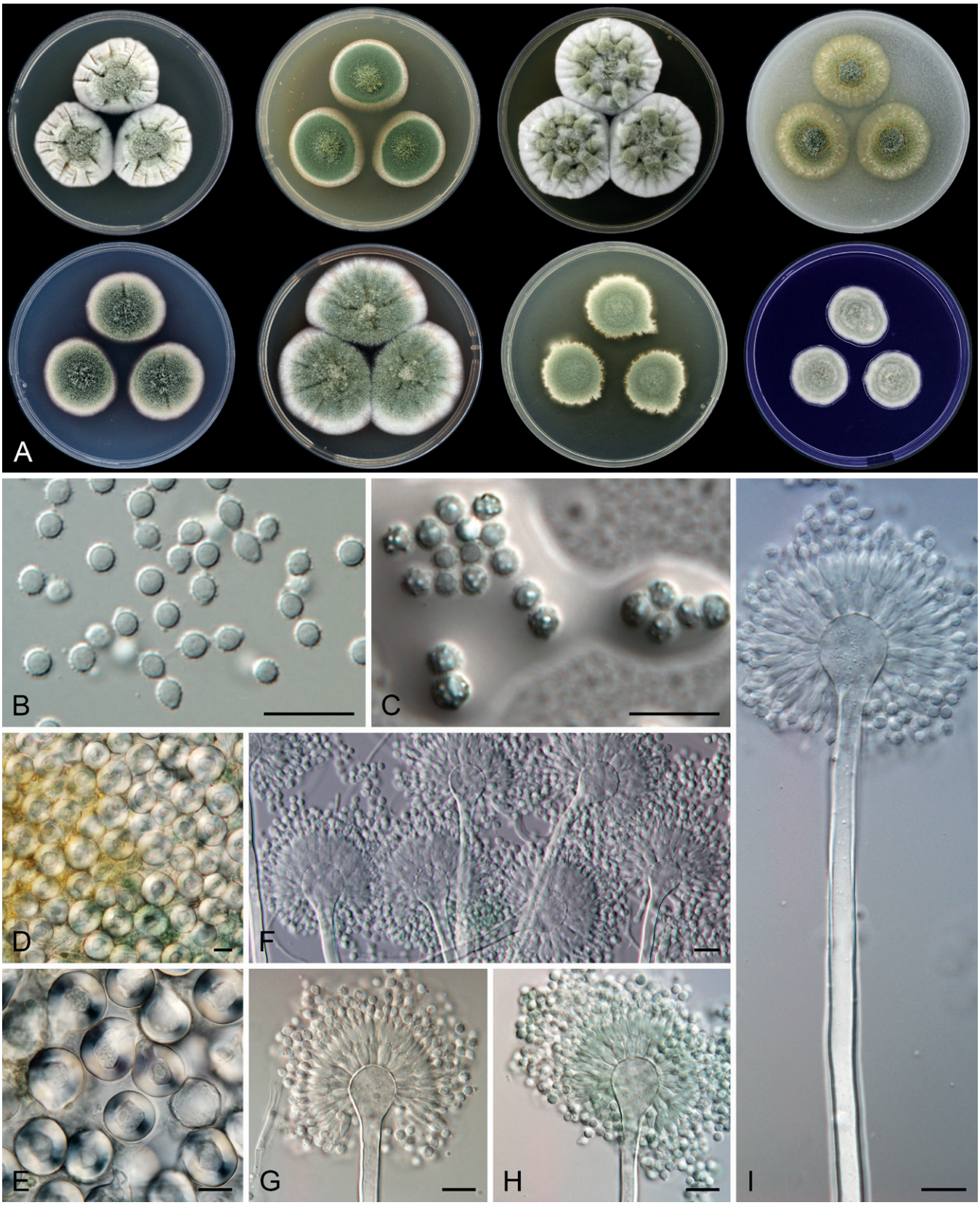

Fig. 14. Macromorphology and micromorphology of *Aspergillus creber*. **A.** Top row left to right: colonies on CYA, MEA, YES and OA after 14 d at 25 °C; bottom row left to right: colonies on CZA, CY20S, DG18 and CREA after 14 d at 25 °C (all colonies from strain NRRL 58592). **B.** Conidia. **C.** Conidia in air bubble. **D, E.** Hülle cells. **F–I.** Conidiophores. Scale bars = 10 µm.

(#f3e5ab) margins. YES: Colonies crateriform (raised with central depression), significantly wrinkled; texture velutinous to floccose; margins undulate to lobate; mycelial areas white to linen (#faf0e6); sporulation dark sea green (#8fbc8f) to green sheen (#6eaea1); reverse centrally earth yellow (#e1a95f) to black bean (#3d0c02), in margins alloy orange (#c46210). DG18: Colonies centrally raised, moderately radially wrinkled; texture velutinous; margins undulate to lobate; mycelial areas hyaline; sporulation green sheen (#6eaea1); reverse saddle brown (#964b00) to alloy orange (#c46210) to naples yellow (#fada5e) in margins. OA: Colonies centrally raised; texture irregularly floccose; margins delicately undulate; mycelial areas hyaline; sporulation deep jungle green (#004b49); reverse

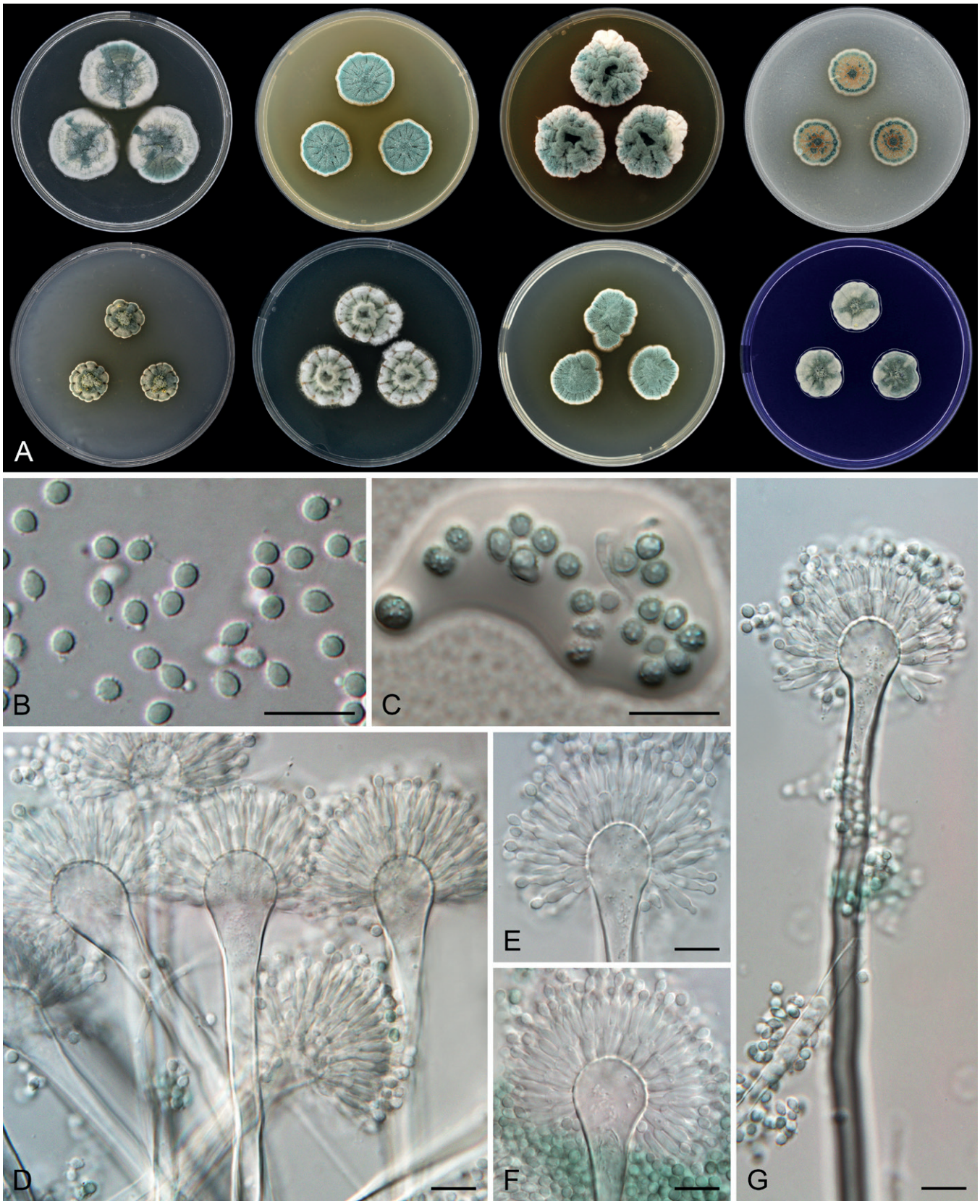

Fig. 15. Macromorphology and micromorphology of *Aspergillus subversicolor*. **A.** Top row left to right: colonies on CYA, MEA, YES and OA after 14 d at 25 °C; bottom row left to right: colonies on CZA, CY20S, DG18 and CREA after 14 d at 25 °C (all colonies from strain NRRL 58999). **B.** Conidia. **C.** Conidia in air bubble. **D–G.** Conidiophores. Scale bars = 10 µm.

centrally alloy orange (#c46210) to medium champagne (#f3e5ab) in margins. CY20S: Colonies crateriform (raised with central depression), radially wrinkled; texture floccose; margins undulate to delicately filiform; mycelial areas white; sporulation dark sea green (#8fbc8f); reverse centrally alloy orange (#c46210) to sunray (#e3ab57), in margins jasmine (#f8de7e). CREA: Colonies centrally raised; texture floccose; margins undulate; exudate present in the form of clear droplets; mycelial areas white to beige (#f5f5dc); sporulation viridian (#40826d) to russian green (#679267); reverse raisin black (#242124), pink lavender (#d8b2d1) in margins; no acid production.

Micromorphology: *Ascomata* absent. *Hülle cells* absent. *Conidial heads* radiate, remaining compact, *conidiophores* biseriate. *Stipes* smooth, hyaline or light brown, 350–450 × 5–6 µm; *vesicles* hyaline, pyriform to spatulate, 14–17 µm diam; *metulae* hyaline, cylindrical to obovate, 6–7 µm long, covering three quarters of the vesicle; *phialides* hyaline, flask-shaped, 7–8 µm long. *Conidia* subglobose to ovoid, verrucose, hyaline 3 (3 ± 0.1) × 2–2.5 (2.3 ± 0.1) µm.

Cardinal temperatures: *Aspergillus subversicolor* does not grow at 10 °C, but grows at 15 °C, and its optimum growth temperature is 30 °C. This species is able to grow restrictedly at 35 °C but not at 37 °C.

Notes: *Aspergillus subversicolor* is phylogenetically distant from other species in the series *Versicolores*, but clearly belongs to the series (Houbraken *et al.* 2020). It is easily distinguishable from other members of the series by its slower growth on almost all cultivation media and on MEA supplied with 5 % NaCl (Fig. 13). Unlike other species, it is unable to grow at 10 °C, but contrary to *A. creber* and *A. versicolor*, it grows restrictedly at 35 °C (Fig. 12).

Aspergillus sydowii (Bainier & Sartory) Thom & Church, Aspergilli: 147. 1926. MycoBank MB 279636. Fig. 16.

Typus: IMI 211384. Culture ex-type: CBS 593.65 = NRRL 250 = IMI 211384 = NRRL 254 = ATCC 16844.

Colony diam, *25 °C (if not otherwise stated)*, *14 d (mm)*: MEA: 34–48; CYA: 36–50; CZA: 32–40; YES: 45–48; DG18: 49–54; OA: 28–39; CY20S: 38–61; CREA: 38–43. MEA 10 °C: 3–5; MEA 15 °C: 11–13; MEA 20 °C: 20–35; MEA 30 °C: 39–50; MEA 35 °C: 10–17; MEA 37 °C: 0–5.

Culture characteristics, *25 °C*, *14 d*: MEA: Colonies centrally raised, moderately radially wrinkled; texture velutinous; margins undulate; mycelial areas white (#ffffff); sporulation celadon green (#2f847c) to dark cyan (#008b8b); reverse centrally dark brown (#654321) to medium champagne (#f3e5ab) in margins or centrally rust (#b7410e) to yellow crayola (#fce883) in margins. CYA: Colonies centrally raised, moderately radially wrinkled in some strains; texture velutinous; margins entire to delicately filiform; exudate present in some strains in the form of clear droplets; mycelial areas white; sporulation centrally deep space sparkle (#4a646c), dark cyan in margins (#008b8b); reverse centrally seal brown (#59260b), in margins windsor tan (#a75502) or banana mania (#fae7b5). CZA: Colonies centrally raised, wrinkled in some strains; texture floccose; margins undulate to delicately filiform; exudate present in the form of clear droplets; bistre (#3d2b1f) soluble pigment present in some strains; mycelial areas white to linen (#faf0e6); sporulation brunswick green (#1b4d3e) to celadon green (#2f847c); reverse centrally bistre (#3d2b1f) or seal brown (#59260b) to banana mania (#fae7b5) in margins. YES: Colonies raised, moderately wrinkled; texture floccose, cottony in margins; margins undulate to irregular; mycelial areas white; sporulation ash gray (#b2beb5) or celadon green (#2f847c); reverse copper (#b87333) to jasmine (#f8de7e). DG18: Colonies centrally raised; texture velutinous; margins entire to delicately filiform; mycelial areas white; sporulation deep jungle green (#004b49) to ash gray (#b2beb5); reverse centrally camel (#c19a6b) to beige (#f5f5dc) in margins. OA: Colonies centrally raised, moderately wrinkled in some strains; texture velutinous to floccose; margins undulate to irregular; mycelial areas white or hyaline; sporulation centrally deep jungle green (#004b49) or russian green (#679267) to ash grey in margins (#b2beb5); reverse centrally saddle brown (#964b00) to medium champagne (#f3e5ab) in margins. CY20S: Colonies centrally raised or crateriform (raised with central depression), radially or irregularly wrinkled; texture centrally floccose to cottony in margins; margins undulate to delicately filiform; mycelial areas white to linen (#faf0e6); sporulation celadon green (#2f847c) or ash gray (#b2beb5); reverse centrally French bistre (#856d4d) to beige (#f5f5dc) in margins. CREA: Colonies centrally raised; texture velutinous to floccose; margins entire to delicately filiform; exudate present in the form of clear droplets; mycelial areas white to tan (#d2b48c); sporulation dark cyan (#008b8b) to middle blue green (#8dd9cc); reverse centrally raisin black (#242124) to charcoal (#36454f), in margins pink lavender (#d8b2d1); no acid production.

Micromorphology: *Ascomata* absent. *Hülle cells* absent. *Conidial heads* radiate, remaining compact, *conidiophores* biseriate. *Stipes* smooth, hyaline or light brown 250–400 × 4–6 µm; *vesicles* hyaline, spatulate to clavate, 10–17(–25) µm diam; *metulae* hyaline, cylindrical to barrel-shaped, 6–7 µm long, covering three quarters of the vesicle; *phialides* hyaline, flask-shaped, 6.5–8 µm long. *Conidia* subglobose to ovate, verrucose, hyaline 3–3.5 (3.1 ± 0.1) × 2.5–3 (2.7 ± 0.1) µm.

Cardinal temperatures: *Aspergillus sydowii* grows restrictedly at 10 °C, and the optimum growth temperature is 30 °C. Some strains of this species are able to grow restrictedly at 37 °C but not at 40 °C.

Distinguishing characters: *Aspergillus sydowii* exhibits some genetic variability, however it was never split into more species and the concept of this species remains the same since its original description in 1926 (Thom & Church). It can be distinguished from other species in series *Versicolores* by its typically blue-green to turquoise colony colours on MEA, CYA, and CZA. Additionally, this species is more osmotolerant than other members of the series as it grows the fastest on media supplied with 5 and 10 % of NaCl (Fig. 13). It is also the only species of the series with some strains capable of growing at 37 °C (Fig. 12).

Aspergillus versicolor (Vuill.) Tirab., Ann. Bot., Roma 7: 9. 1908. MycoBank MB 172159. Fig. 17.
= *Aspergillus amoenus* M. Roberg, Hedwigia 70: 138. 1931. MycoBank MB 250654.
= *Aspergillus austroafricanus* Jurjević, S.W. Peterson & B.W. Horn, IMA Fungus 3: 67. 2012. MycoBank MB 800597.
= *Aspergillus fructus* Jurjević, S.W. Peterson & B.W. Horn, IMA Fungus 3: 70. 2012. MycoBank MB 800600.
= *Aspergillus griseoaurantiacus* Visagie, Hirooka & Samson, Stud. Mycol. 78: 112. 2014. MycoBank MB 809197.
= *Aspergillus hongkongensis* C.C. Tsang *et al.*, Diagn. Microbiol. Infect. Dis. 84: 130. 2016. MycoBank MB 810279.
= *Aspergillus pepii* Despot *et al.*, Mycol. Prog. 16: 67. 2017. MycoBank MB 817073.
= *Aspergillus protuberus* Munt.-Cvetk., Mikrobiologiya 5: 119. 1968. MycoBank MB 326650.
= *Aspergillus tabacinus* Nakaz. *et al.*, J. Agric. Chem. Soc. Japan 10: 177. 1934. MycoBank MB 539544.

Typus: CBS 583.65. Culture ex-type: CBS 583.65 = NRRL 238 = ATCC 9577 = IFO 33027 = IMI 229970 = JCM 10258 = UAMH 4956 = QM 7478 = Thom 5519.57 = WB 238.

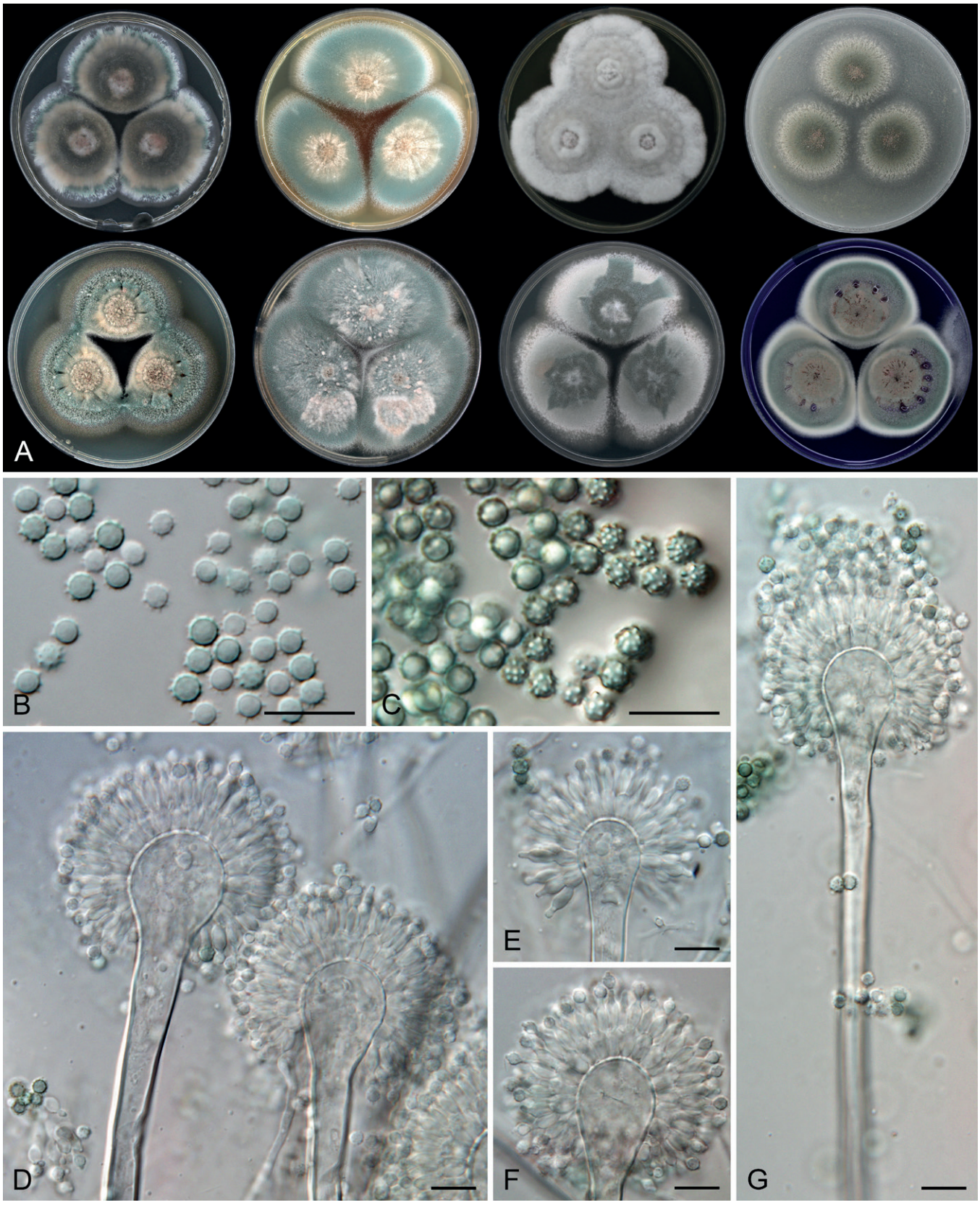

Fig. 16. Macromorphology and micromorphology of *Aspergillus sydowii*. **A.** Top row left to right: colonies on CYA, MEA, YES and OA after 14 d at 25 °C; bottom row left to right: CZA, CY20S, DG18 and CREA after 14 d at 25 °C (all colonies from strain NRRL 254). **B.** Conidia. **C.** Conidia in air bubble. **D–G.** Conidiophores. Scale bars = 10 µm.

Colony diam, *25 °C (if not otherwise stated)*, *14 d (mm)*: MEA: 20–48; CYA: 26–46; CZA: 22–38; YES: 25–60; DG18: 30–49; OA: 22–49; CY20S: 26–60; CREA: 22–45. MEA 10 °C: 2–7; MEA 15 °C: 10–17; MEA 20 °C: 20–32; MEA 30 °C: 18–43; MEA 35 °C: 0.

Culture characteristics, *25 °C*, *14 d*: MEA: Colonies centrally raised, in some strains radially wrinkled; texture velutinous, floccose in the centre; margins entire to delicately filiform; exudate present in the form of clear droplets; mycelial areas white (#ffffff); sporulation forest green crayola (#5fa777), russian green (#679267), viridian (#40826d) or myrtle green (#317873); flax (#eedc82) patches with

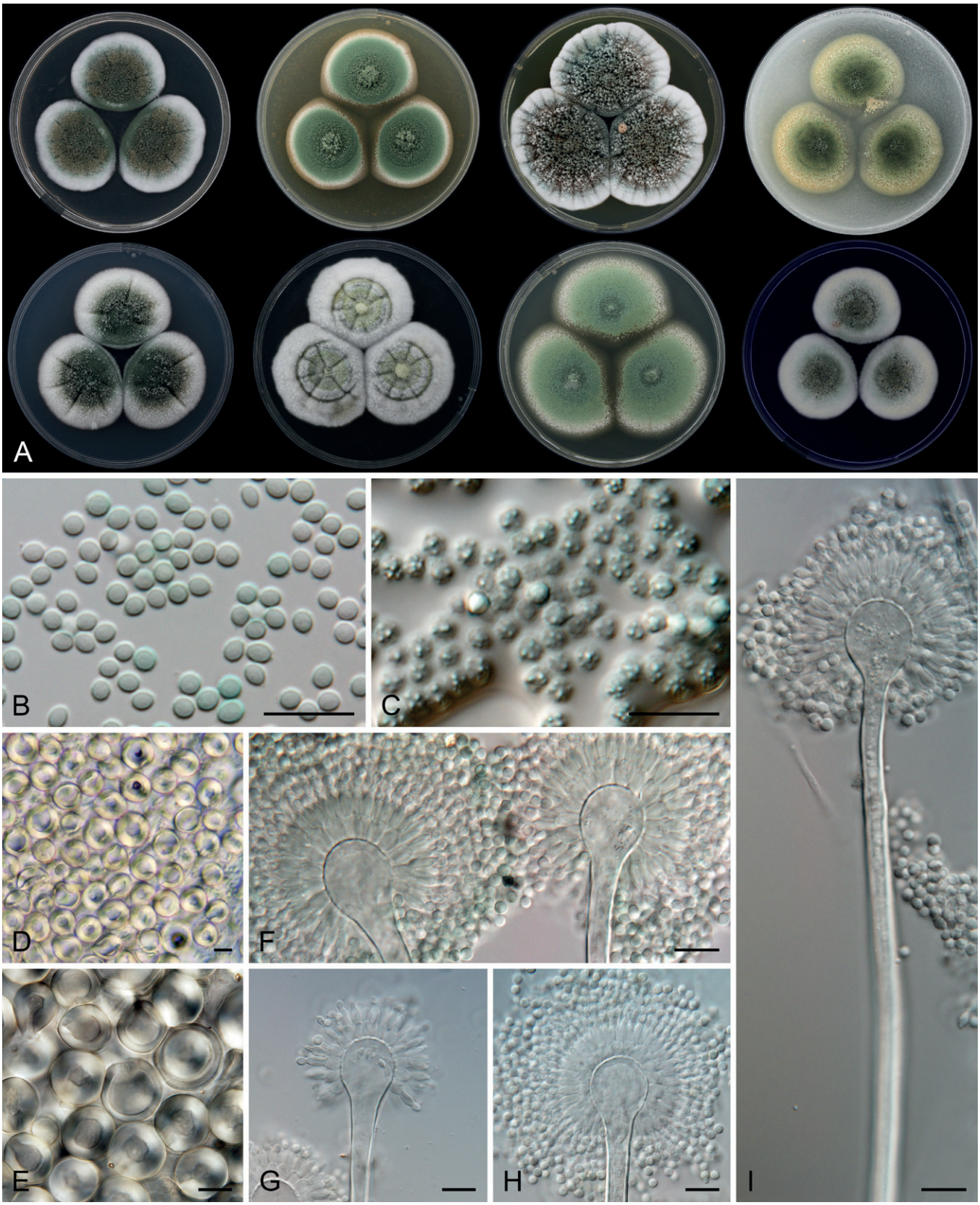

Fig. 17. Macromorphology and micromorphology of *Aspergillus versicolor*. **A.** Top row left to right: colonies on CYA, MEA, YES and OA after 14 d at 25 °C; bottom row left to right: CZA, CY20S, DG18 and CREA after 14 d at 25 °C (all colonies from strain CCF 3690). **B.** Conidia. **C.** Conidia in air bubble. **D, E.** Hülle cells. **F–I.** Conidiophores. Scale bars = 10 µm.

Hülle cells present in some strains; reverse centrally alloy orange (#c46210) or dark brown (#654321) to flax (#eedc82) in margins. CYA: Colonies centrally raised, radially wrinkled; texture velutinous to floccose, with cottony centre in some strains; margins entire, less commonly undulate; exudate present in the form of clear droplets; mycelial areas white; sporulation bottle green (#006a4e), pine green (#01796f) or fern green (#4d744d); reverse centrally bistre brown (#967117) or copper (#b87333) to beige (#f5f5dc) in margins. CZA: Colonies centrally raised, radially (in some strains also concentrically) wrinkled; texture velutinous to floccose; margins entire, seldom undulate; bistre (#3d2b1f) soluble pigment present in some strains; exudate present in the form of clear droplets; mycelial

areas white; sporulation brunswick green (#1b4d3e) or hunter green (#355e3b), seldom white to ash grey (#b2beb5); gold metallic (#d4af37) patches with Hülle cells present in some strains; reverse centrally saddle brown (#964b00) to windsor tan (#a75502) or black bean (#3d0c02) in strains producing soluble pigment, in margins wheat (#f5deb3). YES: Colonies centrally raised, significantly, irregularly wrinkled, texture velutinous to floccose; margins entire, seldom undulate or irregular; exudate present in some strains in the form of clear droplets; mycelial areas white; sporulation deep jungle green (#004b49) shiny shamrock (#5fa778) or cambridge blue (#a3c1ad), seldom white to ash gray (#b2beb5); yellow crayola (#fce883) patches with Hülle cells present in some strains; reverse centrally liver chestnut (#987456) to alloy orange (#c46210), in margins jasmine (#f8de7e). DG18: Colonies centrally raised; texture velutinous, in some strains cottony in the center; margins entire, in some strains irregular; mycelial areas white; sporulation illuminating emerald (#319177) or xanadu (#738678), seldom white to ash gray (#b2beb5); yellow crayola (#fce883) patches with Hülle cells present in some strains; reverse centrally saddle brown (#964b00) to alloy orange (#c46210), in margins straw (#e4d96f). OA: Colonies centrally raised; texture floccose; margins entire to irregular; rust (#b7410e) to ecru (#c2b280) soluble pigment present in some strains; mycelial areas white or hyaline; sporulation deep jungle green (#004b49), fern green (#4d744d) or green sheen (#6eaea1), in some strains with vegas gold (#c5b358) patches formed by conidiophores, not by Hülle cells; reverse centrally dark brown (#654321) to copper (#b87333) or rust (#b7410e) in strains producing soluble pigment, in margins flax (#eedc82). CY20S: Colonies centrally raised, radially wrinkled; texture floccose with cottony patches; margins entire to irregular; mycelial areas white; sporulation green sheen (#6eaea1), fern green (#4d744d) or ash grey (#b2beb5), in some strains with gold metallic (#d4af37) patches (formed by conidiophores, not Hülle cells); canary (#ffff9a) to yellow crayola (#fce883) patches with Hülle cells present in some strains; reverse centrally alloy orange (#c46210) to yellow crayola (#fce883) in margins or centrally olive green (#b5b35c) to beige (#f5f5dc) in margins. CREA: Colonies centrally raised, in some strains moderately wrinkled; texture velutinous to floccose; margins entire to delicately filiform; exudate present in some strains in the form of clear or fire opal (#e95c4b) droplets; mycelial areas white to medium champagne (#f3e5ab); sporulation cambridge blue (#a3c1ad), xanadu (#77897c) or fern green (#4d744d), in some strains ash grey (#b2beb5); reverse centrally dark purple (#301934) to fuchsia crayola (#c154c1) in margins, or centrally charcoal (#36454f) to tuscany (#c09999) in margins; no acid production.

Micromorphology: *Ascomata* absent. *Hülle cells* present in some strains, most commonly on MEA, YES or DG18 (Supplementary Table S3), hyaline, subglobose, usually 18–21 × 15–20 µm. *Conidial heads* radiate, remaining compact, *conidiophores* biseriate. *Stipes* smooth, hyaline or light brown, 300–600 × 4–6 µm; *vesicles* hyaline, pyriform to spatulate, (10–)12–16(–20) µm diam; *metulae* hyaline, cylindrical to barrel-shaped, 5–6 µm long, covering three quarters to the entire vesicle; *phialides* hyaline, flask-shaped, 6–7.5 µm long. *Conidia* subglobose to ovate, finely verrucose, hyaline 2.5–3 (2.6 ± 0.2) × 2–2.5 (2.1 ± 0.1) µm.

Cardinal temperatures: *Aspergillus versicolor* grows restrictedly at 10 °C, and the optimum growth temperature is between 25 and 30 °C. This species is able to grow well at 30 °C but does not grow at 35 °C.

Distinguishing characters: See respective paragraphs of the species above.

DISCUSSION

Larger amounts of molecular data led to a higher rate of description of new species, with phylogenetically defined/cryptic species becoming increasingly common (Struck *et al.* 2018). This is also the case in *Aspergillus*, where the number of accepted species was steadily rising for the last twenty years (Houbraken *et al.* 2020). Recently, studies employing the species delimitation methods often resulted in a reduction in the number of species (Hubka *et al.* 2018, Wang *et al.* 2018, Boluda *et al.* 2019, Li *et al.* 2019, Feng *et al.* 2021, Nguyen *et al.* 2021), even when phylogenomic approaches were used (Parker *et al.* 2022). These studies usually advocate for an integrative approach using as much data of different types as possible. Enough variability in the dataset is often a requirement from species delimitation methods (Mason *et al.* 2020, Burbrink & Ruane 2021, Cicero *et al.* 2021, Magoga *et al.* 2021). Unfortunately, this condition is frequently hard to follow in taxonomic studies because obtaining large numbers of genetically similar isolates from different localities is difficult to achieve especially in uncommon species. Such efforts are often hampered in practice by administrative (*e.g.*, Nagoya protocol), financial and other barriers. A logical outcome in practice is that the fungal species are frequently described based on a low number of isolates with a limited variability due to insufficient sampling. In such cases where intraspecific variability is low or not present at all, it is usually easy to find phenotypic features distinguishing small clusters of strains, or single strains representing different populations/species. True intraspecific variability is often uncovered much later when enough strains representing a broader species variability is collected. In the meantime, however, the species can already be fragmented into several newly described species, which are often cryptic and sometimes introduced only to preserve the monophyly of the other species in the phylogeny. Over time, the concept will become unsustainable until the next overhaul.

The taxonomy of *A. versicolor* and its relatives has been a subject of many taxonomic re-arrangements and repeated expansions followed by reductions in the number of species. Currently, the species number is again at one of the historical peaks and involves 17 species, most of which can be considered cryptic. Over time, the evidence began to accumulate that some isolates cannot be identified satisfactorily to the species level even with the help of molecular methods. Contradictory species identification results based on sequences of different genes were the initial signal that the species concept in series *Versicolores* is becoming unsustainable. To verify this assumption, we gathered a much larger collection of series *Versicolores* members compared to previous taxonomic studies. Most species delimitation methods have consistently suggested a significant reduction in the number of species as summarized below.

Phylogenetic support of species reduction

The species delimitation methods employed in this study broadly agreed on the distinction of four species (*A. creber*, *A. subversicolor*, *A. sydowii* and *A. versicolor*). Only seven out of 28 methods resulted in the delimitation of more than four species but without clear agreement on the arrangement of the additional species. Such conclusive results are probably caused by a sufficient sampling in the majority of subclades. In general, if there are only a few individuals with large genetic distances in the dataset, the species delimitation methods may overestimate the species number, but with a large set of individuals covering genetic diversity and closing the gaps between clades, the probability of methods to delimit species in

their correct boundaries increases (Pante *et al.* 2015, Chambers & Hillis 2020). The multilocus method STACEY gave similar support to the delimitation of four or five species with *A. venenatus* treated as separate species in the setting with a lower *collapseheight* parameter. The uncertainty about *A. venenatus* can probably be attributed to underrepresentation of isolates from this clade (only two strains from similar localities). Delimitation of *A. protuberus* as separate species from *A. versicolor* was also supported by several single-locus delimitation methods but with different arrangements. The incongruences and probable recombination were detected between *A. protuberus* and other species in *benA* and *Tsr1* loci (Fig. 4). Considering all results together with the inability to reliably distinguish these species morphologically, we suggest treating *A. venenatus* as a synonym of *A. creber* and *A. protuberus* as a synonym of *A. versicolor*.

For the independent testing of species hypotheses proposed by delimitation methods, we used a recently developed program DELINEATE (Sukumaran *et al.* 2021), which gives more relevant results compared to the program BPP as discussed previously (Sukumaran & Knowles 2017, Sklenář *et al.* 2021). The results of the analysis were stable, supporting the broad concept of the species in all scenarios (Fig. 7). The tendency to lump the populations into broad species was always present, even in less probable and meaningful scenarios which were tested by us and not shown in Fig. 7. DELINEATE needs some *a priori* defined species that are certainly correctly delimited in the dataset. This requirement is problematic in the series *Versicolores* since the only species that could be conclusively *a priori* defined were *A. sydowii* and *A. subversicolor*. We overcame this fact by setting up more scenarios with additionally defined delimitations in the *A. creber* and *A. versicolor* lineages (both lineages were divided into subgroups based on the species trees calculated by starBEAST - see Fig. 3). Another solution could be the inclusion of several well-defined species from other related series in section *Nidulantes*.

We also compared the amount of intraspecific variability between the broadly defined species and other accepted species from *Aspergillus* with described intraspecific variability. The resulting graph (Fig. 18) shows that the majority of examined species express the phylogenetic variability of up to 4 % (we can also see that there are only a few species of *Aspergillus* that possess intraspecific genetic variability and have the sequences of *Mcm7* and *Tsr1* genes available and some species gather a large amount of variability in the *benA* gene, which is caused by intronic sequences). The species from series *Versicolores* exhibit different amounts of variability with *A. sydowii* having approximately 1 % maximum phylogenetic distance between its strains, *A. creber* between 2 and 3 %, and *A. versicolor* accumulating more than 3 % of variability in all studied loci. However, even this amount of variability does not make *A. versicolor* an outlier among other *Aspergillus* species.

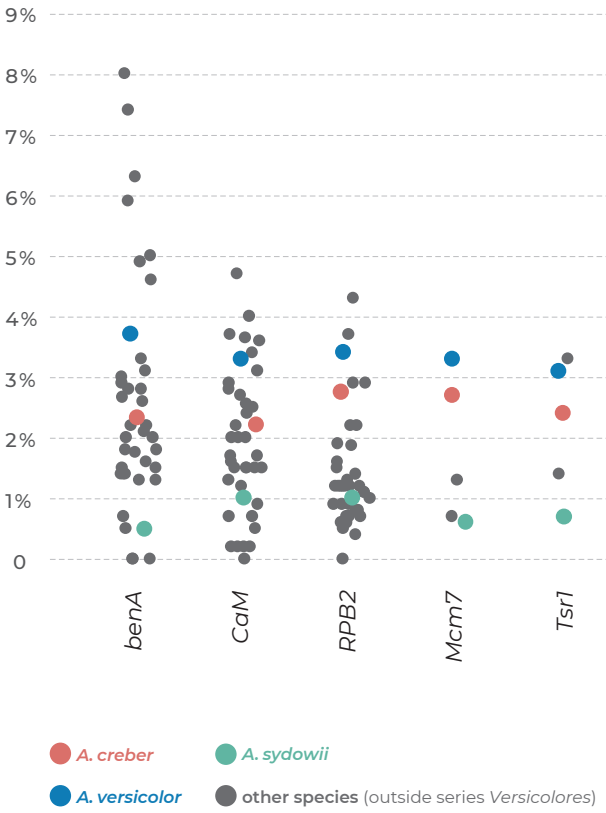

Fig. 18. Graphical representation (jitter plot) of maximum sequence dissimilarity between strains of series *Versicolores* (coloured points) and other *Aspergillus* species (grey points). The comparison includes only species with strains isolated at least from three countries to ensure the presence of representative intraspecific genetic variability. Basic data used for construction of the jitter plot are listed in the Supplementary Table S4.

Morphological and physiological aspects

High morphological variability has always been connected with *A. versicolor* and its relatives (Raper & Fennell 1965, Klich *et al.* 1993, Jurjević *et al.* 2012, Géry *et al.* 2021). This fact also contributed to many re-arrangements in this group before the molecular era. We demonstrated the high intraspecific variability of the series *Versicolores* in macromorphological and micromorphological characters (see Figs 8–11). It is clear from both the colony colours, texture, and dimensions, as well as from boxplots representing micromorphological features that even phylogenetically closely related isolates can exhibit very different phenotypic characteristics. These observations further support reducing the number of species accepted in the series. The linear discriminant analysis (Fig. 10) shows that it is almost impossible to distinguish *A. creber* and *A. versicolor* lineages based on micromorphological characters. The growth curves in the osmotic gradient displayed the same pattern (Fig. 13), *i.e.*, *A. sydowii* and *A. subversicolor* were easily distinguishable, but lineages of *A. creber* and *A. versicolor* grew similarly under changing conditions. From a practical point of view, this means that even after this drastic reduction in the number of species there are still two species that can be considered cryptic from the phenotypic point of view and can only be reliably identified using molecular methods.

Updated taxonomy of series *Versicolores*

Molecular analyses performed in this study indicated that the current species number is overestimated and not sustainable. With a high level of agreement, the majority of methods supported only *A. creber*, *A. subversicolor*, *A. sydowii*, and *A. versicolor* in the series. If we were to consider maintaining the current taxonomic scheme despite the results mentioned above, then we would have to describe at least one new species in the *A. creber* lineage and up to ten new species in the *A. versicolor* lineage (Figs 1, 2). Alternative solutions would be to synonymize some species and describe fewer new species. These solutions were not supported by phenotypic data and receive no or negligible support from phylogenetic methods.

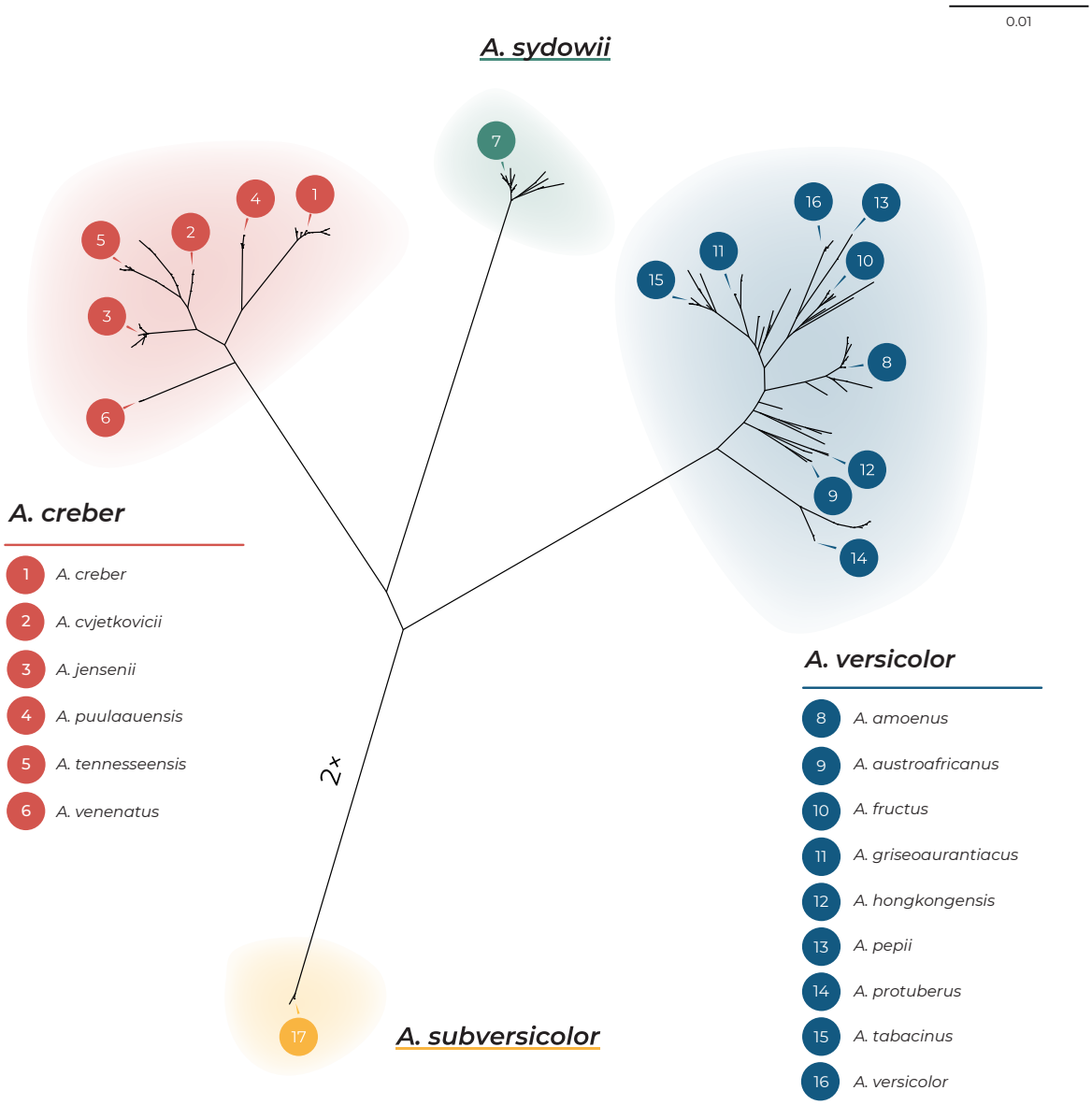

Fig. 19. Taxonomic re-arrangement of series *Versicolores* into four species with marked synonyms. The new taxonomy is schematically shown in the form of the radial tree (ML tree identical to that from Fig. 2).

As a result, a total of 13 species were put in synonymy, five with *A. creber* (*A. cvjetkovicii*, *A. jensenii*, *A. puulaauensis*, *A. tennesseensis*, and *A. venenatus*) and eight with *A. versicolor* (*A. amoenus*, *A. austroafricanus*, *A. fructus*, *A. griseoaurantiacus*, *A. hongkongensis*, *A. pepii*, *A. protuberus*, and *A. tabacinus*). The naming of the two broad species follows the priority rules of the International Code of Nomenclature for algae, fungi, and plants (Turland *et al.* 2018). *Aspergillus versicolor* is the oldest published name in the *A. versicolor* lineage and *A. creber*, simultaneously published with several other new species in its lineage (Jurjević *et al.* 2012), was the highest placed name in the taxonomy section of that article. This new taxonomy is schematically shown by a phylogenetic tree in Fig. 19. This tree is identical to the tree in Fig. 2 but displayed in a radial form, which nicely shows the presence of four wide clades and many small ones representing some of the 17 species accepted before this revision. Additionally, a new species belonging in series *Versicolores*, *A. qilianyuensis*, was described by Wang & Zhuang (2022) based on single strain, but we did not include the species in this study, since it was published during the final preparations of this article and we were unable to obtain the ex-type strain.

We believe that the user community will benefit from this new taxonomy with a lower number of cryptic species. Simplified classification with only four species will facilitate species identification in practices that was complicated by inconsistent identification results when using sequence data of different genes (Fig. 4) and the impossibility of finding species-specific mass spectra within *Aspergillus* when using the MALDI-TOF method (Shao *et al.* 2022). The four supported species in series *Versicolores* can be identified by all of the five genes we used in this study, however identification based on ITS remains problematic. To test the discriminatory power of ITS in the series, we obtained 48 ITS sequences of strains used in this study that are available in the GenBank database (Table 1; alignment available from the Dryad Digital Repository: https://doi.org/10.5061/dryad.63xsj3v5q). There are several substitutions distinguishing *A. sydowii* and *A. subversicolor* from the remaining species, however there is only one substitution separating *A. creber* and *A. versicolor* at the beginning of the ITS1 region and this position is not known for all the strains. A phylogenetic tree based on this dataset calculated by Maximum Likelihood in IQ-TREE (Supplementary Fig. S1) was

poorly resolved, and neither *A. creber*, nor *A. versicolor* formed separate clades. Overall, we cannot recommend ITS as a reliable marker for the identification of series *Versicolores* species, unlike all other loci used in this study.

DECLARATION ON CONFLICT OF INTEREST

The authors declare that there is no conflict of interest.

ACKNOWLEDGEMENTS

František Sklenář was supported by the project of Charles University Grant Agency (GAUK 380821). The project was supported by the Czech Ministry of Health (grant NU21-05-00681), the Charles University Research Centre program no. 204069 and Czech Academy of Sciences Long-term Research Development Project (RVO: 61388971). We are grateful to Radek Zmítko and Jan Karhan for the help with graphical adjustments of some analysis outputs. We thank Milada Chudíčková and Lenka Zídková for their invaluable assistance in the laboratory. VH is grateful for the support from the Japan Society for the Promotion of Science Postdoctoral Fellowships for Research in Japan (Standard) and the support from the Grant-in-aid for JSPS research fellows (grant No. 20F20772). Cobus M Visagie was financially supported by the Future Leaders - African Independent Research fellowship programme (FLAIR, FLR\R1\201831). The FLAIR Fellowship Programme is a partnership between the African Academy of Sciences and the Royal Society funded by the UK Government's Global Challenges Research Fund. We would like to acknowledge Keith A Seifert, Shivan Bezuidenhout, Renan Barbosa, Jiří Řehulka and David Nkwe who provided some strains used in this study.

REFERENCES

Ahlmann-Eltze C, Patil I (2021). ggsignif: R Package for Displaying Significance Brackets for'ggplot2'. *PsyArxiv doi: 10.31234/osf.io/7awm6*.

Ahrens D, Fujisawa T, Krammer HJ, *et al.* (2016). Rarity and incomplete sampling in DNA-based species delimitation. *Systematic Biology* **65**: 478–494.

Beck M (2017). ggord: Ordination Plots with ggplot2. *R package version* **1**: 588.

Boluda C, Rico V, Divakar P, *et al.* (2019). Evaluating methodologies for species delimitation: the mismatch between phenotypes and genotypes in lichenized fungi (*Bryoria* sect. *Implexae*, *Parmeliaceae*). *Persoonia* **42**: 75–100.

Bongomin F, Moore CB, Masania R, *et al.* (2018). Sequence analysis of isolates of *Aspergillus* from patients with chronic and allergic aspergillosis reveals a spectrum of cryptic species. *Future Microbiology* **13**: 1557–1563.

Borgohain P, Barua P, Dutta PJ, *et al.* (2019). Onychomycosis associated with superficial skin infection due to *Aspergillus sydowii* in an immunocompromised patient. *Mycopathologia* **184**: 683–689.

Bouckaert R, Heled J (2014). DensiTree 2: seeing trees through the forest. *bioRxiv* doi: 10.1101/012401.

Bouckaert R, Vaughan TG, Barido-Sottani J, *et al.* (2019). BEAST 2.5: An advanced software platform for Bayesian evolutionary analysis. *PLoS Computational Biology* **15**: e1006650.

Burbrink FT, Ruane S (2021). Contemporary philosophy and methods for studying speciation and delimiting species. *Ichthyology & Herpetology* **109**: 874–894.

Chambers EA, Hillis DM (2020). The multispecies coalescent over-splits species in the case of geographically widespread taxa. *Systematic Biology* **69**: 184–193.

Cicero C, Mason NA, Jiménez RA, *et al.* (2021). Integrative taxonomy and geographic sampling underlie successful species delimitation. *Ornithology* **138**: ukab009.

Danagoudar A, Pratap G, Shantaram M, *et al.* (2021). Antioxidant, cytotoxic and anti-choline esterase activity of green silver nanoparticles synthesized using *Aspergillus austroafricanus* CGJ-B3 (endophytic fungus). *Analytical Chemistry Letters* **11**: 15–28.

De Vries RP, Riley R, Wiebenga A, *et al.* (2017). Comparative genomics reveals high biological diversity and specific adaptations in the industrially and medically important fungal genus *Aspergillus*. *Genome Biology* **18**: 1–45.

Dobolyi C, Inotai K, Bata-Vidács I, *et al.* (2021). Isolation and detailed characterisation of the first sterigmatocystin hyperproducer mould strain in Hungary. *Acta Alimentaria* **50**: 247–258.

Domsch KH, Gams W, Anderson T-H (2007). *Compendium of soil fungi*. 2nd ed. edition. IHW-Verlag, Eching.

Drummond AJ, Xie W, Heled J (2012). Bayesian inference of species trees from multilocus data using *BEAST. *Molecular Biology and Evolution* **29**: 1969–1973.

Feng XY, Wang XH, Chiang YC, *et al.* (2021). Species delimitation with distinct methods based on molecular data to elucidate species boundaries in the *Cycas taiwaniana* complex (*Cycadaceae*). *Taxon* **70**: 477–491.

Fujisawa T, Barraclough TG (2013). Delimiting species using single-locus data and the Generalized Mixed Yule Coalescent (GMYC) approach: a revised method and evaluation on simulated datasets. *Systematic Biology* **62**: 707–724.

Gams W, Christensen M, Onions AHS, *et al.* (1985). Infrageneric taxa of *Aspergillus*. In: *Advances in Penicillium and Aspergillus Systematics.* (R.A. Samson, J.I. Pitt, eds). Plenum Press, New York: 55–62.

Géry A, Lepetit C, Heutte N, *et al.* (2022). Cellular cytotoxicity and oxidative potential of recurrent molds of the genus *Aspergillus* series *Versicolores*. *Microorganisms* **10**: 228.

Géry A, Rioult J-P, Heutte N, *et al.* (2021). First characterization and description of *Aspergillus* series *Versicolores* in French bioaerosols. *Journal of Fungi* **7**: 676.

Glass NL, Donaldson GC (1995). Development of primer sets designed for use with the PCR to amplify conserved genes from filamentous ascomycetes. *Applied and Environmental Microbiology* **61**: 1323–1330.

González-Abradelo D, Pérez-Llano Y, Peidro-Guzmán H, *et al.* (2019). First demonstration that ascomycetous halophilic fungi (*Aspergillus sydowii* and *Aspergillus destruens*) are useful in xenobiotic mycoremediation under high salinity conditions. *Bioresource Technology* **279**: 287–296.

Hall TA (1999). BioEdit: a user-friendly biological sequence alignment editor and analysis program for Windows 95/98/NT. *Nucleic Acids Symposium Series* **41**: 95–98.

Hong S-B, Cho H-S, Shin H-D, *et al.* (2006). Novel *Neosartorya* species isolated from soil in Korea. *International Journal of Systematic and Evolutionary Microbiology* **56**: 477–486.

Houbraken J, Kocsubé S, Visagie CM, *et al.* (2020). Classification of *Aspergillus*, *Penicillium*, *Talaromyces* and related genera (*Eurotiales*): An overview of families, genera, subgenera, sections, series and species. *Studies in Mycology* **95**: 5–169.

Huang C, Feng Y, Patel G, *et al.* (2021). Production, immobilization and characterization of beta-glucosidase for application in cellulose degradation from a novel *Aspergillus versicolor*. *International Journal of Biological Macromolecules* **177**: 437–446.

Hubka V, Barrs V, Dudová Z, *et al.* (2018). Unravelling species boundaries in the *Aspergillus viridinutans* complex (section *Fumigati*): opportunistic human and animal pathogens capable of interspecific hybridization. *Persoonia* **41**: 142–174.

Hubka V, Nováková A, Peterson SW, *et al.* (2016). A reappraisal of *Aspergillus* section *Nidulantes* with descriptions of two new sterigmatocystin-producing species. *Plant Systematics and Evolution* **302**: 1267–1299.

Imbert S, Normand AC, Gabriel F, *et al.* (2019). Multi-centric evaluation of the online MSI platform for the identification of cryptic and rare species of *Aspergillus* by MALDI-TOF. *Medical Mycology* **57**: 962–968.

Jakšić Despot D, Kocsubé S, Bencsik O, *et al.* (2017). New sterigmatocystin-producing species of *Aspergillus* section *Versicolores* from indoor air in Croatia. *Mycological Progress* **16**: 63–72.

Janda-Ulfig K, Ulfig K, Markowska A (2009). Extracellular enzyme profiles of xerophilic fungi isolated from dried materials of medicinal plants. *Polish Journal of Environmental Studies* **18**: 391–397.

Jia J, Chen M, Mo X, *et al.* (2019). The first case report of kerion-type scalp mycosis caused by *Aspergillus protuberus*. *BMC Infectious Diseases* **19**: 1–5.

Jones G (2017). Algorithmic improvements to species delimitation and phylogeny estimation under the multispecies coalescent. *Journal of Mathematical Biology* **74**: 447–467.

Jones G, Aydin Z, Oxelman B (2015). DISSECT: an assignment-free Bayesian discovery method for species delimitation under the multispecies coalescent. *Bioinformatics* **31**: 991–998.

Jurjević Ž, Kubátová A, Kolařík M, *et al.* (2015). Taxonomy of *Aspergillus* section *Petersonii sect. nov.* encompassing indoor and soil-borne species with predominant tropical distribution. *Plant Systematics and Evolution* **301**: 2441–2462.

Jurjević Ž, Peterson SW, Horn BW (2012). *Aspergillus* section *Versicolores*: nine new species and multilocus DNA sequence based phylogeny. *IMA Fungus* **3**: 59–79.

Jurjević Ž, Peterson SW, Solfrizzo M, *et al.* (2013). Sterigmatocystin production by nine newly described *Aspergillus* species in section *Versicolores* grown on two different media. *Mycotoxin Research* **29**: 141–145.

Kato H, Nakahara T, Sugimoto K, *et al.* (2015). Isolation of notoamide S and enantiomeric 6-epi-stephacidin A from the fungus *Aspergillus amoenus*: biogenetic implications. *Organic letters* **17**: 700–703.

Katoh K, Standley DM (2013). MAFFT multiple sequence alignment software version 7: improvements in performance and usability. *Molecular Biology and Evolution* **30**: 772–780.

Kekkonen M, Hebert PD (2014). DNA barcode-based delineation of putative species: efficient start for taxonomic workflows. *Molecular Ecology Resources* **14**: 706–715.

Klich M (1993). Morphological studies of *Aspergillus* section *Versicolores* and related species. *Mycologia* **85**: 100–107.

Klich M, Mullaney E, Daly C (1993). Analysis of intraspecific and interspecific variability of three common species in *Aspergillus* section *Versicolores* using DNA restriction fragment length polymorphisms. *Mycologia* **85**: 852–855.

Kozakiewicz Z (1989). *Aspergillus* species on stored products. *Mycological Papers* **161**: 1–188.

Kubatko LS, Degnan JH (2007). Inconsistency of phylogenetic estimates from concatenated data under coalescence. *Systematic Biology* **56**: 17–24.

Letunic I, Bork P (2016). Interactive tree of life (iTOL) v3: an online tool for the display and annotation of phylogenetic and other trees. *Nucleic Acids Research* **44**: W242–W245.

Li YC, Wen J, Ren Y, *et al.* (2019). From seven to three: Integrative species delimitation supports major reduction in species number in *Rhodiola* section *Trifida* (*Crassulaceae*) on the Qinghai-Tibetan Plateau. *Taxon* **68**: 268–279.

Li Z-X, Wang X-F, Ren G-W, *et al.* (2018). Prenylated diphenyl ethers from the marine algal-derived endophytic fungus *Aspergillus tennesseensis*. *Molecules* **23**: 2368.

Liu YJ, Whelen S, Hall BD (1999). Phylogenetic relationships among ascomycetes: evidence from an RNA polymerse II subunit. *Molecular Biology and Evolution* **16**: 1799–1808.

Magoga G, Fontaneto D, Montagna M (2021). Factors affecting the efficiency of molecular species delimitation in a species-rich insect family. *Molecular Ecology Resources* **21**: 1475–1489.

Mason NA, Fletcher NK, Gill BA, *et al.* (2020). Coalescent-based species delimitation is sensitive to geographic sampling and isolation by distance. *Systematics and Biodiversity* **18**: 269–280.

Micheluz A, Manente S, Tigini V, *et al.* (2015). The extreme environment of a library: Xerophilic fungi inhabiting indoor niches. *International Biodeterioration & Biodegradation* **99**: 1–7.

Minh BQ, Schmidt HA, Chernomor O, *et al.* (2020). IQ-TREE 2: new models and efficient methods for phylogenetic inference in the genomic era. *Molecular Biology and Evolution* **37**: 1530–1534.

Nguyen HT, Nguyen TD, Le TML, *et al.* (2021). Integrative taxonomy of *Mesocriconema onoense* (Tylenchida: Criconematidae) from Vietnam highly suggests the synonymization of *Mesocriconema brevistylus* and related species. *Infection*, *Genetics and Evolution* **95**: 105090.

Nováková A, Hubka V, Saiz-Jimenez C, *et al.* (2012). *Aspergillus baeticus sp. nov.* and *Aspergillus thesauricus sp. nov.*, two species in section *Usti* from Spanish caves. *International Journal of Systematic and Evolutionary Microbiology* **62**: 2778–2785.

Nováková A, Hubka V, Valinová Š, *et al.* (2018). Cultivable microscopic fungi from an underground chemosynthesis-based ecosystem: a preliminary study. *Folia Microbiologica* **63**: 43–55.

O'Donnell K, Cigelnik E (1997). Two divergent intragenomic rDNA ITS2 types within a monophyletic lineage of the fungus *Fusarium* are nonorthologous. *Molecular Phylogenetics and Evolution* **7**: 103–116.

Pante E, Puillandre N, Viricel A, *et al.* (2015). Species are hypotheses: avoid connectivity assessments based on pillars of sand. *Molecular Ecology* **24**: 525–544.

Paradis E (2010). pegas: an R package for population genetics with an integrated-modular approach. *Bioinformatics* **26**: 419–420.

Parker E, Dornburg A, Struthers CD, *et al.* (2022). Phylogenomic species delimitation dramatically reduces species diversity in an Antarctic adaptive radiation. *Systematic Biology* **71**: 58–77.

Peterson SW (2008). Phylogenetic analysis of *Aspergillus* species using DNA sequences from four loci. *Mycologia* **100**: 205–226.

Pitt JI, AD Hocking (2009). *Fungi and food spoilage*. Springer, Dordrecht, Heidelberg, London, New York.

Posada D (2008). jModelTest: phylogenetic model averaging. *Molecular Biology and Evolution* **25**: 1253–1256.

Puillandre N, Lambert A, Brouillet S, *et al.* (2012). ABGD, Automatic Barcode Gap Discovery for primary species delimitation. *Molecular Ecology* **21**: 1864–1877.

R Core Team (2015). *R: A language and environment for statistical computing*. R Foundation for Statistical Computing. Vienna, Austria. R Foundation for Statistical Computing, Vienna, Austria.

Rank C, Nielsen KF, Larsen TO, *et al.* (2011). Distribution of sterigmatocystin in filamentous fungi. *Fungal Biology* **115**: 406–420.

Raper KB, Fennell DI (1965). *The genus Aspergillus*. Williams & Wilkins, Baltimore, MD.

Reid NM, Carstens BC (2012). Phylogenetic estimation error can decrease the accuracy of species delimitation: a Bayesian implementation of the general mixed Yule-coalescent model. *BMC Evolutionary Biology* **12**: 196.

Sakhri A, Chaouche NK, Catania MR, *et al.* (2019). Chemical composition of *Aspergillus creber* extract and evaluation of its antimicrobial and antioxidant activities. *Polish Journal of Microbiology* **68**: 309.

Samson RA, Visagie CM, Houbraken J, *et al.* (2014). Phylogeny, identification and nomenclature of the genus *Aspergillus*. *Studies in Mycology* **78**: 141–173.

Seo T-K (2008). Calculating bootstrap probabilities of phylogeny using multilocus sequence data. *Molecular Biology and Evolution* **25**: 960–971.

Shao J, Wang Q, Wei L, *et al.* (2022). Limitations of matrix-assisted laser desorption/ionization time-of-flight mass spectrometry for the identification of *Aspergillus* species. *Medical Mycology* **60**: myab084.

Shehata AN, Abd El Aty AA, Darwish DA, *et al.* (2018). Purification, physicochemical and thermodynamic studies of antifungal chitinase with production of bioactive chitosan-oligosaccharide from newly isolated *Aspergillus griseoaurantiacus* KX010988. *International Journal of Biological Macromolecules* **107**: 990–999.

Schmitt I, Crespo A, Divakar P, *et al.* (2009). New primers for promising single-copy genes in fungal phylogenetics and systematics. *Persoonia* **23**: 35–40.

Schwab CJ, Straus DC (2004). The roles of *Penicillium* and *Aspergillus* in sick building syndrome. *Advances in Applied Microbiology* **55**: 215–238.

Siqueira JPZ, Sutton DA, García D, *et al.* (2016). Species diversity of *Aspergillus* section *Versicolores* in clinical samples and antifungal susceptibility. *Fungal Biology* **120**: 1458–1467.

Sklenář F, Jurjević Ž, Houbraken J, *et al.* (2021). Re-examination of species limits in *Aspergillus* section *Flavipedes* using advanced species delimitation methods and description of four new species. *Studies in Mycology* **99**: 100120.

Sklenář F, Jurjević Ž, Peterson SW, *et al.* (2020). Increasing the species diversity in the *Aspergillus* section *Nidulantes*: Six novel species mainly from the indoor environment. *Mycologia* **112**: 342–370.

Sklenář F, Jurjević Ž, Zalar P, *et al.* (2017). Phylogeny of xerophilic aspergilli (subgenus *Aspergillus*) and taxonomic revision of section *Restricti*. *Studies in Mycology* **88**: 161–236.

Struck TH, Feder JL, Bendiksby M, *et al.* (2018). Finding evolutionary processes hidden in cryptic species. *Trends in Ecology & Evolution* **33**: 153–163.

Sukumaran J, Holder MT, Knowles LL (2021). Incorporating the speciation process into species delimitation. *PLoS Computational Biology* **17**: e1008924.

Sukumaran J, Knowles LL (2017). Multispecies coalescent delimits structure, not species. *Proceedings of the National Academy of Sciences of the United States of America* **114**: 1607–1611.

Swain SK, Debta P, Sahu MC, *et al.* (2020). Otomycosis due to *Aspergillus versicolor*. *International Journal of Health & Allied Sciences* **9**: 192.

Thom C, Church MB (1926). *The Aspergilli*. Williams & Wilkins, Baltimore, MD.

Thom C, Raper KB (1945). *A manual of the Aspergilli*. Williams &Wilkins, Maryland, MD.

Tsang C-C, Hui TWS, Lee K-C, *et al.* (2016). Genetic diversity of *Aspergillus* species isolated from onychomycosis and *Aspergillus hongkongensis sp. nov.*, with implications to antifungal susceptibility testing. *Diagnostic Microbiology and Infectious Disease* **84**: 125–134.

Turland NJ, Wiersema JH, Barrie FR, *et al.* (2018). International Code of Nomenclature for algae, fungi, and plants (Shenzhen Code) adopted by the Nineteenth International Botanical Congress Shenzhen, China, July 2017. Koeltz Botanical Books, Glashütten.

van Rossum G, Drake FL (2019). *Python language reference, version 3*. Python Software Foundation.

Venables WN, Ripley BD (2002). *Modern applied statistics with S*. Fourth edition. Springer, New York.

Veršilovskis A, De Saeger S (2010). Sterigmatocystin: occurrence in foodstuffs and analytical methods–an overview. *Molecular Nutrition & Food Research* **54**: 136–147.

Vidal-Acuña MR, Ruiz-Pérez de Pipaón M, Torres-Sánchez MJ, *et al.* (2018). Identification of clinical isolates of *Aspergillus*, including cryptic species, by matrix assisted laser desorption ionization time-of-flight mass spectrometry (MALDI-TOF MS). *Medical Mycology* **56**: 838–846.

Visagie CM, Hirooka Y, Tanney JB, *et al.* (2014). *Aspergillus*, *Penicillium* and *Talaromyces* isolated from house dust samples collected around the world. *Studies in Mycology* **78**: 63–139.

Wang PM, Liu XB, Dai YC, *et al.* (2018). Phylogeny and species delimitation of *Flammulina*: taxonomic status of winter mushroom in East Asia and a new European species identified using an integrated approach. *Mycological Progress* **17**: 1013–1030.

Wang X-C, Zhuang WY (2022). New species of *Aspergillus* (*Aspergillaceae*) from tropical islands of China. *Journal of Fungi* **8**: 225.

Wickham H (2016). *ggplot2: elegant graphics for data analysis*. Springer-Verlag, New York.

Yang Z (2015). The BPP program for species tree estimation and species delimitation. *Current Zoology* **61**: 854–865.

Zahradnik E, Kespohl S, Sander I, *et al.* (2013). A new immunoassay to quantify fungal antigens from the indoor mould *Aspergillus versicolor*. *Environmental Science: Processes & Impacts* **15**: 1162–1171.

Zhang J, Kapli P, Pavlidis P, *et al.* (2013). A general species delimitation method with applications to phylogenetic placements. *Bioinformatics* **29**: 2869–2876.

Supplementary Material: https://studiesinmycology.org/

Fig. S1. Phylogenetic tree based on 48 ITS sequences of series *Versicolores* strains available from the NCBI GenBank database (Table 1). The tree was calculated in IQ-TREE v. 2.1.2 with 100 000 ultrafast bootstrap replicates (only support values higher than 70 % are shown). TrNef was selected as the most suitable model of evolution by jModelTest v 2.1.7. The ex-type strains are designated with a superscript T.

Table S1. Strains from *Aspergillus* series *Versicolores* used for calculation of phylogenetic tree based on the partial calmodulin sequences (Fig. 1).

Table S2. Growth rates of selected strains on eight cultivation media after 14 d in mm (average values from at least three measurements).

Table S3. Production of Hülle cells on eight cultivation media after 3 wk of cultivation at 25 °C in the dark.

Table S4. Maximum sequence dissimilarity between isolates of the same *Aspergillus* species whose species limits have been delimited using methods based on multispecies coalescent model; only species represented by isolates from at least three countries were included.

Reducing the number of accepted species in *Aspergillus* series *Nigri*

C. Bian[1], Y. Kusuya[2,3], F. Sklenář[4,5], E. D'hooge[6], T. Yaguchi[2], S. Ban[2], C.M. Visagie[7], J. Houbraken[8], H. Takahashi[2,9,10*], V. Hubka[2,4,5*]

[1]*Graduate School of Medical and Pharmaceutical Sciences, Chiba University, Chiba, Japan;* [2]*Medical Mycology Research Center, Chiba University, Chiba, Japan;* [3]*Biological Resource Center, National Institute of Technology and Evaluation, Kisarazu, Japan;* [4]*Department of Botany, Faculty of Science, Charles University, Prague, Czech Republic;* [5]*Laboratory of Fungal Genetics and Metabolism, Institute of Microbiology, Czech Academy of Sciences, Prague, Czech Republic;* [6]*BCCM/IHEM collection, Mycology and Aerobiology, Sciensano, Bruxelles, Belgium;* [7]*Department of Biochemistry, Genetics, and Microbiology, Forestry and Agricultural Biotechnology Institute, University of Pretoria, Pretoria, South Africa;* [8]*Westerdijk Fungal Biodiversity Institute, Utrecht, the Netherlands;* [9]*Molecular Chirality Research Center, Chiba University, Chiba, Japan;* [10]*Plant Molecular Science Center, Chiba University, Chiba, Japan*

**Corresponding authors*: H. Takahashi, hiroki.takahashi@chiba-u.jp; V. Hubka, vit.hubka@gmail.com

Abstract: The *Aspergillus* series *Nigri* contains biotechnologically and medically important species. They can produce hazardous mycotoxins, which is relevant due to the frequent occurrence of these species on foodstuffs and in the indoor environment. The taxonomy of the series has undergone numerous rearrangements, and currently, there are 14 species accepted in the series, most of which are considered cryptic. Species-level identifications are, however, problematic or impossible for many isolates even when using DNA sequencing or MALDI-TOF mass spectrometry, indicating a possible problem in the definition of species limits or the presence of undescribed species diversity. To re-examine the species boundaries, we collected DNA sequences from three phylogenetic markers (*benA*, *CaM* and *RPB2*) for 276 strains from series *Nigri* and generated 18 new whole-genome sequences. With the three-gene dataset, we employed phylogenetic methods based on the multispecies coalescence model, including four single-locus methods (GMYC, bGMYC, PTP and bPTP) and one multilocus method (STACEY). From a total of 15 methods and their various settings, 11 supported the recognition of only three species corresponding to the three main phylogenetic lineages: *A. niger*, *A. tubingensis* and *A. brasiliensis*. Similarly, recognition of these three species was supported by the GCPSR approach (Genealogical Concordance Phylogenetic Species Recognition) and analysis in DELINEATE software. We also showed that the phylogeny based on *benA*, *CaM* and *RPB2* is suboptimal and displays significant differences from a phylogeny constructed using 5 752 single-copy orthologous proteins; therefore, the results of the delimitation methods may be subject to a higher than usual level of uncertainty. To overcome this, we randomly selected 200 genes from these genomes and performed ten independent STACEY analyses, each with 20 genes. All analyses supported the recognition of only one species in the *A. niger* and *A. brasiliensis* lineages, while one to four species were inconsistently delimited in the *A. tubingensis* lineage. After considering all of these results and their practical implications, we propose that the revised series *Nigri* includes six species: *A. brasiliensis*, *A. eucalypticola*, *A. luchuensis* (syn. *A. piperis*), *A. niger* (syn. *A. vinaceus* and *A. welwitschiae*), *A. tubingensis* (syn. *A. chiangmaiensis*, *A. costaricensis*, *A. neoniger* and *A. pseudopiperis*) and *A. vadensis*. We also showed that the intraspecific genetic variability in the redefined *A. niger* and *A. tubingensis* does not deviate from that commonly found in other aspergilli. We supplemented the study with a list of accepted species, synonyms and unresolved names, some of which may threaten the stability of the current taxonomy.

Key words: *Aspergillus luchuensis*, *Aspergillus niger*, *Aspergillus tubingensis*, clinical fungi, indoor fungi, infraspecific variability, multigene phylogeny, multispecies coalescence model, ochratoxin A, species delimitation.

Citation: Bian C, Kusuya Y, Sklenář F, D'hooge E, Yaguchi T, Ban S, Visagie CM, Houbraken J, Takahashi H, Hubka V (2022). Reducing the number of accepted species in *Aspergillus* series *Nigri*. *Studies in Mycology* **102**: 95–132. doi: 10.3114/sim.2022.102.03
Received: 6 October 2022; **Accepted:** 6 December 2022; **Effectively published online:** 19 December 2022
Corresponding editor: Robert A. Samson

INTRODUCTION

Aspergillus niger and its relatives play important roles in food mycology (Taniwaki *et al.* 2018), biotechnology (Schuster *et al.* 2002, Yang *et al.* 2017), the fermentation industry (Hong *et al.* 2014) and medical mycology (Howard *et al.* 2011). Consequently, *A. niger* is the most frequently cited species name in the genus *Aspergillus* (Samson *et al.* 2017). Since, on most occasions, species in section *Nigri* have been classified as GRAS (generally regarded as safe) by the Food and Drug Administration of the US government, they are suitable organisms for genetic manipulation and thus are used by biotechnology industries to produce hydrolytic enzymes (such as amylases and lipases) or organic acids (such as citric acid and gluconic acid) (Ward 1989, Bennett & Klich 1992, Andersen *et al.* 2011). On the other hand, *Aspergillus* section *Nigri* species (including some *A. niger* strains) cause food spoilage or contaminate a wide variety of food products (Samson *et al.* 2019) and may produce mycotoxins such as ochratoxin A, fumonisins and oxalic acid (Frisvad *et al.* 2011, 2018). *Aspergillus niger*, *A. tubingensis* and their lesser known cryptic species (phylogenetically supported but phenotypically nearly identical or undistinguishable) can also act as opportunistic pathogens that cause invasive mycoses in immunocompromised patients and non-invasive mycoses (aspergilloma, allergic aspergillosis, fungal otitis externa and keratomycosis) in otherwise healthy patients (Hubka *et al*. 2012, D'hooge *et al.* 2019, Hashimoto *et al*. 2017, Salah *et al*. 2019, Vidal-Acuña *et al*. 2019, Gits-Muselli *et al*. 2021, Nargesi *et al*. 2022). Some previous studies also demonstrated that different antifungal susceptibility patterns to azole derivates are present between *A. niger* and *A. tubingensis* complexes (Alcazar-Fuoli *et al*. 2009, Hendrickx *et al*. 2012, Szigeti *et al*. 2012).

The infrageneric classification of *Aspergillus* has a long history with Thom & Church (1926), Thom & Raper (1945) and Raper & Fennell (1965) recognizing that its species could be classified

into "groups" based on their morphological similarities. This infrageneric classification was formalised when Gams *et al*. (1986) introduced names as subgenera and sections in *Aspergillus*, *e.g.,* all black aspergilli were classified in section *Nigri* in the subgenus *Circumdati*. Recently, Houbraken *et al*. (2020) reviewed this infrageneric classification with the help of multigene phylogenies, and showed that it mostly agreed with the infrageneric classification proposed by Gams *et al.* (1986). They introduced series rank and subdivided section *Nigri* into five series. The most economically important section *Nigri* species, including *A. niger*, *A. tubingensis* and *A. luchuensis* belong to the series *Nigri.*

The taxonomy of section *Nigri* at the species level has been turbulent over time. Originally, Mosseray (1934) proposed 35 species. This number was reduced by Raper & Fennell (1965), who recognized 12 species and two varieties, and provided detailed morphological characteristics to distinguish among their accepted species. Al-Musallam (1980) revised the species limits using cluster analysis based on morphological and cultural parameters, suggesting at least seven species, including *A. carbonarius, A. ellipticus, A. helicothrix, A. heteromorphus, A. japonicus, A. foetidus* and *A. niger.* In this classification, *A. niger* was subdivided into six varieties and two forms. Kozakiewicz (1989), who drew her taxonomic conclusions from conidial ornamentation under scanning electron microscopy, distinguished 16 taxa, among which three belong to the current series *Nigri,* namely, *A. acidus*, *A. niger* with six varieties and *A. citricus* with two varieties. Early molecular genetic studies indicated that *A. niger* consisted of at least two cryptic species, *A. niger* and *A. tubingensis* (Kusters-van Someren *et al.* 1991, Varga *et al.* 1994, Peterson 2000), which are morphologically undistinguishable (Pitt & Hocking 2009, Crous *et al.* 2009). Using a polyphasic approach combining morphological features, extrolite profiling and β-tubulin DNA sequences, Samson *et al*. (2004) accepted 15 species in the section, comprising eight species in the clade currently known as series *Nigri*, *i.e., A. brasiliensis*, *A. costaricensis*, *A. foetidus, A. lacticoffeatus*, *A. niger, A. piperis*, *A. tubingensis* and *A. vadensis*. Subsequent phylogenetic studies supported the recognition of several cryptic phylogenetic species in the series *Nigri*, such as *A. awamori* (Perrone *et al*. 2011), later synonymized with another cryptic species, *A. welwitschiae* (Hong *et al.* 2013). Similarly, Varga *et al*. (2011) recognized *A. acidus*, which was later synonymized with the resurrected species *A. luchuensis* (Hong *et al.* 2013). Another two cryptic species related to *A. tubingensis*, *i.e., A. eucalypticola* and *A. neoniger*, were described by Varga *et al*. (2011), who also synonymized *A. foetidus* and *A. lacticoffeatus* with *A. niger*. As a result, the last overview of accepted *Aspergillus* species (Houbraken *et al.* 2020) assigned ten species to the series *Nigri*: *A. brasiliensis*, *A. costaricensis*, *A. eucalypticola*, *A. luchuensis*, *A. neoniger*, *A. niger*, *A. piperis*, *A. tubingensis*, *A. vadensis* and *A. welwitschiae*. Four novel cryptic species have been proposed since. Silva *et al.* (2020) introduced *A. vinaceus* as a close relative of *A. niger* and Khuna *et al*. (2021) introduced *A. chiangmaiensis, A. pseudopiperis* and *A. pseudotubingensis* as close relatives of *A. tubingensis*.

Vesth *et al*. (2018) and de Vries *et al*. (2017) *de novo* sequenced the genomes of the majority of accepted section *Nigri* species and performed phenotypic and genomic comparative analyses. The whole genomes of the ex-neotype strain of *A. niger* (CBS 554.65) and 24 *A. niger sensu stricto* strains were subsequently sequenced, and the mating-type distribution was analysed (Ellena *et al.* 2021, Seekles *et al.* 2022). Isolates with both *MAT1-2-1* and *MAT1-1-1* mating-type gene idiomorphs were found among genome-sequenced strains of *A. niger*, in agreement with previous PCR-based detection studies (Varga *et al.* 2014, Mageswari *et al.* 2016). This fact indicates that the species might have a cryptic sexual cycle, as previously observed in *A. tubingenis* (Horn *et al.* 2013). Additionally, recent phylogenomic studies indicated that section *Nigri* might belong to the subgenus *Nidulantes* (de Vries *et al.* 2017, Steenwyk *et al.* 2019) and not subgenus *Circumdati* (Jurjević *et al.* 2015, Kocsubé *et al.* 2016).

The reliable identification of section *Nigri* species is of great importance, as evidenced by their diverse positive and negative significances for humans. However, there is an increasing number of isolates that cannot be satisfactorily classified into the currently recognized species despite using multilocus sequence data (Howard *et al*. 2011, Negri *et al*. 2014, D'hooge *et al*. 2019). This fact also resulted in the recent description of several cryptic species related to *A. niger* and *A. tubingensis* (Silva *et al.* 2020, Khuna *et al.* 2021). The narrow species definition in the series *Nigri* is also associated with unsatisfactory identification results of MALDI-TOF MS (matrix-assisted laser desorption ionization time-of-flight mass spectrometry), a widely used identification tool in diagnostic laboratories and applied spheres (Gautier *et al.* 2016, D'hooge *et al.* 2019, Ban *et al.* 2021). All of the abovementioned problems may indicate that the species limits are not defined correctly and that the species definitions applied in the series are too narrow. This situation prompted the initiation of this study, where we are concerned with the verification of species boundaries at the molecular level based on a large number of strains.

A common requirement of species delimitation methods is proper sampling (a high number of strains of all studied species ideally isolated from a wide range of substrates and localities) and the presence of intraspecific variability (Carstens *et al.* 2013). This condition is, however, frequently difficult to fulfil in fungal taxonomy (Ahrens *et al*. 2016). From this point of view, series *Nigri* represents a perfect model group for studying species limits on a large scale due to the frequent occurrence of its species in many habitats and a high representation of molecular data in public databases. To do so, we have gathered extensive sequence data and applied a wide range of phylogenetic methods. The synthesis of the resulting data and the consideration of its practical taxonomic implications have led to a significant reduction in the number of species, as detailed below.

METHODS

Molecular studies

The DNA sequences of three loci, β-tubulin (*benA*), calmodulin (*CaM*) and the RNA polymerase II second largest subunit (*RPB2*), were gathered for a total of 276 strains from series *Nigri*. For this process, we removed short sequences or those that contained obvious errors. Additional species from other series of section *Nigri* were selected as outgroups or reference species depending on the analysis. The sequences were either downloaded from the GenBank database and mostly originated from previous studies, or they were taken from genes amplified and sequenced in this study. Sequences downloaded from the GenBank database were mostly from studies by D'hooge *et al*. (2019), Peterson (2008), Jurjević *et al.* (2012), Fungaro *et al.* (2017) and Hashimoto *et al.* (2017). Sequence alignments from the Silva *et al.* (2020) study were kindly provided by the authors. Information about the provenance of all strains is listed in Table 1.

Table 1. List of *Aspergillus* series *Nigri* strains included in the phylogenetic analyses.

				GenBank/ENA/DDBJ accession Nos.[2]			
Species	**Strain No.[1]**	**Country**	**Substrate**	***benA***	***CaM***	***RPB2***	**ITS**
A. brasiliensis	CBS 101740 = IMI 381727 = ATCC MYA 4553 = IBT 21946[T]	Brazil	soil	genome[2]	genome	EF661063	MH862749
	PPRI 26017 = CMV 007D1	South Africa	onion	MK451119	MK451325	MK450774	MK450631
	PPRI 3388 = CMV 010B8	South Africa	garlic (*Allium sativum*)	MK451152	MK451326	MK450775	MK450632
	PPRI 3328 = CMV 004I8	South Africa	mangrove leaves	MK451015	MK451324	MK450773	MK450630
	NRRL 26651	USA	unknown	EF661094	EF661160	EF661064	KC796389
	NRRL 26650	USA	unknown	EF661079	EF661159	EF661062	EF661196
	NRRL 35542	USA	peanut seed	EF661096	EF661162	EU021641	EF661199
	NRRL 26652	USA	unknown	EF661095	EF661161	EF661063	EF661198
	CBS 121619 = DTO 24-D5 = ITEM 6139	Portugal	grapes	AM295185	AM295176	OP081976	AM295181
	CBS 121618 = DTO 24-D2 = ITEM 4539	Portugal	grapes (*Tinta barroca*)	AM295182	AM295179	OP081975	—
	NBRC 9455 = ATCC 16404 = CBS 733.88 = DSM 1387 = DSM 1988 = KCTC 6317 = MUCL 29039 = MUCL 30113 = CECT 2574 = IFO 9455 = NCPF 2275 = IHEM 3766	USA	blueberry (*Vaccinium* sp.)	genome	genome	genome	—
	NBRC 105650 = ATCC 9642 = CBS 246.65 = JCM 16265 = NRRL 3536 = ATHUM 2856 = CECT 2700 = DSM 63263 = IFO 6342 = IMI 091855 = MUCL 19001 = IHEM 3797	Australia	wireless set	genome	genome	genome	—
	IFM 66950 = CCF 3991	Spain	cave air	genome	genome	genome	—
	IFM 66951 = CCF 4962	Romania	microbial mat in cave	genome	genome	genome	—
	IHEM 23046	Belgium	unknown	MH614413	MH644886	OP081977	MH613107
	IHEM 23047	Belgium	unknown	MH614444	MH644887	OP081978	MH613108
	IHEM 5185 = NRRL 2276	Unknown	unknown	MH614565	MH644892	OP081982	MH613109
	IHEM 23049	Belgium	unknown	MH614414	MH644889	OP081979	MH613081
	IHEM 3766	USA	fruit, *Vaccinium* subg. *Cyanococcus*	MH614415	MH644891	OP081980	MH613079
	IHEM 3797	Australia	radio set	MH614416	MH644890	OP081981	MH613110
A. niger	CBS 554.65 = ATCC 16888 = IFO 33023 = IHEM 3415 = JCM 10254 = NRRL 326 = CCFC 222006 = IMI 050566 = NBRC 33023[T]	USA	tannin-gallic acid fermentation	EF661089	EF661154	EF661058	FJ629337
	CBS 101883 = CECT 20581 = IBT 22031[T1]	Indonesia	coffee bean	genome	genome	genome	—
	PPRI 8682 = CMV 005B2	South Africa	mopane debris	MK451027	MK451462	MK450792	—
	PPRI 8734 = CMV 005B7	South Africa	mopane debris	MK451032	MK451464	MK450793	—
	PPRI 26011 = CMV 005G9	South Africa	soil	MK451060	MK451468	MK450794	—
	PPRI 18719 = CMV 004I3	South Africa	frass of *Busseola fusca* feeding inside maize stems	MK451010	MK451458	MK450789	—
	PPRI 3640 = CMV 004I6	South Africa	old photo paper	MK451013	MK451459	MK450790	—
	IFM 63326	Japan	human sputum	MK854742	OP081973	genome	—
	IFM 63604	Japan	human sputum	MK854748	OP081974	genome	—
	IFM 59636	Japan	human abdominal drain	OP081896	OP081969	genome	—
	104	Brazil	coffee bean	OP081838	OP081913	OP082051	—

Table 1. (Continued).

Species	Strain No.[1]	Country	Substrate	GenBank/ENA/DDBJ accession Nos.[2]			
				benA	*CaM*	*RPB2*	ITS
A. niger	1400	Brazil	brazil nuts	OP081842	OP081917	OP082055	—
	1551	Brazil	brazil nuts	OP081848	OP081923	OP082061	—
	2334	Brazil	brazil nuts	OP081860	OP081935	OP082073	—
	2504	Brazil	brazil nuts	OP081861	OP081936	OP082074	—
	4.17	Brazil	grapes	OP081863	OP081938	OP082076	—
	4.18	Brazil	grapes	OP081864	OP081939	OP082077	—
	643	Brazil	coffee bean	OP081878	OP081953	OP082091	—
	6504	Brazil	brazil nuts	OP081879	OP081954	OP082092	—
	7061	Brazil	brazil nuts	OP081884	OP081959	OP082097	—
	8219	Brazil	coffee bean	OP081888	OP081963	OP082101	—
	902	Brazil	brazil nuts	OP081890	OP081965	OP082103	—
	1.2	Brazil	grapes	OP081836	OP081911	OP082049	—
	1357	Brazil	brazil nuts	OP081841	OP081916	OP082054	—
	23.115	Brazil	onions	OP081859	OP081934	OP082072	—
	CBS 117.80	Unknown	unknown	OP081891	GU195632	OP082104	—
	IHEM 18069	French Guiana, France	soil under palm tree	MH614489	MH645000	OP082110	MH613155
	IHEM 2312	Belgium	cosmetics	MH614521	MH645010	OP082127	MH613218
	IHEM 17892	Belgium	chronic sinusitus	MH614520	MH644877	OP082108	KP131598
	IHEM 23979	Belgium	otitis	MH614500	MH645005	OP082139	MH613182
	IHEM 25482	France	human bronchoalveolar lavage	MH614474	MH644860	OP082150	MH613113
	IHEM 23907	Belgium	human ear	MH614492	MH645003	OP082136	MH613168
	IHEM 24459	India	otitis	MH614502	MH645006	OP082144	MH613185
	IHEM 5788	Unknown	Chinese gall	MH614437	MH645007	OP082169	MH613213
	IHEM 21604	Cuba	outdoor air	MH614478	MH644996	OP082117	MH613124
	IHEM 5844	Unknown	unknown	MH614434	MH645002	OP082170	MH613157
	IHEM 5296	Unknown	leather	MH614519	MH645009	OP082167	MH613217
	IHEM 6126	Belgium	human sputum	MH614453	MH644998	OP082171	MH613135
	IHEM 5622	Unknown	unknown	MH614451	MH645001	OP082168	MH613156
	IHEM 4023	Belgium	mycotic otitis externa	MH614496	MH645004	OP082162	KP131606
	IHEM 9673	France	dwelling environment dust	MH614523	MH645012	OP082176	MH613219
	IHEM 25481	France	human bronchoalveolar lavage	MH614473	MH644859	OP082149	MH613112
	IHEM 21605	Cuba	nickel deposit	MH614479	MH644997	OP082118	MH613125
	IHEM 6147	Belgium	human nose	MH614439	MH645008	OP082172	MH613215
	IHEM 9709	France	cement	MH614522	MH645011	OP082177	MH613084
	IFM 56816	Japan	human ear	OP081895	OP081968	genome	—
	2.6	Brazil	grapes	OP081856	OP081931	OP082069	—
	2.8	Brazil	grapes	OP081858	OP081933	OP082071	—
	102.2706	Brazil	grapes	OP081837	OP081912	OP082050	—
	13.09	Brazil	coffee bean	OP081840	OP081915	OP082053	—
	148.727	Brazil	onions	OP081846	OP081921	OP082059	—
	ITAL 47.456 = IBT 35556^{T2}	Brazil	surface of grape berries	MN583579	MN583580	MN583581	MN575692
	ITAL 49.577	Brazil	grapes	OP081869	OP081944	OP082082	—
	ITAL 57.1243	Brazil	grapes	OP081875	OP081950	OP082088	—

Table 1. (Continued).

Species	Strain No.[1]	Country	Substrate	GenBank/ENA/DDBJ accession Nos.[2]			
				benA	*CaM*	*RPB2*	ITS
A. niger	ITAL 62.1583	Brazil	grapes	OP081877	OP081952	OP082090	—
	ITAL 66.1929	Brazil	grapes	OP081881	OP081956	OP082094	—
	ITAL 48.545	Brazil	grapes	OP081867	OP081942	OP082080	—
	47.514	Brazil	grapes	OP081865	OP081940	OP082078	—
	48.544	Brazil	grapes	OP081866	OP081941	OP082079	—
	49.580	Brazil	grapes	OP081870	OP081945	OP082083	—
	55.1175	Brazil	grapes	OP081874	OP081949	OP082087	—
	58.1292	Brazil	grapes	OP081876	OP081951	OP082089	—
	CBS 139.54[T3]	Namibia	*Welwitschia mirabilis*	MN969369	genome	MN969100	MH857271
	PPRI 23385 = CMV 004I5	South Africa	animal feed	MK451012	MK451548	MK450816	MK450663
	PPRI 4966 = CMV 004I1	South Africa	*Chrysomelidae* beetle	MK451008	MK451546	MK450814	MK450661
	PPRI 13255 = CMV 004I2	South Africa	chicken house bedding, mostly sunflower husks	MK451009	MK451547	MK450815	MK450662
	PPRI 26014 = CMV 006G2	South Africa	soil	MK451097	MK451562	MK450819	MK450669
	PPRI 9362 = CMV 005D1	South Africa	twigs and leaves from *Colophospermum mopane*	MK451039	MK451556	MK450818	MK450666
	IFM 50267	Japan	human sputum	OP081894	OP081967	genome	—
	IFM 63309	Japan	human, bronchoalveolar lavage fluid	MK854741	OP081972	genome	—
	IFM 49718	Japan	human sputum	OP081893	OP081966	genome	—
	IFM 62618	Japan	human, bronchoalveolar lavage fluid	MK854725	OP081971	genome	—
	IFM 60653	Japan	human sputum	OP081897	OP081970	genome	—
	15477	Brazil	onions	OP081847	OP081922	OP082060	—
	15580	Brazil	onions	OP081849	OP081924	OP082062	—
	15646	Brazil	onions	OP081850	OP081925	OP082063	—
	16158	Brazil	onions	OP081851	OP081926	OP082064	—
	16285	Brazil	onions	OP081852	OP081927	OP082065	—
	171804	Brazil	onions	OP081854	OP081929	OP082067	—
	181832	Brazil	onions	OP081855	OP081930	OP082068	—
	2.7	Brazil	grapes	OP081857	OP081932	OP082070	—
	48282	Brazil	onions	OP081868	OP081943	OP082081	—
	53295	Brazil	onions	OP081871	OP081946	OP082084	—
	53a	Brazil	yerba mate	OP081872	OP081947	OP082085	—
	54298	Brazil	onions	OP081873	OP081948	OP082086	—
	6573	Brazil	brazil nuts	OP081880	OP081955	OP082093	—
	69363	Brazil	onions	OP081883	OP081958	OP082096	—
	714	Brazil	brazil nuts	OP081885	OP081960	OP082098	—
	77390	Brazil	onions	OP081887	OP081962	OP082100	—
	88430	Brazil	onions	OP081889	OP081964	OP082102	—
	127a	Brazil	yerba mate	OP081839	OP081914	OP082052	—
	145723	Brazil	onions	OP081843	OP081918	OP082056	—
	146.724	Brazil	onions	OP081844	OP081919	OP082057	—
	146725	Brazil	onions	OP081845	OP081920	OP082058	—
	361	Brazil	brazil nuts	OP081862	OP081937	OP082075	—
	670	Brazil	brazil nuts	OP081882	OP081957	OP082095	—
	716	Brazil	brazil nuts	OP081886	OP081961	OP082099	—

Table 1. (Continued).

Species	Strain No.[1]	Country	Substrate	GenBank/ENA/DDBJ accession Nos.[2]			
				benA	*CaM*	*RPB2*	ITS
A. niger	17.179	Brazil	grapes	OP081853	OP081928	OP082066	—
	DTO 267-I3	Thailand	house dust	OP081892	KP330149	OP082105	—
	IHEM 22373	India	otomycosis	MH614468	MH644935	OP082121	KP131600
	IHEM 17902	Belgium	chronic sinusitus	MH614508	MH644965	OP082109	KP131599
	IHEM 25483	France	human sputum	MH614447	MH644929	OP082151	MH613114
	IHEM 3095	Mauritius	soil	MH614488	MH644942	OP082160	MH613151
	IHEM 3090	Mauritius	soil	MH614487	MH644884	OP082159	MH613150
	IHEM 20620	Cuba	soil	MH614516	MH644973	OP082115	MH613208
	IHEM 23644	India	otitis	MH614435	MH644948	OP082129	MH613171
	IHEM 6727	France	bronchopulmonary cancer	MH614450	MH644972	OP082174	KP131609
	IHEM 21970	Mauritius	soil	MH614484	MH644938	OP082120	MH613111
	IHEM 24434	India	otitis	MH614498	MH644952	OP082141	MH613179
	IHEM 18351	French Guiana, France	bark kapok tree	MH614481	MH644934	OP082112	MH613128
	IHEM 23822	India	otitis	MH614493	MH644947	OP082132	MH613169
	IHEM 23651	India	otitis	MH614491	MH644946	OP082131	MH613167
	IHEM 24707	Belgium	otitis	MH614503	MH644957	OP082145	MH613189
	IHEM 25101	Belgium	Unknown	MH614441	MH644961	OP082147	MH613194
	IHEM 21697	Belgium	onion	MH614448	MH644939	OP082119	MH613137
	IHEM 23892	Belgium	human	MH614570	MH644944	OP082134	MH613161
	IHEM 23965	France	otitis	MH614497	MH644951	OP082138	MH613178
	IHEM 15980	Belgium	ball from Pakistan	MH614518	MH644976	OP082107	MH613210
	IHEM 20621	Cuba	soil	MH614480	MH644933	OP082116	MH613126
	IHEM 18080	French Guiana, France	soil of riverside	MH614513	MH644969	OP082111	MH613077
	IHEM 25485	France	human bronchoaspiration	MH614477	MH644932	OP082153	MH613116
	IHEM 5077	Belgium	human ear	MH614515	MH644971	OP082166	MH613078
	IHEM 25340	Belgium	human toenail	MH614506	MH644962	OP082148	MH613195
	IHEM 18676	Peru	guano	MH614446	MH644928	OP082113	MH613082
	IHEM 24328	Unknown	horse (crust) - clinical sample	MH614499	MH644953	OP082140	MH613180
	IHEM 2951	Belgium	mycotic otitis externa	MH614569	MH644963	OP082156	KP131605
	IHEM 2969	India	soil	MH614449	MH644941	OP082157	MH613149
	IHEM 22432	Somalia	otitis	MH614509	MH644966	OP082126	KP131604
	IHEM 26623	Belgium	human ear	MH614486	MH644940	OP082155	MH613146
	IHEM 26214	Belgium	otitis	MH614505	MH644960	OP082154	MH613192
	IHEM 23648	India	otitis	MH614495	MH644950	OP082130	MH613174
	IHEM 24450	India	otitis	MH614469	MH644955	OP082142	MH613184
	IHEM 25484	France	human bronchoaspiration	MH614476	MH644931	OP082152	MH613115
	IHEM 22377	Belgium	conjunctivitis - human eye	MH614483	MH644937	OP082123	KP131602
	IHEM 22378	Somalia	human auditory canal	MH614510	MH644967	OP082124	MH613076
	IHEM 23913	Belgium	human ear	MH614501	MH644954	OP082137	MH613183
	IHEM 4781	Belgium	mycotic otitis externa	MH614454	MH644974	OP082165	KP131608
	IHEM 22374	India	otomycosis	MH614482	MH644936	OP082122	KP131601
	IHEM 23642	India	otitis	MH614452	MH644861	OP082128	MH613170

Table 1. (Continued).

Species	Strain No.[1]	Country	Substrate	GenBank/ENA/DDBJ accession Nos.[2]			
				benA	***CaM***	***RPB2***	**ITS**
A. niger	IHEM 4063	Bahamas	sea water	MH614440	MH644995	OP082163	MH613152
	IHEM 23895	Belgium	human ear secretions	MH614584	MH644945	OP082135	MH613163
	IHEM 14389	Belgium	chronic obstructive bronchopneumopathy (bronchoalveolar lavage)	MH614517	MH644975	OP082106	KP131597
	IHEM 18678	Peru	guano	MH614475	MH644930	OP082114	MH613074
	IHEM 3710	Unknown	unknown	MH614490	MH644943	OP082161	MH613158
	IHEM 24767	India	otitis	MH614507	MH644964	OP082146	MH613198
	IHEM 9388	France	air	MH614438	MH644979	OP082175	MH613220
	IHEM 3019	Zaire	soil from palm grove (*Elaeis guineensis*)	MH614514	MH644970	OP082158	MH613206
	IHEM 24454	India	otitis	MH614470	MH644956	OP082143	MH613186
	IHEM 22379	India	otomycosis	MH614511	MH644968	OP082125	KP131603
	IHEM 4461	Belgium	mycotic otitis externa	MH614585	MH644978	OP082164	KP131607
	IHEM 23888	Belgium	otitis	MH614494	MH644949	OP082133	MH613173
	IHEM 6350	Belgium	dried food for fish	MH614471	MH644977	OP082173	MH613214
A. eucalypticola	CBS 122712 = DTO 53-A2 = IBT 29274^{T}	Australia	leaves of *Eucalyptus* sp.	genome	genome	genome	OL711732
A. luchuensis	CBS 205.80 = IFM 47726 = NBRC 4281 = IFO 428 = KACC 46772 = RIB 2642^{T}	Unknown	awamori-koji	JX500062	JX500071	MN969081	JX500081
	NRRL 4750 = CBS 128.52 = KACC 47005^{T4}	USA	unknown	EF661087	EF661152	EF661052	MH856956
	RIB 2601 = IFO 4033 = NBRC 111188 = ATCC 38854 = IFM 46994	Unknown	unknown	genome	genome	genome	LC573600
	IFO 4308 = NBRC 4308	Unknown	unknown	genome	genome	genome	AB573884
	IHEM 26285	France	human broncho-aspiration	MH614561	MH644869	OP082038	MH613141
	IHEM 25486	France	human trimming liquid	MH614563	MH644862	OP082030	MH613118
	CBS 112811 = CECT 20582 = IBT 26239^{T5}	Denmark	black pepper	genome	genome	genome	OL711715
	IHEM 23904	India	otitis	MH614551	MH644990	OP082022	MH613164
	PPRI 13091 = CMV 010I3	South Africa	soil	MK451175	MK451492	MK450797	—
	IHEM 5316	Belgium	human ear	MH614562	MH644893	OP082046	MH613216
	PPRI 9197 = CMV 005C9	South Africa	soil	MK451038	MK451491	MK450796	MK450641
	PPRI 13230 = CMV 011A9	South Africa	maize roots	MK451187	MK451493	MK450798	—
	PPRI 8983 = CMV 005C2	South Africa	twigs and leaves from *Colophospermum mopane*	MK451035	MK451490	MK450795	MK450640
A. pseudotubingensis	SDBR CMUO2^{T}	Thailand	rhizosphere soil	MK457206	MK457205	MK457208	—
	SDBR CMUO8	Thailand	rhizosphere soil	MW602908	MW602907	MW602909	—
	SDBR CMU20	Thailand	rhizosphere soil	MW602913	MW602912	MW602914	—
A. tubingensis	CBS 133056 = DTO 213-F6 = NRRL 4875^{T}	Unknown	unknown	EF661086	EF661151	EF661055	EF661193
	PPRI 8683 = CMV 005B3	South Africa	soil	MK451028	MK451452	MK450786	—
	PPRI 8733 = CMV 005B6	South Africa	plant debris from *Colophospermum mopane*	MK451031	MK451453	MK450787	—
	PPRI 21344 = CMV 004I4	South Africa	seed of soybean (*Glycine max*)	MK451011	MK451448	MK450782	—
	IFM 57258	Nagasaki, Japan	soil	OP081902	OP081909	genome	—

Table 1. (Continued).

Species	Strain No.[1]	Country	Substrate	GenBank/ENA/DDBJ accession Nos.[2]			
				benA	*CaM*	*RPB2*	ITS
A. tubingensis	IHEM 18329	French Guiana, France	rotten mango	MH614467	MH644992	OP082002	MH613202
	IHEM 18205	French Guiana, France	soil	MH614419	MH644865	OP082001	MH613127
	IHEM 21599	Cuba	rail feather	MH614458	MH644985	OP082008	MH613073
	IHEM 18097	French Guiana, France	rotten mango	MH614417	MH644981	OP081998	MH613119
	IHEM 21607	Cuba	indoor environment	MH614464	MH644988	OP082012	MH613133
	IHEM 18042	French Guiana, France	soil under mango tree	MH614462	MH644980	OP081997	MH613117
	IHEM 21597	Cuba	indoor air	MH614457	MH644984	OP082007	MH613122
	IHEM 2463	Belgium	nutmeg (*Myristica fragrans*)	MH614465	MH644989	OP082028	MH613147
	IHEM 21593	Cuba	cotton cloth	MH614460	MH644987	OP082006	MH613131
	IHEM 18136	French Guiana, France	soil under palm tree	MH614456	MH644983	OP082000	MH613121
	IHEM 21592	Cuba	human ear	MH614420	MH644866	OP082005	MH613130
	IHEM 21606	Cuba	indoor environment	MH614466	MH644991	OP082011	MH613199
	IHEM 21590	Cuba	indoor air	MH614418	MH644986	OP082004	MH613129
	IHEM 22375	India	otomycosis	MH614461	MH644867	OP082015	KP131633
	IHEM 22376	India	otomycosis	MH614463	MH644868	OP082016	KP131634
	IHEM 18106	French Guiana, France	leaf of mango tree	MH614455	MH644982	OP081999	MH613083
	IHEM 21602	Argentina	clinical material	MH614459	MH644864	OP082010	MH613123
	PPRI 21345 = CMV 005A8	South Africa	seed of soybean (*Glycine max*)	MK451024	MK451450	MK450784	—
	PPRI 21347 = CMV 005A9	South Africa	seed of soybean (*Glycine max*)	MK451025	MK451451	MK450785	—
	IHEM 21971	Mauritius	soil	MH614546	MH644993	OP082013	MH613134
	IHEM 25327	Belgium	laboratory contaminant	MH614421	MH644994	OP082029	MH613139
	IHEM 21601	Argentina	clinical material	MH614564	MH644917	OP082009	—
	PPRI 7393 = CMV 005A5	South Africa	unknown	MK451021	MK451542	MK450813	MK450660
	NRRL 4851 = ATCC 16879 = CBS 115.48 = CBS 558.65	Wisconsin, USA	unknown	EF661085	EF661150	EF661054	—
	CBS 134.48 = ITEM 7040	Unknown	unknown	AY820007	AJ964876	EF661055	FJ629354
	IHEM 5802	Unknown	unknown	MH614558	MH644919	OP082048	MH613204
	IHEM 22772	Belgium	human ear	MH614545	MH644871	OP082018	MH613132
	PPRI 25991 = CMV 001B7	South Africa	walnut kernels (*Juglans regia*)	MK450891	MK451540	MK450811	MK450658
	PW3161	Hong Kong	human nail	LC000547	LC000560	LC000573	AB987902
	PPRI 6720 = CMV 005A3	South Africa	beetle (*Aspidimorpha areata*)	MK451019	MK451541	MK450812	MK450659
	IFM 54640	Japan	human sputum	OP081898	OP081905	genome	—
	IFM 55763	Japan	vineyard	OP081899	OP081906	genome	—
	IFM 57143	Japan	human	OP081901	OP081908	genome	—
	IFM 56815	Japan	human ear	OP081900	OP081907	genome	—

Table 1. (Continued).

Species	Strain No.[1]	Country	Substrate	GenBank/ENA/DDBJ accession Nos.[2]			
				benA	***CaM***	***RPB2***	**ITS**
A. tubingensis	IFM 61612	Japan	human, bronchoalveolar lavage fluid	OP081903	OP081910	genome	—
	IHEM 22370	Belgium	otitis	MH614525	MH644894	OP082014	KP131632
	IHEM 1941	Belgium	dust from mattress	MH614550	MH644900	OP082003	MH613159
	IHEM 17170	Belgium	chronic sinusitus	MH614537	MH644923	OP081989	KP131625
	IHEM 25487	France	environment	MH614524	MH644879	OP082031	MH613120
	IHEM 23971	Belgium	mycotic otitis externa	MH614555	MH645013	OP082025	MH613181
	IHEM 17440	Belgium	chronic sinusitus	MH614540	MH644924	OP081991	KP131627
	IHEM 23890	Belgium	human ear	MH614530	MH644905	OP082020	MH613172
	IHEM 16879	Morocco	otitis human ear	MH614559	MH644921	OP081986	MH613211
	IHEM 26291	Belgium	unknown	MH614552	MH644903	OP082039	MH613165
	IHEM 17439	Belgium	chronic sinusitus	MH614539	MH644876	OP081990	KP131626
	IHEM 13662	Belgium	hospital environment	MH614553	MH644898	OP081985	MH613153
	IHEM 17033	Belgium	mycotic otomycosis externa	MH614536	MH644922	OP081987	KP131623
	IHEM 23911	Belgium	otitis	MH614566	MH644908	OP082024	MH613177
	IHEM 17904	Belgium	chronic sinusitus	MH614538	MH644875	OP081996	MH613212
	IHEM 17893	Belgium	chronic sinusitus	MH614542	MH644926	OP081994	KP131630
	IHEM 25949	France	human sputum	MH614528	MH644873	OP082034	MH613144
	IHEM 26200	Belgium	otitis	MH614568	MH644901	OP082036	MH613160
	IHEM 26645	Belgium	human ear secretions	MH614549	MH644897	OP082043	MH613148
	IHEM 26163	Belgium	otitis externa	MH614527	MH644872	OP082035	MH613140
	IHEM 23900	Belgium	otitis	MH614529	MH644904	OP082021	MH613166
	IHEM 26661	Belgium	onychomycosis human toe nail	MH614556	MH644911	OP082044	MH613193
	IHEM 17903	Belgium	chronic sinusitus	MH614543	MH644927	OP081995	KP131631
	IHEM 17441	Belgium	chronic sinusitus	MH614541	MH644925	OP081992	KP131628
	IHEM 26350	France	air	MH614548	MH644883	OP082040	MH613143
	IHEM 17168	Belgium	chronic sinusitus	MH614534	MH644920	OP081988	KP131624
	IHEM 26622	Belgium	human ear	MH614567	MH644896	OP082042	MH613145
	IHEM 25777	Belgium	human wound	MH614423	MH644913	OP082033	MH613197
	IHEM 25773	Belgium	otitis externa	MH614472	MH644912	OP082032	MH613196
	IHEM 4379	unknown	unknown	MH614554	MH644899	OP082045	MH613154
	IHEM 23985	Belgium	otitis	MH614531	MH644907	OP082026	MH613176
	IHEM 26215	Belgium	otomycosis	MH614433	MH644914	OP082037	MH613200
	IHEM 17442	Belgium	chronic sinusitus	MH614533	MH644915	OP081993	KP131629
	IHEM 10349	China	grains	MH614535	MH644918	OP081984	MH613207
	IHEM 23886	Belgium	otitis	MH614424	MH644910	OP082019	MH613188
	IHEM 5615	Unknown	unknown	MH614425	MH644916	OP082047	MH613201
	IHEM 24447	India	otitis	MH614532	MH644909	OP082027	MH613187
	CBS 115574 = IBT 23401 = ITEM 7555 = CECT 20579[T6]	Costa Rica	soil	genome	genome	HE984361	MH862988
	CBS 553.65 = NRRL 5121 = ATCC 16880 = IMI 23599	Costa Rica	soil	FJ629278	OP081904	OP081983	FJ629327
	CBS 115656 = IBT 20973 = NRRL 62634[T7]	Venezuela	mangrove water	KC796361	KC796377	genome	OL711719
	IHEM 23909	India	otitis	MH614422	MH644906	OP082023	MH613175
	IHEM 22394	India	conjunctivitis - human eye	MH614544	MH644870	OP082017	KP131635

Table 1. (Continued).

Species	Strain No.[1]	Country	Substrate	GenBank/ENA/DDBJ accession Nos.[2]			
				benA	*CaM*	*RPB2*	ITS
A. tubingensis	SDBR CMUI4[T8]	Thailand	rhizosphere soil	MK457200	MK457199	MK457202	—
	SDBR CMU15	Thailand	rhizosphere soil	MW602898	MW602897	MW602899	—
	SDBR CMUI1[T9]	Thailand	rhizosphere soil	MK457194	MK457193	MK457196	—
	SDBR CMUI7	Thailand	rhizosphere soil	MW602903	MW602902	MW602904	—
A. vadensis	CBS 113365 = IMI 142717 = CECT 20584 = IBT 24658[T]	Egypt	air	AY585531	genome	HE984371	—
	IHEM 26351	France	human sputum	MH614547	MH644878	OP082041	MH613142
A. carbonarius	CBS 111.26 = ITEM 4503 = NRRL 369 = ATCC 1025 = ATHUM 2854 = CBS 556.65 = IMI 016136 = MUCL 13583 = NCTC 1325 = NRRL 1987 = NRRL 369 = ITEM 5010[T]	Unknown	paper	EF661099	EF661167	EF661068	EF661204
	NRRL 67 = NBRC 5864 = ATCC 8740 = CBS 420.64 = DSM 872 = IFO 5864 = IMI 41875 = MUCL 30479 = NRRL 1737 = NRRL 605	Unknown	unknown	EF661097	EF661165	EF661066	EF661202
	NRRL 4849 = CBS 114.29	USA	unknown	EF661100	EF661168	EF661069	EF661205
	NRRL 346 = ATCC 6277 = CBS 146284	Honduras	unknown	EF661098	EF661166	EF661067	EF661203
Additional strains used only in DELINEATE and STACEY analyses							
A. carbonarius	IHEM 661	France	indoor air in bakery	MH614442	MH645014	—	—
	IHEM 1931	Belgium	dust from mattress	MH61458	MH644880	—	—
	IHEM 25902	France	human sputum	MH614575	MH645015	—	—
	DTO 179-F4	South Africa	house dust	KP329846	KJ775280	—	—
	DTO 179-C6	South Africa	house dust	KP329845	KJ775278	—	—
	CCF 3388	Czech Republic	toenails, human clinical material	HE577803	HE649500	—	—
	144-3-K2	Unknown	unknown	KJ599604	KJ599576	—	—
	A-1759	Israel	grape	KC520549	KC520552	—	—
	G187	Slovakia	dried vine fruits	MT166308	MK046876	—	—
	A-2160	Spain	grape	KC520550	KC520553	—	—
A. ibericus	NRRL 35644 = CBS 121593 = IMI 391429 = DTO 24-F1 = ITEM 4776 = IHEM 23498[T]	Portugal	wine grapes	EF661102	EF661163	XM_025715438	—
	NRRL 35645 = ITEM 6601 = IMI 391430	Portugal	wine grapes	EF661101	EF661164	EF661065	—
A. ellipticus	CBS 707.79 = IMI 172283[T]	Unknown	unknown	AY585530	EF661170	EF661051	—
	CBS 677.79 = IMI 278383 = ITEM 4499[T10]	Costa Rica	unknown	AY819993	AM117810	HE984363	—
A. heteromorphus	NRRL 4747 = CBS 117.55 = ATCC 12064 = IMI 172288 = IHEM 5801 = ITEM 7045[T]	Brazil	culture contaminant	EF661103	EF661169	EF661050	—
	IHEM 18645	France, Martinique	indoor wall	MH614573	MH645030	—	—
A. sclerotiicarbonarius	CBS 121057 = IBT 121057[T]	Unknown	culture contaminant	EU159229	EU159235	MN969091	—
A. sclerotioniger	CBS 115572 = IBT 22905 = ITEM 7560[T]	Unknown	unknown	FJ629304	FN594557	HE984369	—
A. japonicus	CBS 114.51 = ITEM 7034[T]	Unknown	unknown	HE577804	AJ964875	MN969079	—
	PPRI 4286 = CMV 005H7	South Africa	soil	MK451062	MK451430	MK450779	—
	ITEM 14787	USA	indoor air	HE984413	HE984430	HE984377	—

Table 1. (Continued).

Species	Strain No.[1]	Country	Substrate	GenBank/ENA/DDBJ accession Nos.[2]			
				benA	***CaM***	***RPB2***	**ITS**
A. japonicus	ITEM 14805	USA	indoor air	HE984416	—	HE984378	—
	CBS 123.27 = NRRL 360 = ATCC 1042 = IFO 4106 = IMI 358697	Puerto Rico	soil	HE577805	EF661141	EF661047	—
	NRRL 1782 = ATCC 16873 = CBS 568.65 = IMI 211387	Panama	soil	—	EF661144	EF661048	—
	NRRL 35494 = ITEM 15926	Unknown	unknown	—	EU021690	EU021639	—
	NRRL 35541	USA	peanut field soil	EF661104	EF661143	EU021640	—
	NRRL 4839 = IHEM 5627 = NCTC 3792 = MUCL 13578 = IMI 312983 = CBS 113.48	Unknown	unknown	MH614586	EF661142	EF661049	—
	IHEM 26043	France	human sputum	MH614587	MH645026	—	—
	CBS 115571	Bahamas	marine environment	EU482434	EU482432	—	—
	AJP01	Unknown	unknown	JX103558	JX103559	—	—
	CCF 4079	Unknown	unknown	HE577811	FR751423	—	—
	ITEM 14789	USA	indoor air	HE9844174	HE984432	—	—
	NBRC 4408	Unknown	soil	LC573650	LC573708	—	—
	NBRC 32856	Japan	living leaf	LC573651	LC573709	—	—
A. aculeatus	CBS 172.66 = IHEM 5796 = NRRL 5094 = IMI 211388 = CCRC 32190 = ATCC 16872 = ITEM 7046[T]	Unknown	tropical soil	HE577806	EF661148	XM020198603	—
	PPRI 7513 = CMV 005A6	Unknown	unknown	MK451022	MK451291	MK450752	—
	PPRI 26016 = CMV 007C9	South Africa	soil	MK451118	MK451296	MK450756	—
	F-719	Unknown	unknown	HE577810	HE578093	—	—
	PPRI 4070 = CMV 005F1	South Africa	soil	MK451044	MK451292	MK450753	—
	ITEM 14807	USA	indoor air	HE984409	HE984424	HE984372	—

[1]Acronyms of culture collections in alphabetic order: ATCC, American Type Culture Collection, Manassas, Virginia; ATHUM, Athens Collection of Fungi, University of Athens, Athens, Greece; CBS, Westerdijk Fungal Biodiversity Institute (formerly Centraalbureau voor Schimmelcultures), Utrecht, the Netherlands; CCF, Culture Collection of Fungi, Department of Botany, Charles University, Prague, Czech Republic; CCFC,Canadian Collection of Fungal Cultures, living fungal collection associated with the DAOM herbarium (Agriculture and Agri-Food Canada), Ottawa, Canada; CCM (F-), Czech Collection of Microorganisms, Brno, Czech Republic; CCRC (=BCRC), Bioresources Collection and Research Center, Food Industry Research and Development Institute, Hsinchu, Taiwan; CECT, Colección Española de Cultivos Tipo, Universidad de València, Edificio de Investigación, Burjassot, Spain; CMV, working and formal culture collections housed at FABI (Forestry and Agricultural Biotechnology), Innovation Africa, University of Pretoria, South Africa; DSM, Leibniz Institute DSMZ-German Collection of Microorganisms and Cell Cultures, Braunschweig, Germany; DTO, internal culture collection of the Department Applied and Industrial Mycology of the Westerdijk Fungal Biodiversity Institute, Utrecht, The Netherlands; IBT, Culture Collection at the Department of Biotechnology and Biomedicine, Lyngby, Denmark; IFM, Culture Collections for Pathogenic Fungi and Actinomycetes, Medical Mycology Research Center, Chiba University, Chiba, Japan; IFO, Institute for Fermentation, Osaka, Japan (IFO strains were transferred to the NBRC NITE collection); IHEM (BCCM/IHEM), Belgian Coordinated Collections of Micro-organisms, Fungi Collection: Human and Animal Health, Sciensano, Brussels, Belgium; IMI, CABI's collection of fungi and bacteria, Wallingford, UK; JCM, Japan Collection of Microorganisms, Tsukuba, Japan; KACC, Korean Agricultural Culture Collection, Wanju, South Korea; KCTC, Korean Collection for Type Cultures, Korea Research Institute of Bioscience and Biotechnology, Jeongeup, South Korea; MUCL (BCCM/MUCL), Agro-food & Environmental Fungal Collection, Louvain-la-Neuve, Belgium; NBRC (NITE), National Institute of Technology and Evaluation, Biological Resource Center, Department of Biotechnology, Kisarazu, Chiba, Japan; NCTC, National Collection of Type Cultures, Central Public Laboratory Service, London, UK; ITEM, Agri-Food Toxigenic Fungi Culture Collection, Institute of Sciences of Food Production, Bari, Italy; NRRL, Agricultural Research Service Culture Collection, Peoria, Illinois, USA; PPRI, culture collection of the National Collections of Fungi, housed at the Agricultural Research Council - Plant Health and Protection, Roodeplaat, South Africa; RIB, National Research Institute of Brewing, Tax Administration Agency, Higashihiroshima, Hiroshima, Japan; SDBR, Sustainable Development of Biological Resources Laboratory, Faculty of Science, Chiang Mai University, Chiang Mai Province, Thailand. Other acronyms represent personal strain numbers (without permanent preservation).

[2]Accession numbers to genomic sequences analysed in this study are listed in Supplementary Table S3.

[T]ex-type strain. [T1] = *A. lacticoffeatus*; [T2] = *A. vinaceus*; [T3] = *A. welwitschiae*; [T4] = *A. nakazawae;* [T5] = *A. piperis*; [T6] = *A. costaricensis*; [T7] = *A. neoniger*; [T8] = *A. chiangmaiensis*; [T9] = *A. pseudopiperis*; [T10] = *A. helicothrix*.

Total genomic DNA was isolated from 5-d-old cultures using the Zymo Research Fungal/Bacterial DNA Kit™ (Zymo Research, Irvin, CA, USA) or the Invisorb Spin Plant Mini Kit (Invitek, Berlin, Germany). PCR amplification of *CaM* was performed using the primer pairs cmd5 and cmd6 (Hong *et al.* 2006) or CF1L and CF4 (Peterson 2008); *benA* with Bt2a and Bt2b (Donaldson *et al.* 1995) or Ben2f (Hubka & Kolarik 2012) and Bt2b; and *RPB2* with fRPB2-5F and fRPB2-7CR (Liu *et al.* 1999). Samples were amplified using the following cycling parameters: one initial step of 10 min at 95 °C followed by 35 cycles of 1 min at 95 °C, 1 min at 55 °C, and 1 min at 72 °C and a single extension step of 10 min at 72 °C. The PCRs were performed in 25 µL volume containing 2 µL of DNA (2 pM), 2 µL of forward primer, 2 µL of reverse primer, 19 µL of H_2O, and PuReTaq Ready-To-Go PCR beads (GE Healthcare UK, Little Chalfont, UK). The PCR products were sequenced using the BigDye Terminator cycle sequencing ready reaction kit (Applied Biosystems, Foster City, CA, USA) using the same primers used for PCR and analysed on an ABI Prism 3130 genetic analyser (Applied Biosystems) according to the manufacturer's instructions.

Newly obtained DNA sequences were inspected and assembled in Geneious Prime v. 2020.2.4 (Biomatters Ltd.). Sequences were deposited into GenBank with the accession numbers listed in Table 1.

Phylogenetic analyses and species delimitation

Alignments of *benA*, *CaM* and *RPB2* were performed using the FFT-NS-i option implemented in the MAFFT online service (Katoh *et al.* 2019). The alignments were trimmed, concatenated, and then analysed using maximum likelihood (ML), maximum parsimony (MP) and Bayesian inference (BI) methods. The final alignments are available from the DRYAD digital repository (https://doi.org/10.5061/dryad.866t1g1td).

Suitable partitioning schemes and substitution models for the analyses were selected based on the Bayesian information criterion using a greedy strategy implemented in PartitionFinder 2 (Lanfear *et al.* 2017) with settings allowing introns, exons and codon positions to be independent datasets (Supplementary Table S1). ML trees were constructed with IQ-TREE v. 1.4.4 (Nguyen *et al.* 2015) with nodal support determined by ultrafast bootstrapping (BS) with 10^5 replicates. Bayesian posterior probabilities were calculated using MrBayes v. 3.2.6 (Ronquist *et al.* 2012). The analysis ran for 10^7 generations, two parallel runs with four chains each were used, every 1 000th tree was retained, and the first 25 % of trees were discarded as burn-in. The convergence of the runs and effective sample sizes were checked in Tracer v. 1.6 (http://tree.bio.ed.ac.uk/software/tracer). Maximum parsimony (MP) trees were calculated using PAUP* v. 4.0b10 (Swofford 2003). Analyses were performed using the heuristic search option with 100 random taxon additions; tree bisection-reconnection (TBR); maxtrees were set to 1 000. Branch support was assessed by bootstrapping with 500 replications.

The rules for the application of the GCPSR approach were adopted from Dettman *et al*. (2003a, b) and slightly modified for the different design of this study (different numbers of loci and methods used). To recognize a clade as an "evolutionary lineage", it had to satisfy one of two criteria: (a) genealogical concordance - the clade was present in the majority (2/3) of the single-locus genealogies; (b) genealogical nondiscordance - the clade was well supported in at least one single-locus genealogy, as judged by ML ultrafast bootstrap proportions ≥95 %, MP bootstrap proportions ≥70 % and BI posterior probabilities ≥95 %, and was not contradicted in any other single-locus genealogy at the same level of support. When deciding which evolutionary lineages represent "phylogenetic species", two additional criteria were applied and evaluated according to the combined phylogeny of three genes: (a) genetic differentiation - species had to be relatively distinct and well differentiated from other species to prevent minor tip clades from being recognized as a separate species; (b) all individuals had to be placed within a phylogenetic species, and no individuals were to be left unclassified.

Species delimitation analyses based on the multispecies coalescent model were performed as described previously (Sklenář *et al.* 2021). In brief, the haplotype function from R v. 4.0.2 (R Core Team 2016) package PEGAS (Paradis 2010) was used to retain only unique sequences in the alignments. The best fitting models were obtained in jModelTest v. 2.1.7. Parameters and the other settings of the STACEY, GMYC, bGMYC, PTP, and bPTP methods were consistent with previous studies (Sklenář *et al.* 2021, Glässnerová *et al.* 2022). Two different settings were used for the GMYC method. The ultrametric input trees for this method were calculated in BEAST v. 2.6.6 (Bouckaert *et al.* 2014) with a chain length of 10^7 generations. As a model for creating input trees, we set up the coalescent constant population prior and performed two tree reconstruction methods: one with the common ancestor height (CAh) setting and a second with the median height (Mh) setting. We only show the delimitation results of both settings when they were different. The results of all analyses are graphically summarised in iTOL v. 6 (Interactive Tree of Life) (Letunic & Bork 2021).

The multilocus species delimitation method STACEY was performed in BEAST (Bouckaert *et al.* 2014) using the STACEY v. 1.2.5 add-on (Jones 2017). For this and the DELINEATE analysis (see below), we added several additional species from other series of section *Nigri* (Table 1). We set up the length of MCMC chain to 10^9 generations, the species tree prior was set to the Yule model, the molecular clock model was set to a strict clock, the growth rate prior was set to a lognormal distribution (M = 5, S = 2), the clock rate priors for all loci were set to a lognormal distribution (M = 0, S = 1), the PopPriorScale prior was set to a lognormal distribution (M = -7, S = 2) and the relative DeathRate prior was set to a beta distribution (α = 1, β = 1 000). The substitution models were as follows: *benA* - K80+I; *CaM* - TrNef+G; *RPB2* - TrNef+G. The output was processed with SpeciesDelimitationAnalyzer (Jones *et al.* 2015). For the presentation of the STACEY results, we first created a plot showing how the number of delimited species and the probability of the most likely scenarios changed in relation to the value of the *collapseheight* parameter, and then we created similarity matrices using code from Jones *et al.* (2015) with different values of *collapseheight* chosen from the plot (see the Results section).

Independent testing of various species boundary hypotheses was performed in the DELINEATE software (Sukumaran *et al.* 2021). After splitting the dataset into hypothetical populations (Supplementary Table S2) using the "A10" analysis in BPP v. 4.4 (Yang 2015), the species tree for these populations was estimated in starBEAST (Heled & Drummond 2010) implemented in BEAST v. 2.6.7 (Bouckaert *et al.* 2014). The analysis was run in the Python (van Rossum & Drake Jr FL 2014) package DELINEATE (Sukumaran *et al.* 2021). In every simulated model, some populations delimited by BPP were assigned to tentative (fixedly defined) species based on the species delimitation results from previous analyses or were based on the common species definitions from previous studies. Other populations were left free to be delimited (unassigned to any species). As a result, the algorithm implemented in DELINEATE can either recognize the unassigned population as a separate

species, define a wider monophyletic species composed of several unassigned populations, or merge unassigned populations with some of the predefined species.

Whole genome sequencing and assembly

Whole-genome 100 bp paired-end (PE) sequencing was performed in 18 strains with the aid of HiSeq 1500 (Illumina, San Diego, CA) using the HiSeq reagent kit v. 1, according to the manufacturer's instructions. A 300 bp PE sequencing was performed on a MiSeq (Illumina) using the MiSeq Reagent Kit v. 3, according to the manufacturer's instructions. Long read sequencing of IFM 61612 was performed on the MinION platform (ONT; Oxford Nanopore Technologies, Cambridge, UK). A DNA library for ONT sequencing was prepared using a short-read eliminator kit (Nippon Genetics, Tokyo, Japan) and a ligation sequencing kit (SQK-LSK109), and sequencing was performed with a FLO-MIN106D flow cell (R9.4.1) for 48 h, according to the manufacturer's instructions. A total of 83 443 ONT reads were generated with a mean length of 12 011 bp using ONT Guppy v. 2.3.5.

Adapters and low-quality bases of Illumina reads were trimmed by Trim Galore v. 0.6.4 (Krueger 2015) with the default settings selected (http://www.bioinformatics.babraham.ac.uk/projects/trim_galore). The mitochondrial genomes were assembled using GetOrganelle v. 1.6.4 (Jin *et al.* 2020) with trimmed reads. To filter the mitochondrial reads, the trimmed reads were aligned against the mitochondrial genomes by BWA v. 0.7.17-r1188 (Li & Durbin 2009), and the mapped reads were filtered by SAMtools v. 1.9 (Li *et al.* 2009) and SeqKit (Shen *et al.* 2016). For eight isolates sequenced by MiSeq, the filtered reads were used to assemble the nuclear genomes using SPAdes v. 3.14.0 (Bankevich *et al.* 2012) with the options '--cov-cutoff auto' and '--careful'. For six isolates sequenced by HiSeq 1500, the assembly of nuclear genomes was carried out as follows: (1) the filtered reads were used to assemble the contigs using VelvetOptimiser v. 2.2.6 (Zerbino & Birney 2008); (2) the contigs were used to generate *in silico* long mate-pair reads with inserts of 3 000 ± 300 bp using Wgsim v. 0.3.1-r13 (https://github.com/lh3/wgsim) with the options '-e 0 -1 100 -2 100 -r 0 -R 0 -X 0 -d 3000 -s 300 -N 4000000'; (3) Illumina PE and simulated mate-pair (MP) reads were assembled by ALLPATHS-LG v. 52488 (Gnerre *et al.* 2011). The genome of IFM 61612 was assembled using NECAT v. 0.0.1_update20200803 (Chen *et al.* 2021), and polished with the ONT reads by using Racon v. 1.4.20 (Vaser *et al.* 2017) and Medaka v. 1.4.4 (https://github.com/nanoporetech/medaka) and with Illumina PE reads by using HyPo v. 1 (Kundu *et al.* 2019). Most tools were obtained through Bioconda (Grüning *et al.* 2018).

Genome annotation

The annotation of assembled genomes was performed using the Funannotate pipeline v. 1.7.4 (https://funannotate.readthedocs.io/en/latest/). Following the identification of repeat sequences by RepeatModeler v. 1.0.11 (http://www.repeatmasker.org/RepeatModeler.html) and RepeatMasker v. 4.0.7 (https://www.repeatmasker.org), Funannotate *ab initio* prediction was performed with the option '--busco_seed_species=aspergillus_oryzae' by Augustus v. 3.3.3 (Stanke *et al.* 2006), GeneMark-ES v. 4.38 (Ter-Hovhannisyan *et al.* 2008), GlimmerHMM v. 3.0.4 (Majoros *et al.* 2004), and SNAP v. 2006-07-28 (Korf 2004) using exon hints from the proteins of *A. niger* CBS 513.88 and *A. oryzae* RIB40 downloaded from the Aspergillus Genome Database (Bairoch & Apweiler 2000, Cerqueira *et al.* 2014). The functional annotations of predicted genes were performed using the Swiss-Prot, InterPro v. 5.42-78.0 (Jones *et al.* 2014), eggNOG v. 4.5.1 (Buchfink *et al.* 2015, Huerta-Cepas *et al.* 2016), MEROPS v. 12.0 (Rawlings *et al.* 2018, Mitchell *et al.* 2019), and the dbCAN v. 8.0 (Yin *et al.* 2012) databases. Genome annotations of the reference strains were obtained from the Joint Genome Institute (http://genome.jgi.doe.gov/) (Supplementary Table S3). The completeness of the draft genomes and predicted proteins were evaluated using BUSCO v. 4.0.6 (Seppey *et al.* 2019) with the database "eurotiales_odb10".

Phylogenetic analyses based on the genomic sequences

Orthologous genes among the 31 strains (18 newly sequenced and 13 available from previous studies) were identified by OrthoFinder v. 2.3.12 (Emms & Kelly 2019). Then, the amino acid sequences of 5 752 single-copy orthologous proteins were aligned using the G-INS-i option in MAFFT v. 7.471 and concatenated into one long protein sequence. A phylogenetic tree was constructed using multithreaded RAxML (Stamatakis 2014), selecting the PROTGAMMAWAG model and using 100 bootstrap replicates to determine node support.

The predicted protein sets of 31 strains were evaluated with BUSCO protein mode. A total of 2 754 genes present at a single copy were identified among all strains. From these, 200 genes were randomly selected for analyses using the STACEY method and randomly distributed into ten independent analyses, each containing 20 genes (Supplementary Table S4). Coding regions (exons) of the corresponding 200 nucleotide sequences were extracted for each strain from the *de novo* assemblies. Each sequence matrix was aligned using MAFFT, and well-aligned regions were extracted using Gblocks v. 0.91b (Talavera & Castresana 2007) with settings allowing no gap positions.

RESULTS

Combined phylogeny based on three loci

A maximum likelihood (ML) phylogenetic tree based on three loci in 280 strains (276 belonging to the series *Nigri* and four *A. carbonarius* strains used as outgroups) is presented in Fig. 1, with the geographic origin and substrate plotted on the tree in the form of colour strips. The topology of the trees inferred by the maximum parsimony (MP) and Bayesian inference (BI) methods was similar to ML and the bootstrap support values and posterior probabilities, respectively, were appended to the nodes.

There are three main lineages in the tree and for practical reasons, we named them based on the priority rules. The *A. brasiliensis* lineage (ABL) only contains the ex-type isolate of *A. brasiliensis*, while the *A. niger* lineage (ANL) contains the ex-type isolates of *A. lacticoffeatus*, *A. niger*, *A. vinaceus* and *A. welwitschiae* (the old species names, which are usually considered synonyms, are omitted). The *Aspegillus tubingensis* lineage (ATL) contains ex-types of ten species: *A. chiangmaiensis*, *A. costaricensis*, *A. eucalypticola*, *A. luchuensis*, *A. neoniger*, *A. piperis*, *A. pseudopiperis*, *A. pseudotubingensis*, *A. tubingensis* and *A. vadensis*. The sequences of the three recently described species, *A. chiangmaiensis, A. pseudopiperis* and *A. pseudotubingensis* (Khuna *et al.* 2021), were of poor quality and contained a large number of errors (indels) in the coding regions and probably also in the noncoding regions of all three genes. Due to this fact and the

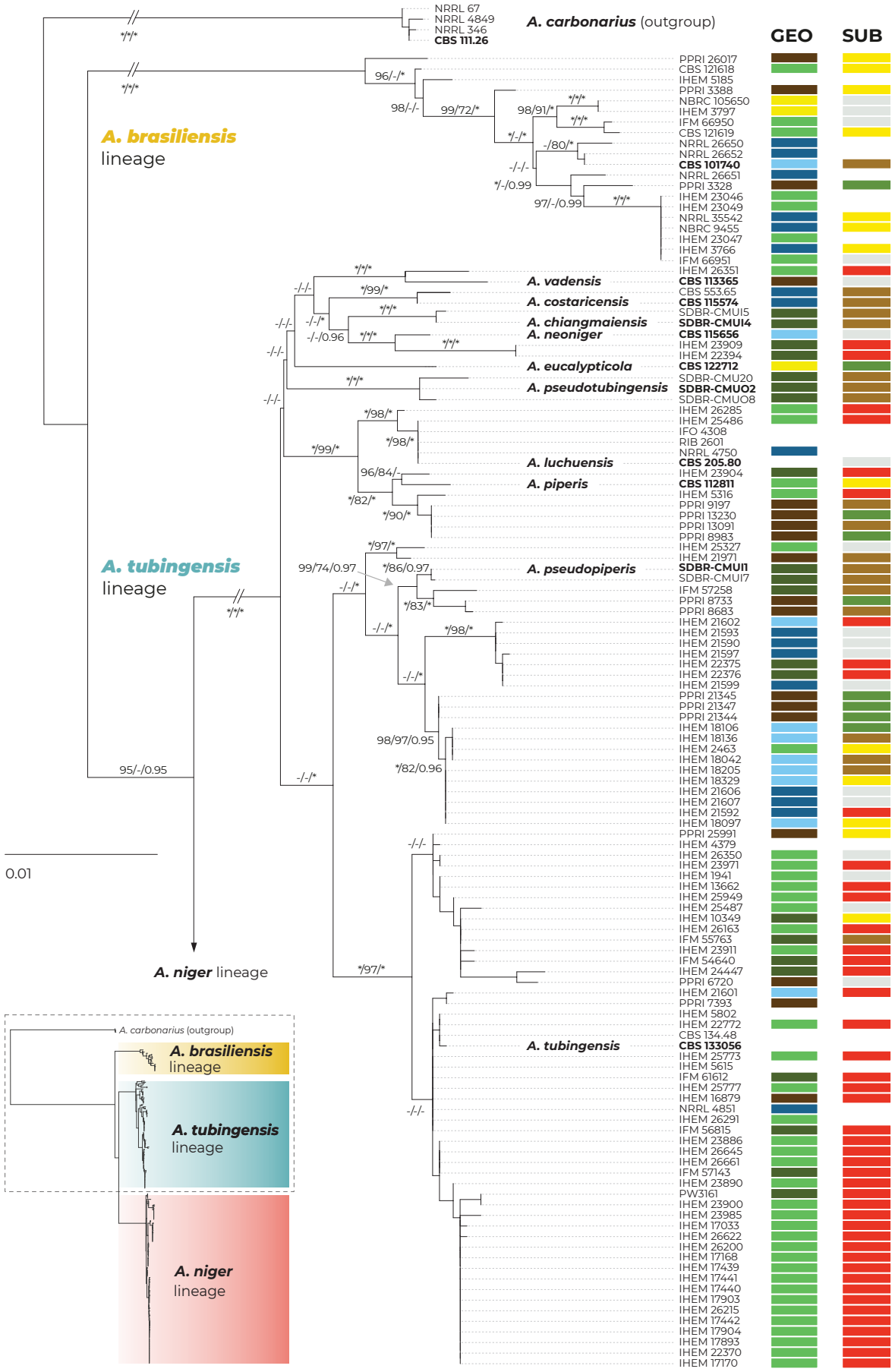

Fig. 1. Multilocus phylogeny of *Aspergillus* series *Nigri* based on three loci (*benA*, *CaM*, *RPB2*) and 276 isolates (and four *A. carbonarius* isolates as an outgroup). The best-scoring maximum likelihood (ML) tree inferred in the IQ-TREE is shown; ultrafast bootstrap support values (ML bs) are appended to nodes along with maximum parsimony bootstrap support values (MP bs) and Bayesian inference posterior probabilities (BI pp); only support values ≥95 %, ≥70 % and ≥0.95, respectively, are shown; a dash indicates lower statistical support for a specific node or the absence of a node in the phylogeny while an asterisk indicates full support; the ex-type strains are designated with a bold print; the information on geographic origin and isolation source is plotted on the tree (see legend). Alignment characteristics, partitioning schemes and substitution models are listed in Supplementary Table S1.

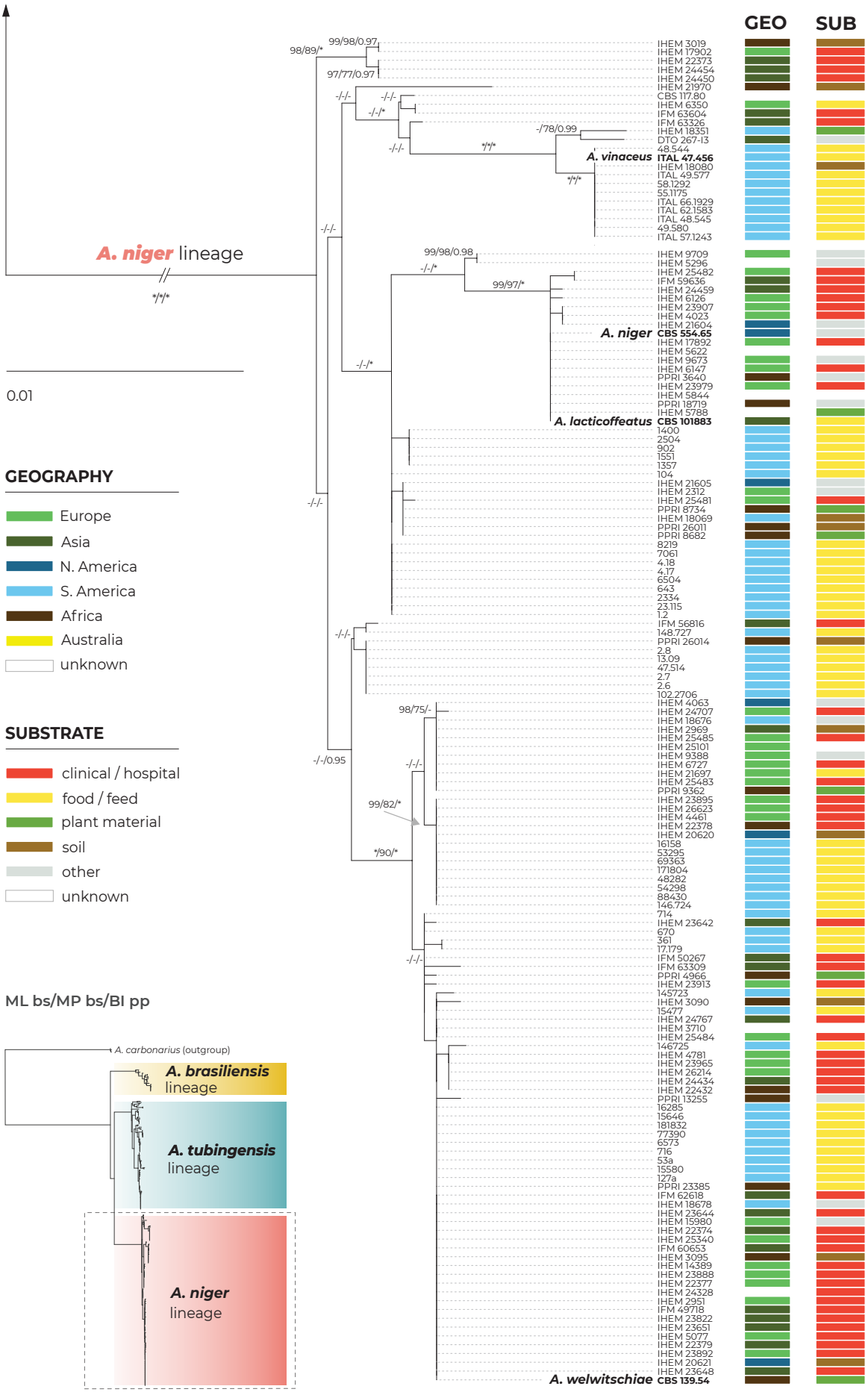

Fig. 1. (Continued).

absence of genomic sequences, we excluded these species from most analyses. However, we manually corrected some apparent errors in the exonic regions (partially revised sequences can be found in the alignments deposited in the Dryad digital repository: https://doi.org/10.5061/dryad.866t1g1td) and added these species to the classical phylogenetic trees based on the ML, MP and BI methods. In these phylogenies, the positions of *A. chiangmaiensis* and *A. pseudotubingensis* differ significantly from the tree presented by Khuna *et al*. (2021). The combined phylogeny without these species is shown in Supplementary Fig. S1.

The bootstrap support values in the combined trees (Fig. 1 and Supplementary Fig. S1) are high on many terminal branches in ATL, and the majority of the currently accepted species form their own well-supported terminal clades. On the other hand, some deeper nodes are poorly supported and the relationships among the species in ATL are mostly unresolved. If only the monophyly and statistical support of branches in these combined phylogenetic trees were considered, all currently recognized species in ATL could be accepted. Bootstrap values in the trees based on concatenated datasets are, however, often falsely high and are not a suitable criterion for deciding about species limits (Kubatko & Degnan 2007, Seo 2008). The boundaries between currently accepted species in ANL are much less clear, as there are several poorly supported clades in the proximity of *A. vinaceus*, *A. niger* and *A. welwitschiae* whose species identification is unclear.

The geography and substrate of isolation showed no clear patterns that could be associated with particular species, although clinical isolates from European countries (mostly strains from the study of D'hooge *et al.* (2019)) were overrepresented in the clade containing the *A. tubingensis* ex-type strain CBS 133056, while isolates from food and South America were more common throughout ANL (strains predominantly from Silva *et al.* (2020)).

Incongruences between single gene trees: consequences for the GCPSR approach and BLAST similarity searches

Single-gene trees based on *benA*, *CaM* and *RPB2* loci are shown in Fig. 2 and Supplementary Fig. S2 (only one isolate per unique multilocus haplotype was included). The coloured connecting lines show changes in the positions of isolates between single-gene trees (Fig. 2); the branches were rotated so that the trees maximally correspond to each other; the trees without connecting lines are shown in Supplementary Fig. S2. There was no conflict in topology among the three main lineages, *i.e.,* there was no isolate changing position between ABL, ANL and ATL in different single-gene trees. When applying the rules of the GCPSR approach in ABL and ANL, only one phylogenetic species (PS) can be recognized in each lineage because the composition of their subclades is variable in terms of the isolates resolved in them, while the statistical support of the subclades is low or unstable between phylogenies. A more complicated situation is present in the ATL, where some clades can be recognized as evolutionary lineages, as they are well supported in at least two phylogenetic trees. For example, the clade containing the two strains of *A. vadensis* (CBS 113365 and IHEM 26351) was present and supported in all phylogenies, while the clade containing seven strains attributed to *A. luchuensis*/*A. piperis* was present and supported in the *benA* and *CaM* trees. The singleton lineage containing the ex-type of *A. eucalypticola* (CBS 122712) was also present in all trees, but it cannot be evaluated by the GCPSR criteria as there are no isolates clustering with this strain. Although the abovementioned evolutionary lineages were recognized by the grouping criteria, they cannot be recognized as PS because doing so would have resulted in a situation where other strains belonging to the ATL and forming several nonmonophyletic clades in the combined tree (Fig. 1) could not be assigned to any phylogenetic species and were left unclassified. As a result, applying GCPSR criteria in the ATL would also lead to the recognition of only one phylogenetic species.

To show the practical consequences of the incongruences between single-gene datasets, we created a local BLAST database containing sequences of *benA*, *CaM* and *RPB2* of the ex-type strains belonging to the series *Nigri*. Then, we performed BLAST searches for all sequences of these genes against this database (only one isolate per unique multilocus haplotype was used) in Geneious PRIME v. 2020.2.4 (https://www.geneious.com). The results of the BLAST searches and the closest similarities to the ex-type strains are presented in Fig. 3. It is apparent that sequences of different genes from the same strain frequently resulted in the closest sequence similarities with ex-type strains of different species and thus resulted in variable species identifications. This phenomenon does not involve *A. brasiliensis*.

In the ANL, different species identifications commonly resulted for different loci, which was observed in 21 out of 53 haplotypes (39.6 %). In seven haplotypes (13 %; CBS 117.80, IFM 63326, IFM 63604, IHEM 6350, 148.727, 2.8 and 102.2706), the three BLAST searches resulted in three different identifications, *i.e., A. niger*, *A. vinaceus* and *A. welwitschiae*. This demonstrates that there are phylogenetic conflicts throughout the entire clade and that there is no barcode gap for these species at any of these loci. These incongruences are also visible in the single-gene phylogenetic trees shown in (Fig. 2, Supplementary Fig. S2).

In ATL, unstable identification based on different genes was less prevalent than in ANL, but was still present in 14 out of 54 haplotypes (24 %). It occurred mostly between *A. tubingensis*, *A. costaricensis*, *A. neoniger*, *A. pseudopiperis*, *A. luchuensis* and *A. piperis*. Four haplotypes (7 %; IHEM 23904, IHEM 25327, IHEM 21971 and IFM 57258) were identified as a different species for each gene region. This phenomenon also has its basis in the single-gene tree incongruences (Fig. 2, Supplementary Fig. S2).

Phylogenomic tree

In Fig. 4, the topology of the phylogenomic tree was compared to the topology of the three-locus ML tree (alignment reduced to unique multilocus haplotypes; *A. chiangmaiensis, A. pseudopiperis* and *A. pseudotubingensis* were excluded; list of haplotypes in Supplementary Table S5) and to the topology of the species tree constructed in starBEAST. The phylogenomic tree was based on 5 752 protein orthologues extracted from 30 whole-genome sequences of series *Nigri* and one sequence of *A. carbonarius* as an outgroup. Nine out of 18 newly sequenced genomes (Supplementary Table S3; designated by bold print in Fig. 4) belonged to ANL, six to ATL and three to ABL. Almost all clades in the phylogenomic tree gained full statistical support, in contrast to the trees based on the *benA*, *CaM* and *RPB2* loci. The topologies among the different analyses were mostly congruent, but several incongruences were observed (most of them were present at unresolved nodes with low statistical support). For example, *A. vadensis* was resolved as a separate branch sister to all other species in the ATL in the phylogenomic and species tree but clustered with *A. costaricensis* and *A. neoniger* with a high support of 95 % in the ML tree. In the phylogenomic and species tree, *A. neoniger* and *A. costaricensis*

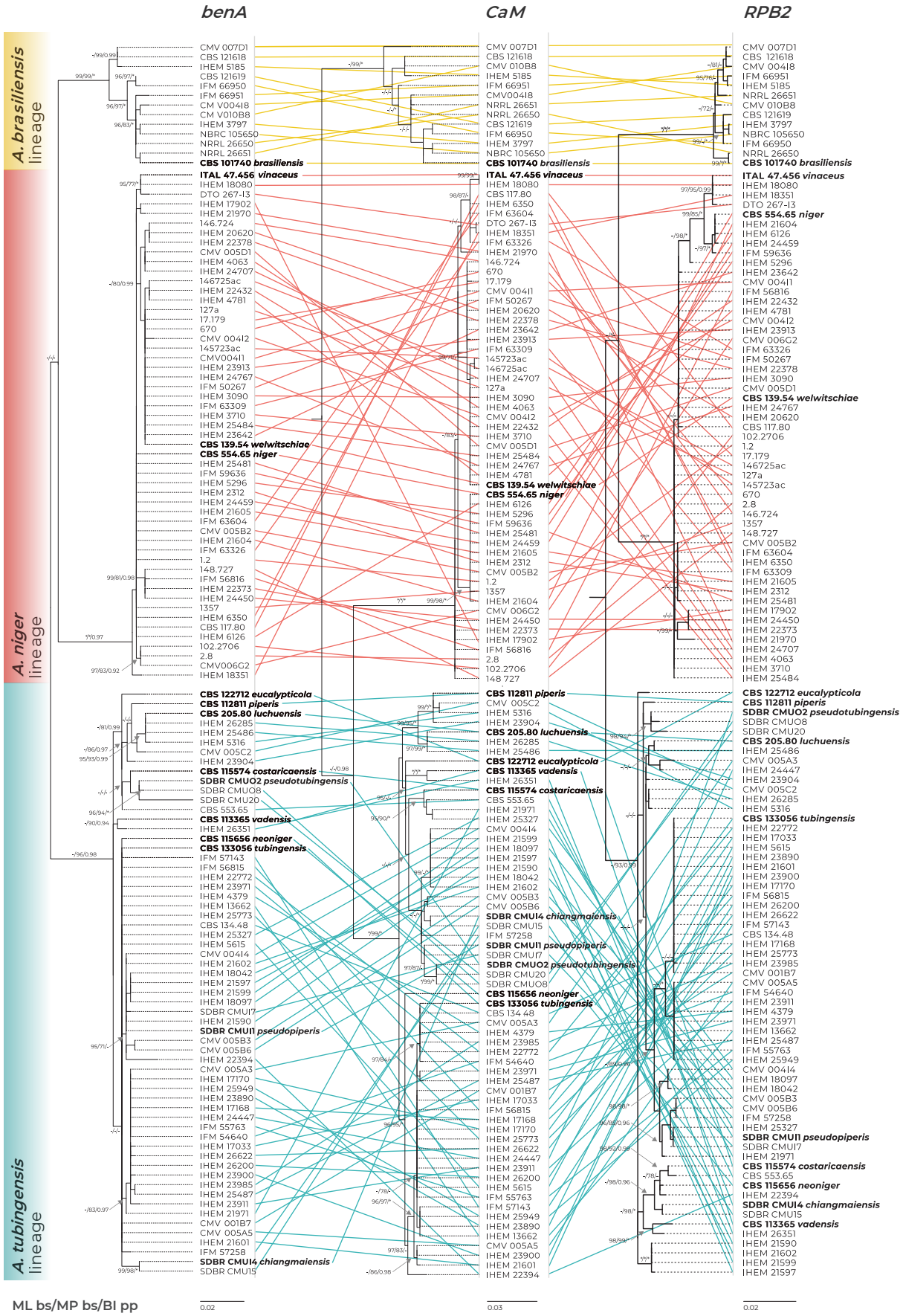

Fig. 2. Comparison of single-gene genealogies based on the *benA*, *CaM* and *RPB2* loci and created by three different phylogenetic methods (only one isolate per unique multilocus haplotype is included in each phylogeny). The coloured connecting lines show changes in the positions of isolates between single-gene trees (the branches were rotated so that the trees maximally correspond to each other). Best-scoring single-locus maximum likelihood (ML) trees are shown; ML ultrafast bootstrap support values (ML bs), maximum parsimony bootstrap support values (MP bs) and Bayesian inference posterior probabilities (BI pp) are appended to nodes. Only support values ≥95 %, ≥70 % and ≥0.95, respectively, are shown. A dash indicates lower statistical support for a specific node, or the absence of a node in the phylogeny, while an asterisk indicates full support. The ex-type strains are designated with a bold print. Alignment characteristics, partitioning schemes and substitution models are listed in Supplementary Table S1.

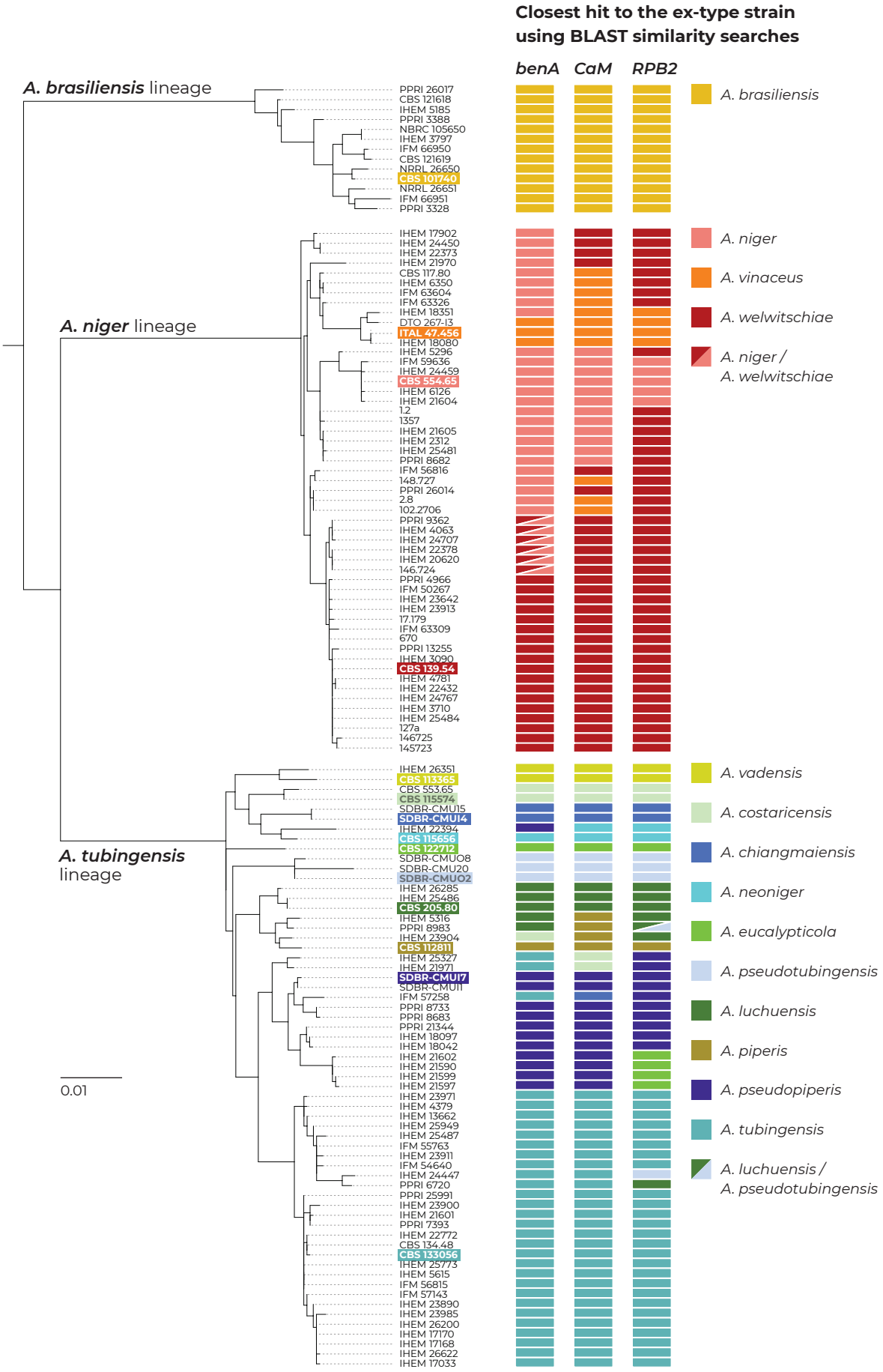

Fig. 3. The results of BLAST similarity searches of three loci (*benA*, *CaM* and *RPB2*) derived from strains with unique multilocus haplotypes across the genetic diversity of series *Nigri*. Coloured rectangles represent the closest hits to one of the 14 ex-type strains (every species has its unique colour; the ex-type of *A. lacticoffeatus* was omitted because it has an identical genotype to the ex-type of *A. niger*). If there was an identical similarity to two ex-type strains, the rectangles were diagonally divided. Ex-type isolates are marked with bold font and a coloured background. The phylogenetic tree was calculated in IQ-TREE using partitioned analysis and 10^5 ultrafast bootstrap replicates.

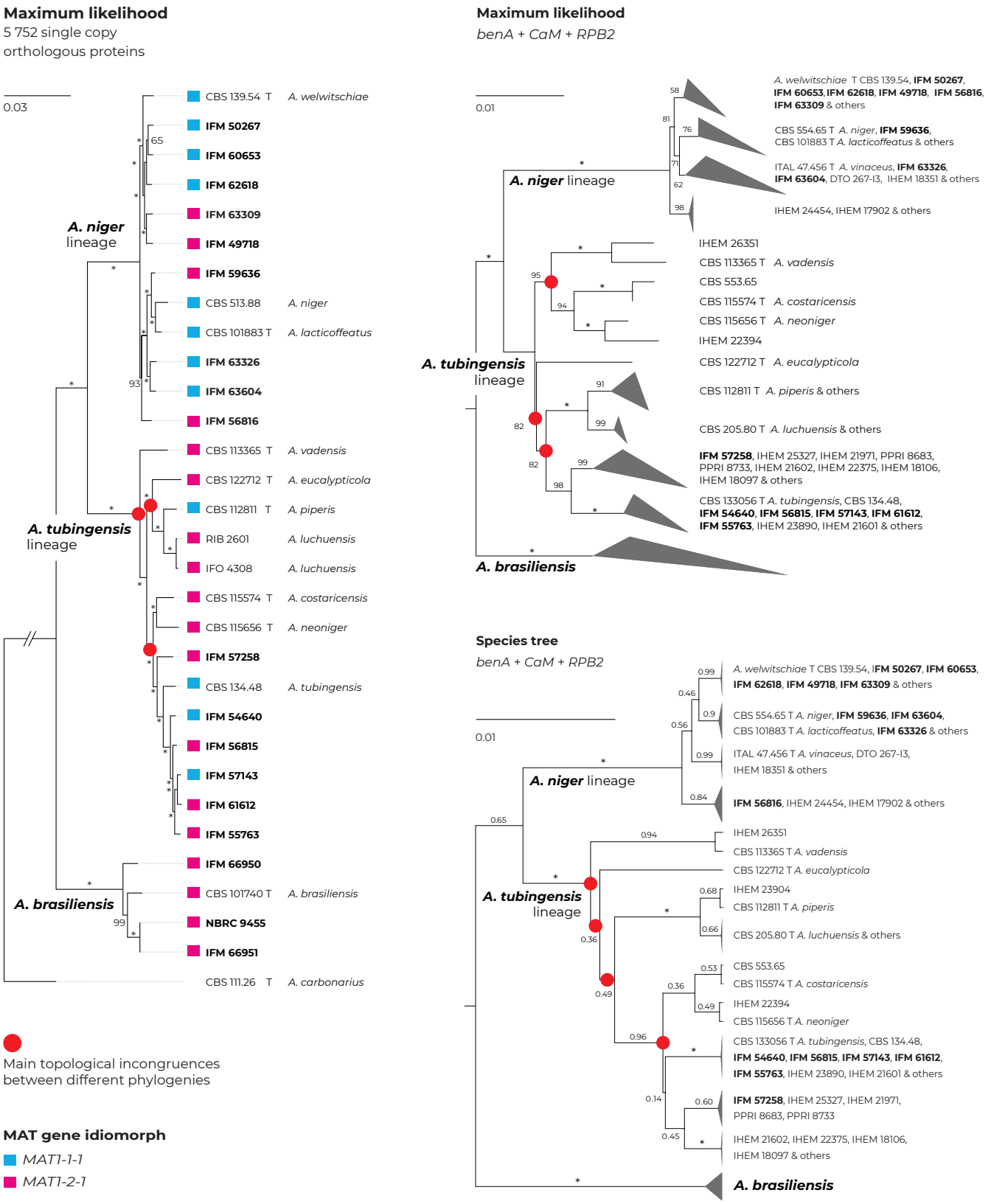

Fig. 4. Comparison of topologies of phylogenetic trees constructed on the basis of different methods and data. Incongruences between phylogenies are designated with red circles. Maximum likelihood (ML) tree constructed based on the 5 752 orthologous proteins extracted from the 31 whole genome sequences (WGS; Supplementary Table S3) (left side); ML tree based on *benA*, *CaM* and *RPB2* loci estimated in IQ-TREE (top right); species tree based on *benA*, *CaM* and *RPB2* loci estimated in starBEAST (bottom right); the last two mentioned trees were constructed from combined three-gene alignments reduced to unique multilocus haplotypes (Table S5), and *A. chiangmaiensis*, *A. pseudopiperis* and *A. pseudotubingensis* were excluded. The most significant differences can be observed in the positions of *A. neoniger*, *A. costaricensis* and *A. eucalypticola*. Bootstrap support values or posterior probabilities are appended to the nodes, the support values equal to 100 % and 1.00, respectively, are designated with an asterisk; the ex-type strains are designated with the letter "T". Isolates for which whole genomic sequences were generated in this study are designated with a bold print; mating-type gene idiomorphs are plotted on the tree based on the WGS data.

clustered with *A. tubingensis* isolates, in contrast to the ML tree, where they clustered distantly from the latter. Last, *A. eucalypticola* clusters with *A. luchuensis* and *A. piperis* in the phylogenomic tree, while in ML and species trees, it formed a long separate branch.

Both *MAT1-2-1* and *MAT1-1-1* mating-type gene idiomorphs were found in the genomes of strains belonging to the ANL and ATL, while only the *MAT1-2-1* idiomorph was found in the *A. brasiliensis* strains (Fig. 4).

Multispecies coalescent model-based (MSC) methods

The results of the species delimitation using four single-locus species delimitation methods (GMYC, bGMYC, PTP and bPTP) and one multilocus method, STACEY, are summarised in Fig. 5. For the GMYC and STACEY methods, we showed the results of two different settings, as they differed in the number of delimited species.

All methods and their settings delimited the entire ANL as a single species without any exception. The method STACEY and all single-locus methods except for three delimited only one species in the *A. brasiliensis* lineage. Three methods (GMYC with a common ancestor height (CAh) setting; bPTP based on *benA*, and bPTP based on *CaM*) recognized isolate PPRI 26017 as a singleton species separated from *A. brasiliensis*. All single-locus methods except for two unequivocally proposed that ATL should be considered a single broad species. The first exception was the GMYC method based on *benA* with a CAh setting that divided the ATL into three species: *A. vadensis* and another two species that are not monophyletic in any multigene phylogeny that are shown in Figs 1 and 3. The second was the bPTP method based on *CaM*, which divided ATL into eight species corresponding to *A. vadensis*, *A. eucalypticola*, *A. tubingensis*, a species comprising both *A. piperis* and *A. luchuensis*, and four additional species whose delimitation has no support in the multigene phylogeny as they are not monophyletic (Figs 1 and 3).

The multilocus method STACEY was performed using two different datasets. The first dataset contained unique multilocus haplotypes from the *Nigri* series and the second dataset was supplemented with eight additional species outside the *Nigri* series. The results of both analyses were identical and supported the delimitation of one or four species in the ATL depending on the value of the *collapseheight* parameter. Detailed results of STACEY based on the second dataset are presented in Fig. 6, where subfigure A illustrates the effect of the *collapseheight* parameter value on the number of delimited species. On the y-axis on the left side, there is the number of delimited species with the given *collapseheight* value (black line). The support for the most likely scenario (yellow line), and the support for the second most likely scenario (blue line) are shown; other less supported scenarios were omitted. The vertical dashed lines in subfigure A represent the scenarios illustrated in detail in Fig. 6B and Fig. 6C in the form of similarity matrices showing posterior probabilities of each pair of isolates being included in the same species. There are three main scenarios that gained reasonable support and which delimited 15 (*collapseheight* = ~0.004–0.006), 14 (*collapseheight* = ~0.006–0.008) and 11 species (*collapseheight* = ~0.009 and higher) (Fig. 6), corresponding to 3 or 7 species in the series *Nigri.* In all three scenarios, the ANL and ABL were always resolved as single species. At *collapseheight* of ~0.005, four species were delimited in the ATL: (1) *A. costaricensis* + *A. neoniger* + *A. tubingensis*; (2) *A. luchuensis* + *A. piperis*; (3) *A. eucalypticola*; and (4) *A. vadensis.* When the *collapseheight* increases and reaches values in the range 0.006–0.008, the support for the delimitation of multiple species in the ATL decreases, but four species are still supported and not lumped together. The only difference in the scenario with 14 species compared to that with 15 species is outside series *Nigri,* namely, *A. aculeatus i*s delimited as one or two species, respectively. In the scenario with 11 species and a *collapseheight* of approximately 0.009 and higher, the whole *A. tubingensis* lineage is delimited as a single species.

Species delimitation using DELINEATE

The species hypotheses were independently tested in DELINEATE software, where we set up 10 different models. These models were divided into three categories based on the broadness of the fixed species predefined within the ANL and ATL: narrow (Models 1–4), medium (Models 5–7) and broad (Models 8–10). The results are summarised in Fig. 7, where every column represents one model with individual populations either assigned into species (grey bars = predefined species), or left unassigned and free to be delimited (brown bars). The red frames show the resulting solution proposed by DELINEATE for every model, *i.e.*, an unassigned population either recognized as a separate species, merged with other unassigned population(s), or merged with some predefined species.

Models 1, 5 and 8 focused on delimitation within the ABL, where four populations were recognized by BPP software. In all three models, these populations were left unassigned, and they were always lumped to form a single broad species regardless of whether the species in the ANL and ATL were predefined as narrow or broad.

Models 2, 6 and 9 focused on the ANL, in which all populations were left free to be delimited, while the populations of the ATL were segregated into eight narrow species (Model 2), four broader species (Model 6) and one broad species (Model 10). In all of these settings, the ANL was always recognized as a single broad species regardless of the species number and species limits in the ATL.

More variable delimitation results were obtained in the ATL. Models 3 and 4 simulated situations where *A. niger* populations (pop1 to pop8) were segregated into four and six species, respectively. In these cases, the ATL populations (pop1 to pop13) were arranged into four species as follows: (1) *A. piperis* + *A. luchuensis*; (2) *A. tubingensis* + *A. costaricensis* + *A. neoniger*; (3) *A. eucalypticola*; and (4) *A. vadensis*. In Models 7 and 10, the populations of the ANL were predefined into two and single species, respectively. In both cases, the ATL was delimited as a single species.

STACEY analysis using genomic data

To analyse species limits using MSC methods on the genome scale, we randomly selected 200 single-copy orthologous genes from the genomes. The alignments of these genes were randomly distributed into ten datasets each containing 20 genes that were analysed separately (Supplementary Table S4). The results are summarized in Fig. 8. The upper part of the figure shows the course of each analysis using different colours and the dependence of the delimitation results on the changing value of the *collapseheight* parameter. For every analysis, there are two curves, the first representing the number of delimited species (left y-axis) and the second representing the probability of the most likely species delimitation scenario at a specific *collapseheight* value (ranging from 0 to 1, right y-axis).

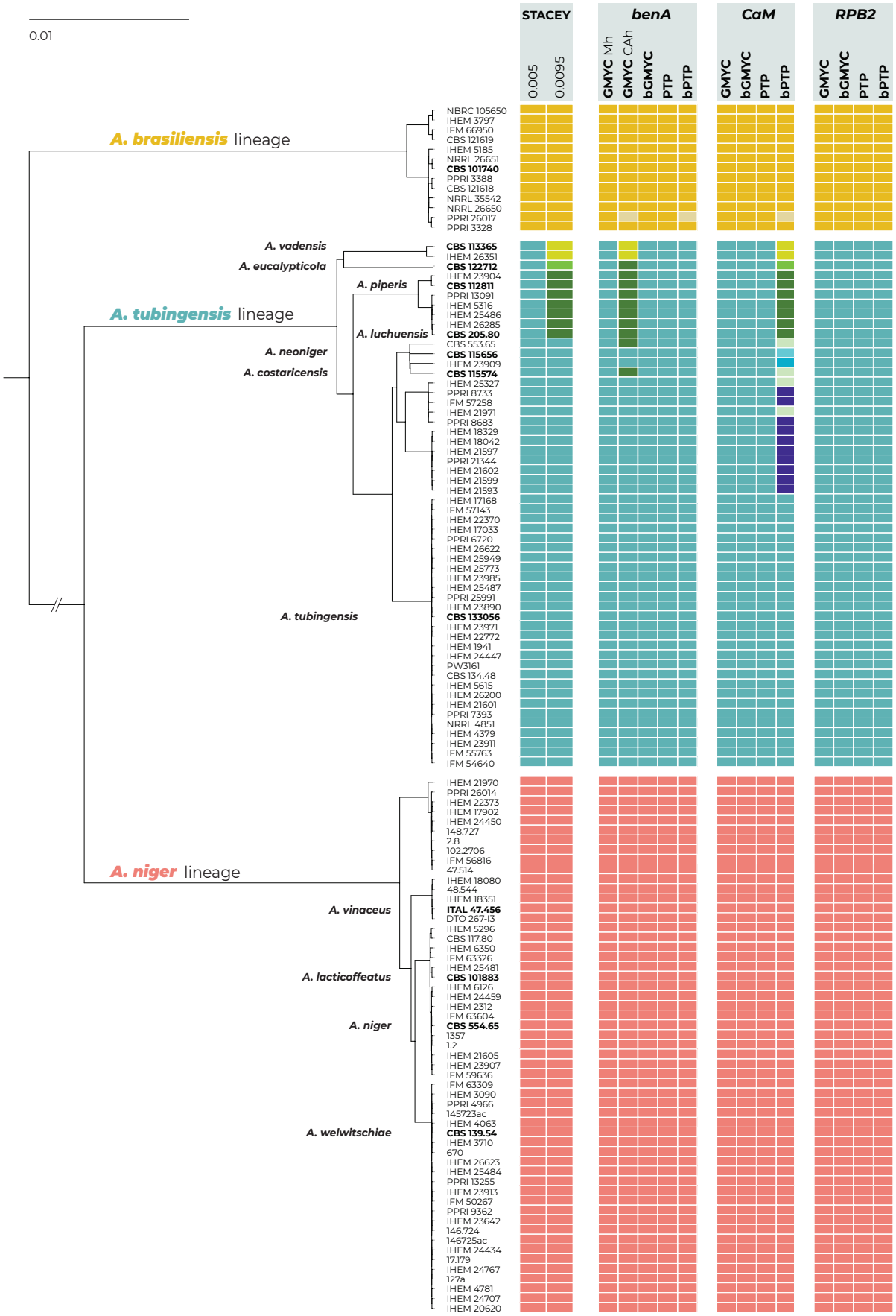

Fig. 5. Schematic representation of the results of species delimitation methods in the series *Nigri*. One multilocus method (STACEY) and four single-locus methods (GMYC, bGMYC, PTP, bPTP) were applied to a dataset of three loci (*benA*, *CaM*, *RPB2*). The results are depicted by coloured bars with different colours or shades indicating species delimited by specific methods and settings. Ex-type isolates are highlighted with a bold print. The STACEY results with two *collapseheight* parameter values, 0.005 and 0.0095, are shown. For the GMYC method, the coalescent constant population tree model was used as an input with both common ancestor heights (CAh) and median height (Mh) settings (both settings are only shown when they produced different delimitation results). The phylogenetic tree was calculated by STACEY analysis and is used solely for the comprehensive presentation of the results from different methods.

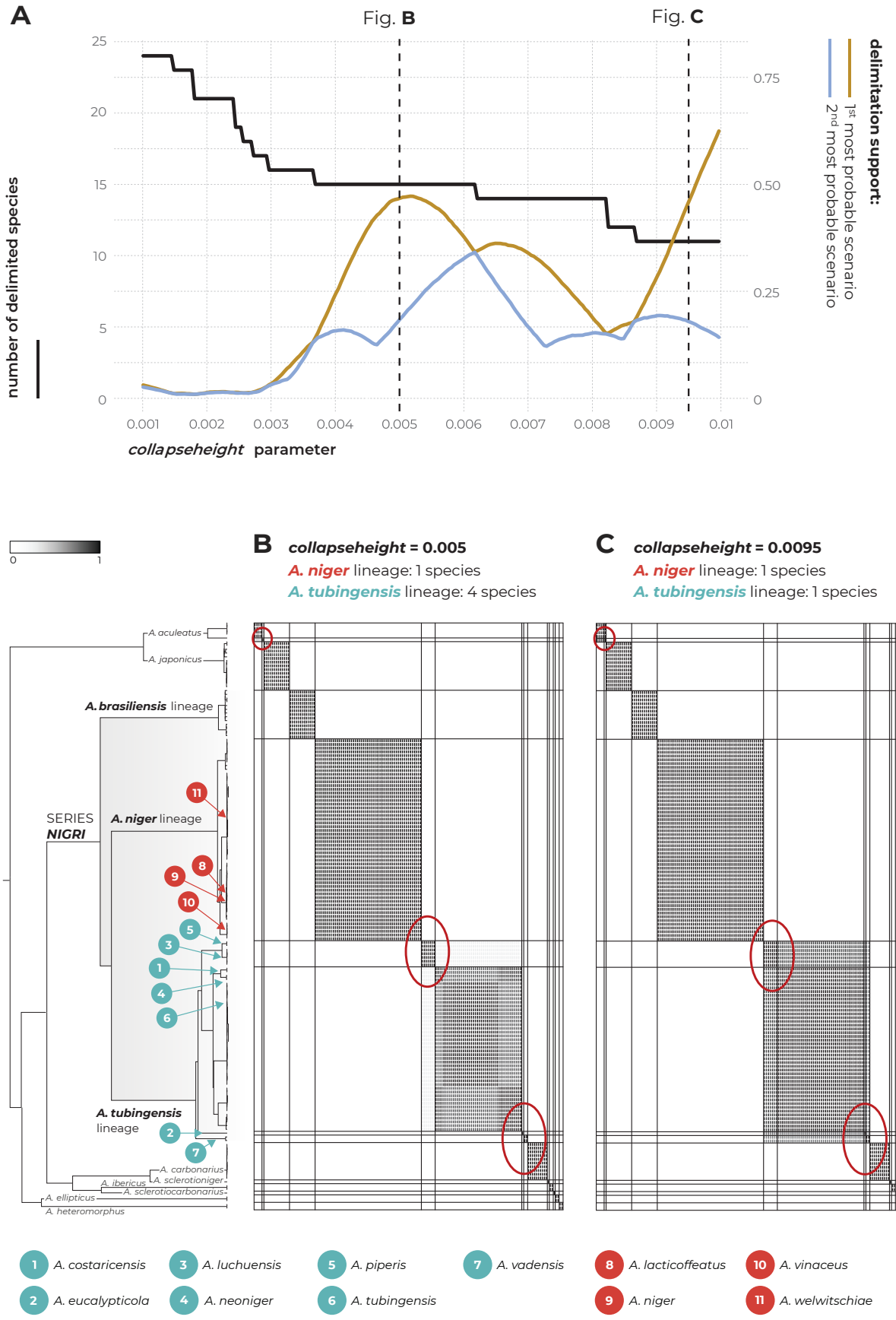

Fig. 6. The results of species delimitation by using the STACEY method based on the three loci: *benA*, *CaM* and *RPB2*. (A) Dependence of the delimitation results on the *collapseheight* parameter. The black solid line represents the number of delimited species (left y-axis) depending on the changing value of the *collapseheight* parameter (x-axis). The yellow line represents the probability (range from 0 to 1, right y-axis) of the most likely scenario at specific *collapseheight* value. The blue line represents the probability of the second most probable scenario at a specific *collapseheight* value; curves representing other less probable scenarios are omitted. Dashed vertical lines mark two values of the *collapseheight* parameter (0.005 and 0.0095) whose results are shown in detail by similarity matrices in subfigures B and C. The similarity matrices give the posterior probability of every two isolates belonging to the same multispecies coalescent cluster (tentative species). The darkest black shade corresponds to a posterior probability of 1, while the white colour is equal to 0. Thicker horizontal and vertical lines in the similarity matrices delimit species or their populations that gained delimitation support in some scenarios.

Fig. 7. Species delimitation using DELINEATE software. In total, ten models of species boundaries were set up and tested. The brown bars represent unassigned populations left free to be delimited, while the grey bars represent the predefined species. The resulting solutions suggested by DELINEATE are depicted by red frames around the bars. The populations were delimited by using BPP software; isolates belonging to each population are listed in Supplementary Table S2. The displayed tree was calculated in starBEAST based on the *benA*, *CaM* and *RPB2* loci and is only used for the comprehensive presentation of the results from different models.

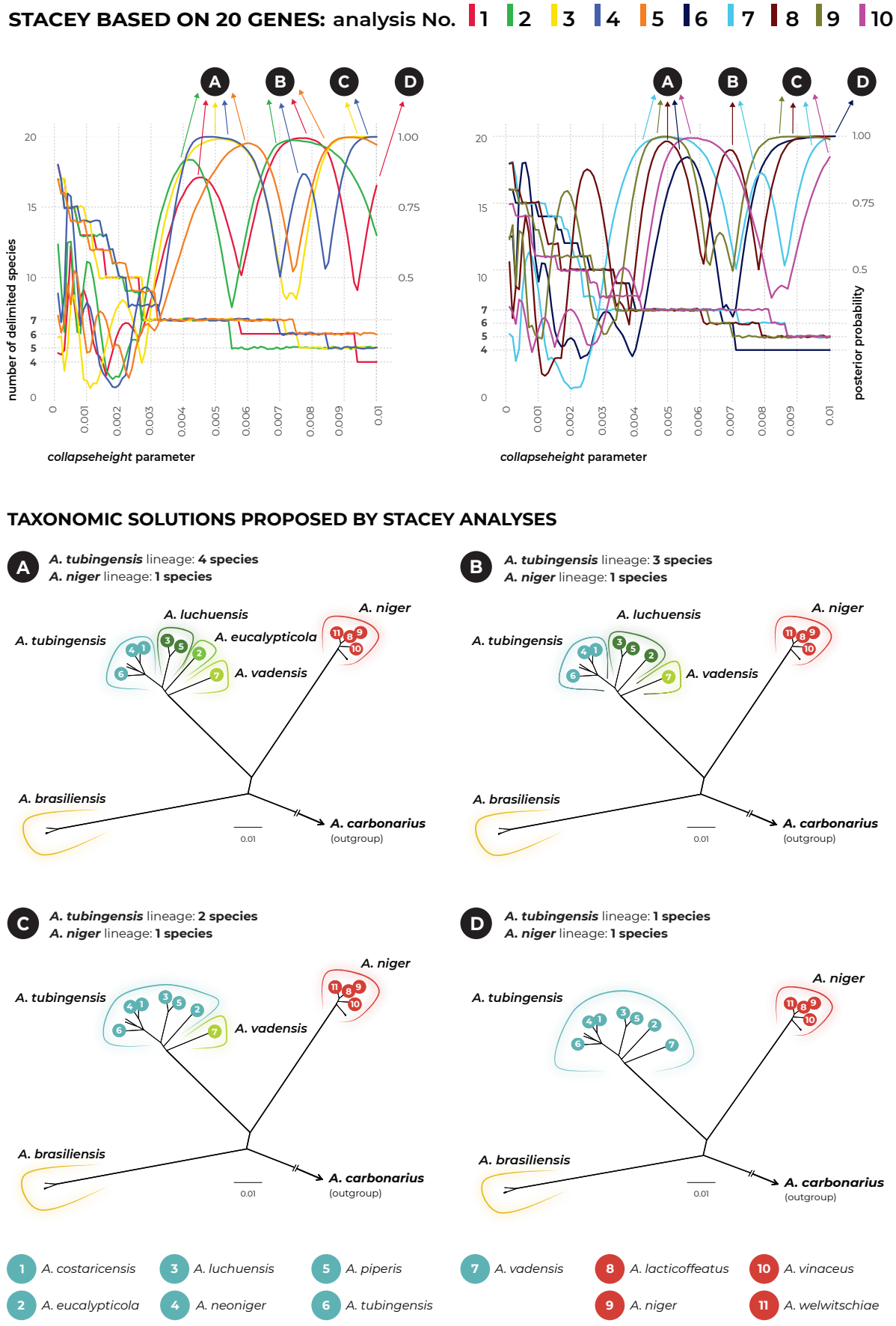

Fig. 8. Species delimitation results from ten independent STACEY analyses, each based on 20 genes randomly selected from genomes of series *Nigri* species (n = 30; plus one genome of *A. carbonarius* as the outgroup). The upper part of the figure shows the dependence of the delimitation results on the changing value of the *collapseheight* parameter; each analysis is designated with a different colour. There are two curves for each analysis, the first representing the number of delimited species (left y-axis) and the second representing the probability of the most likely species delimitation scenario at a specific *collapseheight* value (ranging from 0 to 1, right y-axis). Every analysis proposed two to three taxonomic solutions having similar probabilities. In total, there were four possible scenarios (A, B, C, D) differing in the number of delimited species within the *A. tubingensis* lineage (one to four species). These delimitation results are schematically shown in the lower part of the figure. The list of genes used in every analysis can be found in Supplementary Table S4.

Surprisingly, every analysis proposed two to three taxonomic solutions having high probabilities (two to three major peaks). There were four possible scenarios (A, B, C, D) resulting in 3–6 delimited species in the *Nigri* series. However, none of these analyses supported the division of the ANL or ABL into more species. Thus, all of these scenarios only differed in the number of delimited species in the ATL, ranging from one to four delimited species. These delimitation results are schematically shown in the lower part of Fig. 8. All ten analyses supported the scenario with four species: (1) *A. costaricensis* + *A. neoniger* + *A. tubingensis*; (2) *A. luchuensis* + *A. piperis*; (3) *A. eucalypticola*; and (4) *A. vadensis*. In addition, six analyses supported scenarios with three or two species in the ATL, and only two analyses lumped all species into one at high *collapseheight* values (Fig. 8).

Intraspecific genetic diversity in *Aspergillus* and series *Nigri*

To determine whether the intraspecific genetic variability in the redefined species in the series *Nigri* falls within the range commonly found in *Aspergillus*, we made an intraspecific diversity comparison across *Aspergillus* (basic data in Supplementary Table S6). We downloaded sequences of the *benA*, *CaM* and *RPB2* genes from 34 species outside section *Nigri* (fewer common markers, such as *Mcm7*, *Tsr1* and *Act,* were available for only some species). The criteria for inclusion were as follows: (1) species boundaries were re-examined using MSC methods, and (2) the strains of the species were obtained from at least three countries (sufficient sampling).

The results of the comparison (Fig. 9) showed that dissimilarites in the common taxonomic markers were usually lower than 4 % except in *benA*, where a higher degree of dissimilarity was found occasionally.

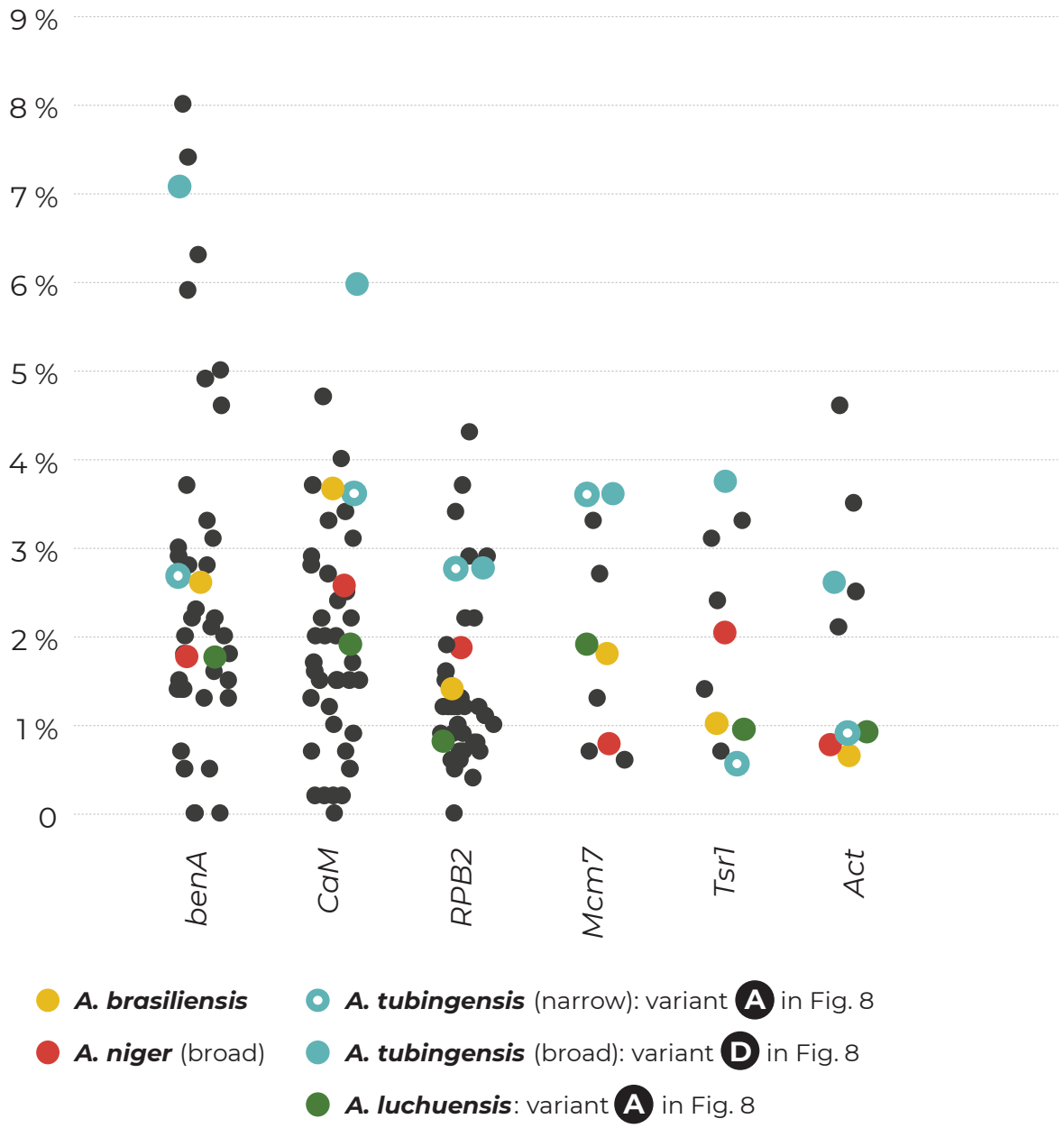

Fig. 9. Jitter plot showing maximum sequence dissimilarity between isolates of the same *Aspergillus* species whose species limits have been delimited using methods based on a multispecies coalescent model. Only species represented by isolates from at least three countries were included to ensure relevant sampling and thus representative intraspecific genetic variability. In total, 34 species were included that were classified outside section *Nigri.* The data from *benA*, *CaM* and *RPB2* were collected from all 34 species, while less common markers (minichromosome maintenance factor 7 - *Mcm7*, ribosome biogenesis protein - *Tsr1* and actin - *Act*) were available for only a limited number of species. Species belonging to the series *Nigri* are designated with coloured circles. The basic data used for construction of the jitter plot are listed in the Supplementary Table S6.

This was mainly caused by long intronic regions in *benA*. However, the two highest dissimilarity values in *benA* belong to *A. vitricola* (sect. *Restricti*) and *A. subalbidus* (sect. *Candidi*), which could each be a complex of two species because the species delimitation results were ambiguous (Sklenář *et al*. 2017, Glässnerová *et al*. 2022). Thus, the real maximum sequence dissimilarity in *benA* may be lower than that displayed in Fig. 9.

The intraspecific variability in the broadly defined *A. niger* (corresponding to the whole ANL) and in *A. brasiliensis* falls comfortably within the range frequently found in *Aspergillus*. The intraspecific genetic diversity of the broadly defined *A. tubingensis* in *benA* and *CaM* is higher than that commonly found in *Aspergillus*, while the variability within the narrowly defined *A. tubingensis* (excluding *A. luchuensis*/*A. piperis*, *A. eucalypticola* and *A. vadensis*) is within the range common for *Aspergillus* (Fig. 9).

TAXONOMY

The following list contains the names of accepted species in the series *Nigri* and their synonyms. Illegitimate and invalid names are also included as some of them are still used in the applied sphere. This list builds on previously published lists of accepted species and their synonyms in section *Nigri* (Thom & Church 1926, Thom & Raper 1945, Raper & Fennell 1965, Al-Musallam 1980, Kozakiewicz 1989). Compared to previous lists, this list is primarily based on available molecular data. If this data is missing, the names are included in the sub-list of unresolved or doubtful names.

One of the main goals of this list is to point out that the taxonomy of series *Nigri* is still unresolved and to stimulate further research to resolve names for which original material is available in the form of cultures or herbarium specimens. Some of these names may still threaten the stability of the taxonomy of series *Nigri*. Most importantly, some of the synonyms or unresolved names compete for priority with economically significant species such as *A. tubingensis*, *A. luchuensis* or even *A. niger*. Althoug *A. niger* Tiegh. 1867 was conserved against *Ustilago ficuum* Reichard 1867 and *Ustilago phoenicis* Corda 1840 (Kozakiewicz *et al.* 1992), it can still be predated by *A. phaeocephalus* Durieu & Mont. 1848 (no specimens available), *A. nigrescens* C.P. Robin 1853 (no specimens available) and *A. nanus* Mont. 1856 whose type is preserved in the Muséum National d'Histoire Naturelle in France but no DNA data are available. The situation is even more complicated with *A. tubingensis* Mosseray 1934. This species is conspecific with several older species names, such as *A. pulverulentus* (basionym *Sterigmatocystis pulverulenta* McAlpine 1896), *A. schiemanniae* Thom 1916, *A. elatior* Mosseray 1934, *A. pseudoniger* Mosseray 1934 and possibly some other species listed among unresolved species. *Aspergillus tubingensis* is the most frequently used name compared to other competing names and members of the International Commission of *Penicillium* and *Aspergillus* (ICPA) are thus currently in discussions about its possible conservation.

Accepted species and their synonyms in *Aspergillus* section *Nigri* series *Nigri*

1. *Aspergillus brasiliensis* Varga, Frisvad & Samson, Int. J. Syst. Evol. Microbiol. 57: 1929. 2007. MycoBank MB 510581. — Type: CBS 101740. Ex-type: CBS 101740 = IMI 381727 = IBT 101740. DNA barcodes: ITS = FJ629321; *benA* = FJ629272; *CaM* = FN594543; *RPB2* = EF661063.

2. *Aspergillus eucalypticola* Varga, Frisvad & Samson, Stud. Mycol. 69: 9. 2011. MycoBank MB 560387. — Type: CBS H-20627. Ex-type: CBS 122712 = IBT 29274. DNA barcodes: ITS = EU482439; *benA* = EU482435; *CaM* = EU482433; *RPB2* = MN969070.

3. *Aspergillus luchuensis* Inui, J. Coll. Sci. Imp. Univ. Tokyo 15: 469. 1901. MycoBank MB 151291. — Type: CBS H-24280. Ex-type: CBS 205.80 = NBRC 4281 = KACC 46772 = IFM 47726 = RIB 2642. DNA barcodes: ITS = JX500081; *benA* = JX500062; *CaM* = JX500071; *RPB2* = MN969081.

Synonym: *Aspergillus perniciosus* Inui, J. Coll. Sci. Imp. Univ. Tokyo 15: 473. 1901. [no MycoBank record]. Synonymized by Hong *et al.* (2013). No living culture available.

Synonym: *Aspergillus awamori* Nakaz., Rep. Govt. Res. Inst. Formosa: 1. 1907. [MycoBank MB 119955]. Synonymized by Hong *et al.* (2014). Culture ex-type: JCM 2261 = IAM 2112 = KACC 47234.

Synonym: *Aspergillus velutinus* Mosseray, La Cellule 43: 252. 1934. [MycoBank MB 255342]. The *benA* sequence (FJ629283) derived from the ex-type strain CBS 139.48 (= NRRL 4877 = CCM F-286 = VKM F-2084 = WB 4877) is identical to the ex-type of *A. luchuensis.*

Synonym: *Aspergillus aureus* var. *acidus* Nakaz., Simo & A. Watan., Bull. Agric. Chem. Soc. Japan 12: 960. 1936. [MycoBank MB 493809]. Not validly published [Art. 39.1; Turland *et al.* (2018)]. Synonymized by Hong *et al.* (2013). Culture ex-type: NBRC 4121 = NRRL 4796 = CBS 564.65 = KACC 45131.

Synonym: *Aspergillus aureus* var. *pallidus* Nakaz., Simo & A. Watan., Bull. Agric. Chem. Soc. Japan 12: 961. 1936. [MycoBank MB 372388]. Not validly published [Art. 39.1; Turland *et al.* (2018)]. Synonymized by Hong *et al.* (2014). Culture ex-type: NBRC 4123 = NRRL 4797 = CBS 565.65 = KACC 47004.

Synonym: *Aspergillus awamori* var. *piceus* Nakaz., Simo & A. Watan., Bull. Agric. Chem. Soc. Japan 12: 956. 1936. [MycoBank MB 250923]. Not validly published [Art. 39.1; Turland *et al.* (2018)]. Synonymized by Hong *et al.* (2013). Representative strain: CBS 119.52 = NRRL 4846.

Synonym: *Aspergillus kawachii* Kitahara & Yoshida. J. Ferment. Technol. 27. 1949. [No MycoBank record]. Not validly published [Art. 39.1; Turland *et al.* (2018)]. Synonymized by Hong *et al.* (2013). Culture ex-type: NBRC 4308 = CBS 117.80 = NRRL 4886 = KACC 46771. Hong *et al*. (2013) and Ban *et al*. (2021) examined phylogenetic position of *A. kawachii* based on strains KACC 46771 and NBRC 4308, respectively. Their sequences are identical with the ex-type of *A. kawachii* in contrast to the sequences from strain CBS 117.90 that belong to the ANL (Table 1). Our conclusion is that the strain CBS 117.90 is contaminated with *A. niger*.

Synonym: *Aspergillus citricus* var. *pallidus* (Nakaz., Simo & A. Watan.) Kozak., Mycol. Pap. 161: 114. 1989. [MycoBank MB 127748]. Not validly published – basionym *A. aureus* var. *pallidus* Nakaz., Simo & A. Watan. is not a validly published [Art. 41.5; Turland *et al.* (2018)].

Synonym: *Aspergillus inuii* Sakag., Iizuka & M. Yamaz., J. Agric. Chem. Soc. Japan 3: 97. 1950. [Mycobank MB 309227]. Not validly published [Art. 39.1; Turland *et al.* (2018)]. Synonymized by Hong *et al.* (2014). Culture ex-type: JCM 22302 = IAM 2255 = CBS 125.52 = KACC 47235.

Synonym: *Aspergillus nakazawae* [as *nakazawai*] Sakag., Iizuka & M. Yamaz., J. Agric. Chem. Soc. Japan 4: 3.

1950. [Mycobank MB 309232]. Not validly published [Art. 39.1; Turland *et al.* (2018)]. Synonymized by Hong *et al.* (2014). Culture ex-type: NRRL 4750 = CBS 128.52 = KACC 47005.

Synonym: *Aspergillus foetidus* var. *acidus* (Nakaz., Simo & A. Watan.) Raper & Fennell, The Genus *Aspergillus*: 326. 1965. [MycoBank MB 353273]. Synonymized by Hong *et al.* (2013). Not validly published – basionym *A. aureus* var. *acidus* Nakaz., Simo & A. Watan. is not a validly published name [Art. 41.5; Turland *et al.* (2018)].

Synonym: *Aspergillus foetidus* var. *pallidus* (Nakaz., Simo & A. Watan.) Raper & Fennell, The Genus *Aspergillus*: 325. 1965. [MycoBank MB 353274]. Synonymized by Hong *et al.* (2014). Not validly published – basionym *A. aureus* var. *pallidus* Nakaz., Simo & A. Watan. is not a validly published name [Art. 41.5; Turland *et al.* (2018)].

Synonym: *Aspergillus niger* var. *awamori* (Nakaz.) Al-Musallam, Revision of the black *Aspergillus* species: 60. 1980. Doctoral diss., Rijksuniversiteit Utrecht, Netherlands. [MycoBank MB 118405]. Hong *et al.* (2014) showed that the ex-type strain NRRL 4948 (= CBS 557.65 = KACC 46996 = ATCC 16877) is closely related to the ex-type of *A. welwitschiae* (ANL) and is synonymized here with *A. niger*.

Synonym: *Aspergillus acidus* Kozak., Mycol. Pap. 161: 110. 1989. [MycoBank MB 127765]. Synonymized by Hong *et al.* (2013). Culture ex-type: KACC 45131 = CBS 564.65 = ATCC 16874 = NBRC 4121 = IMI 104688 = NRRL 4796.

Synonym: *Aspergillus coreanus* Yu T.S. *et al.*, J. Microbiol. Biotechnol. 14:182. 2004. [No Mycobank record]. Illegitimate name [Art. 54.1; Turland *et al.* (2018)] and *nomen nudum.* Synonymized by Hong *et al.* (2013). Authentic strain: KACC 41731 = CBS 119384.

Synonym: *Aspergillus piperis* Samson & Frisvad, Stud. Mycol. 50: 57. 2004. [MycoBank MB 500009]. Synonymized in this study.

Synonym: *Aspergillus luchuensis* mut. *kawachii* (Kitahara & Yoshida) S.B. Hong, O. Yamada & R.A. Samson, Appl. Microbiol. Biotechnol. 98: 560. 2014. [No Mycobank record]. Not validly published: basionym was not validly published [Art. 41.5; Turland *et al.* (2018)] and protologue does not include citation of the identifier issued for the name by a recognized electronic repository, *e.g.* MycoBank [Art. F.5.1; Turland *et al.* (2018)].

4. *Aspergillus niger* Tiegh., Ann. Sci. Nat., Bot. ser. 5, 8: 240. 1867. MycoBank MB 284309. *Nomen conservandum* taking precedence over *Ustilago phoenicis* Corda and *Ustilago ficuum* Reichard which were published earlier (Kozakiewicz *et al.* (1992). — Type: CBS 554.65. Ex-type: CBS 554.65 = NRRL 326 = ATCC 16888 = IFO 33023 = IHEM 3415 = IMI 050566ii = IMI 50566 = JCM 10254 = QM 9270 = QM 9946 = Thom 2766 = WB 326. DNA barcodes: ITS = EF661186; *BenA* = EF661089; *CaM* = EF661154; *RPB2* = EF661058.

Synonym: *Ustilago ficuum* Reichardt, Verh. Zool.-Bot. Ges. Wien 17: 335. 1867. [MycoBank MB 187740]. *Nomen rejiciendum*, rejected name in favour of *A. niger* Tiegh. – see Kozakiewicz *et al.* (1992). The ex-type strain IHEM 3710 (= WB 364 = NRRL 364 = IMI 91881 = CBS 555.65 = ATCC 16882) derived from the type IMI 91881 (Kozakiewicz *et al.* 1992) is located in the ANL (Fig. 1).

Synonym: *Eurotium nigrum* (Tiegh.) de Bary, Beiträge zur Morphologie und Physiologie der Pilze: 21. 1870. [No MycoBank record]. *Basionym*: *A. niger* Tiegh.

Synonym: *Sterigmatocystis nigra* (Tiegh.) Tiegh., Bull. Soc. Bot. France 24: 102. 1877. [MycoBank MB 231646]. *Basionym*: *A. niger* Tiegh.

Synonym: *Ustilago welwitschiae* Bres. in Sacc, Bol. Soc. Brot. 11: 68. 1893. [MycoBank MB 176748]. Synonymized in this study.

Sterigmatocystis ficuum (Reichardt) Henn., Hedwigia 34: 86. 1895. [MycoBank MB 100573]. See *Ustilago ficuum* Reichardt (basionym).

Synonym: *Sterigmatocystis welwitschiae* (Bres.) Henn. in H. Baum, Kunene-Zambesi Expedit., Berlin: 168. 1903. [MycoBank MB 233714]. See *Ustilago welwitschiae* Bres. in Sacc. (basionym).

Synonym: *Aspergillus batatas* [as *batatae*] Saito, Zentralbl. Bakteriol. Parasitenkn. Abt. II, 18: 34. 1907. [MycoBank MB 214829]. Synonymized by Hong *et al.* (2014). Culture ex-type: NRRL 4785 = CBS 115.34 = NBRC 4034 = KACC 46995.

Synonym: *Aspergillus welwitschiae* (Bres.) Henn. in Wehmer, Zentrbl. Bakteriol. ParasitK. Abt. II, 18: 294. 1907. [MycoBank MB 490584]. See *Ustilago welwitschiae* Bres. in Sacc. (basionym).

Synonym: *Aspergillopsis nigra* (Tiegh.) Speg., Anales Mus. Nac. Hist. Nat. Buenos Aires, ser. 3, 13: 435. 1911. [MycoBank MB 210007]. *Basionym*: *A. niger* Tiegh.

Synonym: *Rhopalocystis nigra* (Tiegh.) Grove, J. Econ. Biol. 6: 41. 1911. [MycoBank MB 432029]. *Basionym*: *A. niger* Tiegh.

Synonym: *Aspergillus niger* var. *altipes* E. Schiemann, Z. Indukt. Abstamm. Vererbungsl. 8: 1–35. 1912. [Mycobank MB 493817]. This variety belongs to the ANL based on the ITS sequence (MH854603) derived from the ex-type strain CBS 102.12 (= ATCC 10549 = IBT 19348 = IBT 26343 = IFO 4067 = MUCL 13608 = NRRL 4863 = WB 4863).

Synonym: *Sterigmatocystis batatas* [as *batatae*] (Saito) Sacc. Syll. Fung. 22: 1261. 1913. [MycoBank MB 209678]. See *A. batatas* Saito (basionym).

Synonym: *Aspergillus aureus* Nakazawa, Rep. Govt. Res. Inst. Formosa 4: 215–222. 1915. [No MycoBank record]. Synonymized by Hong *et al.* (2014). Culture ex-type: CBS 121.28 = NRRL 4784 = NBRC 4031 = RIB 2014 = KACC 47003 = IFO 4031 = IMI 104687 = WB 4784. Illegitimate name [Art. 54.1; Turland *et al.* (2018)]. Not *A. aureus* Berk. 1836 [MycoBank MB 214770].

Synonym: *Aspergillus ficuum* (Reichardt) Thom & Currie, J. Agric. Res. 7: 12. 1916. [MycoBank MB 101909]. See *Ustilago ficuum* Reichardt (basionym).

Synonym: *Aspergillus citricus* Mosseray, Ann. Univ. Sci. Budap. Rolando Eotvos Nominatae Biol. 43: 262. 1934. [MycoBank MB 251457]. Synonymized by Frisvad *et al.* (2011) and Houbraken *et al.* (2014). The genotype of the ex-type strain IHEM 5622 (= CBS 126.48 = WB 337 = NRRL 337 = NCTC 1692 = MUCL 28130 = IMI 15954 = IFO 6428 = DSM 734 = CCRC 30206 = ATCC 10254) is identical to the ex-type strains of *A. niger* (Fig. 1).

Synonym: *Aspergillus bainieri* Mosseray, Ann. Soc. Sci. Brux. 54: 79. 1934. [No MycoBank record]. The description is based on the same strain like *A. longobasidia* Bainier ex Mosseray (CBS 121.48).

Synonym: *Aspergillus longobasidia* Bainier ex Mosseray, La Cellule 43: 227. 1934. [MycoBank MB 253086]. The ex-

type strain CBS 121.48 (= NRRL 4857) belongs to the ANL (Hong *et al.* 2013).

Synonym: *Aspergillus pseudocitricus* Mosseray, La Cellule 43: 228. 1934. [Mycobank MB 254148]. The ex-type strain CBS 127.48 (= NRRL 4869) can be identified as *A. niger* based on *benA* (Hong *et al.* 2013).

Synonym: *Aspergillus niger* mut. *fusca* Blochwitz, Ann. Mycol. 32: 87. [No MycoBank record]. The ex-type strain CBS 113.33 (= NRRL 4864 = ATCC 10548 = WB 4864) can be identified as *A. niger* based on *benA* (Hong *et al.* 2013).

Synonym: *Aspergillus hennebergii* Blochwitz, Ann. Mycol. 33: 238. 1935. [MycoBank MB 266969]. Not validly published [Art. 39.1; Turland *et al.* (2018)]. The ex-type strain CBS 118.35 (= NRRL 4883 = CECT 2801 = QM 9704 = WB 4883 = VKM F-4392) can be identified as *A. niger* based on *benA* (Hong *et al.* 2013).

Synonym: *Aspergillus aureus* var. *brevior* [as *brevius*] Nakaz., Simo & A. Watan. Bull. Agric. Chem. Soc. Japan 12: 962. 1936. [MycoBank MB 493810]. Not validly published [Art. 39.1; Turland *et al.* (2018)]. The representative strain CBS 113.52 (= WB 4841) can be identified as *A. niger* based on *benA* (Hong *et al.* 2013).

Synonym: *Aspergillus awamori* var. *fuscus* Nakaz., Simo & A. Watan., Bull. Agric. Chem. Soc. Japan 12: 959. 1936. [MycoBank MB 250921]. Not validly published [Art. 39.1; Turland *et al.* (2018)]. Synonymized by Hong *et al.* (2013, 2014). Representative strain: CBS 117.52 = NRRL 4844 = WB 4844.

Synonym: *Aspergillus awamori* var. *minimus* Nakaz., Simo & A. Watan., Bull. Agric. Chem. Soc. Japan 12: 955. 1936. [MycoBank MB 250922]. Not validly published [Art. 39.1; Turland *et al.* (2018)]. Synonymized by Hong *et al.* (2013). Representative strain: CBS 118.52 [the whole-genome sequence was generated by Seekles *et al.* (2022)].

Synonym: *Aspergillus miyakoensis* Nakaz., Simo & A. Watan., Bull. Agric. Chem. Soc. Japan 12: 963. 1936. [MycoBank MB 253392]. Not validly published [Art. 39.1; Turland *et al.* (2018)]. Synonymized by Hong *et al.* (2014). Culture ex-type: NRRL 4859 = CBS 117.51 = KACC 46998.

Synonym: *Aspergillus pyri* W.H. English, Res. Stud. State Coll. Wash. 8: 127. 1940. [MycoBank MB 453796]. *Nomen nudum.* Subsequent work by English led to recognition of the name as a synonym of *A. niger* and withdrawal of the name (Thom & Raper 1945, Raper & Fennell 1945).

Synonym: *Aspergillus foetidus* Thom & Raper, A manual of the Aspergilli: 219. 1945. [Mycobank MB 284300]. Synonymized by Varga *et al.* (2011). Culture ex-type: CBS 121.28 = NRRL 4784 = NBRC 4031 = RIB 2014 = KACC 47003 = IFO 4031 = IMI 104687 = WB 4784.

Synonym: *Aspergillus usamii* Sakag., Iizuka & M. Yamaz., J. Appl. Mycol. Japan 4: 1. 1950. [No MycoBank record]. Not validly published [Art. 39.1; Turland *et al.* (2018)]. Validly published later – see *A. usamii* Sakag., Iizuka & M. Yamaz. ex Iizuka & K. Sugiy.

Synonym: *Aspergillus usamii* mut. *shirousamii* Iizuka & Yamaguchi. J. Gen. Appl. Microbiol. 1: 194–200. 1954. [No MycoBank record]. Not validly described. Synonymized by Hong *et al.* (2014). Culture ex-type: NRRL 4889 = KACC 47001.

Synonym: *Aspergillus usamii* Sakag., Iizuka & M. Yamaz. ex Iizuka & K. Sugiy., J. Jap. Bot.: 232. 1965. [MycoBank MB 326664]. Synonymized by Yamada *et al.* (2011) and Hong *et al.* (2014). Culture ex-type: CBS 139.52 = NRRL 4760 = ATCC 11364 = ATCC 14331 = NBRC 4388 = RIB 2602 = IAM 2185 = KACC 47000 = IFO 4388 = QM 8164 = WB 4760.

Synonym: *Aspergillus niger* f. *hennebergii* Blochwitz ex Al-Musallam, Revision of the black *Aspergillus* species: 68. 1980. Doctoral diss., Rijksuniversiteit Utrecht, Netherlands. [MycoBank MB 118404]. See *A. hennebergii* Blochwitz (basionym).

Synonym: *Aspergillus niger* var. *usamii* (Sakag., Iizuka & M. Yamaz. ex Iizuka & K. Sugiy.) Al-Musallam, Revision of the black *Aspergillus* species: 64. 1980. Doctoral diss., Rijksuniversiteit Utrecht, Netherlands. [MycoBank MB 118400]. See *A. usamii* Sakag., Iizuka & M. Yamaz. ex Iizuka & K. Sugiy. (basionym).

Synonym: *Aspergillus niger* var. *ficuum* (Reichardt) Kozak., Mycol. Pap. 161: 112. 1989. [MycoBank MB 127745]. See *Ustilago ficuum* Reichardt (basionym).

Synonym: *Aspergillus lacticoffeatus* Frisvad & Samson, Stud. Mycol. 50: 52. 2004. [Mycobank MB 500008]. Synonymized by Varga *et al.* (2011) and confirmed in this study.

Synonym: *Aspergillus vinaceus* Ferranti *et al.*, J. Fungi 6: 371 - p14. 2020. [MycoBank MB 833399]. Synonymized in this study.

5. *Aspergillus tubingensis* Mosseray, La Cellule 43: 245. 1934. [MycoBank MB 255209]. — Type: CBS H-24288. Ex-type: NRRL 4875 = CBS 133056 = QM 8904 = WB 4875. DNA barcodes: ITS = EF661193; *benA* = EF661086; *CaM* = EF661151; *RPB2* = EF661055.

Synonym: *Sterigmatocystis pulverulenta* McAlpine, Agric. Gaz. N.S.W., Sydney 7: 302. 1896 (1897). [MycoBank MB 194998]. Synonymized by Houbraken *et al.* (2014). The ex-type strain IHEM 5615 (= CBS 558.65 = CBS 115.48 = MUCL 13592 = MUCL 15630 = NRRL 4851 = WB 4851 = IMI 211396 = ATCC 16879) is close to the ex-type of *A. tubingensis* (Fig. 1).

Synonym: *Aspergillus pulverulentus* (McAlpine) Wehmer, Zentralbl. Bakteriol. Parasitenkd., Abt. II, 18: 394. 1907. [MycoBank MB 121243]. See *Sterigmatocystis pulverulenta* McAlpine (basionym).

Synonym: *Aspergillus cinnamomeus* E. Schiemann, Z. Indukt. Abstamm. Vererbungsl. 8: 1–35. 1912. [MycoBank MB 122195]. The *benA* sequence (FJ629307) derived from the ex-type strain CBS 103.12 = ATCC 1027 = IBT 16906 = IBT 28139 = IBT 29892 = IFO 4043 = IMI 016148 = LSBH Ac42 = MZKI A-76 = NCTC 3774 = NRRL 348 = QM 326 = Thom 3534B = WB 348) is identical with the ex-type of *A. tubingensis*.

? Synonym: *Aspergillus fuscus* E. Schiem., Z. Indukt. Abstamm. Vererbungsl. 8: 1–35. 1912. [MycoBank MB 450741]. Illegitimate name [Art. 54.1; Turland *et al.* (2018)]. Not *A. fuscus* Bonord. 1861 [MycoBank MB 206602]. Illegitimate name *A. fuscus* was replaced by *nomen novum A. schiemanniae* Thom 1916 (see *A. schiemanniae*).

? Synonym: *Aspergillus proteus* E. Schiem., Z. Indukt. Abstamm. Vererbungsl. 8: 1–35. 1912. [No MycoBank record]. Illegitimate name – not accepted by the author itself in the original publication [Art. 36.1; Turland *et al.* (2018)].

Synonym: *Aspergillus pulverulentus* (McAlpine) Thom, J. Agric. Res. 7: 11. 1916. [No MycoBank record]. Illegitimate name [Art. 54.1; Turland *et al*. (2018)] - a later homonym of *A. pulverulentus* (McAlpine) Wehmer 1907.

? Synonym: *Aspergillus schiemanniae* Thom [as *schiemanni*], J. Agric. Res. 7: 11. 1916. [MycoBank MB 102113]. The ITS sequence (MH854950) derived from the ex-type strain CBS 122.28 (= ATCC 1040 = NRRL 361 = IFO 4091 = IMI 091895 = IMI 16269 = LSHB AC.37 = NCTC 3781 = QM 327 = Thom 3534C = WB 361) belongs to the ATL.

Synonym: *Aspergillus elatior* Mosseray, Ann. Univ. Sci. Budap. Rolando Eotvos Nominatae Biol. 43: 253. 1934. [MycoBank MB 251950]. The ex-type strain IHEM 5615 (= CBS 558.65 = CBS 115.48 = MUCL 13592 = MUCL 15630 = NRRL 4851 = WB 4851 = IMI 211396 = ATCC 16879) is similar to the ex-type of *A. tubingensis* (Fig. 1).

Synonym: *Aspergillus pseudoniger* Mosseray, La Cellule 43: 256. 1934. [MycoBank MB 472168]. The ex-type strain IHEM 4379 (= CBS 128.48 = IMI 313491 = WB 4870 = MUCL 31312) is similar to *A. tubingensis* (Fig. 1).

Synonym: *Aspergillus niger* mut. *cinnamomeus* (E. Schiemann) Thom & Raper, A manual of the Aspergilli: 223. 1945. [MycoBank MB 440825]. See *A. cinnamomeus* E. Schiemann (basionym).

? Synonym: *Aspergillus niger* mut. *schiemanniae* (Thom) Thom & Raper [as *schiemanni*], A manual of the Aspergilli: 224. 1945. [MycoBank MB 123940]. See *A. schiemanniae* Thom (basionym).

Synonym: *Aspergillus saitoi* Sakag., Iizuka & M. Yamaz., J. Appl. Mycol. Japan 3: 68. 1950. [No MycoBank record]. Not validly published [Art. 39.1; Turland *et al.* (2018)]. Validly published later – see *A. saitoi* Sakag., Iizuka & M. Yamaz. ex Iizuka & K. Sugiy.

Synonym: *Aspergillus saitoi* var. *kagoshimaensis* Sakag., Iizuka & M. Yamaz., J. Appl. Mycol. Japan 4: 3. 1950. [No MycoBank record]. Not validly published [Art. 39.1; Turland *et al.* (2018)]. Validly published later – see *A. saitoi* var. *kagoshimaensis* Sakag., Iizuka & M. Yamaz. ex Iizuka & K. Sugiy.

Synonym: *Aspergillus awamori* var. *hominis* Bat. & Maia, An. Soc. Biol. Pernambuco 15: 186. 1957. [MycoBank MB 351895]. The *benA* sequence (FJ629318) derived from the ex-type strain CBS 107.55 (= NRRL 4740 = ATCC 12074 = WB 4740) is almost identical (419/420 bp) to the ex-type of *A. tubingensis*.

Synonym: *Aspergillus saitoi* Sakag., Iizuka & M. Yamaz. ex Iizuka & K. Sugiy., J. Jap. Bot. 40: 230. 1965. [Mycobank MB 326655]. Synonymized by Hong *et al.* (2014). Culture ex-type: CBS 136.52 = CBS 552.65 = NRRL 4757 = IAM 2209 = ATCC 11362 = IMI 211395 = KACC 46993 = WB 4757.

Synonym: *Aspergillus saitoi* var. *kagoshimaensis* Sakag., Iizuka & M. Yamaz. ex Iizuka & K. Sugiy., J. Jap. Bot. 40: 231. 1965. [MycoBank MB 349043]. Synonymized by Hong *et al.* (2014). Culture ex-type: CBS 137.52 = NRRL 4758 = IMI 214827 = ATCC 11363 = KACC 46994 = QM 8162 = IAM 2190 = WB 4758.

Synonym: *Aspergillus niger* f. *pulverulentus* (McAlpine) Al-Musallam, Revision of the black *Aspergillus* species: 58. 1980. Doctoral diss., Rijksuniversiteit Utrecht, Netherlands. [MycoBank MB 118403]. See *Sterigmatocystis pulverulenta* McAlpine (basionym).

Synonym: *Aspergillus niger* var. *pulverulentus* (McAlpine) Kozak., Mycol. Pap. 161: 113. 1989. [MycoBank MB 127747]. See *Sterigmatocystis pulverulenta* McAlpine (basionym).

Synonym: *Aspergillus niger* var. *tubingensis* (Mosseray) Kozak., Mycol. Pap. 161: 112. 1989. [MycoBank MB 127746]. *Basionym*: *A. tubingensis* Mosseray.

Synonym: *Aspergillus costaricensis* [as *costaricaensis*] Samson & Frisvad, Stud. Mycol. 50: 52. 2004. [MycoBank MB 369151]. Synonymized in this study.

Synonym: *Aspergillus neoniger* Varga, Frisvad & Samson, Stud. Mycol. 69: 16. 2011. [MycoBank MB 560390]. Synonymized in this study.

Synonym: *Aspergillus chiangmaiensis* S. Khuna, N. Suwannarach & S. Lumyong, Front. Microbiol. 12: 705896 - p6. 2021. [Mycobank MB 830887]. Synonymized in this study.

Synonym: *Aspergillus pseudopiperis* S. Khuna, N. Suwannarach & S. Lumyong, Front. Microbiol. 12: 705896 - p6. 2021. [MycoBank MB 830888]. Synonymized in this study.

6. *Aspergillus vadensis* Samson, de Vries, Frisvad & Visser, Antonie van Leeuwenhoek 87: 201. 2005. [MycoBank MB 340234]. — Type: CBS 113365. Ex-type: CBS 113365 = CECT 20584 = IMI 313493 = IBT 24658. DNA barcodes: ITS = AY585549; *benA* = AY585531; *CaM* = FN594560; *RPB2* = HE984371.

Synonym: *Aspergillus vadensis* de Vries *et al.*, Appl. Environ. Microbiol. 70: 3954. 2004. [MycoBank MB 560390]. Not validly described (*nomen nudum*).

Unresolved or doubtful names most probably belonging to the series *Nigri*

Aspergillus phaeocephalus Durieu & Mont., Exploration scientifique de l'Algérie 1: 342. 1848. [MycoBank MB 179669]. No specimens are available.

Synonym: *Sterigmatocystis phaeocephala* (Durieu & Mont.) Sacc., Syll. Fung. 4: 76. 1886. [MycoBank MB 233071].

Aspergillus nigrescens C.P. Robin, Histoire naturelle des végétaux parasites: 518. 1853. [MycoBank MB 182212]. Considered either *A. fumigatus* or *A. niger* by various authors (Wilhelm 1877, Wehmer 1901, Raper & Fennell 1965), no material is available (species described from pathological specimens only).

Aspergillus nanus Mont., Syll. Gen. Sp. Crypt. (Paris): 300. 1856. [MycoBank MB 193617]. Typus in Muséum National d'Histoire Naturelle , France, Paris (PC); no DNA sequence available. The strains of *A. niger* var. *nanus* examined by Al-Musallam (1980) belong either to the ANL or ATL, e.g., CBS 105.47 (MH856174; ATL), CBS 106.47 (FJ629281; ATL), CBS 110.30 (MH855092; ANL), CBS 115.50 (MH856565; ANL), CBS 131.52 (the whole-genome sequence was generated by Seekles *et al.* (2022); ANL).

Synonym: *Aspergillus niger* var. *nanus* (Mont.) Al-Musallam, Revision of the black *Aspergillus* species: 62. 1980. Doctoral diss., Rijksuniversiteit Utrecht, Netherlands. [MycoBank MB 118406].

Sterigmatocystis antacustica C.E. Cramer, Vierteljahrsschr. Naturforsch. Ges. Zürich 4: 325. 1859. [MycoBank MB 209963].

Synonym: *Rhopalocystis antacustica* (C.E. Cramer) Grove, J. Econ. Biol.: 41. 1911. [MycoBank MB 503610].

Aspergillus nigricans Wreden, C. R. Hebd. Seances Acad. Sci. 65: 368. 1867. [No MycoBank record]. No specimen is available.

Aspergillus fuliginosus Peck, Bull. Buffalo Soc. Nat. Sci. 1: 69. 1873. [MycoBank MB 208679]. Typus in New York State Museum, USA (NYSf 1265); no DNA sequence available.

Synonym: *Sterigmatocystis fuliginosa* Bainer, Bull. Soc. Bot. France 28: 78. 1881. [No MycoBank record].

Aspergillus nigricans Cooke, Grevillea 6: 127. 1878. [MycoBank

MB 182128]. Illegitimate name. Not *A. nigricans* Wreden 1867.

Alliospora sapucaya [as *sapucayae*] Pim, J. Bot. London 21: 234. 1883. [Mycobank MB 215122].

Aspergillus cookei Sacc., Syll. Fung. 4: 71. 1886. [MycoBank MB 206435]. A replaced synonym for illegitimate name *A. mucoroides* Cooke.

Basionym: *Aspergillus mucoroideus* Cooke, Grevillea 12: 9. 1883. [MycoBank MB 187861]. Illegitimate name [Art. 54.1; Turland et al. (2018)]. Not *A. mucoroides* Corda 1838 [MycoBank MB 187771].

Aspergillus subfuscus Johan-Olsen, Nordiskt Med. Ark. 18: 14. 1886. [MycoBank MB 184212].

Basionym: *Sterigmatocystis subfusca* (Johan-Olsen) Sacc., Syll. Fung. 10: 526. 1892. [MycoBank MB 226258].

Aspergillus nigriceps Berk. & Curt., Grevillea 17: 21. 1888. [No MycoBank record]. A slide from material in the Harvard Collection (Curtis collection, Wright no. 927) showed species inseparable from *A. niger* (Raper & Fennell 1965).

Aspergillus ustilago Beck in H. Wawra, Itinera Principum S. Coburgi 2: 148. 1888. [MycoBank MB 161832].

Synonym: *Sterigmatocystis ustilago* (Beck) Sacc., Syll. Fung. 10: 526. 1892. [MycoBank MB 198044].

Sterigmatocystis castanea F. Patt., Bull. Torrey Bot. Club 27: 284. 1900. [MycoBank MB 195664]. Typus in BPI Herbarium (BPI 410863).

Aspergillus gallomyces Calmette, Germ. Pat. Abstr. 129: 164. 1902. [No MycoBank record].

Aspergillus strychni Lindau, Hedwigia 43: 306. 1904. [MycoBank MB 183848].

Synonym: *Sterigmatocystis strychni* (Lindau) Sacc. & D. Sacc., Syll. Fung. 18: 516. 1906. [MycoBank MB 225824].

Sterigmatocystis pseudonigra Costantin & Lucet, Bull. Soc. Mycol. France 19: 33. 1903. [MycoBank MB 195028]. No specimen available.

Synonym: *Aspergillus pseudoniger* (Costantin & Lucet) Saincl., Centralbl. Gesammte Forstwesen: 103. 1949. [MycoBank MB 292856]. Illegitimate name. Not *A. pseudoniger* Mosseray 1934. [MycoBank MB 472168].

Sterigmatocystis luteonigra M.L. Lutz, Bull. Soc. Bot. France 53: 50. 1907. [MycoBank MB 228634].

Synonym: *Aspergillus luteoniger* (M.L. Lutz) Thom & Church, The Aspergilli: 166. 1926. [MycoBank MB 269972].

Aspergillopsis intermedia Speg., Anales Mus. Nac. Hist. Nat. Buenos Aires, ser. 3, 13: 435. 1911. [MycoBank MB 209760]. Typus deposited in the Herbarium of Museo de La Plata, Argentiva (LPS 12691); no DNA sequence is available. The strains considered *A. niger* var. *intermedius* by Al-Musallam (1980) belong either to the ANL or ATL, *e.g.*, CBS 117.32 (MH855233; ATL), CBS 115.29 (MH855018; ATL), CBS 117.52 (MH856951; ANL), CBS 130.52 (FJ629359, FJ629310; ATL), CBS 107.55 (FJ629367, FJ629318; ATL).

Synonym: *Aspergillus niger* var. *intermedius* (Speg.) Al-Musallam, Revision of the black *Aspergillus* species: 66. 1980. Doctoral diss., Rijksuniversiteit Utrecht, Netherlands. [MycoBank MB 118402].

Aspergillus phoenicis (Corda) Thom, J. Agric. Res. 7: 14. 1916. [MycoBank MB 101952].

Basionym: *Ustilago phoenicis* Corda, Icones fungorum hucusque cognitorum 4: 9. 1840. [MycoBank MB 169060]. *Nomen rejiciendum*, rejected name in favour of *A. niger* Tiegh. (Kozakoewict *et. al.* 1992). Type located in Corda´s herbarium (PRM, Czech Republic) but no sequence derived from the original material is available. Representative strains NRRL 363, NRRL 365 and NRRL 1956 do either belong to ANL or ATL (Houbraken *et al.* 2014).

Synonym: *Sterigmatocystis phoenicis* (Corda) Pat. & Delacr., Bull. Soc. Mycol. France 7: 119. 1891. [MycoBank MB 232882].

Synonym: *Aspergillus niger* var. *phoenicis* (Corda) Al-Musallam, Revision of the black *Aspergillus* species: 56. 1980. Doctoral diss., Rijksuniversiteit Utrecht, Netherlands. [MycoBank MB 118401].

Aspergillopsis tropicalis Speg., Bol. Acad. Nac. Cienc. Córdoba 23: 588. 1918. [MycoBank MB 209817].

Aspergillus fumaricus Wehmer ex Thom & Church, The Aspergilli: 181. 1926. [MycoBank MB 122538].

Sterigmatocystis gigantea Mattlet, Ann. Soc. Belge Méd. Trop. 6: 31. 1926. [MycoBank MB 252349].

Synonym: *Aspergillus giganteus* (Mattlet) C.W. Dodge, Medical Mycology: 629. 1935. [No MycoBank record]. Illegitimate name. Not *A. giganteus* Wehmer 1901 [MycoBank MB 206765].

Synonym: *Aspergillus mattletii* Hendr., Publ. Inst. Nat. Étude Agron. Congo Belge 35: 7. 1948. [MycoBank MB 284307].

Aspergillus atropurpureus Blochwitz, Ann. Mycol. 32: 86. 1934. [No MycoBank record]. Illegitimate name. Not *A. atropurpureus* Zimm. 1902 [MycoBank MB 214593].

Aspergillus biourgei Mosseray, La Cellule 43: 241. 1934. [MycoBank MB 251009].

Aspergillus buntingii Mosseray, La Cellule 43: 236. 1934. [MycoBank MB 251145].

Aspergillus churchii Mosseray, La Cellule 43: 242. 1934. [MycoBank MB 251413].

Aspergillus densus Mosseray, La Cellule 43: 232. 1934. [MycoBank MB 251792].

Aspergillus granulatus Mosseray, La Cellule 43: 249. 1934. [MycoBank MB 252446]. Culture ex-type: CBS 120.48 = NRRL 4855 = WB 4855 (no DNA sequence available).

Aspergillus guttifer Mosseray, La Cellule 43: 235. 1934. [MycoBank MB 252493].

Aspergillus microcephalus Mosseray, La Cellule 43: 225. 1934. [MycoBank MB 253336]. The strain CBS 122.48 is considered the ex-type strain (Al-Musallam 1980) but no DNA sequence is available.

Aspergillus niger var. *fermentarius* Nakaz., Simo & A. Watan., J. Agric. Chem. Soc. Japan 10: 171. 1934. [No MycoBank record].

Aspergillus olivaceofuscus Mosseray, La Cellule 43: 258. 1934. [MycoBank MB 253675].

Aspergillus praecox Mosseray, Ann. Soc. Sci. Brux. 54: 79. 1934. [No MycoBank record].

Aspergillus pseudoelatior Mosseray, La Cellule 43: 255. 1934. [MycoBank MB 254152].

Aspergillus rutilans Mosseray La Cellule 43: 234. 1934. [MycoBank MB 254522].

Aspergillus sclerotifer Mosseray, Ann. Soc. Sci. Brux. 54: 79. 1934. [No MycoBank record].

Aspergillus variegatus Mosseray La Cellule 43: 238. 1934. [MycoBank MB 255332].

Aspergillus macfiei C.W. Dodge, Medical Mycology: 629. 1935. [MycoBank MB 253139]. Not validly described [Art. 39.1, 40.1; Turland *et al.* (2018)].

Aspergillus aureus var. *minor* Nakaz., Simo & A. Watan., Bull. Agric. Chem. Soc. Japan 12: 958. 1936. [MycoBank MB 534300]. Not validly published [Art. 39.1; Turland *et al.* (2018)].

Aspergillus aureus var. *murinus* Nakaz., Simo & A. Watan., Bull. Agric. Chem. Soc. Japan 12: 959. 1936. [MycoBank MB 534301]. Not validly published [Art. 39.1; Turland *et al.* (2018)].
Aspergillus awamori var. *ferrugineus* Nakaz., Simo & A. Watan., Bull. Agric. Chem. Soc. Japan 12: 957. 1936. [Mycobank MB 250919]. Not validly published [Art. 39.1; Turland *et al.* (2018)].
Aspergillus awamori var. *fumeus* Nakaz., Simo & A. Watan., Bull. Agric. Chem. Soc. Japan 12: 961. 1936. [MycoBank MB 250920]. Not validly published [Art. 39.1; Turland *et al.* (2018)]. Representative strain: CBS 116.52 = NRRL 4843 = WB 4843 = IBT 16908 (no DNA sequence availabele).
Aspergillus luchuensis var. *rubeolus* Y.K. Shih, Lingnan Sci. J. 15: 374. 1936. [Mycobank MB 253092]. The ITS sequence (DQ196202) derived from the representative strain CBS 114.37 (= IAM 2185 = IBT 4944 = IBT 29898 = IMI 313493 = NRRL 4856 = WB 4856) belongs to the ATL.
Cladosarum olivaceum E. Yuill & J.L. Yuill, Trans. Brit. Mycol. Soc. 22: 199. 1938. [MycoBank MB 272878]. Culture ex-type: CBS 147.38 (no DNA sequence available).
Aspergillus niger var. *arecae* Lal & Ram Chandra, J. Scient. Res. Banaras Hindu Univ. 3: 123. 1953. [MycoBank MB 349040]. Not validly published [Art. 39.1; Turland *et al.* (2018)].
Aspergillus niger var. *taxi* D.P. Zhou, K. Zhao & Ping, J. Appl. Microbiol. 107: 1206. 2009. [MycoBank MB 542212]. Not validly described [Art. 39.1, 40.1; Turland *et al.* (2018)]. The ITS sequence (EU853157) derived from the original strain belongs to the ATL.
Aspergillus pseudotubingensis S. Khuna, N. Suwannarach & S. Lumyong, Front. Microbiol. 12: 705896 - p9. 2021. [MycoBank MB 830889]. See comments in sections Results and Discussion.

DISCUSSION

Taxonomic studies on *A. niger*, *A. tubingensis* and their related species have been the subject of many taxonomic controversies, rearrangements, name resurrections and repeated synonymizations. Currently, the species number in series *Nigri* is at one of its historical peaks and involves 14 accepted species (Houbraken *et al.* 2020, Silva *et al.* 2020, Khuna *et al.* 2021). Distinguishing among these species using morphology is impossible, and DNA sequencing is the gold standard for reliable classification and species identification (Howard *et al.* 2011, Varga *et al.* 2011). Therefore, these species can be considered cryptic in the truest sense. However, even when using molecular methods, some isolates cannot be identified satisfactorily at the species level (Howard *et al.* 2011, Negri *et al.* 2014, D'hooge *et al.* 2019). Contradictory species identifications in significant part of isolates using BLAST similarity searches with different genes (Fig. 3) can serve as evidence of taxonomic issues and may indicate the need for a taxonomic reclassification. To verify this assumption, we gathered a large dataset of a series *Nigri* sequences from three common phylogenetic markers and *de novo* sequenced 18 genomes and employed various species delimitation methods. All of these methods unequivocally suggested species number reduction.

Phylogenetic support of species reduction

We demonstrated that MSC delimitation methods using three genes broadly agreed on the distinction of only three species in the series *Nigri* (*A. brasiliensis*, *A. niger* and *A. tubingensis*). Only four analyses from among the 15 depicted in Fig. 5 proposed the delimitation of more species. These conclusive results, especially in the *A. niger* lineage (ANL) and *A. brasiliensis* lineage (ABL), are supported by the collection of a large number of strains well representing the intraspecific genetic variability.

In the *A. tubingensis* lineage (ATL), the multilocus method STACEY gave similar support to the delimitation of one or four species. This dilemma has not been satisfactorily resolved even at the genome level because ten STACEY analyses based on 20 genes each proposed several solutions ranging from one to four species in the ATL (Fig. 8), with four species being most preferred. The datasets containing 20 genes (and not higher) were selected due to the relatively high computational requirements of the method and because 20 genes are usually enough to resolve the phylogeny with a similar level of accuracy to the genome-wide data (Rokas *et al.* 2003, Yang & Rannala 2010, 2014). The uncertainty regarding the number of delimited species can probably be attributed to the underrepresentation of isolates related to *A. vadensis* and *A. eucalypticola* and, to a lesser extent, other species in the ATL, with the exception of *A. tubingensis* itself. Generally, it is thought that when a dataset contains a few isolates with large genetic distances, the delimitation methods may be prone to over delimitation, but with a large set of isolates representing genetic variability of every species, the probability of methods finding real species boundaries increases (Pante *et al.* 2015, Chambers & Hillis 2020). Another reason for the conflicting results can be the widely present incongruences between single-gene genealogies as typically present in recently speciating species or in populations that have not completed their speciation process. In recently diverged species, it is typically caused by retaining ancestral polymorphisms (incomplete lineage sorting), or it can be caused by past hybridization events (Hubka *et al.* 2018, Steenkamp *et al.* 2018, Matute & Sepúlveda 2019).

At this point, it is appropriate to mention that the single-gene phylogenies based on *benA*, *CaM* and *RPB2* loci were highly incongruent (Fig. 2, Supplementary Fig. S2) and that the topology of the resulting multigene phylogeny shows several conflicts or poorly resolved clades compared to the whole-genome phylogeny, as we demonstrated in Fig. 4. Suboptimal phylogenetic signals contained in these three loci can further contribute to the discrepancy between the results of the MSC methods (support of a single species in the ATL) and those of the STACEY analyses based on 20 loci randomly selected from genomes (predominant support of four species in the ATL) (Fig. 8). When species limits are evaluated using the GCPSR approach (Taylor *et al.* 2000, Dettman *et al.* 2003a) using the *benA*, *CaM* and *RPB2* loci only, the obvious conclusion is the recognition of only three species in the series *Nigri*: *A. brasiliensis*, *A. niger* and *A. tubingensis*. The recently proposed *A. vinaceus* (Silva *et al.* 2020) from the ANL was also described based on the GCPSR approach, but the phylogeny lacked some isolates with intermediate genotypes included here. The presence of these strains in the phylogenies contradicts the delimitation of *A. vinaceus* as a separate phylogenetic species.

Another independent testing of species hypotheses was performed in the recently released software DELINEATE (Sukumaran *et al.* 2021). The software needs some a priori defined species that are correctly delimited in the dataset. This requirement was fulfilled by the inclusion of some species belonging to the other series of section *Nigri.* In addition, *A. brasiliensis* is well defined and can serve as a "reference species" when dealing with delimitation in *A. niger* and *A. tubingensis* lineages. The results of the various models were relatively stable, always supporting the broad concept of *A. niger* (comprising *A. niger*, *A. welwitschiae* and *A. vinaceus*) and *A. brasiliensis (*Fig. 7). In the ATL a broad species definition (comprising all species in the lineage) gained support in Models

7 and 10 when *A. niger* was defined as a broad species as well. In models where the ANL was divided into four and six species, the unassigned ATL populations were segregated into four tentative species. This scenario is, however, improbable because the ANL was never divided into several species in Models 2, 6 and 9. Model 6 shows the situation where populations of the ATL are predefined into four species identical to those delimited by Models 3 and 4, while populations of the ANL are unassigned. In this situation, *A. niger* was also delimited as a single broad species. In summary, DELINEATE analysis convincingly supported that the series *Nigri* contains only three species based on *benA*, *CaM* and *RPB2*.

Phenotype and sexual reproduction in series *Nigri*

Species in the series *Nigri* are all biseriate and present colonies with brown, dark brown to black sporulating areas and white to yellowish white mycelial areas. Generally, the species exhibit largely overlapping characteristics in terms of both macromorphology (colony diameter and colour) and micromorphology (size, shape and ornamentation of conidia, diameter and shape of vesicle, and length and width of stipes) (Table 2). Not only particular species but also the main lineages of *A. niger* and *A. tubingensis* are indistinguishable from each other using morphology. Additionally, species identification is sometimes complicated by the occurrence of atypical strains exhibiting unusual morphological characteristics. For example, *A. lacticoffeatus* was described based on its different colony colour and a specific extrolite pattern (Samson *et al.* 2004). However, it was later synonymized with *A. niger*, because it was phylogenetically inseparable (Varga *et al.* 2011). Within the ATL, *A. vadensis* stands out among the others for its slow growth and short stipes (Table 2), but the original description is based on only one isolate (Vries *et al.* 2005).

Series *Nigri* species are known for producing a wide range of extrolites, and their spectra were summarised by Samson *et al*. (2007), Nielsen *et al*. (2009) and Frisvad *et al*. (2018). It is often asserted that species in series *Nigri* could be identified by different secondary metabolite patterns. However, the extrolite profiles can vary among strains, which makes its use to distinguish between species complicated. Additionally, the usability of secondary metabolite production for taxonomy and evolutionary biology in general might be limited due to the potential for horizontal gene transfer of secondary metabolism gene clusters between species of the same genus or even between fungal genera (Richards 2011, Slot & Rokas 2011, Szöllősi *et al.* 2015). The high frequency of this phenomenon is also suggested from the genomes of series *Nigri* species (Vesth *et al.* 2018). Considering our proposed reclassification of series *Nigri*, the extrolite profiles of the six species we accepted need to be reassessed to determine if they support the delineation proposed here based on a phylogenetic species concept.

Sexual reproduction in heterothallic fungi is governed by mating-type (*MAT*) genes (Dyer & O'Gorman 2011). In section *Nigri*, the development of asci and ascospores occurs in the stroma of sclerotia (Horn *et al.* 2013). Therefore, sclerotia formation is considered a prerequisite for sexual reproduction. In the ATL, sclerotia were reported in most species except for *A. eucalypticola, A. pseudotubingensis* and *A. vadensis*. In the ANL, sclerotia were formed in some strains of *A. vinaceus* and *A. niger* (Frisvad *et al.* 2014, Silva *et al.* 2020). Sclerotia in the ATL were mostly pink to yellow, while those in the ANL were white to cream (Table 2). Despite the heterogeneity in sclerotia production among series *Nigri* species, most of them were proven to be heterothallic or protoheterothallic, which means that mating-type gene idiomorph(s) associated with heterothallism have been detected among the examined strains of these species (Houbraken *et al*. 2020). Currently, *A. tubingensis* is the only species in series *Nigri* with an experimentally proven sexual cycle (Horn *et al.* 2013). In this study, we detected both *MAT1-1-1* and *MAT1-2-1* idiomorphs among isolates of ANL and ATL (Fig. 4), in agreement with previous studies (Horn *et al.* 2013, Varga *et al.* 2014, Mageswari *et al.* 2016, Seekles *et al.* 2022). An interesting observation was made by Horn *et al*. (2013), who sequenced five genes in the parental isolates of *A. tubingensis* and their progeny resulting from sexual reproduction. The authors found that *A. neoniger* cannot be separated from *A. tubingensis* in the *benA* or *tsr1* phylogenies, while in the other phylogenies (*CaM*, *Mcm7* and *RPB2*), it is resolved outside the least inclusive clade containing all *A. tubingensis* strains and its ex-type. In our opinion, this fact demonstrates gene flow between *A. tubingensis* and *A. neoniger* and supports the synonymization made in this study. *Aspergillus costaricensis* was not included by Horn *et al.* (2013), but it is a close relative of *A. neoniger* and must be synonymized together to retain the monophyly of the redefined *A. tubingensis* (Fig. 5).

Updated taxonomy of series *Nigri* and species identification

We showed based on various independent species delimitation analyses that the number of accepted species in the *Nigri* series is too high and needs to be reduced. The methods broadly agreed that the ABL and ANL contain only one species each. The only uncertainty was about the species number in the ATL, where single-gene MSC methods and the GCPSR approach based on the commonly used phylogenetic markers *benA*, *CaM* and *RPB2* supported only one species, while STACEY analyses supported up to four species: *A. tubingensis*, *A. luchuensis*, *A. eucalypticola* and *A. vadensis*. After considering all results and practical consequences, we decided on a conservative solution by retaining four species in the ATL. This newly proposed taxonomic treatment of series *Nigri* with six accepted species overall is shown in Fig. 10.

The following findings played a major role in our decision-making process. *Aspergillus luchuensis* is industrially extremely important (Hong *et al.* 2013, 2014), and its imprudent synonymization without further confirmation could cause unnecessary taxonomic instability. The phylogenetic signal from the dataset containing only *benA*, *CaM* and *RPB2* loci may be suboptimal when compared to the predominant signal obtained from whole genome data (Fig. 4); thus, the results should be considered with caution before data from more genes/genomes are evaluated. We also showed that the intraspecific genetic diversity of the broadly defined *A. tubingensis* would be higher than that commonly found for *Aspergillus* species, while the variability within *A. tubingensis*, excluding *A. luchuensis*, *A. eucalypticola* and *A. vadensis* comfortably falls within this range (Fig. 9).

We believe that the user community will benefit from the simplified taxonomy of series *Nigri* with a lower number of species. This new classification will facilitate species identification that is currently complicated by inconsistent identification results when using sequence data of different genes (Fig. 3) and the impossibility of finding species-specific mass spectra for some narrow species when using the MALDI-TOF method (Gautier *et al*. 2016, D'hooge *et al.* 2019, Ban *et al*. 2021). DNA sequence identification of these newly defined species is possible by using *benA*, *CaM* and *RPB2* markers, although in a minority of cases, there can be conflicting identification in the ATL (Fig. 3). Because of this, we recommend that if identification to a species level is required in the ATL, it should be

Table 2. Overview of macro- and micromorphological features of species belonging to the series *Nigri*.

Species	CYA, 7 d (mm)		MEA, 7 d, 25 ˚C (mm)	Prevailing colony colour(s) on CYA	Vesicle diam (µm), shape	Stipe (µm)		Conidia: diam (µm), shape, surface	Sclerotia (mm), colour	References[1]
	25 ˚C	37 ˚C				Length	Width			
A. brasiliensis	71–76	71–76	52–70	cream-coloured to light brown	30–45, nearly globose	700–1 700	8–13	3.5–4.8, subglobose, echinulate	1–1.5, white	Varga *et al.* (2007)
A. niger	70–85	70–85	n/a	black	45–80, globose	1 500–3 000	15–20	3.5–5.5, globose, finely to distinctly roughened	0.5–0.7, cream	Crous *et al.* (2009), Samson *et al.* (2010), Frisvad *et al.* (2014)
A. lacticoffeatus	71–76	59–75	52–70	cream to light brown	40–65, nearly globose	(200–)300–1 200	(7–)10–15(–18)	3.5–4.1 × 3.4–3.9, subglobose, usually smooth to very finely roughened	not observed	Samson *et al.* (2004)
A. vinaceus	64–66	60–63.5	35–39	black	63–75, globose to subglobose	1 300–1 800	16–21	3–5.5, globose to subglobose, finely roughened to echinulate	0.9–1.5, white to cream	Silva *et al.* (2020)
A. welwitschiae	similar to *A. niger*	similar to *A. niger*	similar to *A. niger*	black	45–85, globose	similar to *A. niger*	n/a	3.5–5.5, globose, finely to distinctly roughened	not observed	Hong *et al.* (2013), Silva *et al.* (2020)
A. chiangmaiensis	62–63	57–66	68–70	dark brown to black	35–68, globose to ellipsoidal	370–1 430	10–15	3–4.5, globose to subglobose, echinulate	0.4–1.4, white	Khuna *et al.* (2021)
A. costaricensis	63–78	58–62	26–62	white with sparse black-sporulating areas	40–90, globose	(800–)1 000–1 700(–1 900)	(12–)13–20(–22)	3.1–4.5, globose to subglobose, smooth to distinctly roughened	1.2–1.8, pink to yellow	Samson *et al.* (2004)
A. eucalypticola	68–72	30–50	46–51	beige to cream yellow	30–55, globose	n/a	8–14	2.5–3.5, globose, smooth to coarsely roughened	not observed	Varga *et al.* (2011)
A. luchuensis[2]	37–80	30–67	43–68	white, gray, brown, black	15–90, subglobose to globose	1500	10–22	3–4.5, globose, smooth	0.8–1.3, cream	Samson *et al.* (2010), Varga *et al.* (2011), Hong *et al.* (2013), Frisvad *et al.* (2014)
A. neoniger	72–80	37–67	54–61	gray to black	30–50, globose	n/a	8–12	3.5–5, globose, coarsely roughened to echinulate	observed (without description)	Varga *et al.* (2011), Frisvad *et al.* (2014)
A. piperis	60–75	64–82	59–78	cream-coloured with sparse black-sporulating areas	40–55, subglobose	(300–)400–3 000	(7–)12–15(–20)	2.8–3.6, subglobose to broadly ellipsoidal, distinctly roughened	1–1.7, yellow to pink brown	Samson *et al.* (2004)
A. pseudopiperis	63–65	61–64	55–60	greenish brown to dark brown	15–39, globose to ellipsoidal	200–2 125	10–18	3–5, globose to subglobose, roughened to spinulose	0.2–1 × 0.2–0.8, light yellow to pinkish orange	Khuna *et al.* (2021)
A. pseudotubingensis	51–58	55–68	62–63	grayish brown to dark brown	20–70, globose to ellipsoidal	740–3 060	10–18	3–6, globose to subglobose, fine spiny surface	not observed	Khuna *et al.* (2021)
A. tubingensis	n/a	n/a	40–65	beige, grayish brown, brown to black	27–80, globose	550–2 300(–6 000)	10–35	3–5, globose, coarsely roughened	0.4–1.8, cream to pinkish tan	Samson *et al.* (2007), Varga *et al.* (2007), Hong *et al.* (2013), Horn *et al.* (2013), Ismail (2017)
A. vadensis	25	n/a	30	light brown to olive green brown	25–35, globose	up to 150	6–15	3–4, globose, rough-walled to finely echinulate	not observed	de Vries *et al.* (2005)

n/a - exact data not available.

[1]if there are multiple studies in the column "references", the description and dimensions are shown as a summary from all these sources.

[2]the dimensions shown here represent summary from description of *A. luchuensis* and its synononym *A. acidus* as they appeared in the publications of Varga *et al.* (2011) and Hong *et al.* (2013).

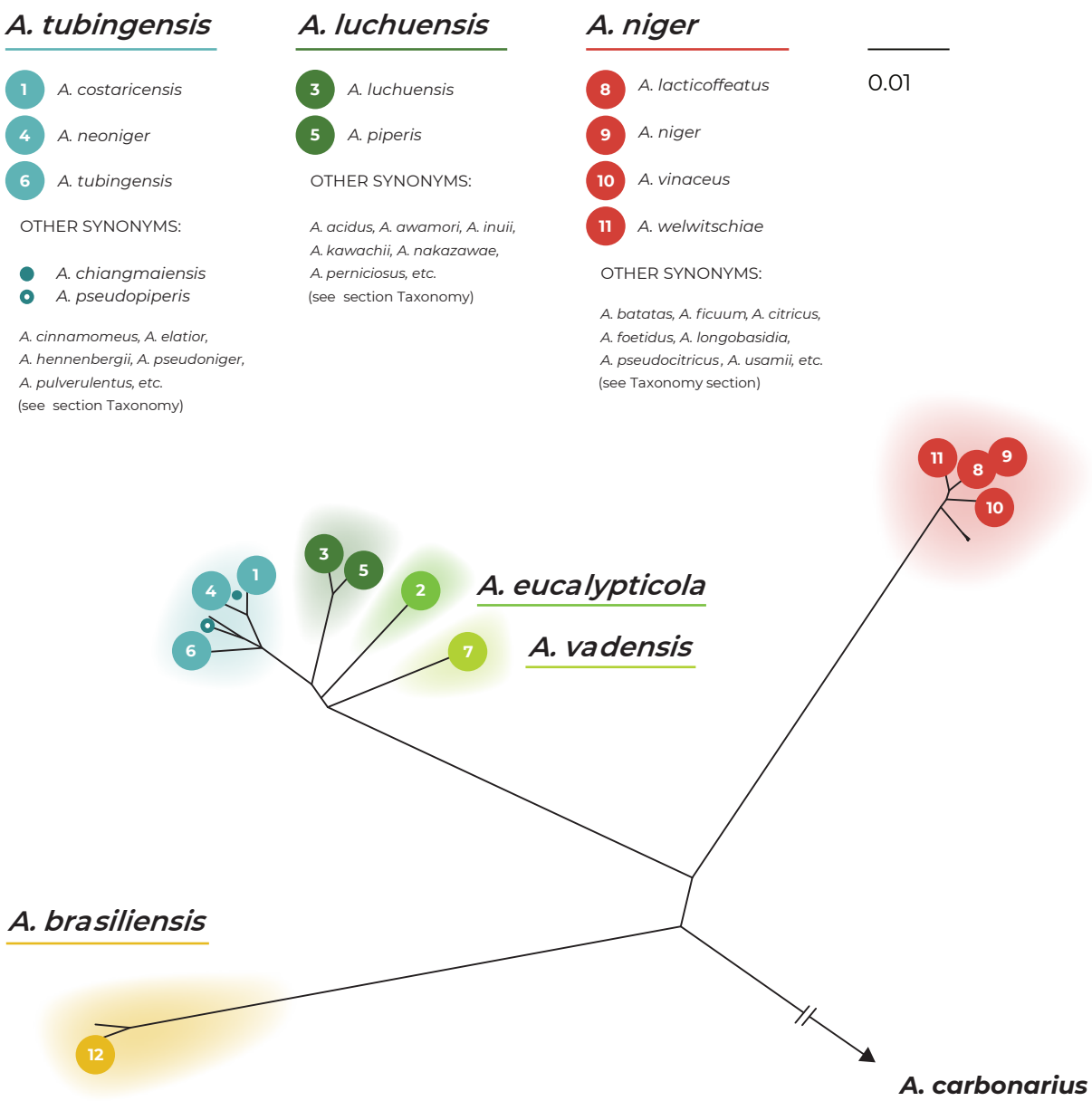

Fig. 10. Taxonomic rearrangement of series *Nigri* into six species with marked synonymizations. The proposed taxonomy is schematically shown in the form of a radial tree (species tree based on *benA*, *CaM* and *RPB2* calculated in starBEAST). The positions of *A. chiangmaiensis* and *A. pseudopiperis* are approximated based on the tree shown in Figs 1, 3 as they were not included in this phylogenetic analysis.

done through DNA sequencing of all three markers and performing phylogenetic analysis. The ITS barcoding sequence can only distinguish among ABL, ANL and ATL (Supplementary Fig. S3).

As mentioned above, we excluded three newly described species, *A. chiangmaiensis, A. pseudopiperis* and *A. pseudotubingensis* (Khuna *et al.* 2021), from the analyses based on the MSC model because of the poor quality of their available sequences. However, we propose that *A. chiangmaiensis* and *A. pseudopiperis* are synonyms of *A. tubingensis*, as their phylogenetic position in the combined ML, MP and BI trees is within the redefined *A. tubingensis*: the *A. pseudopiperis* ex-type strain (SDBR-CMUI1) is located in a clade sister to the clade containing the *A. tubingensis* ex-type (CBS 133056), and *A. chiangmaiensis* is closely related to *A. costaricensis* and *A. neoniger* (Figs 1, 3), which are also synonymized with *A. tubingensis*. The status of *A. pseudotubingensis* remains uncertain and needs to be revised in the future as it forms a relatively separate lineage in the combined phylogeny based on three loci similar to *A. eucalypticola* (Figs 1, 3). The phylogeny presented by Khuna *et al.* (2021) is affected by numerous errors in the DNA sequences of the newly described species and it shows clear signs of the long branch attraction phenomenon (Kück *et al.* 2012). We believe that a more reliable position is shown in our phylogenies constructed based on partially corrected sequences (Figs 1, 3).

The species reduction proposed in this study is in line with some other studies using MSC model-based methods, genomic data or more complex approaches for species delimitation in fungi. For example, species number was significantly reduced in the plant pathogens from the *Diaporthe eres* complex (Hilário *et al.* 2021) and *Alternaria* section *Alternaria* (Woudenberg *et al.* 2015), the edible mushroom *Flammulina* (Wang *et al.* 2018), the lichen-forming fungus *Bryoria* (Boluda *et al.* 2019), the indoor fungi from *Aspergillus* series *Versicolores* (Sklenář *et al.* 2022) and the opportunistic human and animal pathogens from *Aspergillus* series *Viridinutantes* (Hubka *et al.* 2018). Numerous examples can also be found outside the *Fungi* kingdom (Li *et al.* 2019, Feng *et al.* 2021, Parker *et al.* 2021). These studies demonstrate that species over splitting similar to that observed in series *Nigri* is relatively common

in extensively studied groups and species number reduction can become an increasingly common trend in taxonomy.

Future prospects

Further reduction of species number in the series *Nigri* cannot be ruled out in the future after collecting more strains and more whole genome sequences from underrepresented taxa such as *A. eucalypticola* and *A. vadensis*. Inclusion of more variability from these rare taxa should resolve persistent ambiguities in the definition of species limits and increase the probability of methods to delimit species more conclusively. As mentioned above, the position of *A. pseudotubingensis* should be re-examined, and higher quality DNA sequences should be obtained, ideally whole genome sequences. For now, we recommend avoiding using this name until the abovementioned issues are resolved.

Advanced phylogenetic methods spanning the whole genome will allow for a systematic and comparable metric of species differentiation. For example, reciprocal monophyly and a high level of concordance between thousands of markers on the genome scale should allow better differentiation between processes such as recombination, incomplete lineage sorting and speciation in most cases (Kobmoo *et al.* 2019, Matute & Sepúlveda 2019, Mavengere *et al.* 2020). A dense population-level representation in genome-scale phylogenetic studies is important for accurate identification of species boundaries and for resolving evolutionary relationships between species and higher-level taxonomic ranks in *Aspergillus* (Steenwyck *et al.* 2022). Our efforts in the following years will be directed towards achieving this goal.

DECLARATION ON CONFLICT OF INTEREST

The authors declare that there is no conflict of interest.

ACKNOWLEDGMENTS

Vit Hubka was supported by the Czech Ministry of Health (grant NU21-05-00681), the Charles University Research Centre program no. 204069 and the Czech Academy of Sciences Long-term Research Development Project (RVO: 61388971). František Sklenář was supported by the project of Charles University Grant Agency (GAUK 380821). This work has been partly supported by JST SPRING awarded to Cai Bian (JPMJSP2109). CMV acknowledges the Plant Health and Protection - Agricultural Research Council (ARC-PHP), where research on the PPRI strains included in this study was initiated and financially supported by a grant (nr 110441; reference FBIS170406226088) received from the Foundational Biodiversity Information Programme (FBIP) of the National Research Foundation of South Africa. VH is grateful for the support from the Japan Society for the Promotion of Science - Postdoctoral Fellowships for Research in Japan (Standard) and Grant-in-aid for a JSPS research fellow (No. 20F20772). We are grateful to Jan Karhan for the help with graphical adjustments of analysis outputs. We thank Kateřina Glässnerová for her assistance in the laboratory and Osamu Yamada for providing copies of some old taxonomic studies.

REFERENCES

Ahrens D, Fujisawa T, Krammer H-J, *et al*. (2016). Rarity and incomplete sampling in DNA-based species delimitation. *Systematic Biology* **65**: 478–494.

Alcazar-Fuoli L, Mellado E, Alastruey-Izquierdo A, *et al*. (2009). Species identification and antifungal susceptibility patterns of species belonging to *Aspergillus* section *Nigri*. *Antimicrobial Agents and Chemotherapy* **53**: 4514–4517.

Al-Musallam (1980). *A revision of the black Aspergillus species.* Ph.D. dissertation. Rijksuniversiteit Utrecht, Netherlands.

Andersen MR, Salazar MP, Schaap PJ, *et al*. (2011). Comparative genomics of citric-acid-producing *Aspergillus niger* ATCC 1015 versus enzyme-producing CBS 513.88. *Genome Research* **21**: 885–897.

Bairoch A, Apweiler R (2000). The SWISS-PROT protein sequence database and its supplement TrEMBL in 2000. *Nucleic Acids Research* **28**: 45–48.

Ban S, Kasaishi R, Kamijo T, *et al*. (2021). An exploratory MALDI-TOF MS library based on SARAMIS superspectra for rapid identification of *Aspergillus* section *Nigri*. *Mycoscience* **62**: 224–232.

Bankevich A, Nurk S, Antipov D, *et al*. (2012). SPAdes: a new genome assembly algorithm and its applications to single-cell sequencing. *Journal of Computational Biology* **19**: 455–477.

Bennett JW, Klich MA (1992). *Aspergillus: biology and industrial applications.* Butterworth-Heinemann, USA.

Boluda CG, Rico VJ, Divakar PK, *et al*. (2019). Evaluating methodologies for species delimitation: the mismatch between phenotypes and genotypes in lichenized fungi (*Bryoria* sect. *Implexae*, *Parmeliaceae*). *Persoonia* **42**: 75–100.

Bouckaert R, Heled J, Kühnert D, *et al*. (2014). BEAST 2: a software platform for Bayesian evolutionary analysis. *PLoS Computational Biology* **10**: e1003537.

Buchfink B, Xie C, Huson DH (2015). Fast and sensitive protein alignment using DIAMOND. *Nature Methods* **12**: 59–60.

Carstens BC, Pelletier TA, Reid NM, Satler JD (2013). How to fail at species delimitation. *Molecular Ecology* **22**: 4369–4383.

Cerqueira GC, Arnaud MB, Inglis DO, *et al*. (2014). The *Aspergillus* Genome Database: multispecies curation and incorporation of RNA-Seq data to improve structural gene annotations. *Nucleic Acids Research* **42**: D705–710.

Chambers EA, Hillis DM (2020). The multispecies coalescent over-splits species in the case of geographically widespread taxa. *Systematic Biology* **69**: 184–193.

Chen Y, Nie F, Xie S-Q, *et al*. (2021). Efficient assembly of nanopore reads via highly accurate and intact error correction. *Nature Communications* **12**: 60.

Crous PW, Verkley GJM, Groenewald JZ, *et al*. (eds) (2009). *Fungal Biodiversity. CBS Laboratory Manual Series No. 1.* Centraalbureau voor Schimmelcultures, Utrecht, The Netherlands.

de Vries RP, Riley R, Wiebenga A, *et al*. (2017). Comparative genomics reveals high biological diversity and specific adaptations in the industrially and medically important fungal genus *Aspergillus*. *Genome Biology* **18**: 28.

Dettman JR, Jacobson DJ, Taylor JW (2003a). A multilocus genealogical approach to phylogenetic species recognition in the model eukaryote *Neurospora*. *Evolution* **57**: 2703–2720.

Dettman JR, Jacobson DJ, Turner E, *et al*. (2003b). Reproductive isolation and phylogenetic divergence in *Neurospora*: comparing methods of species recognition in a model eukaryote. *Evolution* **57**: 2721–2741.

D'hooge E, Becker P, Stubbe D, *et al*. (2019). Black aspergilli: A remaining challenge in fungal taxonomy? *Medical Mycology* **57**: 773–780.

Donaldson GC, Ball LA, Axelrood PE, *et al*. (1995). Primer sets developed to amplify conserved genes from filamentous ascomycetes are useful in differentiating *Fusarium* species associated with conifers. *Applied and Environmental Microbiology* **61**: 1331–1340.

Dyer PS, O'Gorman CM (2011). A fungal sexual revolution: *Aspergillus* and *Penicillium* show the way. *Current Opinion in Microbiology* **14**: 649–654.

Ellena V, Seekles SJ, Vignolle GA, *et al*. (2021). Genome sequencing of the neotype strain CBS 554.65 reveals the MAT1–2 locus of *Aspergillus niger*. *BMC Genomics* **22**: 679.

Emms DM, Kelly S (2019). OrthoFinder: phylogenetic orthology inference for comparative genomics. *Genome Biology* **20**: 238.

Feng X, Wang X, Chiang Y, *et al*. (2021). Species delimitation with distinct methods based on molecular data to elucidate species boundaries in the *Cycas taiwaniana* complex (*Cycadaceae*). *Taxon* **70**: 477–491.

Frisvad JC, Larsen TO, Thrane U, *et al*. (2011). Fumonisin and ochratoxin production in industrial *Aspergillus niger* strains. *PLoS ONE* **6**: e23496.

Frisvad JC, Møller LLH, Larsen TO, *et al*. (2018). Safety of the fungal workhorses of industrial biotechnology: update on the mycotoxin and secondary metabolite potential of *Aspergillus niger, Aspergillus oryzae*, and *Trichoderma reesei*. *Applied Microbiology and Biotechnology* **102**: 9481–9515.

Frisvad JC, Petersen LM, Lyhne EK, *et al*. (2014). Formation of sclerotia and production of indoloterpenes by *Aspergillus niger* and other species in section *Nigri*. *PLoS ONE* **9**: e94857.

Fungaro MHP, Ferranti LS, Massi FP, *et al*. (2017). *Aspergillus labruscus sp. nov.*, a new species of *Aspergillus* section *Nigri* discovered in Brazil. *Scientific Reports* **7**: 1–9.

Gams W, Christensen M, Onions AH, *et al*. (1986). Infrageneric Taxa of *Aspergillus*. In: *Advances in Penicillium and Aspergillus Systematics*. Springer, US: 55–62.

Gautier M, Normand A-C, Ranque S (2016). Previously unknown species of *Aspergillus*. *Clinical Microbiology and Infection* **22**: 662–669.

Gits-Muselli M, Hamane S, Verillaud B, *et al*. (2021). Different repartition of the cryptic species of black aspergilli according to the anatomical sites in human infections, in a French University hospital. *Medical Mycology* **59**: 985–992.

Glässnerová K, Sklenář F, Jurjević Ž, *et al*. (2022). A monograph of *Aspergillus* section *Candidi*. *Studies in Mycology* **102**: 1–51.

Gnerre S, MacCallum I, Przybylski D, *et al*. (2011). High-quality draft assemblies of mammalian genomes from massively parallel sequence data. *Proceedings of the National Academy of Sciences of the United States of America* **108**: 1513–1518.

Grüning B, Dale R, Sjödin A, *et al*. (2018). Bioconda: sustainable and comprehensive software distribution for the life sciences. *Nature Methods* **15**: 475–476.

Hashimoto A, Hagiwara D, Watanabe A, *et al*. (2017). Drug sensitivity and resistance mechanism in *Aspergillus* section *Nigri* strains from Japan. *Antimicrobial Agents and Chemotherapy* **61**: e02583-16.

Heled J, Drummond AJ (2010). Bayesian inference of species trees from multilocus data. *Molecular Biology and Evolution* **27**: 570–580.

Hendrickx M, Beguin H, Detandt M (2012). Genetic re-identification and antifungal susceptibility testing of *Aspergillus* section *Nigri* strains of the BCCM/IHEM collection. *Mycoses* **55**: 148–155.

Hilário S, Gonçalves MFM, Alves A (2021). Using genealogical concordance and coalescent-based species delimitation to assess species boundaries in the *Diaporthe eres* complex. *Journal of Fungi* **7**: 507.

Hong S-B, Cho HS, Shin HD, *et al*. (2006). Novel *Neosartorya* species isolated from soil in Korea. *International Journal of Systematic and Evolutionary Microbiology* **56**: 477–486.

Hong S-B, Lee M, Kim DH, *et al*. (2013). *Aspergillus luchuensis*, an industrially important black *Aspergillus* in east Asia. *PLoS ONE* **8**: e63769.

Hong S-B, Yamada O, Samson RA (2014). Taxonomic re-evaluation of black koji molds. *Applied Microbiology and Biotechnology* **98**: 555–561.

Horn BW, Olarte RA, Peterson SW, *et al*. (2013). Sexual reproduction in *Aspergillus tubingensis* from section *Nigri*. *Mycologia* **105**: 1153–1163.

Houbraken J, de Vries RP, Samson RA (2014). Modern taxonomy of biotechnologically important *Aspergillus* and *Penicillium* species. *Advances in Applied Microbiology* **86**: 199–249.

Houbraken J, Kocsubé S, Visagie CM, *et al*. (2020). Classification of *Aspergillus, Penicillium, Talaromyces* and related genera (*Eurotiales*): an overview of families, genera, subgenera, sections, series and species. *Studies in Mycology* **95**: 5–169.

Howard SJ, Harrison E, Bowyer P, *et al*. (2011). Cryptic species and azole resistance in the *Aspergillus niger* complex. *Antimicrobial Agents and Chemotherapy* **55**: 4802–4809.

Hubka V, Barrs V, Dudová Z, *et al*. (2018). Unravelling species boundaries in the *Aspergillus viridinutans* complex (section *Fumigati*): opportunistic human and animal pathogens capable of interspecific hybridization. *Persoonia* **41**: 142–174.

Hubka V, Kolarik M (2012). β-tubulin paralogue *tubC* is frequently misidentified as the *benA* gene in *Aspergillus* section *Nigri* taxonomy: primer specificity testing and taxonomic consequences. *Persoonia* **29**: 1–10.

Hubka V, Kubatova A, Mallatova N, *et al*. (2012). Rare and new etiological agents revealed among 178 clinical *Aspergillus* strains obtained from Czech patients and characterized by molecular sequencing. *Medical Mycology* **50**: 601–610.

Huerta-Cepas J, Szklarczyk D, Forslund K, *et al*. (2016). eggNOG 4.5: a hierarchical orthology framework with improved functional annotations for eukaryotic, prokaryotic and viral sequences. *Nucleic Acids Research* **44**: D286–D293.

Ismail MA (2017). Incidence and significance of black aspergilli in agricultural commodities: a review, with a key to all species accepted to-date. *European Journal of Biological Research* **7**: 207–222.

Jin JJ, Yu W bin, Yang JB, *et al*. (2020). GetOrganelle: a fast and versatile toolkit for accurate *de novo* assembly of organelle genomes. *Genome Biology* **21**: 241.

Jones G (2017). Algorithmic improvements to species delimitation and phylogeny estimation under the multispecies coalescent. *Journal of Mathematical Biology* **74**: 447–467.

Jones G, Aydin Z, Oxelman B (2015). DISSECT: an assignment-free Bayesian discovery method for species delimitation under the multispecies coalescent. *Bioinformatics* **31**: 991–998.

Jones P, Binns D, Chang HY, *et al*. (2014). InterProScan 5: genome-scale protein function classification. *Bioinformatics* **30**: 1236–1240.

Jurjević Ž, Peterson SW, Stea G, *et al.* (2012). Two novel species of *Aspergillus* section *Nigri* from indoor air. *IMA Fungus* **3**: 159–173.

Jurjević Ž, Kubátová A, Kolařík M, Hubka V (2015). Taxonomy of *Aspergillus* section *Petersonii sect. nov.* encompassing indoor and soil-borne species with predominant tropical distribution. *Plant Systematics and Evolution* **301**: 2441–2462.

Katoh K, Rozewicki J, Yamada KD (2019). MAFFT online service: multiple sequence alignment, interactive sequence choice and visualization. *Briefings in Bioinformatics* **20**: 1160–1166.

Khuna S, Suwannarach N, Kumla J, *et al*. (2021). Growth enhancement of *Arabidopsis* (*Arabidopsis thaliana*) and onion (*Allium cepa*) with inoculation of three newly identified mineral-solubilizing fungi in the genus *Aspergillus* section *Nigri*. *Frontiers in Microbiology* **12**: 705896.

Kocsubé S, Perrone G, Magistà D, *et al.* (2016). *Aspergillus* is monophyletic: evidence from multiple gene phylogenies and extrolites profiles. *Studies in Mycology* **85**: 91–105.

Korf I (2004). Gene finding in novel genomes. *BMC Bioinformatics* **5**: 59.

Kozakiewicz Z (1989). *Aspergillus* species on stored products. *Mycological Papers* **161**: 1–188.

Kozakiewicz Z, Frisvad JC, Hawksworth DL, Pitt JI, Samson RA, Stolk AC (1992). Proposal for *nomina specifica conservanda* and *rejicienda* in *Aspergillus* and *Penicillium* (Fungi). *Taxon* **41**: 109–113.

Krueger F (2015). Trim Galore!: a wrapper tool around Cutadapt and FastQC to consistently apply quality and adapter trimming to FastQ files. *Babraham Institute* https://www.bioinformatics.babraham.ac.uk/projects.

Kubatko LS, Degnan JH (2007). Inconsistency of phylogenetic estimates from concatenated data under coalescence. *Systematic Biology* **56**: 17–24.

Kück P, Mayer C, Wägele J-W, *et al*. (2012). Long branch effects distort maximum likelihood phylogenies in simulations despite selection of the correct model. *PLoS ONE* **7**: e36593.

Kundu R, Casey J, Sung WK (2019). HyPo: super fast & accurate polisher for long read genome assemblies. *bioRxiv* doi: 10.1101/2019.12.19.882506.

Kusters-van Someren MA, Samson RA, Visser J (1991). The use of RFLP analysis in classification of the black Aspergilli: reinterpretation of the *Aspergillus niger* aggregate. *Current Genetics* **19**: 21–26.

Lanfear R, Frandsen PB, Wright AM, *et al*. (2017). PartitionFinder 2: new methods for selecting partitioned models of evolution for molecular and morphological phylogenetic analyses. *Molecular Biology and Evolution* **34**: 772–773.

Letunic I, Bork P (2021). Interactive Tree Of Life (iTOL) v5: an online tool for phylogenetic tree display and annotation. *Nucleic Acids Research* **49**: W293–W296.

Li H, Durbin R (2009). Fast and accurate short read alignment with Burrows-Wheeler transform. *Bioinformatics* **25**: 1754–1760.

Li H, Handsaker B, Wysoker A, *et al*. (2009). 1000 genome project data processing subgroup. The sequence alignment/map format and Samtools. *Bioinformatics* **25**: 2078–2079.

Li Y, Wen J, Ren Y, *et al*. (2019). From seven to three: integrative species delimitation supports major reduction in species number in *Rhodiola* section *Trifida* (*Crassulaceae*) on the Qinghai-Tibetan Plateau. *Taxon* **68**: 268–279.

Liu YJ, Whelen S, Hall BD (1999). Phylogenetic relationships among ascomycetes: evidence from an RNA polymerse II subunit. *Molecular Biology and Evolution* **16**: 1799–1808.

Mageswari A, Kim J, Cheon K-H, *et al*. (2016). Analysis of the *MAT1-1* and *MAT1-2* gene ratio in black Koji molds isolated from Meju. *Mycobiology* **44**: 269–276.

Majoros WH, Pertea M, Salzberg SL (2004). TigrScan and GlimmerHMM: two open source *ab initio* eukaryotic gene-finders. *Bioinformatics* **20**: 2878–2879.

Matute DR, Sepúlveda VE (2019). Fungal species boundaries in the genomics era. *Fungal Genetics and Biology* **131**: 103249.

Mitchell AL, Attwood TK, Babbitt PC, *et al*. (2019). InterPro in 2019: improving coverage, classification and access to protein sequence annotations. *Nucleic Acids Research* **47**: D351–D360.

Mosseray R (1934). Les *Aspergillus* de la section" Niger" Thom & Church. *La Cellule* **43**: 203–285.

Nargesi S, Jafarzadeh J, Najafzadeh MJ, *et al*. (2022). Molecular identification and antifungal susceptibility of clinically relevant and cryptic species of *Aspergillus* sections *Flavi* and *Nigri*. *Journal of Medical Microbiology* **71**: 001480.

Negri CE, Gonçalves SS, Xafranski H, *et al*. (2014). Cryptic and rare *Aspergillus* species in Brazil: prevalence in clinical samples and *in vitro* susceptibility to triazoles. *Journal of Clinical Microbiology* **52**: 3633–3640.

Nguyen L-T, Schmidt HA, von Haeseler A, *et al*. (2015). IQ-TREE: a fast and effective stochastic algorithm for estimating maximum-likelihood phylogenies. *Molecular Biology and Evolution* **32**: 268–274.

Nielsen KF, Mogensen JM, Johansen M, *et al*. (2009). Review of secondary metabolites and mycotoxins from the *Aspergillus niger* group. *Analytical and Bioanalytical Chemistry* **395**: 1225–1242.

Noonim P, Mahakarnchanakul W, Nielsen KF, *et al*. (2008). Isolation, identification and toxigenic potential of ochratoxin A-producing *Aspergillus* species from coffee beans grown in two regions of Thailand. *International Journal of Food Microbiology* **128**: 197–202.

Pante E, Puillandre N, Viricel A, *et al*. (2015). Species are hypotheses: avoid connectivity assessments based on pillars of sand. *Molecular Ecology* **24**: 525–544.

Paradis E (2010). pegas: an R package for population genetics with an integrated-modular approach. *Bioinformatics* **26**: 419–420.

Parker E, Dornburg A, Struthers CD, *et al*. (2021). Phylogenomic species delimitation dramatically reduces species diversity in an Antarctic adaptive radiation. *Systematic Biology* **71**: 58–77.

Perrone G, Stea G, Epifani F, *et al*. (2011). *Aspergillus niger* contains the cryptic phylogenetic species *A. awamori*. *Fungal Biology* **115**: 1138–1150.

Peterson SW (2000). Phylogenetic relationships in *Aspergillus* based on rDNA sequence analysis. In: *Integration of Modern Taxonomic Methods for Penicillium and Aspergillus Classification* (Samson RA, Pitt JI, eds). Harwood Academic Publishers, UK: 323–355.

Peterson SW (2008). Phylogenetic analysis of *Aspergillus* species using DNA sequences from four loci. *Mycologia* **100**: 205–226.

Pitt JI, Hocking AD (2009). *Aspergillus* and related teleomorphs. In: *Fungi and Food Spoilage*. Springer, USA: 275–337.

R Core Team (2016). *R: a language and environment for statistical computing*. R foundation for statistical computing, Vienna, Austria.

Raper KB, Fennell DI (1965). The genus *Aspergillus*. Williams & Wilkins, USA.

Rawlings ND, Barrett AJ, Thomas PD, *et al*. (2018). The MEROPS database of proteolytic enzymes, their substrates and inhibitors in 2017 and a comparison with peptidases in the PANTHER database. *Nucleic Acids Research* **46**: D624–D632.

Richards TA (2011). Genome evolution: horizontal movements in the fungi. *Current Biology* **21**: R166–R168.

Rokas A, Williams BL, King N, *et al*. (2003). Genome-scale approaches to resolving incongruence in molecular phylogenies. *Nature* **425**: 798–804.

Ronquist F, Teslenko M, van der Mark P, *et al*. (2012). MrBayes 3.2: efficient Bayesian phylogenetic inference and model choice across a large model space. *Systematic Biology* **61**: 539–542.

Salah H, Lackner M, Houbraken J, *et al*. (2019). The emergence of rare clinical *Aspergillus* species in Qatar: molecular characterization and antifungal susceptibility profiles. *Frontiers in Microbiology* **10**: 1677.

Samson RA, Houbraken J, Thrane U, *et al*. (2010). *Food and indoor fungi. CBS Laboratory Manual Series 2*. CBS-KNAW Fungal Biodiversity Centre, The Netherlands.

Samson RA, Houbraken J, Thrane U, *et al*. (2019). *Food and Indoor Fungi*. Westerdijk Fungal Biodiversity Institute, The Netherlands.

Samson RA, Houbraken JAMP, Kuijpers AFA, *et al*. (2004). New ochratoxin A or sclerotium producing species in *Aspergillus* section *Nigri*. *Studies in Mycology* **50**: 45–61.

Samson RA, Hubka V, Varga J, *et al*. (2017). Response to Pitt & Taylor 2016: conservation of *Aspergillus* with *A. niger* as the conserved type is unnecessary and potentially disruptive. *Taxon* **66**: 1439–1446.

Samson RA, Noonim P, Meijer M, *et al*. (2007). Diagnostic tools to identify black aspergilli. *Studies in Mycology* **59**: 129–145.

Schuster E, Dunn-Coleman N, Frisvad J, *et al*. (2002). On the safety of *Aspergillus niger* - a review. *Applied Microbiology and Biotechnology* **59**: 426–435.

Seekles SJ, Punt M, Savelkoel N, *et al*. (2022). Genome sequences of 24 *Aspergillus niger sensu stricto* strains to study strain diversity, heterokaryon compatibility, and sexual reproduction. *G3 (Bethesda)* **12**: jkac124.

Seo T-K (2008). Calculating bootstrap probabilities of phylogeny using multilocus sequence data. *Molecular Biology and Evolution* **25**: 960–971.

Seppey M, Manni M, Zdobnov EM (2019). BUSCO: assessing genome assembly and annotation completeness. *Methods in Molecular Biology* **1962**: 227–245.

Shen W, Le S, Li Y, *et al*. (2016). SeqKit: a cross-platform and ultrafast toolkit for FASTA/Q file manipulation. *PLoS ONE* **11**: e0163962.

Silva JJ da, Iamanaka BT, Ferranti LS, *et al*. (2020). Diversity within *Aspergillus niger* clade and description of a new species: *Aspergillus vinaceus sp. nov. Journal of Fungi* **6**: 371.

Sklenář F, Glässnerová K, Jurjević Ž, *et al*. (2022). Taxonomy of *Aspergillus* series *Versicolores*: species reduction and lessons learned about intraspecific variability. *Studies in Mycology* **102**: 53–93.

Sklenář F, Jurjević Ž, Houbraken J, *et al*. (2021). Re-examination of species limits in *Aspergillus* section *Flavipedes* using advanced species delimitation methods and description of four new species. *Studies in Mycology* **99**: 100120.

Sklenář F, Jurjević Ž, Zalar P, *et al*. (2017). Phylogeny of xerophilic aspergilli (subgenus *Aspergillus*) and taxonomic revision of section *Restricti*. *Studies in Mycology* **88**: 161–236

Slot JC, Rokas A (2011). Horizontal transfer of a large and highly toxic secondary metabolic gene cluster between fungi. *Current Biology* **21**: 134–139.

Stamatakis A (2014). RAxML version 8: a tool for phylogenetic analysis and post-analysis of large phylogenies. *Bioinformatics* **30**: 1312–1313.

Stanke M, Schöffmann O, Morgenstern B, *et al*. (2006). Gene prediction in eukaryotes with a generalized hidden Markov model that uses hints from external sources. *BMC Bioinformatics* **7**: 62.

Steenkamp ET, Wingfield MJ, McTaggart AR, *et al*. (2018). Fungal species and their boundaries matter – definitions, mechanisms and practical implications. *Fungal Biology Reviews* **32**: 104–116.

Steenwyk JL, Shen X-X, Lind AL, *et al*. (2019). A robust phylogenomic time tree for biotechnologically and medically important fungi in the genera *Aspergillus* and *Penicillium*. *mBio* **10**: e00925-19.

Steenwyk JL, Balamurugan C, Raja HA *et al.* (2022). Phylogenomics reveals extensive misidentification of fungal strains from the genus *Aspergillus*. bioRxiv doi: 10.1101/2022.11.22.517304.

Sukumaran J, Holder MT, Knowles LL (2021). Incorporating the speciation process into species delimitation. *PLoS Computational Biology* **17**: e1008924.

Swofford DL (2003). PAUP* Phylogenetic analysis using parsimony, (*and other methods); version 4.0 b10. Sinauer Associates, USA.

Szigeti G, Sedaghati E, Mahmoudabadi AZ, *et al*. (2012). Species assignment and antifungal susceptibilities of black aspergilli recovered from otomycosis cases in Iran. *Mycoses* **55**: 333–338.

Szöllősi GJ, Davín AA, Tannier E, *et al*. (2015). Genome-scale phylogenetic analysis finds extensive gene transfer among fungi. *Philosophical Transactions of the Royal Society B*: *Biological Sciences* **370**: 20140335.

Talavera G, Castresana J (2007). Improvement of phylogenies after removing divergent and ambiguously aligned blocks from protein sequence alignments. *Systematic Biology* **56**: 564–577.

Taniwaki MH, Pitt JI, Magan N (2018). *Aspergillus* species and mycotoxins: occurrence and importance in major food commodities. *Current Opinion in Food Science* **23**: 38–43.

Taylor JW, Jacobson DJ, Kroken S, *et al*. (2000). Phylogenetic species recognition and species concepts in fungi. *Fungal Genetics and Biology* **31**: 21–32.

Ter-Hovhannisyan V, Lomsadze A, Chernoff YO, *et al*. (2008). Gene prediction in novel fungal genomes using an *ab initio* algorithm with unsupervised training. *Genome Research* **18**: 1979–1990.

Thom C (1916). *Aspergillus niger* group. *Journal of Agricultural Research* 8: 1–15.

Thom C, Church MB (1926). *The Aspergilli*. Baltimore: Williams & Wilkins.

Thom C, Raper KB (1945). *A Manual of the Aspergilli*. Baltimore: Williams & Wilkins.

Turland NJ, Wiersema JH, Barrie FR, *et al.* (2018). *International Code of Nomenclature for algae, fungi, and plants (Shenzhen Code) adopted by the Nineteenth International Botanical Congress Shenzhen, China, July 2017.* Regnum Vegetabile 159. Glashütten: Koeltz Botanical Books.

van Rossum G, Drake Jr FL (2014). *The python language reference*. Python software foundation.

Varga J, Szigeti G, Baranyi N, *et al*. (2014). *Aspergillus*: sex and recombination. *Mycopathologia* **178**: 349–362.

Varga J, Frisvad JC, Kocsubé S, *et al*. (2011). New and revisited species in *Aspergillus* section *Nigri*. *Studies in Mycology* **69**: 1–17.

Varga J, Kevei F, Vriesema A, *et al*. (1994). Mitochondrial DNA restriction fragment length polymorphisms in field isolates of the *Aspergillus niger* aggregate. *Canadian Journal of Microbiology* **40**: 612–621.

Vaser R, Sović I, Nagarajan N, *et al*. (2017). Fast and accurate *de novo* genome assembly from long uncorrected reads. *Genome Research* **27**: 737–746.

Vesth TC, Nybo JL, Theobald S, *et al*. (2018). Investigation of inter- and infraspecies variation through genome sequencing of *Aspergillus* section *Nigri*. *Nature Genetics* **50**: 1688–1695.

Vidal-Acuña MR, Ruiz M, Torres MJ, *et al*. (2019). Prevalence and *in vitro* antifungal susceptibility of cryptic species of the genus *Aspergillus* isolated in clinical samples. *Enfermedades Infecciosas y Microbiologia Clinica (English ed.)* **37**: 296–300.

Wang PM, Liu X bin, Dai YC, *et al*. (2018). Phylogeny and species delimitation of *Flammulina*: taxonomic status of winter mushroom in East Asia and a new European species identified using an integrated approach. *Mycological Progress* **17**: 1013–1030.

Ward OP (1989). *Fermentation Biotechnology.* Prentice Hall, Englewood Cliffs, New York, USA.

Wehmer C (1907). Zur Kenntnis einiger *Aspergillus*-Arten. *Centralblatt für Bakteriologie und Parasitenkunde, Abt. II* **18**: 385–395.

Wilhelm KA (1877). *Beiträge zur Kenntnis des Pilzgattung Aspergillus*. Doctoral Dissertation, Strasburg, Germany.

Woudenberg JHC, Seidl MF, Groenewald JZ, *et al*. (2015). *Alternaria* section *Alternaria*: species, *formae speciales* or pathotypes? *Studies in Mycology* **82**: 1–21.

Yamada O, Takara R, Hamada R, *et al.* (2011). Molecular biological researches of Kuro-Koji molds, their classification and safety. *Journal of Bioscience and Bioengineering* **112**: 233–237.

Yang L, Lübeck M, Lübeck PS (2017). *Aspergillus* as a versatile cell factory for organic acid production. *Fungal Biology Reviews* **31**: 33–49.

Yang Z (2015). The BPP program for species tree estimation and species delimitation. *Current Zoology* **61**: 854–865.

Yang Z, Rannala B (2010). Bayesian species delimitation using multilocus sequence data. *Proceedings of the National Academy of Sciences* **107**: 9264–9269.

Yang Z, Rannala B (2014). Unguided species delimitation using DNA sequence data from multiple loci. *Molecular Biology and Evolution* **31**: 3125–3135.

Yin Y, Mao X, Yang J, *et al*. (2012). dbCAN: a web resource for automated carbohydrate-active enzyme annotation. *Nucleic Acids Research* **40**: W445–451.

Yu T-S, Yeo S-H, Kim H-S (2004). A new species of hyphomycetes, *Aspergillus coreanus sp. nov.*, isolated from traditional Korean nuruk. *Journal of Microbiology and Biotechnology* **14**: 182–187.

Zerbino DR, Birney E (2008). Velvet: algorithms for *de novo* short read assembly using *de Bruijn* graphs. *Genome Research* **18**: 821–829.

Supplementary Material: https://studiesinmycology.org/

Fig. S1. Multilocus phylogeny of *Aspergillus* series *Nigri* based on three loci (*benA*, *CaM* and *RPB2*) without species *A. chiangmaiensis*, *A. pseudopiperis* and *A. pseudotubingensis*. Best-scoring Maximum Likelihood (ML) tree inferred in the IQ-TREE is shown; ultrafast bootstrap support values (ML bs) are appended to nodes; only support values ≥95 % are shown; the ex-type strains are designated with a bold print; the information on geographic origin and isolation source is plotted on the tree (see the legend).

Fig. S2. Comparison of single-gene genealogies based on the *benA*, *CaM* and *RPB2* loci and created by three different phylogenetic methods (only one isolate per unique multilocus haplotype is included in each phylogeny). Best-scoring single-locus maximum likelihood (ML) trees are shown; ML ultrafast bootstrap support values (ML bs), maximum parsimony bootstrap support values (MP bs) and Bayesian inference posterior probabilities (BI pp) are appended to nodes. Only support values ≥95 %, ≥70 % and ≥0.95, respectively, are shown. A dash indicates lower statistical support for a specific node, or the absence of a node in the phylogeny, while an asterisk indicates full support. The ex-type strains are designated with a bold print. Alignment characteristics, partitioning schemes and substitution models are listed in Supplementary Table S1.

Fig. S3. Best scoring maximum likelihood tree inferred in IQ-TREE based on ITS rDNA region sequences of series *Nigri* members (Table 1). It is apparent from the tree that a limited variability present in this locus can only differentiate the three main lineages, and more detailed differentiation is not possible. The ITS sequence of the *A. vadensis* ex-type was excluded from the analysis because it contains numerous errors and unresolved positions (accession number AY585549). Alignment characteristics, partitioning schemes and substitution models are listed in Supplementary Table S1.

Table S1. Characteristics of alignments, partition-merging results and best substitution model for each partition according to the Bayesian information criterion.

Table S2. Assignment of strains into populations for analysis in DELINEATE based on BPP v. 4.3.

Table S3. *Aspergillus* series *Nigri* genomes analyzed in this study and their basic characteristics.

Table S4. Distribution of 200 orthologous genes into ten separate STACEY analyses.

Table S5. List of unique multilocus haplotypes.

Table S6. Maximum sequence dissimilarity between isolates of the same *Aspergillus* species whose species limits have been delimited using methods based on a multispecies coalescent model; only species represented by isolates from at least three countries were included.

Studies in Mycology (ISSN 0166-0616)

The Westerdijk Fungal Biodiversity Institute taxonomy series “Studies in Mycology” is issued as individual booklets. Regular subscribers receive each issue automatically. Prices of back-volumes are specified below.

For more information and ordering of other Westerdijk Institute books and publications see www.wi.knaw.nl and www.studiesinmycology.org.

102 Samson RA (ed) June 2022. Diversity and taxonomy of food and indoor *Aspergillus* 132 pp., online only. No hardcopy available.
101 Samson RA (ed) March 2022. Regular issue. 564 pp., online only. No hardcopy available.
100 Samson RA (ed) September 2021. Human fungal pathogens. 117 pp., online only. No hardcopy available.
99 Samson RA (ed) June 2021. Regular issue. 218 pp., online only. No hardcopy available.
98 Samson RA (ed) March 2021. Genera of fusarioid fungi in *Nectriaceae*. 184 pp., online only. No hardcopy available.
97 Samson RA (ed) September 2020. Regular issue. 92 pp., online only. No hardcopy available.
96 Samson RA (ed) June 2020. Regular issue. 396 pp., online only. No hardcopy available.
95 Samson RA, Crous PW (eds) March 2020. Genera of Hyphomycetes: a Tribute to Keith A. Seifert. 462 pp., online only. No hardcopy available.
94 Samson RA (ed) September 2019. Regular issue. 298 pp., online only. No hardcopy available.
93 Samson RA (ed) June 2019. Taxonomy of industrially important fungi. 252 pp., online only. No hardcopy available.
92 Samson RA (ed) March 2019. Regular issue. 415 pp., online only. No hardcopy available.
91 Samson RA (ed) December 2018. A (post-) genomic view on the diversity in *Aspergillus*. 100 pp., online only. No hardcopy available.
90 Crous PW (ed) June 2018. Regular issue. 190 pp., online only. No hardcopy available.
89 Samson RA (ed) March 2018. Leading women in fungal biology. 302 pp., online only. No hardcopy available.
88 Samson RA (ed) December 2017. Diversity and taxonomy of Food and Indoor Fungi. 268 pp., online only. No hardcopy available.
87 Crous PW (ed) June 2017. Dothideomycetes. 422 pp., online only. No hardcopy available.
86 Samson RA (ed) March 2017. Regular issue. 296 pp., online only. No hardcopy available.
85 Crous PW (ed) September 2016. Regular issue. 214 pp., online only. No hardcopy available.
84 Samson RA (ed) June 2016. Diversity and taxonomy of Indoor Fungi 1. 224 pp., online only. No hardcopy available.
83 Samson RA (ed) March 2016. Regular issue. 234 pp., online only. No hardcopy available.
82 Crous PW, Groenewald JZ (eds) 2015. Saprobic and phytopathogenic *Dothideomycetes*. 222 pp., online only. No hardcopy available.
81 Boekhout T, Bai F-Y (eds) 2015. Multigene phylogeny and reclassification of yeasts and related filamentous taxa in Basidiomycota. 190 pp., online only. No hardcopy available.
80 Lombard L, Groenewald JZ, Crous PW (eds) (2015). Hypocrealean lineages of industrial and phytopathological importance. 245 pp., € 70.00
79 Crous PW, Groenewald JZ (eds) (2014). Fungal pathogens of food and fibre crops. 288 pp., € 65.00
78 Samson RA, Visagie CM, Houbraken J (eds) (2014). Species diversity in *Aspergillus*, *Penicillium* and *Talaromyces*. 451 pp., € 75.00
77 Stadler M, Læssøe T, Fournier F, Decock C, Schmieschek B, Tichy H-V, Peršoh D (2014). A polyphasic taxonomy of *Daldinia* (*Xylariaceae*). 143 pp., € 60.00
76 Phillips AJL, Slippers B, Groenewald JZ, Crous PW (eds) (2013). Plant pathogenic and endophytic *Botryosphaeriales* known from culture. 167 pp., € 65.00
75 Crous PW, Verkley GJM, Groenewald JZ (eds) (2013). Phytopathogenic *Dothideomycetes*. 406 pp., € 70.00
74 Dijksterhuis J, Wösten H (eds) (2013). Development of *Aspergillus niger*. 85 pp., €40.00
73 Damm U, Cannon PF, Crous PW (eds) (2012). *Colletotrichum*: complex species or species complexes? 217 pp., € 65.00
72 Bensch K, Braun U, Groenewald JZ, Crous PW (2012). The genus *Cladosporium*. 401 pp., € 70.00
71 Hirooka Y, Rossmann AY, Samuels GJ, Lechat C, Chaverri P (2012). A monograph of *Allantonectria*, *Nectria*, and *Pleonectria* (*Nectriaceae*, *Hypocreales*, *Ascomycota*) and their pycnidial, sporodochial, and synnematous anamorphs. 210 pp., € 65.00
70 Samson RA, Houbraken J (eds) (2011). Phylogenetic and taxonomic studies on the genera *Penicillium* and *Talaromyces*. 183 pp., € 60.00
69 Samson RA, Varga J, Frisvad JC (2011). Taxonomic studies on the genus *Aspergillus*. 97 pp., € 40.00
68 Rossman AY, Seifert KA (eds) (2011). Phylogenetic revision of taxonomic concepts in the *Hypocreales* and other *Ascomycota* - A tribute to Gary J. Samuels. 256 pp., € 65.00
67 Bensch K, Groenewald JZ, Dijksterhuis J, Starink-Willemse M, Andersen B, Summerell BA, Shin H-D, Dugan FM, Schroers H-J, Braun U, Crous PW (2010). Species and ecological diversity within the *Cladosporium cladosporioides* complex (*Davidiellaceae*, *Capnodiales*). 96 pp., € 40.00
66 Lombard L, Crous PW, Wingfield BD, Wingfield MJ (2010). Systematics of *Calonectria*: a genus of root, shoot and foliar pathogens. 71 pp., € 40.00
65 Aveskamp M, Gruyter H de, Woudenberg J, Verkley G, Crous PW (2010). Highlights of the *Didymellaceae*: A polyphasic approach to characterise *Phoma* and related pleosporalean genera. 64 pp., € 40.00
64 Schoch CL, Spatafora JW, Lumbsch HT, Huhndorf SM, Hyde KD, Groenewald JZ, Crous PW (2009). A phylogenetic re-evaluation of *Dothideomycetes*. 220 pp., € 65.00
63 Jaklitsch WA (2009). European species of *Hypocrea*. Part I. The green-spored species. 93 pp., € 40.00
62 Sogonov MV, Castlebury LA, Rossman AY, Mejía LC, White JF (2008). Leaf-inhabiting genera of the *Gnomoniaceae*, *Diaporthales*. 79 pp., € 40.00
61 Hoog GS de, Grube M (eds) (2008). Black fungal extremes. 198 pp., € 60.00
60 Chaverri P, Liu M, Hodge KT (2008). Neotropical *Hypocrella* (anamorph *Aschersonia*), *Moelleriella*, and *Samuelsia*. 68 pp., € 40.00
59 Samson RA, Varga J (eds) (2007). *Aspergillus* systematics in the genomic era. 206 pp., € 65.00
58 Crous PW, Braun U, Schubert K, Groenewald JZ (eds) (2007). The genus *Cladosporium* and similar dematiaceous hyphomycetes. 253 pp., € 65.00
57 Sung G-H, Hywel-Jones NL, Sung J-M, Luangsa-ard JJ, Shrestha B, Spatafora JW (2007). Phylogenetic classification of *Cordyceps* and the clavicipitaceous fungi. 63 pp., € 40.00

For a complete list of the Studies in Mycology see www.wi.knaw.nl.